M.O. 499 e

AIR MINISTRY

METEOROLOGICAL OFFICE

Geophysical Memoirs No. 85

(FIFTH NUMBER, VOLUME X)

UPPER WINDS OVER THE WORLD

BY

C. E. P. BROOKS, D.Sc., C. S. DURST, B.A., N. CARRUTHERS, B.Sc.,
D. DEWAR, B.Sc. and J. S. SAWYER, M.A.

LONDON: HIS MAJESTY'S STATIONERY OFFICE

1950

Decimal Index
551.587
551.557
551.501.7

Geophys. Mem., London
10, No. 85, 1950

TABLE OF CONTENTS

PAGE

INTRODUCTION .. 1

PART I—WIND ROSES

Section 1. Statement of the problem .. 1
2. Construction of a wind rose .. 3

PART II—SEASONAL CHARTS OF MEAN HEIGHTS OF ISOBARIC SURFACES

Section 3. General .. 9
4. Data used .. 9
5. Southern hemisphere .. 11
6. Details of construction of the charts .. 11
7. Accuracy of the charts .. 12
8. Measurement of vector mean winds from the charts .. 12

PART III—SEASONAL CHARTS OF STANDARD VECTOR DEVIATION

Section 9. General .. 14
10. Data available for direct computation of σ .. 14
11. Estimates of σ over the oceans .. 16
12. Variation of σ with height .. 17
13. Details of construction of the charts .. 24
14. Variation of σ with latitude .. 30
15. Final adjustments of the charts .. 31

PART IV—SEASONAL CHARTS OF WINDS AT STANDARD PRESSURE LEVELS IN THE TROPICS

Section 16. General .. 33
17. Data used in constructing the charts .. 33
18. Method of construction of the charts .. 33
19. Note on use of the charts .. 34

BIBLIOGRAPHY .. 35

APPENDICES

I Computation of height differences between successive standard pressure levels from 500 mb. upwards .. 38
II Use of pilot-balloon observations in the construction of wind roses .. 41
III List of symbols .. 49
IV Tables for the construction of wind roses; frequency distribution .. 51

LIST OF ILLUSTRATIONS

Figure 1. Larkhill (51° N., 2° W.), winds at 500 mb. .. 2
2. Mombasa (4° S., 40° E.), winds at 14,000 ft. .. 2
3. Diagram showing relation between q, σ, V_R and V_S .. 5
4. Variation of σ with height over Larkhill and Lerwick .. 18
5. Variation of σ with height over 53° N., 14° E. .. 19
6. Variation of σ with height over Constanţa (44° N., 29° E.) .. 20
7. Variation of σ with height over Mahlsdorf (53° N., 13° E.) (year) .. 21
8. Variation of σ with height over Karachi (25° N., 67° E.) illustrating the rule $\sigma\rho$ = constant .. 22
9. Relation between the level of σ_m and the mean height of the tropopause .. 23
10. Plot of V_a/V_g (theoretical) .. 24
11. Salisbury (18° S., 31° E.), winds at 10,000 ft. Plot of V_a .. 25
12. Bordeaux (45° N., 1° W.), winds at 10,000 ft. Plot of V_a .. 26
13. Relation between σ_{130} and σ_{500} .. 29
14. Variation of σ with latitude over 30° E. .. 30
15. Variation of σ with height over 30° E. .. 32
16. Variation of temperature with height—schematic .. 39
17. Positions of pressure levels P and P' for case 3(a) and corresponding temperatures 40
18. Values of r'' and V_R/V_R'' for given values of q and q'' .. 47
19. Frequencies in range 10-20 kt. at 20,000 ft. over Bahrein .. 49

Charts showing contours, standard vector deviation and stream-lines at 700 mb., 500 mb., 300 mb., 200 mb. and 130 mb. .. 58–150

UPPER WINDS OVER THE WORLD

INTRODUCTION

The idea of compiling charts of upper winds over the world by the use of two parameters was first suggested by C. S. Durst early in 1945. This was discussed with C. E. P. Brooks and the major part of the development took place under his guidance. The preparation of charts of vector mean wind, either directly (for the tropics) or in the form of charts of absolute topography of pressure, was primarily in the hands of D. Dewar and those of standard vector deviation in the hands of N. Carruthers. Frequent discussions took place at the various stages of drawing the charts, and in these the criticisms of J. S. Sawyer were very cogent.

PART I—WIND ROSES

§ 1—STATEMENT OF THE PROBLEM

For the greater part of the world, data of wind velocity in the free air are very scanty or non-existent. In many countries pilot-balloon observations have been taken for many years, but the wind roses obtained from these are inaccurate and misleading for two reasons: (*a*) because data are obtained only for days on which the balloon was not hidden by cloud; and (*b*) because with increase of height fewer and fewer occasions of strong winds are included owing to the disappearance of the balloon in the distance. The first of these difficulties is insuperable, since it is known that the upper winds on days of much cloud differ systematically from those on clear days. The second difficulty can be partly overcome by a method, described in Appendix II, which reconstructs the complete distribution of wind speeds and directions from the incomplete observed distribution.

Radio methods of observation give a much more accurate representation of the actual wind distribution. They are independent of cloud, and it is only at the highest levels that, on occasions of exceptionally strong wind, the balloon passes out of the range of the receiver. But as yet the radio-wind stations are too few, and have mostly been in operation for too short a time, to describe the general circulation of the atmosphere at great heights. It was therefore of prime importance to find a method of constructing wind-rose charts of the upper atmosphere, with some approach to accuracy, by extrapolating from the known data.

The method adopted depended on the assumption that upper winds, away from the influence of the surface features, are distributed about the vector mean wind in accordance with the normal law of errors. If that assumption is correct, it is possible to represent any wind rose by only two parameters, the vector mean wind $\mathbf{V}_R$* and the standard vector deviation σ of the individual winds about the vector mean. Conversely, given these two parameters it is possible to reconstruct a wind rose. It has been shown[4]† that the proportion of occasions on which the

* A list of symbols used in this paper is given in Appendix III, p. 49.

† These numbers refer to the Bibliography on p. 35.

speed V and direction ϕ of the wind lie between V_1 and V_2 and between ϕ_1, and ϕ_2 is

$$\frac{1}{\pi\sigma^2}\int_{V_1}^{V_2}\int_{\phi_1}^{\phi_2} e^{-v^2/\sigma^2}\, V \,.\, dV \,.\, d\phi \qquad \ldots\ \ldots \quad (1)$$

where $v^2 = V^2 + V_R^2 - 2V \,.\, V_R \,.\, \cos\phi$ and V_R is the magnitude of $\mathbf{V_R}$. The assumption of normality was tested for a number of points by comparing the estimated wind roses with those actually observed, and found to be correct within the limits of error of observed wind roses.

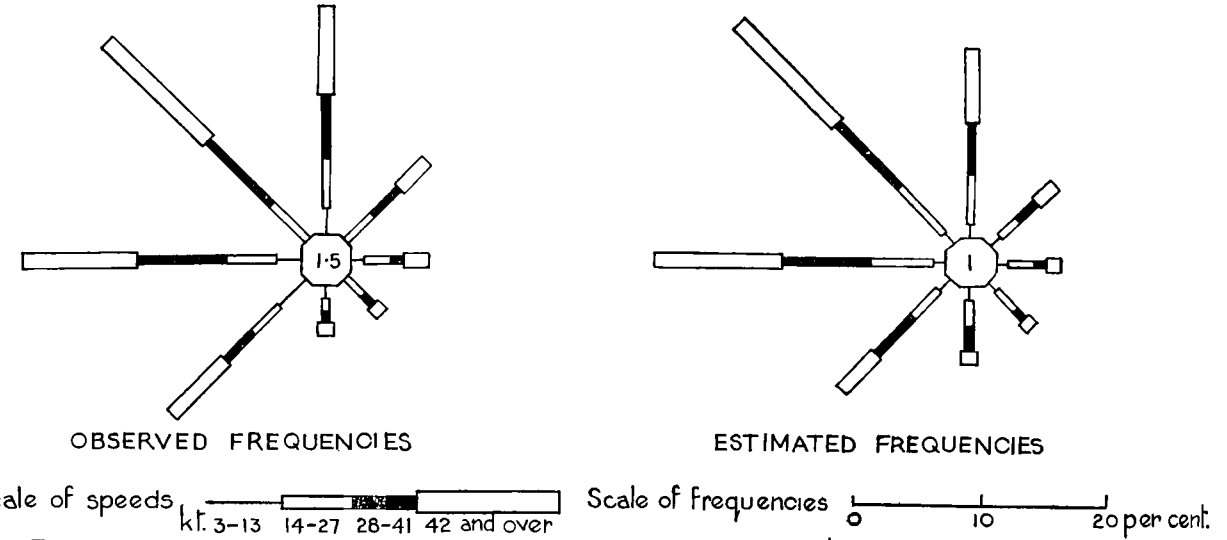

FIG. 1—LARKHILL (51° N., 2° W.), WINDS AT 500 MB.
December–February 1939–40 to 1944–45

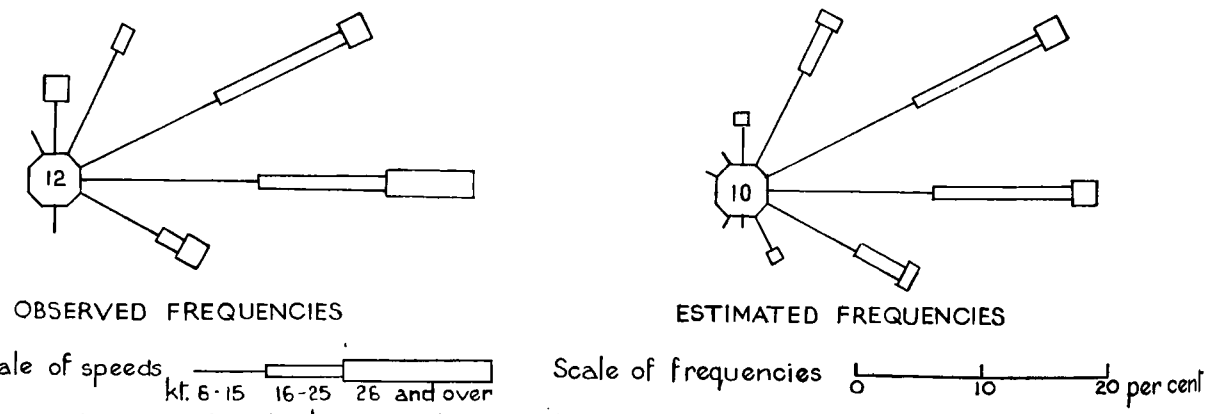

FIG. 2—MOMBASA (4° S., 40° E.), WINDS AT 14,000 FT.
December 1943 and January 1944

The details are given in the *Quarterly Journal of the Royal Meteorological Society*.[4] We reproduce here two examples (Figs. 1 and 2) in which the observed frequencies are compared with those estimated from these two parameters. The agreement is seen to be as good as can be expected.

The problem was now reduced to constructing charts of the distribution of $\mathbf{V_R}$ and σ. These can be found with reasonable accuracy from shorter series of observations than would be required to construct accurate wind roses directly, but this still left very large gaps for which not even this minimum of observations was available. These gaps were filled by extrapolation from surface data and by analogy with parts of the world represented by observations. The greater part of this memoir describes the construction of world charts of $\mathbf{V_R}$ and σ, for each of the four seasons, for pressure levels of 700, 500, 300, 200 and 130 mb., though the charts for the last two levels are incomplete.

The approximate geometric heights of these pressure levels are shown in Table I.

TABLE I—APPROXIMATE GEOMETRIC HEIGHT OF PRESSURE LEVELS

	Pressure levels (mb.)				
	700	500	300	200	130
	thousands of feet				
I.C.A.N. atmosphere	10·0	18·3	30·1	38·8	47·6
Arctic atmosphere	9·0	17·1	28·6	37·0	46·1
Temperate atmosphere	9·9	18·4	29·9	38·9	47·6
Subtropical atmosphere	10·2	19·0	31·5	40·6	49·5

§ 2—CONSTRUCTION OF A WIND ROSE

The method of constructing a wind rose from $\mathbf{V_R}$ and σ was described by Brooks, Durst and Carruthers[4], but as it is essential for using the charts in this memoir, it is repeated here, together with the basic tables which are given in Appendix IV. In practice the standard vector deviation was converted into the " constancy " q, which is defined as $100V_R/V_S$, where V_S is the mean speed of the wind, and Appendix IV was constructed in terms of q and V/V_R. The constancy q is uniquely determined by σ/V_R, except when V_R approaches zero. When q also approaches zero but σ/V_R becomes indefinite. In such a case σ approximates to $1{\cdot}13\ V_S$. The conversion of σ/V_R to q is based on the expression

$$\frac{100}{q} = \frac{2}{\sigma^2}\int_0^\infty Qve^{-v^2/\sigma^2}\,dV \qquad \ldots\ \ldots\ (2)$$

where v is the magnitude of the vector difference of an individual wind from the vector mean wind, and Q is defined by the expression

$$Q = \frac{1}{\pi V_R}\int_0^\pi V\,d\theta = \frac{1}{\pi}\int_0^\pi (1 + x^2 + 2x\cos\theta)^{\frac{1}{2}}\,d\theta \qquad \ldots\ \ldots\ (3)$$

θ being the angle which the vector deviation makes with the positive direction of the vector mean wind, and x the ratio v/V_R.

It was found that Q was given approximately by

$$Q = (1 - m/10)\ (V_R^2 + v^2)^{\frac{1}{2}}/V_R \qquad \ldots\ \ldots\ (4)$$

where $m = v/V_R$ or V_R/v according as v is less or greater than V_R. Subsequently G. C. Watt suggested the following approximations Q_1 and Q_2 for Q, *viz.*:—

$$\left.\begin{aligned} Q_1 &= 1 + \frac{x^2}{4} + \frac{x^6}{44} \text{ when } x \leqslant 1 \\ Q_2 &= x + \frac{1}{4x} + \frac{1}{44x^5} \text{ when } x \geqslant 1 \end{aligned}\right\} \quad .. \quad .. \quad (5)$$

With these approximations for Q expression (2) is integrable in terms of the normal probability integral and, for σ/V_R less than one, they give better results than the method first adopted. The latter seems preferable however when σ/V_R exceeds one. In constructing Table II, Watt's approximations were employed for values of q exceeding 78 per cent.

TABLE II—CONVERSION OF σ/V_R TO q

σ/V_R (range)	q	σ/V_R	q	σ/V_R	q
Over 45	0	2·86–3·36	35	1·17–1·33	70
15 –45	5	2·47–2·86	40	1·01–1·17	75
9·0 –15·0	10	2·18–2·47	45	0·87–1·01	80
6·4 – 9·0	15	1·91–2·18	50	0·72–0·87	85
4·9 – 6·4	20	1·69–1·91	55	0·56–0·72	90
4·03– 4·9	25	1·51–1·69	60	0·40–0·56	95
3·36– 4·03	30	1·33–1·51	65	0·33–0·40	97
				0·25–0·33	98

The relations between q, σ, V_R and V_S are shown graphically in Fig. 3.

To aid in computing frequency tables of wind speed and direction, a series of tables for different values of q was compiled, giving frequencies calculated for steps of 20° of ϕ, the angle which an individual wind vector makes with the resultant direction, and suitable limits of V/V_R. These are given in Appendix IV. In order to construct a wind rose from given values of q and V_R, it is then necessary only to express the limits of the directions and speeds in the rose in terms of ϕ and V/V_R and group or subdivide the frequencies in these tables as necessary. It should be noted that in using Table XXXIII (for $q = 0$) speeds are to be expressed in terms of σ and not V_R; further, since there is no distinction as to direction, the totals for "All directions" can be used, divided by the number of directions required. Frequencies for 20° limits are given for comparison with Tables XXI–XXXII. For general purposes, especially in view of the probable error in the estimate of q or σ, it seems sufficient to calculate q to the nearest 5 per cent. (1–2½ per cent. between 90 and 100 per cent.), and to use the frequency table applicable to this approximate value, or interpolate between the frequency tables on either side.

In compiling the tables it was found that the double integration of (1) was not practicable. It appeared however that, with the number of subdivisions of V/V_R and ϕ adopted (see Appendix IV), a sufficient degree of accuracy could be obtained by substituting for the double integral the expression

$$F = \frac{1}{\pi\sigma^2} e^{-v^2/\sigma^2} \,.\, V \,.\, \delta\phi \,.\, \delta V \quad .. \quad .. \quad (6)$$

which, for intervals of 20°, reduces to

$$\frac{1}{9} \cdot \frac{V_R^2}{\sigma^2} \cdot \frac{V}{V_R} \cdot e^{-v^2/\sigma^2} \cdot \frac{\delta V}{V_R} \quad (7)$$

Expression (7) is computed from the central values of V/V_R and ϕ for any given cell.

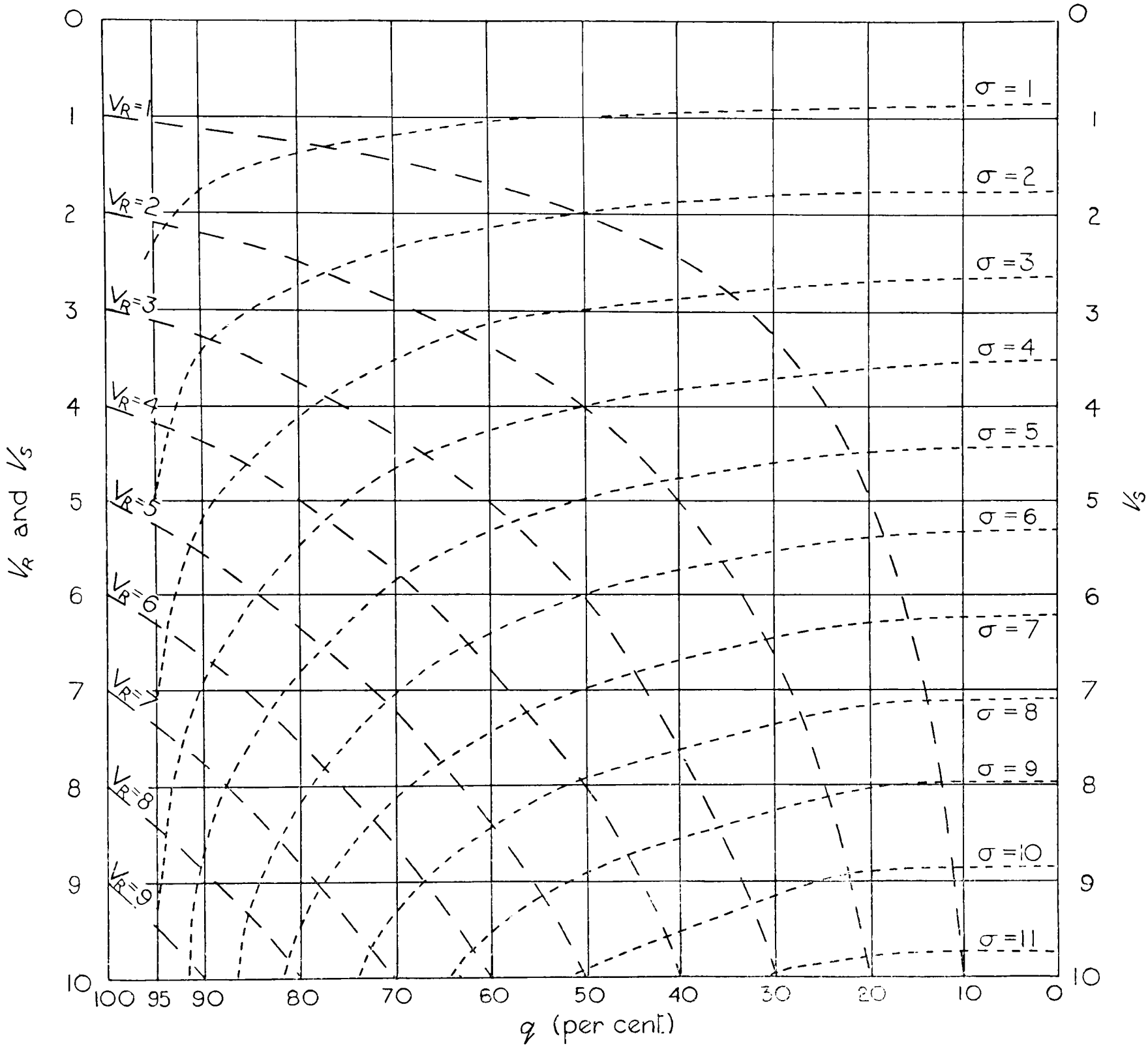

FIG. 3—DIAGRAM SHOWING RELATION BETWEEN q, σ, V_R AND V_S

An example of the calculation.—As an example, the frequency distribution of winds at the 500-mb. level over Larkhill was calculated from March to May using 536 observations for the years 1940–45. The "observed" frequencies (Table III) gave a vector mean of 16·5 kt. from 283° east of north, and a scalar mean of 33·0 kt., so that $q = 50$ and the theoretical frequencies were calculated from Table XXVIII.

The first step is to combine or subdivide the speed groups of Table XXVIII. This is shown in Table IV. The first column gives the divisions between the speed ranges required for the complete summary (in this case those of Table III). The second column gives the ratio of the "dividing" speeds to V_R (in this case 16·5 kt.), so that the speeds are reduced to the units given in the Appendix table. Since in Table XXVIII the ranges of V/V_R are 0·4 in width, V/V_R, in computing the theoretical summary, is expressed to the nearest 0·04 (a tenth of the width

TABLE III—WINDS AT 500 MB. AT LARKHILL

March–May 1940–45, 536 observations, $V_R = 16{\cdot}5$ kt., $q = 50$

Speed	N.	NE.	E.	SE.	S.	SW.	W.	NW.	All directions
kt.									
0–3	..	..	..	..	..	..	..	..	6
3–14	7	8	6	6	7	15	13	7	69
14–27	29	12	11	10	26	29	30	27	174
27–41	20	5	7	4	16	32	43	26	153
41–54	11	5	2	..	2	14	21	19	74
54–68	4	..	..	1	3	3	14	8	33
68–81	4	..	..	..	1	2	4	7	18
81–95	1	..	..	..	..	..	4	4	9
All speeds	76	30	26	21	55	95	129	98	536

TABLE IV—COMPUTATION OF THEORETICAL WIND SUMMARY, STAGES 1 AND 2

$V_R = 16{\cdot}5$ kt. $q = 50$

V	V/V_R*	Ratio of division	Angle between resultant wind direction and individual wind vector (ϕ) 0–20°	20–40°	40–60°	60–80°	80–100°	100–120°	120–140°	140–160°	160–180°	All directions
kt.		0·5	..	..	..	.	..	..	..	..	..	15·0 15·0
3	0·20	0·5	0·9	0·9	0·9	0·9	0·8	0·8	0·8	0·8	0·7	15·0
			6·2 8·1	5·9 7·8	5·6 7·4	5·1 6·8	4·6 6·1	4·2 5·6	3·8 5·1	3·6 4·8	3·5 4·6	85·0 112·6
		0·1	1·0	1·0	0·9	0·8	0·7	0·6	0·5	0·4	0·4	12·6
14	0·84	0·9	9·6	9·0	8·1	7·0	5·9	5·0	4·3	4·0	3·7	113·2
			14·3 25·6	13·2 23·7	11·3 20·6	9·2 17·1	7·4 14·0	5·8 11·3	4·7 9·4	4·1 8·4	3·8 7·8	147·6 275·8
		0·1	1·7	1·5	1·2	0·9	0·7	0·5	0·4	0·3	0·3	15·0
27	1·64	0·9	14·6	13·2	10·9	8·4	6·2	4·6	3·6	3·0	2·6	134·2
			16·3 33·8	14·4 30·1	11·4 24·2	8·3 18·0	5·8 12·9	4·0 9·2	2·9 6·9	2·3 5·6	2·0 4·8	134·8 291·0
		0·2	2·9	2·5	1·9	1·3	0·9	0·6	0·4	0·3	0·2	22·0
41	2·48	0·8	11·8	10·2	7·7	5·3	3·4	2·2	1·5	1·1	1·0	88·4
			12·0 25·6	10·1 21·8	7·3 16·0	4·7 10·6	2·9 6·7	1·8 4·2	1·1 2·7	0·8 2·0	0·7 1·7	82·8 182·6
		0·2	1·8	1·5	1·0	0·6	0·4	0·2	0·1	0·1	..	11·4
54	3·28	0·8	7·0	5·8	4·0	2·5	1·4	0·8	0·5	0·3	0·4	45·4
			6·0 14·1	4·8 11·5	3·2 7·8	1·8 4·6	1·0 2·5	0·5 1·4	0·3 0·8	0·2 0·5	0·2 0·6	36·0 87·6
		0·3	1·1	0·9	0·6	0·3	0·1	0·1	..	..	..	6·2
68	4·12	0·7	2·6	2·0	1·2	0·7	0·4	0·1	0·1	0·1	0·1	14·6
			2·1 5·0	1·6 3·9	1·0 2·3	0·5 1·3	0·2 0·6	0·1 0·2	0·1 0·2	.. 0·1	.. 0·1	11·2 27·4
		0·3	0·3	0·3	0·1	0·1	..	..	..	..	..	1·6
81	4·92	0·7	0·8	0·5	0·4	0·1	0·1	0·1	..	..	..	4·0
			0·5 1·4	0·4 1·0	0·2 0·6	0·1 0·2	0·1 0·2	.. 0·1	.. ..	.. ..	.. ..	2·6 7·0
		0·4	0·1	0·1	..	..	..	..	..	..	..	0·4
95	5·76	0·6	0·1	0·1	0·1	..	..	..	..	..	..	0·6
			0·1 0·2	0·1 0·2	.. 0·1	.. ..	.. ..	.. ..	.. ..	.. ..	.. ..	0·4 1·0
												1000·0

* To nearest 0·04.

of the range). The body of Table IV shows the splitting up and combining of the per mille frequencies of Table XXVIII. For example, for the division at $V/V_R = 0{\cdot}20$, the first line of Table XXVIII is divided in half, 0·5 being included in the " calms " (0–3 kt.) and 0·5 in the speed range 3–14 kt.; for the division at $V/V_R = 0{\cdot}84$, 0·1 of the line for V/V_R between 0·8 and 1·2 is included in the range 3–14 kt. and the remaining 0·9 in the range 14–27 kt. The total " All directions " is expressed to the nearest 0·2 and the sum of the figures along each line, adjusted if necessary, should be exactly half the right-hand total. The central line (in Table IV) of each speed group is compounded of the frequencies of the speed ranges between the divisions for the group. In the group 3–14 kt., for example, the middle line is the line 0·4 – 0·8 of Table XXVIII.

Totals of the cells are given at the right-hand side of each column in Table IV. It is convenient to underline these (stage 2 of the computation). Each of the horizontal lines of underlined figures should add up to half the corresponding frequency (also underlined) in the " All directions " column and the total of this column should be 1000·0.

In the example chosen $q = 50$ so that only one table of the Appendix has been used. If, for example, q had a value between 43 and 47, stages 1 and 2 would be repeated using Table XXIX. For this table, V/V_R (at the divisions between the speed groups) would be expressed to the nearest 0·06 to facilitate computation, *viz.*:—

$V =$	3	14	27	41	54	.....
$V/V_R =$	0·18	0·84	1·62	2·46	3·30	.....

A new table would then be formed such that the frequency in each cell was the mean of the corresponding frequencies underlined (stage 2) for $q = 50$ and $q = 40$. " All directions" frequencies should still be given to the nearest 0·2 and should total 1000·0, and the " throwing " of the means should be arranged so that each " All directions " frequency is exactly twice the sum of the line at the end of which it stands. Up to this stage we are dealing with only half the summary, from $\phi = 0°$ to $\phi = 180°$, because it is symmetrical about $\phi = 0$.

The next step, shown in Table V, is the splitting up and combining of the frequencies for different ranges of ϕ to give the larger direction grouping of (in this case) an eight-point summary. It is sufficient to work to the nearest $2\frac{1}{2}°$ in direction, that is to one-eighth of the range given in each column of Table IV. Thus the direction of the vector mean wind (283° east of north) is taken to be $282\frac{1}{2}°$, distant $77\frac{1}{2}°$ from the centre of the direction group, N. and the frequencies for N. are therefore those lying between $\phi = 55°$ and $\phi = 100°$. Similarly those for NE. lie between $\phi = 100°$ and $\phi = 145°$. Divisions are made at 55°, 100°, 145°, . . . in much the same way as for the speeds in stage 1 (Table IV). The division at 55°, for example, is made by throwing one-quarter of the column 40–60° of Table IV into the group for N. and the remaining

TABLE V—COMPUTATION OF THEORETICAL SUMMARY, STAGE 3

Resultant direction = 283° east of north (taken as $282\frac{1}{2}°$)

V	N.		NE.		E.			SE.			S.		SW.		W.			NW.		
	55°		100°		145° – 180° – 170°			125°			80°		35°		– 0° –		10°			55°
kt.		½		½	¾		½	½		¾	¼			¼	¾		½	½		¾
3–14	1·9	12·9	10·7	1·2	3·6	4·6	2·3	2·3	4·8	3·8	1·3	11·7	14·2	1·9	5·9	8·1	4·1	4·0	7·8	5·5
14–27	5·1	31·1	20·7	2·1	6·3	7·8	3·9	3·9	8·4	7·1	2·3	25·3	37·7	5·9	17·8	25·6	12·8	12·8	23·7	15·5
27–41	6·1	30·9	16·1	1·4	4·2	4·8	2·4	2·4	5·6	5·2	1·7	22·1	42·2	7·5	22·6	33·8	16·9	16·9	30·1	18·1
41–54	4·0	17·3	6·9	0·5	1·5	1·7	0·9	0·8	2·0	2·0	0·7	10·9	26·6	5·5	16·3	25·6	12·8	12·8	21·8	12·0
54–68	1·9	7·1	2·2	0·1	0·4	0·6	0·3	0·3	0·5	0·6	0·2	3·9	12·4	2·9	8·6	14·1	7·1	7·0	11·5	5·9
68–81	0·6	1·9	0·4	..	0·1	0·1	0·1	..	0·1	0·1	0·1	0·8	3·6	1·0	2·9	5·0	2·5	2·5	3·9	1·7
81–95	0·1	0·4	0·1	..	..	..		..	..		..	0·3	0·8	0·3	0·7	1·4	0·7	0·7	1·0	0·5
Over 95	..	..	..	..	..	..		..	..		..	..	0·1	0·1	0·1	0·2	0·1	0·1	0·2	0·1
	19·7			5·3	16·1				18·8		6·3			25·1	74·9					59·3

TABLE VI—COMPUTATION OF THEORETICAL SUMMARY, STAGE 4

V	N.	NE.	E.	SE.	S.	SW.	W.	NW.	All directions
kt.				*frequencies per mille*					
0–3	..	..	..	..	..	..	..	..	15·0
3–14	14·8	11·9	10·5	10·9	13·0	16·1	18·1	17·3	112·6
14–27	36·2	22·8	18·0	19·4	27·6	43·6	56·2	52·0	275·8
27–41	37·0	17·5	11·4	13·2	23·8	49·7	73·3	65·1	291·0
41–54	21·3	7·4	4·1	4·8	11·6	32·1	54·7	46·6	182·6
54–68	9·0	2·3	1·3	1·4	4·1	15·3	29·8	24·4	87·6
68–81	2·5	0·4	0·3	0·2	0·9	4·6	10·4	8·1	27·4
81–95	0·5	0·1	..	..	0·3	1·1	2·8	2·2	7·0
Over 95	..	..	..	..	..	0·2	0·4	0·4	1·0
All speeds	121·3	62·4	45·6	49·9	81·3	162·7	245·7	216·1	1000·0

TABLE VII—COMPARISON OF COMPUTED FREQUENCIES WITH OBSERVED FREQUENCIES

Larkhill, March–May, 1940–45, 536 observations

Vector mean wind : resultant direction = 283°, speed = 16·5 kt. ; constancy (q) = 50

The observed frequencies are given in brackets

V	N.	NE.	E.	SE.	S.	SW.	W.	NW.	All directions
kt.				*per cent.*					
0–3	..	..	..	..	..	..	..	..	1·5 (1·1)
3–14	1·5 (1·3)	1·2 (1·5)	1·1 (1·1)	1·1 (1·1)	1·3 (1·3)	1·6 (3)	1·8 (2)	1·7 (1·3)	11 (13)
14–27	4 (5)	2 (2)	1·8 (2)	1·9 (1·9)	3 (5)	4 (5)	6 (6)	5 (5)	28 (32)
27–41	4 (4)	2 (0·9)	1·1 (1·3)	1·3 (0·7)	2 (3)	5 (6)	7 (8)	6 (5)	29 (29)
41–54	2 (2)	0·7 (0·9)	0·4 (0·4)	0·5 (0·0)	1·2 (0·4)	3 (3)	5 (4)	5 (3)	18 (14)
54–68	0·9 (0·7)	0·2	0·1	0·1 (0·2)	0·4 (0·6)	1·5 (0·6)	3 (2)	3 (1·5)	9 (6)
68–81	0·3 (0·7)	..	..	..	0·1 (0·2)	0·5 (0·4)	1·0 (0·8)	0·8 (1·3)	3 (3)
81–95	0·1 (0·2)	..	..	..	..	0·1	0·3 (0·8)	0·2 (0·7)	0·7 (1·7)
All speeds	13 (14)	6 (5)	5 (5)	5 (4)	8 (11)	16 (18)	24 (24)	22 (18)	100 (100)

three-quarters into the group for NW. It is useful to sum the two portions of each column divided in this way and check that they are in the correct ratio. For the division at 55° the sum, 19·7, is nearly one-third of the other sum, 59·3. For an eight- or sixteen-point summary, it is preferable to work in eighths, since the range for each direction point is a multiple of $2\frac{1}{2}°$; otherwise however, as for example for units of ten degrees of direction, tenths are simpler.

Stage 3 is reasonably simple, but care must be taken to see that the components of any division are thrown into the correct direction groups especially near $\phi = 0°$ and $\phi = 180°$. In group N., the column commencing with 12·9 is the sum of columns 60–80° and 80–100° of Table IV; no splitting up is required at 100° (in this example). The column, starting 10·7, of NE. is composed of the columns 100–120° and 120–140°, and then a division must be made at 145° throwing one-quarter to NE. and three-quarters to E. The next division occurs at 170°, but, although this is in the column 160–180°, the whole of the column (160–180°) also must be inserted in E. to make up the 45 degrees of direction:—

15 degrees from column 140–160°
20 degrees from column 160–180°
and a further 10 degrees from column 160–180°.

Since each direction group (for an eight-point summary) is composed of 45 degrees, the columns of stage 2 (Table IV) each occur twice (whole or divided) in stage 3 (Table V), and so when the

components of the frequency cells have been totalled as in stage 4 (Table VI) the sums of the lines will equal the totals ("All directions") at the ends.

Table VI gives the theoretical frequencies per mille according to the cell divisions required. The particular arrangement of cells adopted in this example is for comparison with the given summary of observations in Table III. The frequencies, however, are not correct to 0·1 per mille as given in the table. The reason for retaining all the digits is solely for ease in checking. Percentage frequencies (derived from Table VI) are given in Table VII with the "observed" values (derived from Table III) for comparison. These have been adjusted slightly so that the "rounded off" figures agree with the totals.

The magnitude of variations about the vector mean wind.—It is sometimes convenient to have, in addition to the conventional wind rose, a measure of the range of variation about the vector mean wind, *i.e.* of the vector differences between the individual winds and the vector mean wind. This is given by the radii of the circles which enclose various proportions of the total number of observations. These radii, in terms of σ, are given in Table VIII.

TABLE VIII—RADII OF CIRCLES WHICH CONTAIN SPECIFIED PROPORTIONS OF THE END POINTS OF THE VECTORS

Percentage proportion of observations (100γ)	25	50	75	80	85	90	95
Radius / [standard vector deviation (σ)]	0·54	0·83	1·18	1·27	1·38	1·52	1·73

The values in the lower line of Table VIII are computed from the expression $\sqrt{[\log_e\{1/(1-\gamma)\}]}$. The mean vector departure from the resultant is $\frac{1}{2}\sigma\sqrt{\pi} = 0{\cdot}89\sigma$.

PART II—SEASONAL CHARTS OF MEAN HEIGHTS OF ISOBARIC SURFACES

§ 3—GENERAL

We have shown that one of the two parameters required for the estimation of a wind rose is the vector mean wind $\mathbf{V}_R$. For latitudes outside the tropics, this can be obtained by the geostrophic relation from charts of the mean pressure at various heights, or, in the more modern manner, from charts of contours of absolute topography of pressure. Since the dynamical equations of atmospheric motion are non-linear, the mean motion cannot be deduced exactly from the mean pressure distribution. Mr. A. F. Crossley has deduced that the use of the geostrophic relation on the charts of mean contours requires a correction but this is not likely to exceed 3 kt. The uncertainty in reading the contours is greater than this, and so the geostrophic wind measured from the mean contours is sufficiently accurate.

As the equator is approached the reliability of the method decreases, and in this work it was considered that the limiting latitudes for the use of the geostrophic relation were 25° N. and 25° S. Seasonal charts of contours were accordingly constructed for the required levels, and in addition, for the intertropical zone, charts of stream-lines and isopleths of vector mean speed.

§ 4—DATA USED

The data used to produce the charts of mean seasonal contours consisted of published values of results of sounding-balloon, radio-sonde and aircraft ascents, daily charts of contours of the 500-mb. and 300-mb. surfaces, values computed from surface data of pressure and temperature, and vector mean winds which indicate approximately the direction and magnitude of the pressure gradient.

Upper air soundings.—All available data were assembled.* For Europe they were mainly long-period averages based on sounding-balloon ascents. For the U.S.A. results of radio-sonde ascents for about three years (1941–43) were used. Monthly summaries of aircraft ascents at British overseas stations and of American radio-sonde ascents at stations in west Africa covered periods of about two years. For other regions data were generally scanty.

Most of the published data gave monthly averages of temperature at kilometre heights. These were first combined into seasonal averages, and the thicknesses of the layers of air were computed for steps of 50 mb. Where the data included pressures at geometric or geodynamic heights, the height of the required pressure level was found by logarithmic interpolation.

Daily charts of contours.—Average heights of the 500-mb. and 300-mb. levels were computed from daily upper air charts drawn in the Meteorological Office for two to three years. For the 500-mb. level there were two sets covering the areas 30–70°N., 30°E. westwards to the United States, and 30–40°N., 10°W.–50°E. For the 300-mb. level the area covered was 30–70°N., 30°E.–40°W.

Heights computed from surface observations.—Over large parts of the world, including all the oceans except the North Atlantic, the upper air data were quite insufficient and had to be supplemented by extrapolation from surface data. Seasonal mean values of surface pressure and temperature were found for land stations; values for the oceans were read from the monthly charts of the oceans. The lapse rate was assumed to be 1·5°C./1,000 ft. from the surface to 700 mb., and 1·8°C./1,000 ft. from 700 to 500 mb. A table was constructed to give the height of the 700-mb. level. It is easily shown that this is given by the relation

$$Z_{700} = \frac{T_0}{\beta}\left[1 - \left(\frac{p}{p_0}\right)^{R\beta/g}\right] \quad .. \quad .. \quad (8)$$

where Z_{700} is the height of the 700-mb. level in dynamic units, T_0 and p_0 the temperature and pressure at the surface, R the gas constant, g the value of gravity and β the lapse rate; in this instance $p = 700$ mb. The small corrections required to convert from dynamic to geometric heights were also tabulated.

Another table gave the height difference between 700 and 500 mb. in terms of surface temperature.

Above the 500-mb. level, over land areas, the surface temperatures were not regarded as a sufficiently reliable guide to the upper air temperature and charts of T_{500} were constructed from the available upper air observations. Over the oceans the data were insufficient and the surface temperatures had to be used; the relation adopted was

$$T_{500} = T_0 - 1{\cdot}65\, Z_{500} \quad .. \quad .. \quad (9)$$

where temperatures are in degrees Centigrade and Z_{500} is the height of the 500-mb. level in thousands of feet.

The mean temperature of the layer between 500 mb. and 300 mb. can be expressed in terms of the temperature at 500 mb. and the height of the tropopause, and a table was constructed for these two factors. Charts of the seasonal mean heights of the tropopause were specially drawn for this purpose.

The thicknesses of the layers 300–200 mb. and 200–130 mb. were calculated in the same way, using charts of seasonal mean temperature at the 300-mb. and 200-mb. levels. The details of the calculation are given in Appendix I.

The heights of the various pressure levels calculated in this way agreed reasonably well with those obtained directly from upper air ascents. A correction chart was constructed from the differences between the observed and computed levels where observations were available, and modifications by analogy were made over the remaining parts of the world.

* Bibliography Nos. 7–8, 14, 16–29, 31–2, 34, 37–8, 50–1, 56, 59–60, 67, 69–70.

Vector mean winds.—The relation between pressure gradient and wind at any level being known, the direction and magnitude of the gradient could be calculated at any point where the vector mean wind was known. The resultant winds obtained in the calculation of values of the standard vector deviation σ (see Part III of this paper) were accordingly plotted on the charts, arrows showing the direction of the contour lines and broken lines at right angles showing the distance apart of the contour lines appropriate to the speed.

§ 5—SOUTHERN HEMISPHERE

Over the southern hemisphere the contours for the 200-mb. level have been omitted. Tentative charts were drawn but these had to be produced almost entirely by analogy with the northern hemisphere as data for the southern hemisphere was almost non-existent. It was not considered justifiable to publish them.

§ 6—DETAILS OF CONSTRUCTION OF THE CHARTS

700-mb. and 500-mb. charts.—The procedure adopted for these two levels was practically the same. Three charts were drawn for each level and each season. The first of these was a chart of corrections to be applied to the heights computed from surface values. Differences between actual observations and values computed from surface pressure and temperature for places for which both values had been obtained were plotted as positive or negative according to whether the observed height was greater or less than the computed height. This gave about 80 correction points and enabled correction lines to be drawn with a fair degree of confidence over much of the northern hemisphere. Over regions where there was little guidance, the lines were drawn by analogy with corresponding regions for which information was available. As a general rule more weight was given to long-period values than to short-period values as it was considered that a fair number of observations spread over a period of 10 years or more gave a better indication of the normal value than a larger number of daily observations for a period of only 2 or 3 years.

Correction lines to the computed heights over the oceans were more difficult to assess than those over land areas. Small-scale seasonal charts of differences over the North Atlantic were drawn and studied in the hope that they would give guiding principles which could be applied to the other ocean areas. Certain features such as large positive corrections over cold currents were evident but all differences could not be satisfactorily accounted for, and it was finally decided to adopt one correction chart for all seasons, all major corrections being embodied in this. These ocean lines were transferred to the large charts, adjustments being made where necessary to fit in with land values, and corrections to other ocean areas completed by analogy with those for the North Atlantic.

The correction lines were transferred to a tracing-paper working chart, blue lines being used for positive corrections and red for negative. On a third chart were plotted all the heights estimated from surface data; using these heights pencil contour lines were drawn at 200-ft. intervals and then traced on to the working chart. The corrections were added graphically to these contour lines by drawing green lines through the intersections of appropriate lines. The pencil lines on the third chart having been rubbed out, the green lines from the working chart were traced on to it. Observed heights were then entered on this final chart together with all vector mean winds available, and the contours finally smoothed to remove kinks introduced during the process of graphical addition and to give the best possible fit to the data.

300-mb. charts.—These charts were constructed in three stages. Temperatures at 500 mb. over the oceans were computed as described using the lapse rates given in §4, p. 10 and plotted on

a working chart, positive values in black, negative in red, together with differences between 500-mb. and 300-mb. heights over land areas obtained from observations at a number of stations. These were entered in red in units of 1,000 ft. By referring to the tropopause charts and the tables of thicknesses of the 500–300-mb. layer, an estimate of the height of the 300-mb. surface above the 500-mb. was obtained to the nearest ten feet and entered in green ink near the appropriate temperature. Thickness isopleths were then drawn. The 500-mb. contours were traced on a second working chart in red ink together with these thickness isopleths in green ink, and rough 300-mb. contours obtained by graphical addition. These contours were then traced in pencil on a final sheet on which were entered all available values of observed height and vector mean winds. It was found that the general agreement between the rough contours obtained in this way and the observed values was satisfactory, though over the North Atlantic they appeared to be about 200 ft. too high. This discrepancy was investigated and appeared to be due to the use of a constant lapse rate, whereas average values for different latitudes showed a slight increase in lapse with increasing latitude. It was decided to allow for this by adjusting the lines to fit the observed values and making a corresponding adjustment in the southern hemisphere.

Owing to the very scanty observations for the Arctic regions and Siberia it was not possible to draw contours with much confidence in this area, and the distortion introduced by Mercator's projection tended to give a false impression of the run of the lines. There were also inconsistencies between heights obtained for Russian stations in the Arctic, and it was difficult to decide which to accept. Observations north of about 50° N. were therefore plotted on small circumpolar maps to give a better picture of this region. Having decided upon the best drawing for the most northerly lines, this presentation was transferred to the Mercator charts and used to fix the lines over Siberia.

200-mb. and 130-mb. charts.—The method of drawing both the 200-mb. and 130-mb. charts (northern hemisphere) was similar to that for the 300-mb. charts so it is unnecessary to give full details.

The charts of contours for 700, 500, 300, 200 and 130 mb. obtained in this way are reproduced on pp. 58–97.

§ 7—ACCURACY OF THE CHARTS

These contour lines of isobaric surfaces over the world are inevitably based on somewhat inadequate data. It is considered that they can be used with a fair degree of confidence over Europe, the Atlantic and North America. They are regarded as rather uncertain over Siberia and the Aleutian Islands and over South America, South Africa and the Southern Ocean south of about 40° S. Over the rest of the world they should be fairly reliable at the two lowest levels, but it will be evident that the uncertainty increases with height, and this is particularly the case in the southern hemisphere. For the 700- and 500-mb. charts, some distinction has been made in the relative reliability of the lines. In high northern latitudes where the course of the lines is very uncertain they are shown as broken lines.

§ 8—MEASUREMENT OF VECTOR MEAN WINDS FROM THE CHARTS

The lines show the height above mean sea level of the appropriate isobaric surface, figures giving height in hundreds of feet.

The direction of the vector mean wind, assumed geostrophic, at any place is given by the direction of the contour lines; in the northern hemisphere the wind is directed counter-clockwise round the regions where the height is low, in the southern hemisphere, clockwise. The speed of the vector mean wind is given by the distance apart of the contours. It has been found better to measure the distance apart of the lines and then read off the corresponding speed from a table than to use a scale for measuring speeds directly from the chart. Table IX gives, for various

latitudes, the wind speed (in knots) for different distances apart (in centimetres) of successive 200-ft. contours on a chart of scale 1 : $1 \cdot 151 \times 10^8$ at the equator. If a measurement is made using 100-ft. intervals the speed derived from the table should be halved. For intermediate latitudes or distances it will be sufficiently accurate to obtain the required value by linear interpolation. For a given latitude, speeds are inversely proportional to the distance between lines, hence a value not shown in the table may be obtained by finding a suitable sub-multiple of the required distance and dividing the speed given for this sub-multiple by the appropriate factor, *e.g.* if a value is required for 3·0 cm. in latitude 75° N. a suitable sub-multiple is 1·0 cm., the corresponding speed, 27 kt., divided by the factor 3 gives 9 kt. as the required value.

Owing to minor irregularities in the drawing of the lines, it is often better to make measurement embrace the adjacent lines and take a mean value provided this does not smooth out an obviously real change in the spacing of the lines.

Table IX is applicable to charts for any pressure level, provided they are on Mercator's projection of the same scale. The figures in the first column have been adjusted to fit the reduced scale of the charts published in this memoir.

TABLE IX—MEAN VECTOR WIND IN RELATION TO THE DISTANCE APART OF SUCCESSIVE 200-FT. CONTOUR LINES

Scale of chart $1 \cdot 151 \times 10^8$	Latitude N. or S.*									
	75°	70°	68°	66°	26° 64°	28° 62°	30° 60°	35° 55°	40° 50°	45°
cm.	*knots*									
0·28	97	76	70	66	62	59	56	52	50	49
0·29	94	73	68	63	60	57	54	50	48	47
0·31	90	70	65	61	57	55	52	48	46	45
0·32	87	68	63	59	55	53	50	46	44	44
0·33	84	66	61	57	53	51	49	45	43	42
0·34	81	63	59	55	52	49	45	43	41	41
0·40	70	54	50	47	44	42	40	37	35	35
0·45	61	48	44	41	39	37	35	32	31	30
0·51	54	42	39	37	34	33	31	29	28	27
0·57	49	38	35	33	31	29	28	26	25	24
0·7	41	32	29	27	26	25	23	22	21	20
0·8	35	27	25	23	22	21	20	19	18	17
0·9	30	24	22	21	19	18	18	16	15	15
1·0	27	21	20	18	17	16	16	14	14	14
1·1	24	19	18	16	15	15	14	13	12	12
1·2	22	17	16	15	14	13	13	12	11	11
1·4	20	16	15	14	13	12	12	11	10	10
1·5	19	15	14	13	12	11	11	10	10	9
1·6	17	14	13	12	11	11	10	9	9	9
1·7	16	13	12	11	10	10	9	9	8	8
1·8	15	12	11	10	10	9	9	8	8	8
1·9	14	11	10	10	9	9	8	8	7	7
2·0	13	11	10	9	9	8	8	7	7	7
2·2	13	10	9	9	8	8	7	7	7	6
2·3	12	10	9	8	8	7	7	6	6	6

* Owing to the increase in scale with latitude of the Mercator projection, the wind speed corresponding with a given distance between contours on a Mercator chart is the same for latitude ϕ as for $90°-\phi$, hence the alternative headings to the table. The table should not be used for latitudes below 25°.

PART III—SEASONAL CHARTS OF STANDARD VECTOR DEVIATION

§ 9—GENERAL

Brooks, Durst and Carruthers[4] described methods by which it is comparatively simple to calculate the value of the standard vector deviation σ from the table of frequencies of winds tabulated in a grid of speeds and directions or alternatively from the constancy q which is related to V_R and V_S by the identity $q = 100\ V_R/V_S$. Wind data in the form of elements of wind roses or of vector and scalar mean winds are thus readily reduced to standard vector deviation.

It is to be noted that σ does not in itself depend on the wind distribution being a normal one, and the derivation of σ from a grid of wind frequencies in speeds and directions in no way invalidates the accuracy of σ. The derivation of σ from a value of the constancy is, however, only strictly accurate if the distribution is normal.

§ 10—DATA* AVAILABLE FOR DIRECT COMPUTATION OF σ

Radio and radar observations.—As has already been indicated truly representative summaries of winds are very few. Our best records are the radio-wind observations in the British Isles, and certain of the observations (mainly radar) made by the German Meteorological Service during the war in various parts of Europe which were subsequently summarised in Hamburg.

Of the British stations, Larkhill (51° N., 2° W., 5–6 years), Lerwick (60° N., 1° W., 3–4 years) and Downham Market (52½° N., ½° E., 3 years) were worked in detail, σ being computed for most levels available up to 80 mb. The summaries at the higher levels were tested for normality because it was thought that there might be a bias against strong winds owing to the balloon drifting out of range of the radio direction-finders under such conditions. In general, it seems safe to assume that values of σ up to 130 mb. are substantially correct and show only random errors. In testing for normality, the frequency distribution of speeds for each set of data was compared with the theoretical frequency distribution, given by the same values of q and V_R, deduced from the "All directions" column of the appropriate table in Appendix IV. The chi-square test was applied to see whether the discrepancies were only such as might be expected to arise by reason of the paucity of the observations.

The German data have been summarised in groups of ascents according to location. Group 3, for instance, comprised all ascents in the neighbourhood of Trondhjem and is considered to apply to the approximate mean position 63° N., 9° E. Of these groups, as many as were available were used at the time of drawing up the chart of σ for any particular level. They vary considerably as to the length of the period of the observations and as to the heights attained. For the 700-mb. chart 14 groups were used, for the 500-mb. 17, for the 300-mb. 21, and only five gave data (and these, for the most part, extrapolated) for the 130-mb. chart.

Pilot-balloon observations.—These exist in large numbers, but are subject to bias for two reasons :—

(i) Even in clear weather the visual range of a pilot balloon is limited, and with strong winds a balloon is likely to disappear in the distance. There is a high correlation between the wind in successive layers of the atmosphere, and hence the winds most likely to be lost are those with the higher speeds.

(ii) In cloudy weather the balloon disappears into the cloud and may be lost at a low height. In many places cloud amount is correlated with wind direction and a summary of pilot-balloon observations may give an entirely false impression of the winds at heights of 10,000 ft. and upwards.

Methods of making the best use of these biassed observations were worked out and are described below.

* Bibliography Nos. 11–13, 15, 35–6, 39–41, 45–7, 52–5, 57, 61–3, 65–6.

The correction of pilot-balloon observations.—With so few radio-wind and radar data available it was of prime importance that every use should be made of summaries of pilot-balloon observations. To do this it was necessary to " complete " the missing observations which had been lost through the disappearance at a lower level of the balloons in distance, haze or cloud. The problem was tackled by two of us, Brooks and Carruthers, and since it may be a matter of considerable interest in other fields the discussion is given in full in Appendix II.

Broadly the method adopted is to consider from the laws of chance the most likely wind values on occasions when the balloon was (*a*) lost in the distance, (*b*) lost in haze and (*c*) lost in cloud. Occasions when the balloon burst or was lost in the sun, or the ascent was abandoned for other reasons, were considered to be casual losses which were irrelevant to the problem.

Certain representative stations in various parts of the world were examined. Table X gives the percentage frequency with which pilot balloons were lost from different causes below certain heights.

TABLE X—PERCENTAGE OF ASCENTS LOST BELOW GIVEN HEIGHTS

R = Random, C = in cloud, D = in distance or haze

Height	Addu Atoll			Reykjavik			Akureyri			Lisbon			Khartoum		
	R	C	D	R	C	D	R	C	D	R	C	D	R	C	D
ft.	*per cent.*														
40,000	83	15	2	26	55	19	23	41	36	52	29	16	66	9	25
30,000	82	15	1	26	55	19	22	41	34	45	29	15	66	9	25
20,000	78	14	0	24	55	19	17	41	24	29	29	11	63	9	24
10,000	50	14	0	10	50	7	7	24	5	6	21	4	32	4	13
5,000	13	4	0	4	30	1	0	6	0	2	8	1	6	1	2
3,000	2	1	0	2	11	0	0	0	0	1	1	0	2	1	1
No of ascents	1,000			609			83			373			623		

This table brings out how in the dusty atmosphere of Khartoum the losses at 10,000 ft. are mainly due to distance, whereas at Reykjavik cloud limits the height to less than 5,000 ft. on many occasions.

If all the balloons were lost in distance or haze or from purely random causes it would be possible to deduce from these figures how many balloons would have been observed at each height had there been no limitations imposed by strong winds and haze. Ignoring those lost in cloud, the number (N) of balloons, which should have been followed to certain heights had there been none lost in strong winds and haze, has been expressed as a ratio of the actual number (n) observed at those heights (see Appendix II). At Addu Atoll the ratio was found to be 1·01 at 10,000 ft., 1·04 at 20,000 ft. and 1·2 at 30,000 ft.; at Khartoum where haze is troublesome the corresponding figures were 1·2, 3 and 5. This gives a measure of the problem that has to be faced.

In regions of clear skies the problem can be solved by trial and error on the assumption that the distribution of winds when " completed " will be a " normal " circular distribution. A worked example is set out in Appendix II. The general experience is that at 700 mb. (10,000 ft.) losses in the distance are usually negligible, and in clear regions the available pilot-balloon summaries for this level have been taken as fair samples. In more cloudy regions the method of completion could not be applied except with extreme caution.

Other data.—A few wind summaries based on estimates during aircraft flights across the Indian Ocean were available. The station at Eismitte in central Greenland lies at a height of about 10,000 ft and was used, with a correction for friction, for the 700-mb. level, but mountain stations in general proved unsatisfactory owing to eddies.

§ 11—ESTIMATES OF σ OVER THE OCEANS

Over the oceans pilot-balloon results are of doubtful use even at 700 mb. owing to cloud, and at 500 mb. values of σ from such sources have been found to be consistently too low. The only regular wind data for the oceans were geostrophic winds measured from contour charts at 500 mb. The measurements made at 39 points covering the area from 35° to 60° N. and from 110° W. to 30° E. were summarised in seasons for the period June 1943–May 1945, and values of σ were calculated and plotted. It was at once apparent that these contour charts suffered from a lack of observations in mid ocean so that there was a tendency for σ to be too low over the centre of the ocean. With the help of Mr. C. H. B. Priestley, who was intimate with the day-to-day preparation of the original charts, the values were rectified. Account was taken of the knowledge possessed of the tracks of depressions and the positions of the polar and arctic fronts. Later the values of σ were modified to agree with values computed subsequently from observations over land stations in the area. In this way the best estimates practicable were obtained and the correlations described below were computed.

The main problem was that of estimating by analogy with the North Atlantic, the distribution of σ at 500 mb. over the remaining oceans of the world. The most promising data for comparison were the summaries of "surface" winds used in the construction of ocean charts prepared by the Marine Branch of the Meteorological Office, and so values of σ were computed from these, and charts were drawn of the distribution of the standard vector deviation of "surface" winds over all the oceans between 65° N. and 45° S.

Close to the coasts, the values of "surface" σ decrease very rapidly owing to the frictional effect of the land which causes a general decrease in wind speeds, but in mid ocean, a high correlation was found between σ at 500 mb. and σ at the "surface". After several trials, it was decided to estimate σ at 500 mb. by means of the regression on "surface" σ and mean surface pressure. Taking 35 points in the North Atlantic at 10-degree intervals of longitude and 5-degree intervals of latitude from 20° N. to 60° N. (omitting points near the coasts), the following results were obtained:—

TABLE XI—CORRELATION OF σ AT 500 MB. WITH SURFACE σ AND SURFACE PRESSURE OVER THE NORTH ATLANTIC

σ_{500} (kt.) = standard vector deviation at 500 mb.
σ_0 (kt.) = standard vector deviation at the surface.
p (mb.) = excess of mean surface pressure over 1,000 mb.
$r_{\sigma_{500}\,\sigma_0}$ = correlation coefficient between σ_{500} and σ_0.
$r_{\sigma_{500}\,\sigma_0 \cdot p}$ = partial correlation coefficient between σ_{500} and σ_0 with the effect of variation of p eliminated.

		Dec.–Feb.	Mar.–May	June–Aug.	Sept.–Nov.
Total correlation:	$r_{\sigma_{500}\,\sigma_0}$	+·93	+·97	+·96	+·91
	$r_{\sigma_{500}\,p}$	−·85	−·84	−·78	−·71
	$r_{\sigma_0\,p}$	−·68	−·83	−·82	−·62
Partial correlations:	$r_{\sigma_{500}\,\sigma_0 \cdot p}$	+·92	+·91	+·91	+·85
	$r_{\sigma_{500}\,p.\sigma_0}$	−·81	−·31	+·09	−·46

Admittedly there is no immediately apparent physical reason why σ at 500 mb. should be correlated with surface pressure. The coefficients, however, are certainly significant, and the regression equations can reasonably be used for estimating σ_{500} although, for the time being, they must be regarded as empirical. These equations are as follows:—

North Atlantic

$$\left.\begin{aligned}
&\text{Winter (December–February)} && \sigma_{500} = 1{\cdot}42\,\sigma_0 - 0{\cdot}44\,p + 13{\cdot}6\\
&\text{Spring (March–May)} && \sigma_{500} = 1{\cdot}40\,\sigma_0 - 0{\cdot}20\,p + 13{\cdot}0\\
&\text{Summer (June–August)} && \sigma_{500} = 1{\cdot}64\,\sigma_0 + 2{\cdot}3\\
&\text{Autumn (September–November)} && \sigma_{500} = 1{\cdot}28\,\sigma_0 - 0{\cdot}32\,p + 13{\cdot}8
\end{aligned}\right\} \quad .. \quad .. \quad (10)$$

These were taken to apply to all oceans in latitudes of not less than 20° for the seasons specified on the left-hand side. The first equation, for example, refers to December–February north of the equator and June–August south of the equator. For the equator and latitudes 10° N. and 10° S., alternative methods of estimation were tried:

(*a*) The values at the equator were taken as the mean between opposite seasons *viz.*:—

$$\left.\begin{aligned}
&\text{December–February and June–August} && \sigma_{500} = 1{\cdot}53\,\sigma_0 - {\cdot}22\,p + 8{\cdot}0\\
&\text{March–May and September–November} && \sigma_{500} = 1{\cdot}34\,\sigma_0 - {\cdot}26\,p + 13{\cdot}4
\end{aligned}\right\} \quad .. \quad .. \quad (11)$$

and those at 10° N. and 10° S. as given by equations intermediate between these and the appropriate equations for higher latitudes.

(*b*) The equations for latitude 10° were deduced directly from the total correlation of σ_{500} with σ_0 with the following results.

$$\left.\begin{aligned}
&\text{Winter} && \sigma_{500} = 1{\cdot}98\,\sigma_0 - 3{\cdot}0\\
&\text{Spring} && \sigma_{500} = 1{\cdot}57\,\sigma_0 + 7{\cdot}1\\
&\text{Summer (as before)} && \sigma_{500} = 1{\cdot}64\,\sigma_0 + 2{\cdot}3\\
&\text{Autumn} && \sigma_{500} = 1{\cdot}54\,\sigma_0 + 4{\cdot}9
\end{aligned}\right\} \quad .. \quad .. \quad (12)$$

ɔns for the equator were then given by the means of these equations for opposite

The decision as to which method was preferable was based upon the goodness of fit with the Australian values for Port Moresby and Darwin, both sets of results (at 10-degree intervals of longitude) having been plotted on the working charts. It was found that method (*a*) gave the best fit for June–August and December–February and method (*b*) for September–November and March–May. Since σ at 700 mb. did not differ greatly from σ at 500 mb. in September–November and March–May, values for 700 mb. (*see* § 12) for all seasons were based upon the larger values, *i.e.* upon method (*a*).

§ 12—VARIATION OF σ WITH HEIGHT

It was early realised that over the British Isles $\sigma\rho$ is practically constant with height up to some point near the tropopause, and subsequent investigation suggested that the same law holds for other parts of the world. In the range of height covered by the oscillations of the tropopause there is a decrease in σ, and above this it is suspected that σ remains approximately constant with height for any particular station.

To simplify the extrapolation of σ, the convention was adopted of representing the variation of σ by three straight lines on a diagram in which σ is plotted against T/P or $1/\rho$. In this and subsequent sections a standard pressure level is indicated by P.

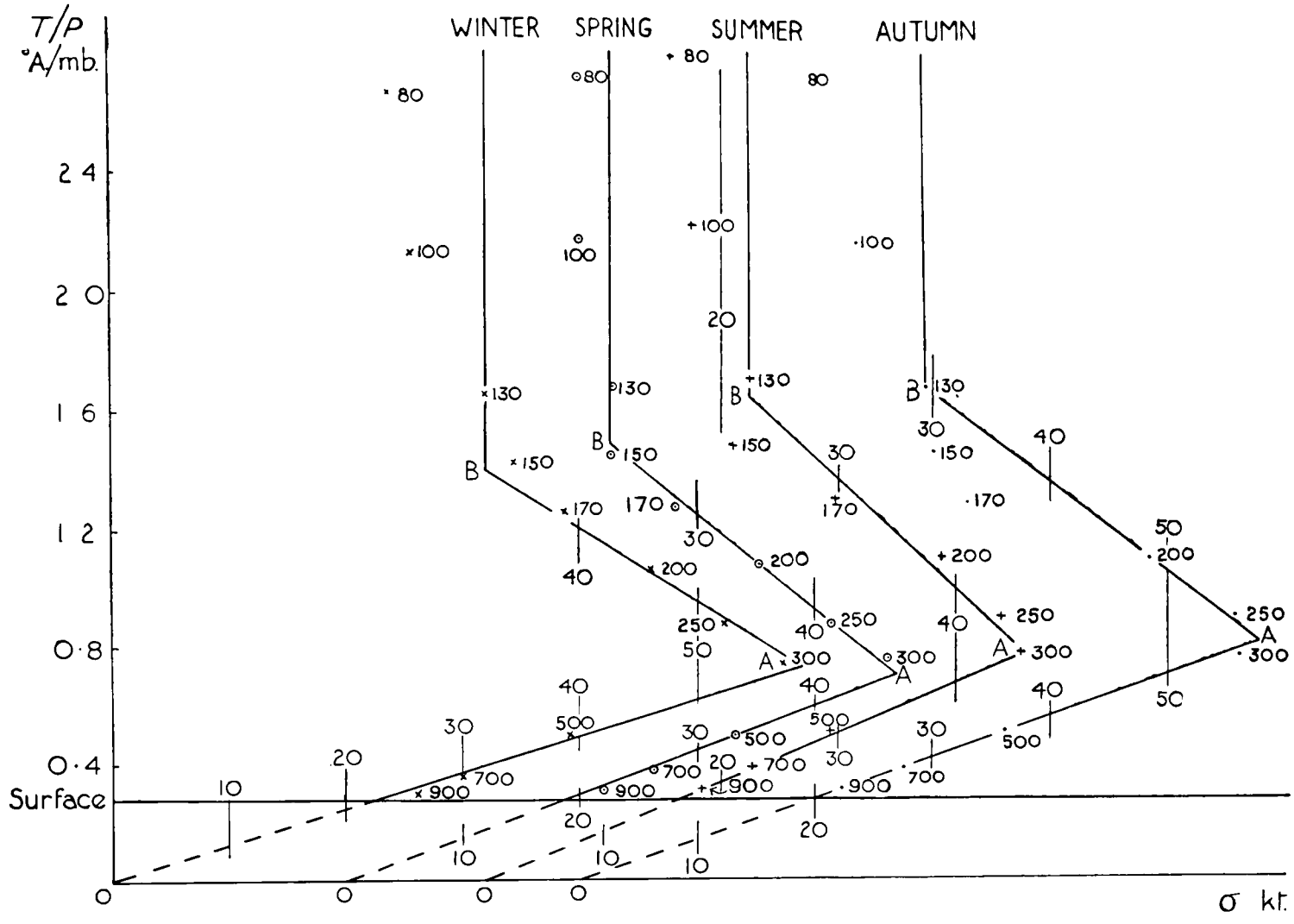

Larkhill (51° N., 2° W.)

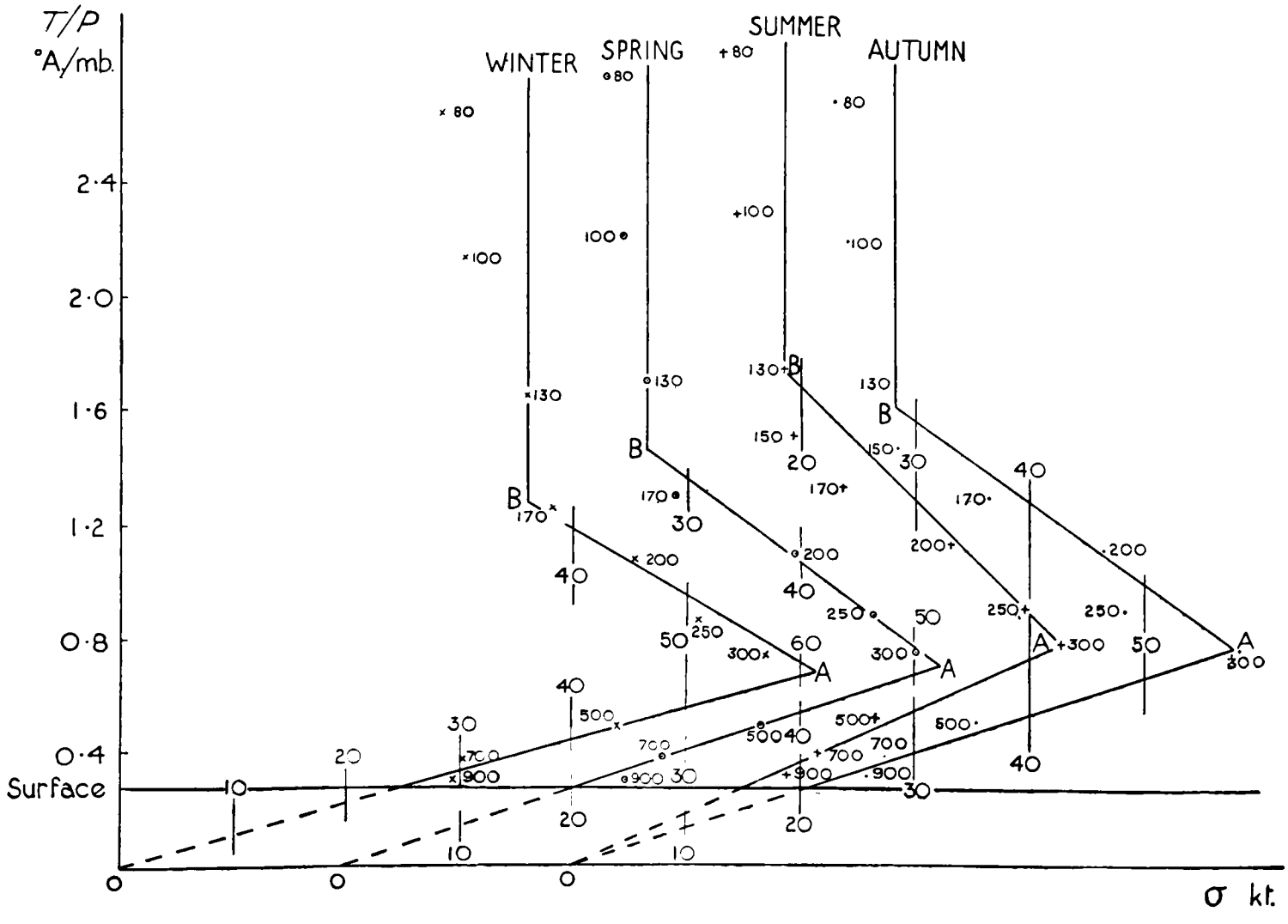

Lerwick (60° N., 1° W.)

FIG. 4—VARIATION OF σ WITH HEIGHT OVER LARKHILL AND LERWICK
Small figures denote pressure in millibars. Horizontal scale: σ in knots

Figs. 4–7 show the variation of σ with height in temperate latitudes. Fig. 4 is from radio-wind observations over Larkhill and Lerwick and Figs. 5 and 6 from the two German groups of radar ascents for which most observations were available. For each graph, the abscissa gives the value of σ in knots; in Figs. 4–6 the scale is shifted in successive seasons to allow all four seasons to be shown on the same diagram. The ordinate is the ratio of the mean temperature in degrees absolute to the mean pressure in millibars, *i.e.* it is very nearly proportional to the reciprocal of the air density. In Fig. 7, which shows the variation of σ at Mahlsdorf (Berlin) for the year as a whole, since actual values of mean density were available, the ordinate used is the reciprocal of the density expressed in grams per cubic decimetre. Small figures by the plotted points indicate either pressure in millibars or height in kilometres.

The seasons each refer to three months of the year; "Winter" is December–February; "Spring", March–May; "Summer", June–August; "Autumn", September–November.

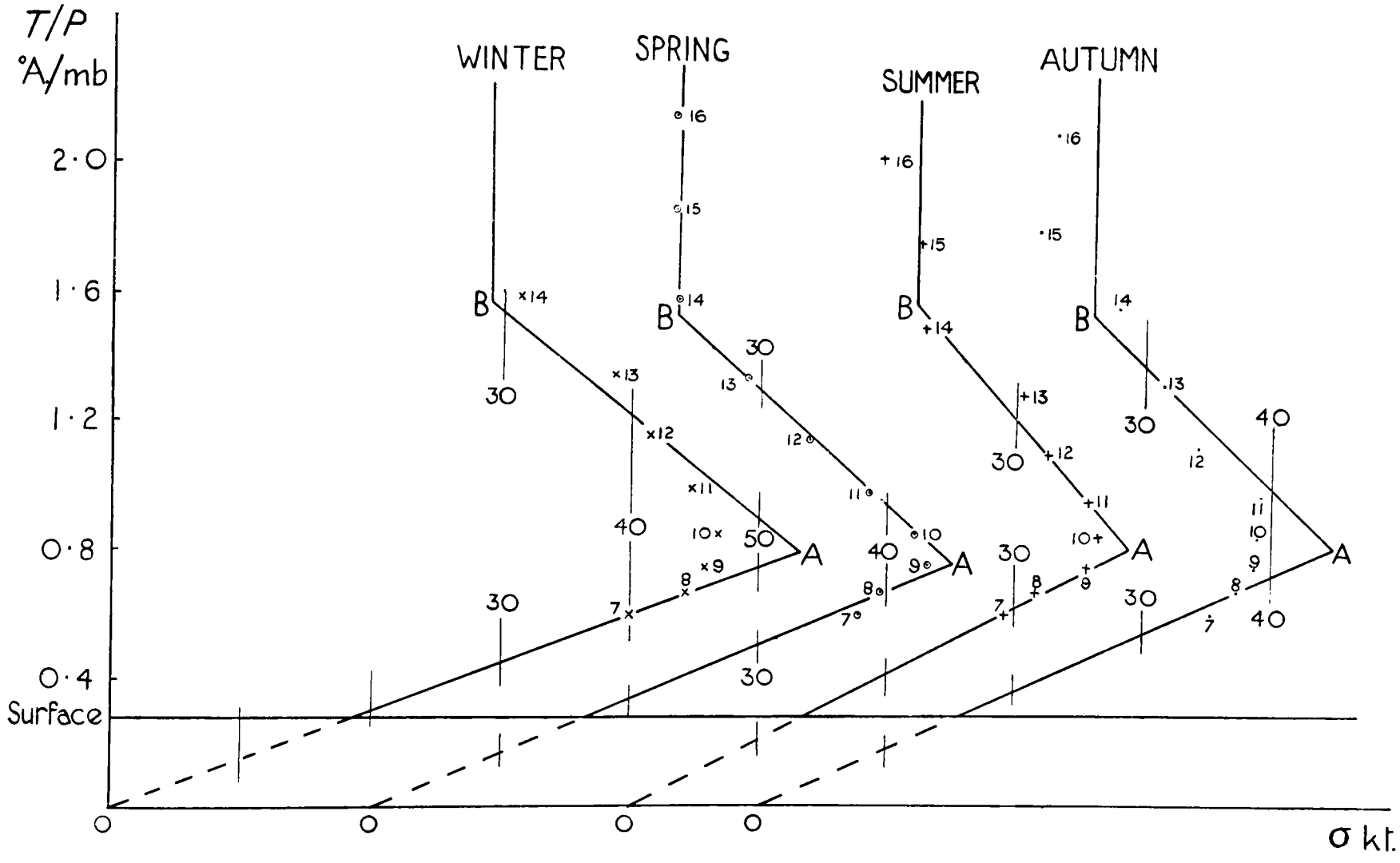

FIG. 5—VARIATION OF σ WITH HEIGHT OVER 53° N., 14° E.
Small figures denote height in kilometres; 1 Km. = 3,280 ft.
Horizontal scale: σ in knots

Variation of σ in the troposphere.—The points from about 900 mb. (1 Km.) up to the maximum value of σ (henceforth referred to as σ_m) fall close to straight lines which, when produced, pass through the origin. This confirms the rule, $\sigma\rho$ = constant, which appears to hold for all places for which sufficient data are available. Fig. 8 shows this for Karachi, in 25° N., for the clear-weather seasons; unfortunately sufficient data are available only to 8 Km. The rule implies that the horizontal pressure gradient, regarded as a vector, has the same standard vector deviation at all levels in the troposphere up to the level of σ_m, the velocity of the wind at each level being proportional to the reciprocal of the air density. This simple law is very useful, for we need to know only the value of σ at any one pressure level (above the surface) and the

density (or temperature) at other levels in order to calculate the value of σ at any level below that of σ_m. The application of the law is described later in § 13.

In the neighbourhood of 500 mb., the boundaries between opposing superposed air currents complicate the variation of σ with height in the tropics. The rule, $\sigma\rho$ = constant, cannot be applied rigidly but, in the absence of data contradicting it, it was assumed to operate at higher levels. In the present draft of the charts the equatorial isopleths of σ are very tentative. They will be revised when radio-wind data become available near the equator.

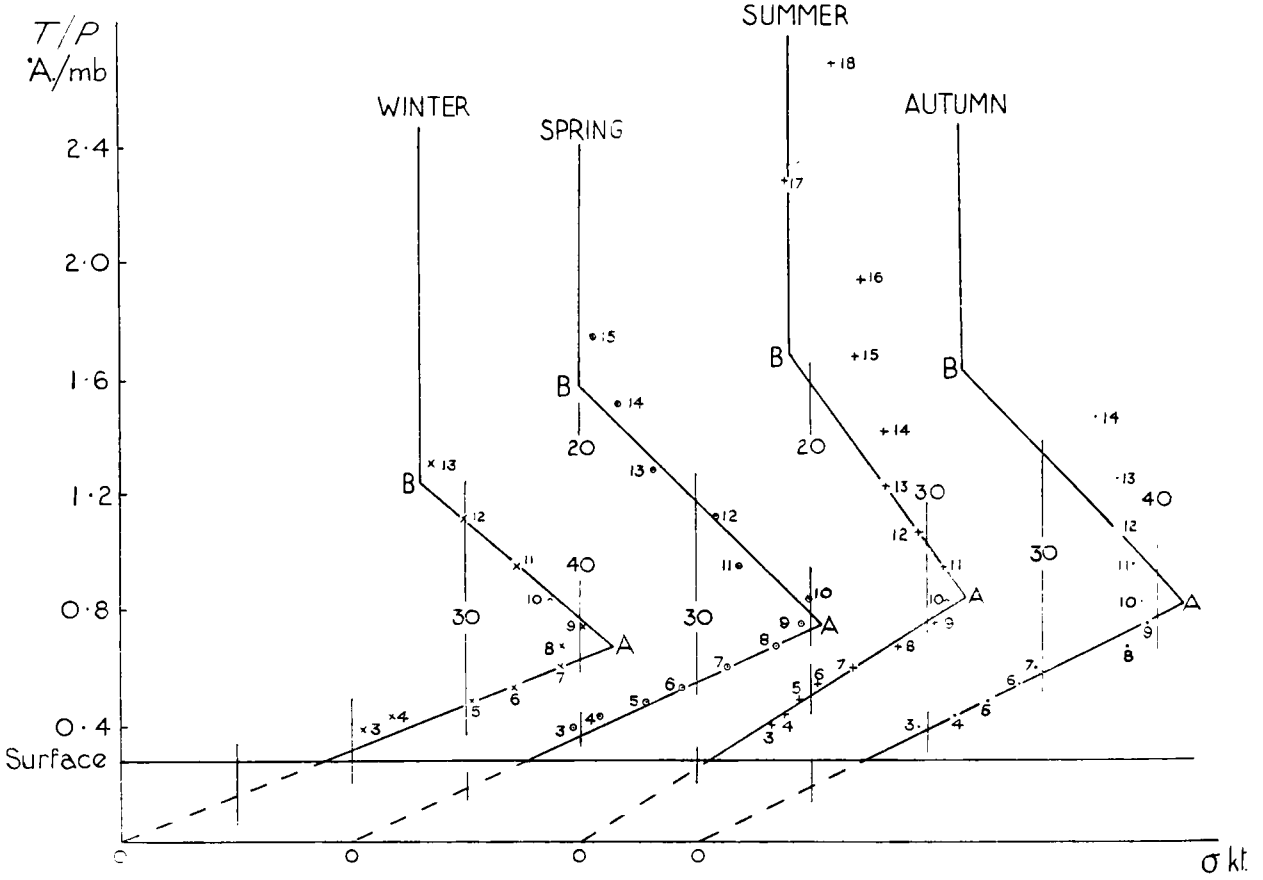

FIG. 6—VARIATION OF σ WITH HEIGHT OVER CONSTANȚA (44° N., 29° E.)

Small figures denote height in kilometres ; 1 Km. = 3,280 ft.

Horizontal scale : σ in knots

Determination of the level of σ_m.—The maximum value of σ lies 50 mb. or more below the mean height of the tropopause and, over Larkhill and Lerwick, corresponds to the lower ten-percentile of tropopause heights, as derived roughly from frequencies given by Mr. C. H. B. Priestley (in unpublished work). It appears likely that the distance of the σ_m level below the tropopause depends upon the variability of the tropopause height, being greatest in latitudes 25° to 45°, where the mean height of the tropopause is changing rapidly with latitude.

Estimates of the pressure level, P_m, of σ_m were made for a number of European stations or groups of stations. These are plotted (in millibars) against the cosine of latitude in Fig. 9. Points plotted for lower latitudes have been deduced from the variation of average speed with height which is similar to that of the standard vector deviation. For winter and summer, the approximate levels of maximum interdiurnal pressure variation, estimated from graphs for

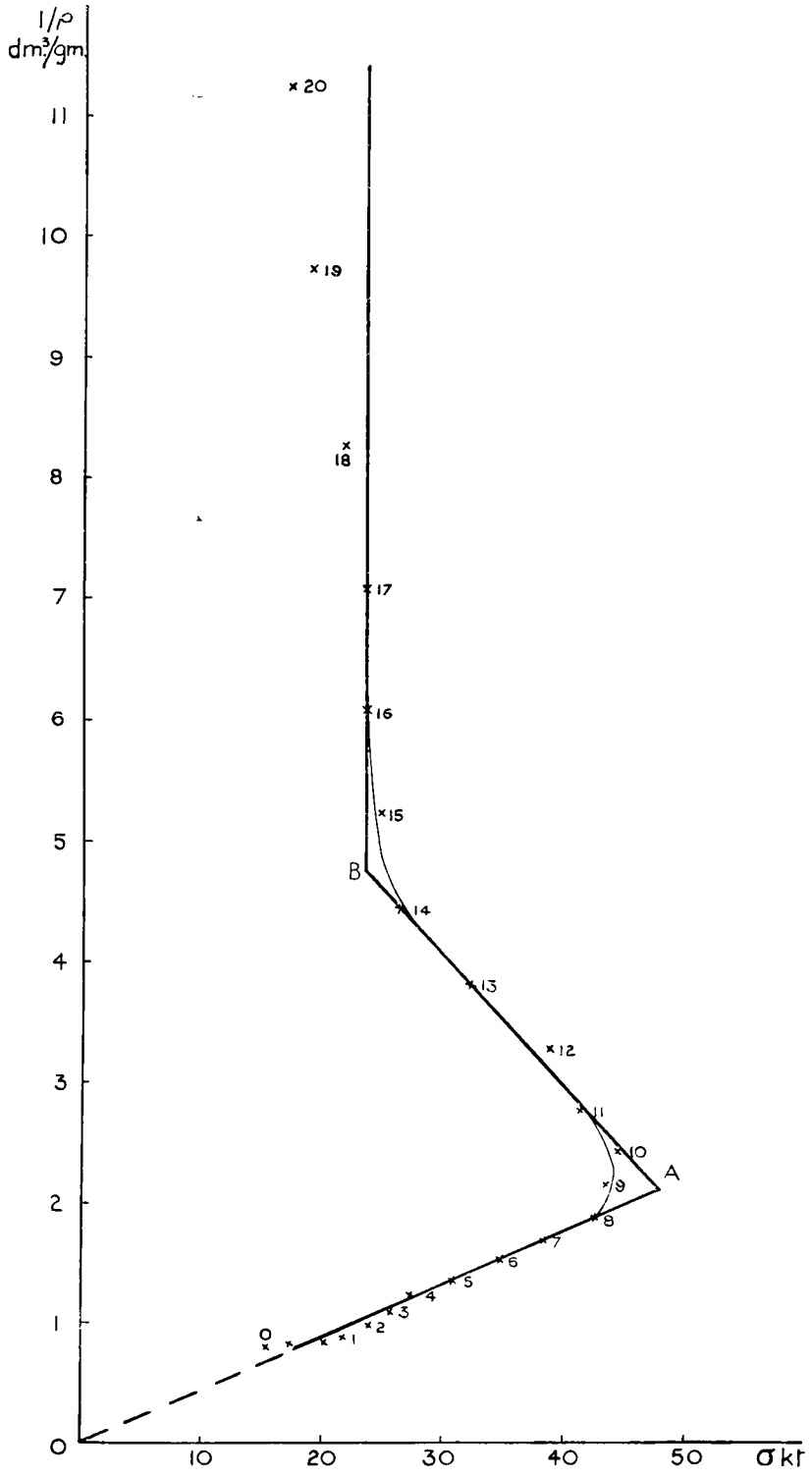

FIG. 7—VARIATION OF σ WITH HEIGHT OVER MAHLSDORF (53° N., 13° E.) (YEAR)
Small figures denote height in kilometres ; 1 Km. = 3,280 ft.

February and August given by T. F. Malone,[58] are also plotted. These are shown by a different type of cross. The pressure, P_t, corresponding to mean height of tropopause for the places for which wind data have been plotted, is shown by a smooth curve in the same figure.

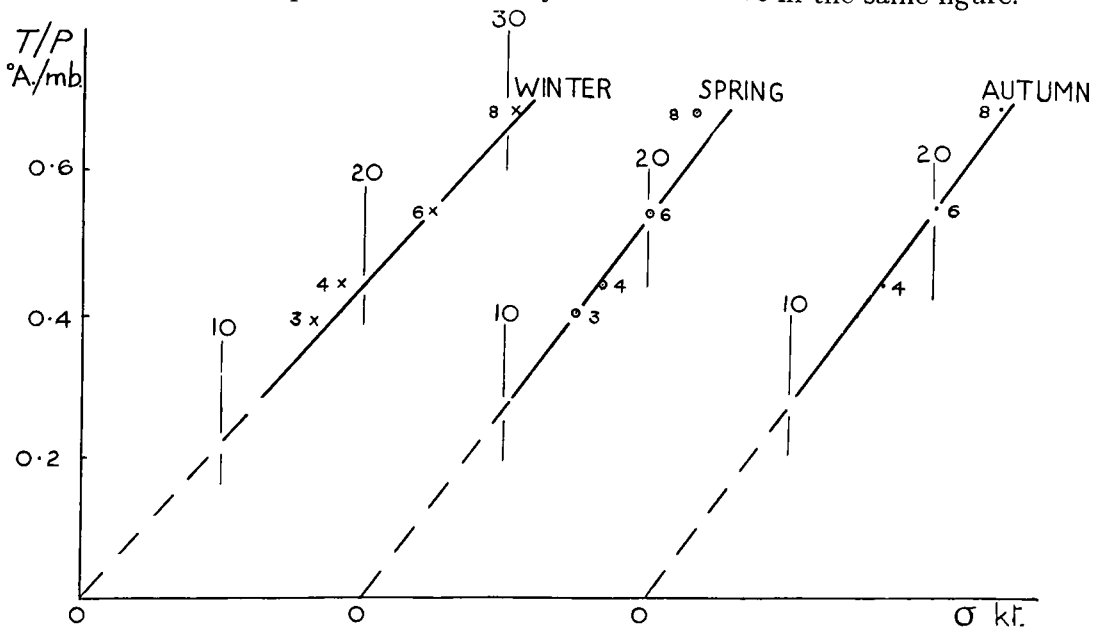

FIG. 8—VARIATION OF σ WITH HEIGHT OVER KARACHI (25° N., 67° E.) ILLUSTRATING THE RULE $\sigma\rho$ = CONSTANT
Small figures denote the height in Kilometres ; 1 Km. = 3,280 ft.

The seasonal variation of the difference between P_m and P_t is not large, and, for the purposes of extrapolation of σ, it seemed sufficient to adopt the same value for all four seasons. Modal values of $P_m - P_t$, estimated from the distances between the points giving P_m and the curve of P_t, were plotted directly against latitude and smoothed by a free-hand curve. From this curve were read the values of $P_m - P_t$ shown in Table XII.

TABLE XII—APPROXIMATE VARIATION OF $P_m - P_t$

Latitude (degrees)	⩾65	60	55	50	45	40	35	30	25	20	10	0
$P_m - P_t$ (mb.)	50	55	70	80	100	115	120	110	100	90	70	50

The curve of P_m in Fig. 9 was derived from Table XII.

Variation of σ near the tropopause and in the stratosphere.— Above the level of σ_m, σ decreases through practically the whole of the remaining range of positions of the tropopause, reaching a value of the order of 20–30 kt. at about 140 mb. ; after which, as far as can be determined from the scanty data, σ remains constant with height (see Figs. 4–7). This statement refers only to latitudes greater than about 45°. For the tropics there are no reliable data at high levels, but it seems probable that the decrease in σ, also occurs, above the mean height of the tropopause (about 90–100 mb. at the equator).

The adoption of 140 mb. as the upper turning point of the σ curve in European latitudes is based upon an examination of Figs. 4–7 and upon the feasibility of extrapolation made from curves of other German wind groups which do not reach the 140-mb. level. The apparent decrease in σ above the upper turning point is thought to be due to the paucity of observations in the corresponding wind summaries combined with a bias against strong winds at these high levels. The

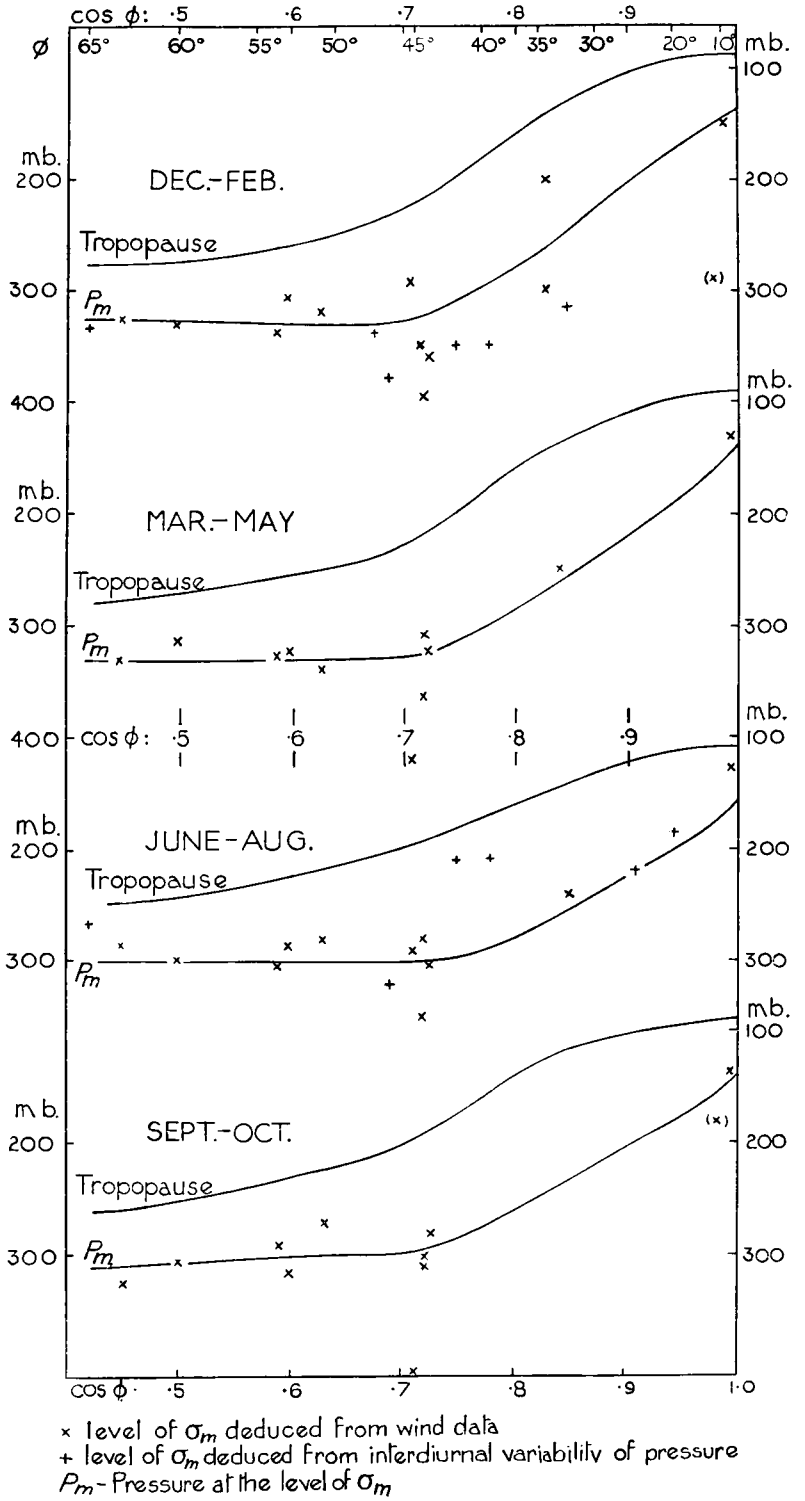

FIG. 9—RELATION BETWEEN THE LEVEL OF σ_m AND THE MEAN HEIGHT OF THE TROPOPAUSE

summaries at 100 mb. and 80 mb. over Larkhill and Lerwick are almost certainly biassed. Since about 90 per cent. of the ascents reached the 200-mb. level, it seems evident that bias against occasions of strong wind in the troposphere may be discounted. Losses at 100 mb. and 80 mb., apart from those due to random causes, will occur mainly with strong winds in the stratosphere. There is a high correlation between winds at different heights, and so, if a balloon is lost in strong wind a little above the 130-mb. level, it may be presumed that the winds at 100 mb. and 80 mb. were also strong.

§ 13—DETAILS OF CONSTRUCTION OF THE CHARTS

It was now possible to proceed to construct the charts. This was carried out in steps, working from 700 mb. upwards and checking the results at each level from such actual values as were available and also by means of tests for consistency.

Charts of σ_{700}.— These were drawn directly over land areas. All the available data for land stations were plotted, including pilot-balloon observations where these seemed to be sufficiently reliable. At this level very few balloons are lost in the distance, and in clear regions (cloud amount less than 3 tenths) the available observations were taken as fair samples of all days. The calculations of σ were from values of q and V_R derived mainly from manuscript summaries of the

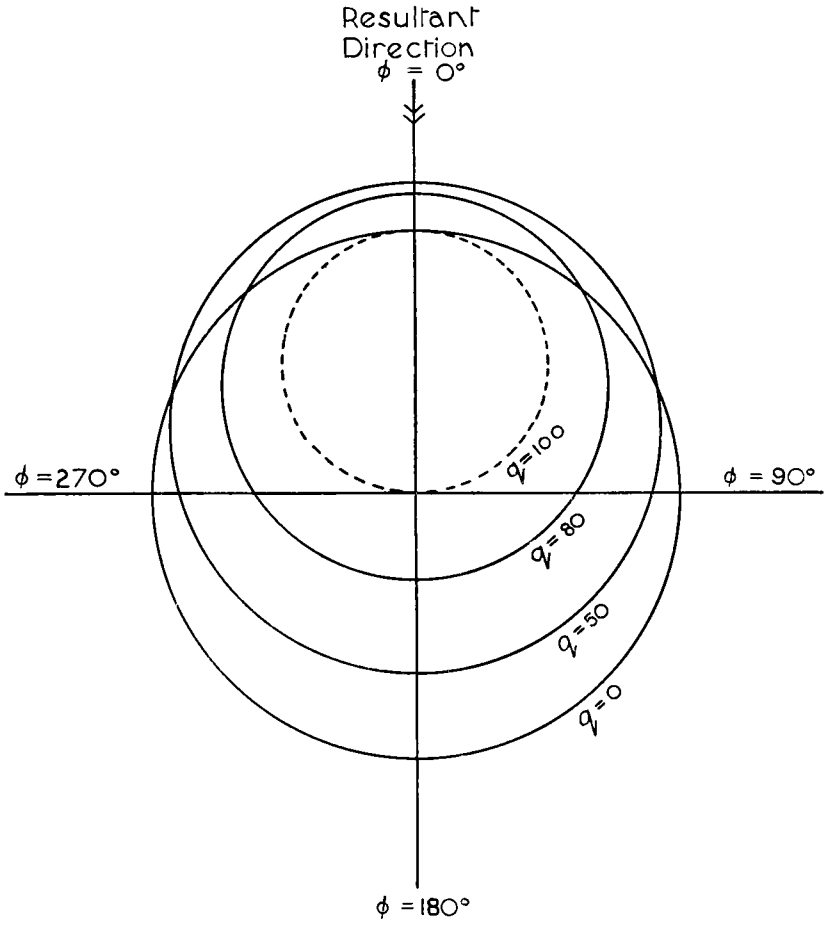

FIG. 10—PLOT OF V_a/V_s (THEORETICAL)

form approved by the International Commission for Air Navigation (I.C.A.N.). One of the properties of the normal circular distribution was used to check these values, as follows:—

When average speeds from different directions, deduced from the theoretical summaries of Appendix IV were plotted, they were seen to fall very nearly on circles as shown in Fig. 10. In this figure, the values plotted are average speed in the specified direction (V_a) divided by the average speed for the whole distribution. Thus the diagram indicates the way in which the circle of V_a changes in position and magnitude over the whole range of q (from 0 to 100) for a fixed value of V_S.

By means of equation (1), it can be shown, on integration, that the average speed in a direction making an angle ϕ with the resultant direction is given by

$$V_a = \frac{\bar{x}e^{-\bar{x}^2/\sigma^2} + \left(1 + 2\frac{\bar{x}^2}{\sigma^2}\right)\left(\frac{\sigma}{2}\sqrt{\pi} + \sigma\int_0^{\bar{x}/\sigma} e^{-z^2}\,dz\right)}{e^{-\bar{x}^2/\sigma^2} + 2\frac{\bar{x}}{\sigma^2}\left(\frac{\sigma}{2}\sqrt{\pi} + \sigma\int_0^{\bar{x}/\sigma} e^{-z^2}\,dz\right)} \qquad \ldots\ \ldots (13)$$

where $\bar{x} = V_R \cos\phi$ and $z = (V - \bar{x})/\sigma$, V being the wind speed on any particular occasion. At right angles to the resultant direction, $\phi = \pi/2$ or $3\pi/2$ so that $\bar{x} = 0$ and V_a reduces exactly to $\frac{1}{2}\sigma\sqrt{\pi}$.

Equation (13) is too complex for practical use, but it was found that a close approximation to the plot of V_a is given by the circle,

$$V_a = \tfrac{1}{2}(\pi\sigma^2 + V_R^2\cos^2\phi)^{\frac{1}{2}} + \tfrac{1}{2}V_R\cos\phi. \qquad \ldots\ \ldots (14)$$

This circle has a radius $\frac{1}{2}(\pi\sigma^2 + V_R^2)^{\frac{1}{2}}$ and its centre is distant $V_R/2$ from the origin.

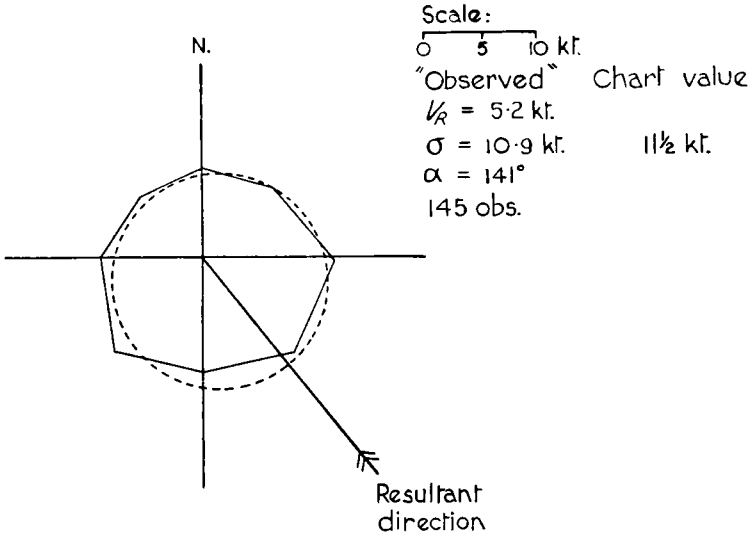

FIG. 11—SALISBURY (18° S., 31° E.) WINDS AT 10,000 FT.; PLOT OF V_a
September–November
Theoretical circle based on " observed " values shown by broken line

To check a computed value of σ, values of the average speed, V_a, for each of the eight directions of the I.C.A.N. summary were plotted, and a line indicating the resultant direction (computed from the summary) was drawn through the origin. Taking as centre the point on this line distant $V_R/2$ from the origin, a circle was drawn through the two points distant $\frac{1}{2}\sigma\sqrt{\pi}$ on either side of the resultant direction on the perpendicular through the origin.

A convenient scale was found to be one inch to represent ten knots. A correctly computed value of σ gave, in most cases, a circle corresponding fairly closely with the area bounded by the plots of V_a. The fit was not always good in the directions furthest from the resultant direction, especially when q was fairly high, on account of the paucity of observations. This discrepancy was heightened by the practice of assuming for all observations in a specified speed range the mean speed of the range. A typical example is shown in Fig. 11.

Even in seasons or regions of more than 3-tenths cloud, it was sometimes possible to estimate σ. When the average cloud amount did not exceed 4 tenths, the computed value was accepted after checking as described above. For 4–5-tenths cloud, σ could generally be estimated from the circle of V_a, the computed circle being modified to fit the plotted values. This, quite often, necessitated only a shift of the circle towards the origin, the discrepancies being due to too large a value of V_R (such as would arise from insufficient scatter of direction).

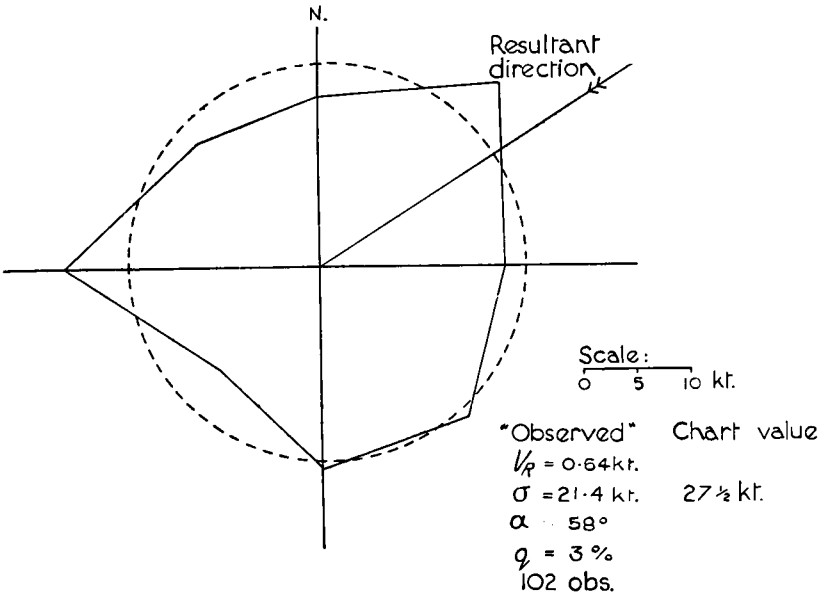

FIG. 12—BORDEAUX (45° N., 1° W.) WINDS AT 10,000 FT.; PLOT OF V_a
December–February 1929–36

Theoretical circle based on " observed " values shown by broken line. It is suspected that the " observed " wind distribution is unrepresentative owing to loss of balloons in cloud; the " observed " σ is too small

Where the average cloud amount was more than 5 tenths, the resultant direction and approximate constancy of " surface " winds sometimes served as a guide to the probable bias of direction due to cloud in estimating the true size and position of the V_a circle, so that with moderate values of " constancy " an estimate of σ to within one or two knots was frequently possible. When q (and therefore V_R) was apparently very near zero, a good fit for V_a might be obtained, however, when actually the computed value of σ was far too small. This was due, we think, to the fact that stronger winds were associated with conditions of low cloud so that clear weather showed only light winds at 10,000 ft., the frequencies of which did not vary appreciably with difference in direction. An example is shown in Fig. 12.

Over the oceans the values of σ at 700 mb. were deduced from the values which were estimated for 500 mb. by method (*a*) described in § 11. Use was made of the relation $\sigma\rho$ = constant. The ratio of σ_{500} to σ_{700} deduced on this basis from observations of upper air temperature was found to be practically constant and equal to 1·32.

When all the available data for 700 mb. for a particular season had been assembled and plotted, isopleths were drawn in for the whole world, most weight being given to values based on radio wind and radar. Over Siberia, Tibet and Canada the run of the lines was estimated to accord with topographical features, for it had been found, in other regions, that there was a tendency for σ to be lower over high ground. This was probably due to friction which causes a general decrease in wind speed. Over the oceans σ tends to be larger than over the land. The first draft of the chart was subjected to considerable smoothing, care being taken, however, to ensure that the differences between the final lines and the original data did not exceed the errors estimated as possible in the data.

Charts of σ_{500}.—For σ_{500} the data available were much fewer since, except in regions of little cloud, pilot-balloon summaries are quite unreliable at this level. The charts of σ_{700} were multiplied graphically by 1·32, corrected by means of the available observations and smoothed, since the effect of surface topography was expected to be less marked at 500 mb. than at 700 mb. The general agreement between the isopleths derived graphically and the available land data was good. The values of σ_{500} over the oceans were derived directly from those of σ at the surface, as described in § 11.

Interpolated values of σ_{300} *and* σ_{200}.—The first step in interpolating values of σ at 300 and 200 mb. was to find the pressure (P_m in millibars) and temperature (T_m in degrees Absolute) at the level of maximum σ. For this were used charts of mean tropopause height drawn specially and the Washington charts[10]. Points were selected to give a fairly uniform network over both land and sea in the northern hemisphere. For each point the mean height of the tropopause was read off the chart for the appropriate season and pressures were read from the two Washington charts immediately above and below this height. The pressure (P_t) associated with mean tropopause height was interpolated by assuming an exact linear relation of log (pressure) with height, and the addition of $P_m - P_t$ from Table XII gave P_m. The temperature (T_m), was interpolated from temperatures and log pressures read from the Washington charts at the two heights next below the mean tropopause height.

Charts of temperature at 500 mb. (T_{500}) had been drawn in the construction of the contour charts. Having read T_{500} from these for the appropriate season, and σ_{500} from the chart of σ at 500 mb., we were able to apply the rule

$$\sigma \frac{P}{T} \simeq \sigma\rho = \text{constant}$$

to obtain the maximum value of σ by the formula:—

$$\sigma_m = \frac{T_m}{T_{500}} \times \frac{500}{P_m} \times \sigma_{500} \qquad \ldots \ldots (15)$$

This value, σ_m, corresponds to the intersection A of the lines OA and OB representing the variation of σ against T/P (Figs. 4–7). The actual variation of σ near this point of intersection is more likely to be a smooth curve, as shown by the thinner line in Fig. 7, and so the true maximum value will tend to be lower than σ_m. B is the point (given by the intersection of two straight lines) at which σ becomes constant with height; it is clearly seen that a reliable estimate of σ_{200} would be obtained by interpolating linearly with respect to $1/\rho$ or T/P between A and B.

The pressure difference between A and B is of the order of 50 to 70 per cent. of the pressure at A, except when P_m approaches 200 mb., while the mean temperature difference was estimated to be less than 10 per cent. of the mean temperature at A. In view of the uncertainty of the values of σ and of P at B, it therefore seemed sufficient to interpolate according to the reciprocals of the pressures between P_m at A and 140 mb. at B. This was effected by the simple formula,

$$\sigma_{200} = \{P_m(0{\cdot}7\sigma_{130} + 0{\cdot}3\sigma_m) - 140\sigma_{130}\}/(P_m - 140) \qquad \ldots \ldots (16)$$

where σ_{130} is a provisional value for σ at 140 mb. (see p. 29).

For $P_m > 300$, interpolation for σ_{300} was also necessary and this is given by:

$$\sigma_{300} = \sigma_{200} + 0{\cdot}233P_m\,(\sigma_m - \sigma_{130})/(P_m - 140) \qquad \ldots\ \ldots (17)$$

These interpolated values of σ_{300} and σ_{200} were plotted in green on the charts and P_m was also given for the more southerly points.

In drawing up the 300-mb. charts, the position of $P_m = 300$ was estimated and inserted as a coloured pencil line across the chart. Equatorwards of this line, isopleths of $1{\cdot}5\ \sigma_{500}$, given by the rule $\sigma\rho$ = constant, were drawn and were continued across the line to fit the interpolated values. Near the line, they were curved in towards the centres of high σ so as to give values 3 or 4 kt. less than those given by the interpolations or by $1{\cdot}5\ \sigma_{500}$. This was to allow for the rounding of the curve of σ against T/P at the level of σ_m. All isopleths, of course, were modified to fit values computed from actual wind observations except where there was reason to suspect that these were unrepresentative. The charts for 200 mb. were treated in the same way, the line $P_m = 200$ (further south than $P_m = 300$) being shown for this level. We now had charts for 300 and 200 mb. covering the northern hemisphere and extending a little way south of the equator. It was still necessary to deduce the distribution of σ in the southern hemisphere at these levels.

TABLE XIII—COMPARISON OF σ_{130} WITH σ_{500}

European latitudes

	Position	Season	σ_{130}	σ_{500}
			kt.	kt.
Group 3	63° N. 9° E.	Sept.–Nov.	23	33
Lerwick	60° N. 1° W.	Dec.–Feb.	36	41
		Mar.–May	26	37
		June–Aug.	18	27
		Sept.–Nov.	28	35
Group 6	54° N. 34° E.	June–Aug.	22	23
Group 11	53° N. 14° E.	Dec.–Feb.	35	38
		Mar.–May	24*	32
		June–Aug.	21*	26
		Sept.–Nov.	27	32
Downham Market ..	52½° N. ½° E.	Dec.–Feb.	32	40
		Mar.–May	23	34
		June–Aug.	23	30
		Sept.–Nov.	28	35
Larkhill	51° N. 2° W.	Dec.–Feb.	32	40
		Mar.–May	23	33
		June–Aug.	22	29
		Sept.–Nov.	29	36
Group 20	44½° N. 10° E.	Sept.–Nov.	28	29
Constanţa	44° N. 29° E.	Dec.–Feb.	21	32
		Mar.–May	22*	27

* It will be found that the values shown for Group 11 (53° N. 14° E.) and Constanţa differ from those indicated by the vertical lines in Figs. 5 and 6. The latter have been drawn to agree with the final drafts of the charts of σ at 130 mb.

Provisional estimate of σ above 140 mb.—The 130-mb. level was considered the highest at which values of σ computed from the British radio-wind data could be accepted with confidence (see § 10). The only representative data approaching this level are for places in Europe. These suggest that there is a level, near the upper limit of the range of positions of the tropopause, at which σ becomes constant with height. In extratropical regions, as stated in § 12, this level appears to be in the neighbourhood of 140 mb. Table XIII gives the more reliable of the values of σ above 140 mb. deduced from actual wind data. For Larkhill, Lerwick and Downham Market, σ has been computed directly from summaries of observations at 130 mb. For most of the German data the line of decreasing σ (above σ_m) has been extrapolated to $T/P = 1{\cdot}50$ (roughly equivalent to $P = 140$) and this point taken to give σ_{130}, representing the value of σ for all levels above 140 mb. The entries starred in Table XIII have been deduced without extrapolation.

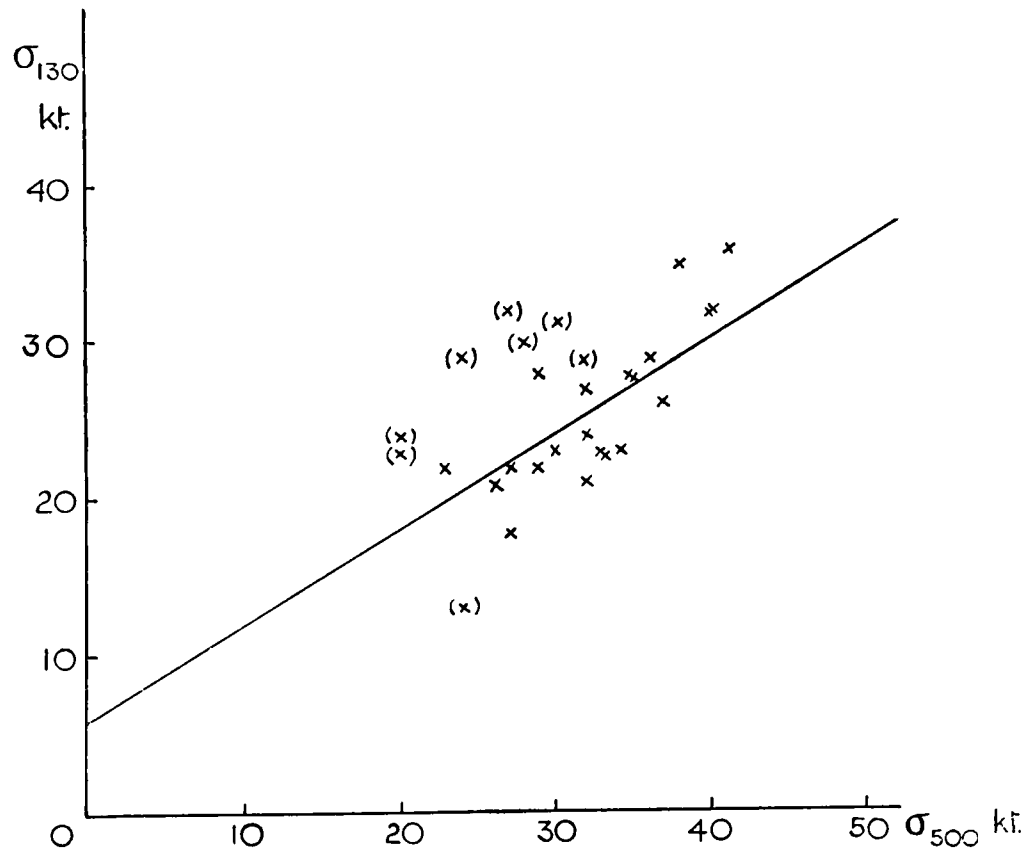

FIG. 13—RELATION BETWEEN σ_{130} AND σ_{500}
Doubtful values are shown in brackets

The corresponding values of σ at 500 mb., the highest level for which, at this stage of the investigation, σ had been charted, are shown on the right of Table XIII. These values of σ_{130} and σ_{500} have been plotted in Fig. 13 from which it will be seen that there is definitely a correlation between σ_{130} and σ_{500} in European latitudes. This is mainly a seasonal effect, but it seemed worth while making use of whatever rule could be deduced from it. Owing to the scatter of the data, only a linear relation was attempted. The 21 pairs of values in Table XIII gave a correlation coefficient of + ·82, and the corresponding regression of σ_{130} on σ_{500} is

$$\sigma_{130} = 0{\cdot}609\sigma_{500} + 5{\cdot}9 \text{ (standard error: 2·7 kt.)} \quad .. \quad .. \quad (18)$$

Other more doubtful values are shown plotted in brackets in Fig. 13.

Rough first approximations to the charts of σ at 130 mb. were drafted by applying relation (18) graphically to the charts of σ_{500} and smoothing the result. These were considered sufficiently correct to use in interpolating for values of σ_{200} and σ_{300} in latitudes as far south as 30° N., for where the errors in σ_{130} were greatest (*i.e.* between 30° and 45° N.) the level of σ_m would be above 300 mb. and very near 200 mb., and so the error of the interpolated values would not be large.

§ 14—VARIATION OF σ WITH LATITUDE

The charts at 300 mb. were not difficult to draw ; σ was still highest over the North Atlantic and North Pacific Oceans and decreased to a minimum near the equator. At 200 mb., however, secondary maxima occurred in about latitude 20° N. and the charts presented a much more complicated appearance so that a check of the reasonableness of the variations of σ with height and with latitude was felt to be necessary. For this purpose, plots of σ against latitudes were made for each of eight different meridians of longitude, the curves for 700, 500, 300 and 200 mb. being plotted on the same diagram in the way shown in Fig. 14. For each ten degrees of latitude,

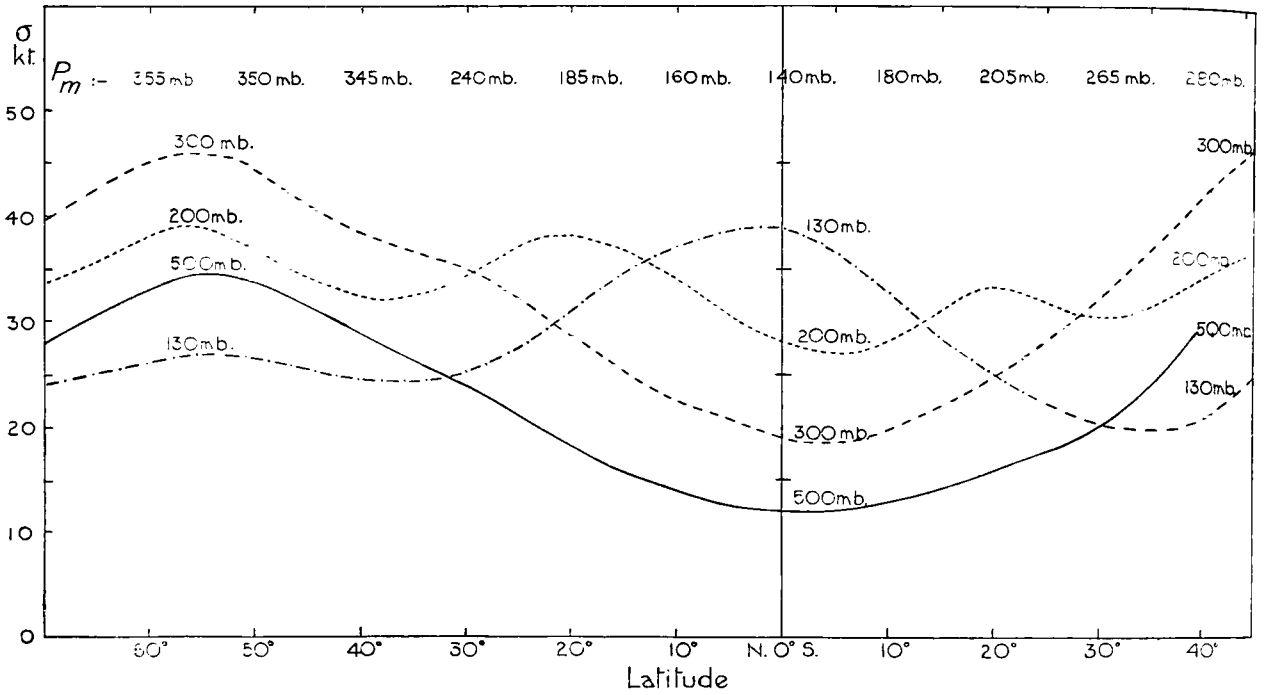

FIG. 14—VARIATION OF σ WITH LATITUDE OVER 30° E.
December–February

an estimate of P_m was made from the mean height of the tropopause and the value of $P_m - P_t$ given in Table XII. This aided in checking the variation of σ from one curve to another, for P_m indicated the level at which σ reached its maximum value and started to decrease with height. The values of P_m associated with the points of intersection of the curve of σ_{200} with those of other levels are, roughly, as follows:

Curve intersected	Values of P_m
	mb.
σ_{500}	300
σ_{300}	240 to 260

Slight modifications were made to the charts of σ in the light of this examination.

By means of the curves of σ plotted against latitude, extrapolation to the southern hemisphere was effected. Five meridians of longitude in the southern hemisphere were compared with one or more of the equivalent season in the northern hemisphere, as indicated in Table XIV. In the first instance, the amount was determined by which σ_{500} for a longitude in the second column

exceeded the average value of σ_{500} at the same latitude for the corresponding longitudes in the third column. This was then added (algebraically) to the average values at 300 mb. and at 200 mb. to give points on the curves required for the southern hemisphere (longitude as in the second column), and the resulting curves were modified to make them consistent with values of P_m computed directly for the southern hemisphere.

TABLE XIV—COMPARISONS FOR EXTRAPOLATION TO THE SOUTHERN HEMISPHERE AT 300 AND 200 MB.

December–February in the southern hemisphere is compared with June–August in the northern hemisphere

	Longitudes		
	Southern hemisphere		Northern hemisphere
Mid ocean	Indian Ocean Pacific Ocean	70° E. 140° W.	25° W., 180°
Coastal	Africa South America	30° E. 60° W.	0°, 70° W., 140° W., 140° E.
Monsoon	Australia	140° E.	70° E.

§ 15—FINAL ADJUSTMENTS OF THE CHARTS

A final check was provided by constructing, from the charts, curves of σ plotted against T/P for latitudes 15° S. and 40° S., longitudes 0°, 30° E., 70° E., 140° E., 140° W and 60° W. for each season. The curves for December–February in 30° E. are shown in Fig. 15. T/P was estimated from the Washington charts of the northern hemisphere, being taken as constant at a given pressure level for a particular latitude. The values of σ read from charts at 700 and 500 mb. and those given by the first draft of the curves at 300 and 200 mb. are shown by small crosses; those finally adopted are shown by circles. The line OA is a straight line through the origin and the 500-mb. point, produced to the level of maximum σ. For 15° S., the pressure (P_m) at this level was estimated and the corresponding value of T/P interpolated between values at 200 and 130 mb. At 40° S., readings from the charts of mean tropopause height are subject to error, and estimation of the position of σ_m in this way seemed too uncertain.

Another problem was to estimate the slope of the line AC showing the variation of σ within the range of variation of the tropopause. The points in this region for each of the European stations (diagrams such as Figs. 4–7) were in the first place fitted by a straight line as nearly as possible by eye. It was found that the inclination to the vertical of this line was generally about half that of the troposphere line, OA. The mean ratio given by the eight graphs for Larkhill and Lerwick was 0·46, and so, for Figs. 4–7, the lines were re-drawn to give inclinations (to the vertical) in this ratio. It will be seen that the fit is reasonably good. The values of σ (Fig. 4) calculated for 150 mb. (actually 46,000 ft.) were based on a much shorter period than the remaining levels; the high values in summer and autumn for Constanța (Fig. 6) are due largely to irregularities in the summaries, somewhat intensified by the grouping of the velocities. In the absence of any other information, the ratio 0·46, was taken to apply in latitudes 15° S. and 40° S. Thus, given the values of σ at 500 mb. and estimates of T/P at A, the graphs for 15° S. were fully determined.

For each of the positions in 40° S., the value of σ_{130} given by equation (18) was computed and attributed to the level $T/P = 1{\cdot}50$ (about 140 mb.), point C in Fig. 15. AC was then

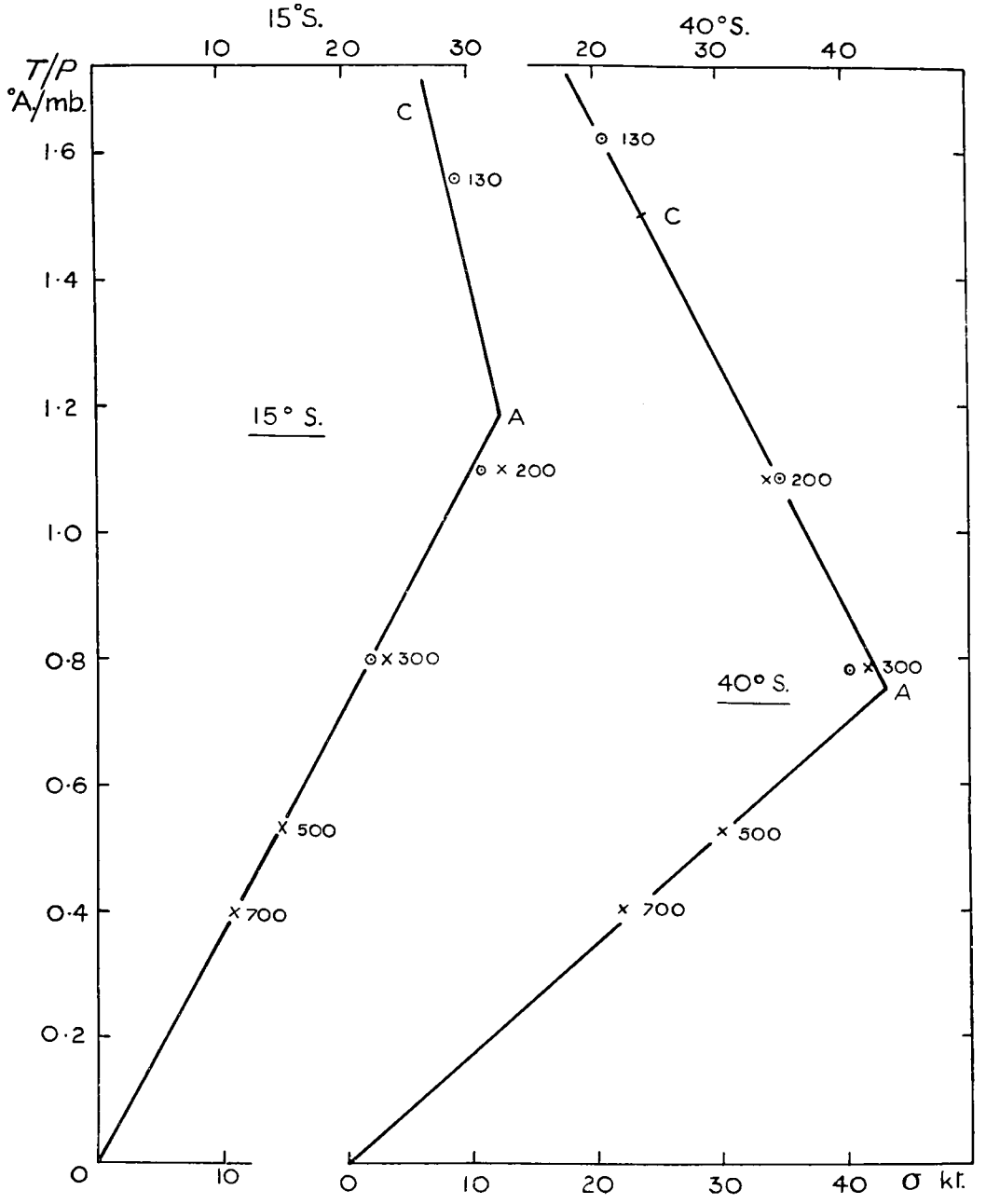

FIG. 15—VARIATION OF σ WITH HEIGHT OVER 30° E.
December–February

determined as a straight line through C, of inclination 0·46 times that of OA, meeting OA in A. In latitudes 45–60° with this construction, the variation of σ would be indicated by OA, AC and a vertical line through C ; but in latitude 40°, the height at which σ becomes constant is probably appreciably greater due to a much greater range of tropopause heights; and so, the value of σ computed from (18) is taken as referring only to the 140-mb. level and not to the whole range of height between 140 and, say, 80 mb. The value at 130 mb. is given by a point on the continuation of the straight line AC.

The curves relating σ with latitude (as Fig. 14) were re-drawn with the help of the graphs for 15° S. and 40° S. The values finally adopted for σ_{300} and σ_{200} (and σ_{130}), shown by circles in Fig. 15, do not deviate from the graphs by more than the error in drawing them, considering that the values for 500 mb. were read from the charts only to the nearest half knot.

The position of the isopleths of σ (30, 35, . . . kt.) given by the curves were marked along the appropriate longitudes on the charts for 300 mb. and 200 mb. In drawing up these charts, further adjustments were made to the curves to ensure smooth and reasonable distributions of the isopleths.

The final isopleths of σ at 700, 500, 300, 200 and 130 mb. are shown on pp. 98–137.

PART IV—SEASONAL CHARTS OF WINDS AT STANDARD PRESSURE LEVELS IN THE TROPICS

§ 16—GENERAL

As geostrophic winds become increasingly unreliable as the equator is approached, it was considered necessary to produce separate charts for the region 25° N. to 25° S. showing wind direction by stream-lines and speeds by isopleths.

At first it was intended to issue these charts for the same pressure levels as the contour charts, but at the 200-mb. level it was found that information was so scanty that it was only practicable to produce a cross-sectional diagram indicating the probable general direction and speed of the air currents. For the 130-mb. level there is practically no information and it would be of little use to attempt even a diagram at present.

§ 17—DATA USED IN CONSTRUCTING THE CHARTS

A list of publications from which data were taken is given in the Bibliography.* The observations used were mainly vector mean wind velocities worked up from pilot-balloon ascents. As far as possible, to avoid bias, only ascents made in fairly clear weather were used, but over many parts of the area, where observations were very scanty, it was found necessary to consider all available information.

Near the northern and southern boundaries of the zone, at 25° N. and 25° S., speeds and directions were obtained from the contour charts for the appropriate level.

For the 300-mb. level observations of the movements of cirrus clouds[6] were used, though with discrimination.

§ 18—METHOD OF CONSTRUCTION OF THE CHARTS

The following technique was adopted and used for all levels (except the 200-mb. diagram). All available information was plotted on a base map; wind directions were shown by heavy arrows and corresponding speeds by figures placed near the arrowhead, red ink being used for winds having an easterly component and black for winds having a westerly component; geostrophic speeds and directions near the boundaries of the charts were shown by small black figures and arrows and cirrus cloud movements by green arrows; indicators and marginal notes were used as necessary to draw attention to data which it was desirable to use with caution. This method of presentation was found to be of assistance in assessing the data, and the use of red and black arrows for easterly and westerly winds made the different currents stand out clearly on the 700-mb. chart where there were a considerable number of observations.

---

* Bibliography Nos. 1–3, 6, 30, 33, 42–4, 46, 48–50, 64, 68, 71–4.

This base map was then covered with a sheet of tracing paper and stream-lines only were drawn. These were necessarily based mainly on the wind directions, but account was taken of speed V_R when planning the lines. A chart of lines of air flow which fitted the observations and appeared to give a coherent picture was ultimately produced though sometimes only after considerable redrafting.

The question of the extent of convergence at the 700-mb. level led to considerable discussion. Observations were too scattered to give a definite answer to this question. Considerable convergence is indicated on some stream-line charts published by the India Meteorological Department[33], but it was doubtful to what extent it prevailed in a particular region over a period of three months. It was therefore considered best to omit stream-lines in regions where the speed was less than $2\frac{1}{2}$ kt. as the precise direction of the lines of flow in these regions is uncertain. In regions where speeds were between $2\frac{1}{2}$ and 5 kt. it was decided to show broken stream-lines to denote that some uncertainty was felt about these areas also; elsewhere full lines were to be used.

After the general stream-line pattern had been decided the V_R isopleths were drawn using observed values as far as possible. The remainder of the chart was completed with the help of geostrophic winds near the boundary and from a consideration of the air flow which would be expected from the stream-line pattern. Actually, as the two are complementary it was often necessary to modify the provisional stream-lines slightly while drawing the isopleths.

As might be expected with inadequate data, particularly at the 500-mb. and 300-mb. levels, alternative constructions were possible in places; in some regions, where short-period data had had to be used, the actual observations were sometimes difficult to reconcile and were occasionally conflicting. It is not possible to discuss all such cases but as an example of a difficult decision the winds for the December–February chart at 300 mb. at Medan (4° N. 99° E.), Padang (1° S. 100° E.) and Batavia ($6\frac{1}{2}$° S. 107° E.) may be mentioned. All these stations might have been expected to show an easterly current; actually, while Batavia gave an ESE. wind of about 7 kt. the other two stations gave west-north-westerly winds of about 10 kt., according to a chart of upper winds from which the seasonal mean winds had been obtained. Reference to Braak[44], who gives more details of the ascents, showed that there were only five observations of winds at 30,000 ft. over Padang, and that these had been made during one season, December 1920-February 1921; on the other hand the ascents showed a steady NW.–WNW., current of about 10 kt. from 23,000–30,000 ft. and the results had apparently been accepted without question by Braak. Details of the Medan ascents could not be found. After considerable discussion it was decided that there was not sufficient justification for disregarding the only available data and the stream-lines were drawn to fit them, though this meant introducing a very marked transfer of air across the equator together with a sharp change in the direction of a 10-kt. air stream.

In the charts on pp. 138–150 air streams of different speeds are shown by different types of shading. A key to this shading is given on the charts.

§ 19—NOTE ON USE OF THE CHARTS

The charts are seasonal means and, in the monsoon regions especially, the conditions in a particular month may not be represented satisfactorily by the seasonal chart. Hence when using a chart it is sometimes desirable to refer also to the chart for the preceding or following season, particularly if the period for which information is wanted is near the beginning or end of the season.

It will be appreciated that these charts have, for the most part, had to be constructed using inadequate data; particularly for South America and the Pacific Ocean. Though they are admittedly of a tentative nature they are the best estimates at present possible of air currents in this region.

BIBLIOGRAPHY

GENERAL

1. ALPERT, L. ; The intertropical convergence zone of the eastern Pacific region. *Bull. Amer. met. Soc., Lancaster Pa*, **26**, 1945, p. 426, and **27**, 1946, pp. 15 and 62.
2. BROOKS, C. E. P. ; The movement of volcanic dust over the globe. *Met. Mag., London*, **67**, 1932, p. 81.
3. BROOKS, C. E. P. ; Studies on the mean atmospheric circulation. *Bull. Amer. met. Soc., Milton Mass.*, **18**, 1937, p. 313.
4. BROOKS, C. E. P., DURST, C. S. and CARRUTHERS, N. ; Upper winds over the world. Part. I. The frequency distribution of winds at a point in the free air. *Quart. J.R. met. Soc., London*, **72**, 1946, p. 55.
5. DOBSON, G. M. B. ; Winds and temperature gradients in the stratosphere. *Quart. J.R. met. Soc., London*, **46**, 1920, p. 54.
6. HILDEBRANDSSON, H. H. ; Rapport sur les observations internationales des nuages au Comité International Météorologique. I. Historique circulation générale de l'atmosphère. Uppsala, 1903.
7. KÖPPEN, W. and GEIGER, R. ; Handbuch der Klimatologie. Band I, Teil F. : Klimatologie der freien Atmosphäre, by A. Wagner. Berlin, 1931.
8. MÖLLER, F. ; Der Jahresgang der Temperatur in der Stratosphäre. *Met. Z., Braunschweig*, **55**, 1938, p. 161.
9. PETTERSSEN, S. ; Weather analysis and forecasting. New York and London, 1940.
10. Washington, Weather Bureau. Normal weather maps. Northern hemisphere, upper level : 10,000 feet (3,050 meters) and 20,000 feet (6,100 meters), 10, 13, 16 and 19 kilometers.

ARCTIC

11. Ann Arbor, University of Michigan. Reports of the Greenland expeditions of the University of Michigan (1926–31). Part I. Aerology, Expeditions of 1926 and 1927–29. *Univ. Mich. Stud., Ann Arbor*, **5**, 19 31
12. Deutsche Grönland–Expedition Alfred Wegener 1929 and 1930–31. Wissenschaftliche Ergebnisse. Band IV. Meteorologie. 1. Halbband : Das Beobachtungsmaterial, von J. Georgi, R. Holzapfel und W. Kopp. Leipzig, 1935.
13. MACGREGOR, G. J. ; The MacGregor Arctic expedition to Etah, Greenland, July 1, 1937 to October 4, 1938. *Mon. Weath. Rev., Washington, D.C.*, **67**, 1939, p. 366.
14. MOLCHANOV, P. ; Results of 6 years (1930–1936) of application of the radio-sounding balloons method in the investigation of the atmosphere. *Bull. arctic. Inst., Leningrad*, No. 6. 1936, p. 274.
15. SVERDRUP, H. U. ; Norwegian North Polar expedition with the " Maud " 1918–1925. Scientific results. Vol. III. Meteorology, Part II, Tables. Bergen 1930.
16. TOMMILA, M. and RAUNIO, N. ; Aerologische Beobachtungen mit Radiosonden in Sommer 1937. *Mitt. Met. Inst. Univ., Helsinki*, No. 41, 1939,

EUROPE

17. GAMBA, P. ; Le caratteristiche dell'atmosfera libera sulla Valle Padana. Venice, 1923.
18. Hamburg, Deutsche Seewarte. Die Hamburger Registrierballonfahrten von 1926 bis 1930. *Aus. d. Arch. dtsch Seew., Hamburg*, **50**, 1931, No. 5.
19. KOFLER, M. ; Die Temperaturverhältnisse der freien Atmosphäre über Wien. *Beih. Jb. Zent.–Anst. Met., Wien*, 1928, Vienna, 1931, p. 23.
20. London, Meteorological Office. *Observatories Year Book*. 1931–38.
21. London, Meteorological Office. Weather in Home Waters and the north-eastern Atlantic. Vol. II, Part I. The Atlantic from the Azores to the African coast with an Appendix on Gibraltar. London, 2nd edn. 1944, pp. 128 and 247.

22. Paris, Office Nationale Météorologique. Étude climatologique sur le bassin méditerranéen. *Études, Paris*, No. 1, 1940.

23. REICHEL, E.; Ferdinand Steinhausen, Die Meteorologie des Sonnblicks. *Met. Z., Braunschweig*, **55**, 1938, p. 448.

24. ROSSI, V.; Über Temperatur and Feuchtigkeitsverhältnisse der freien Atmosphäre nach aerologischen Flugzeugaufstiegen in Finnland. *Mitt. Met. Zent-Anst., Helsinki*, No. 25, 1945.

25. Stockholm, Statens Meteorologisk-Hydrografiska Anstalt. *Årsbok*, **21–5**, 1940–44.

26. Warsaw, Institut Météorologique d'État de Pologne. *Résultats des observations de Sondages aerologiques*. 1936–37.

ASIA

Siberia

27. FLOHN, H.; Zum Klima der freien Atmosphäre über Siberien. *Met. Z., Braunschweig*, **61**, 1944, p. 50.

China

28. TU, CHANG WANG; A preliminary study on the climatological conditions of the free atmosphere of China. *Mem. nat. Res. Inst. Met., Chungking*, **13**, No. 2, 1939.

29. HEYWOOD, G. S. P.; Upper temperatures and the properties of air masses over Hong Kong. *Met. results, Hongkong* 1940, Appendix B, Hongkong, 1940.

30. GHERZI, E.; The winds and the upper currents along the China coast and in the Yangtse Valley. Shanghai, 1931.

31. Washington, U.S.A.A.F., Weather Division. Weather and climate of China. Washington D.C., 1945.

India

32. ANANTHAKRISHNAN, R.; Discussion of upper air data obtained from aeroplane meteorological flights over Peshawar and Quetta during the years 1927–36. *Mem. India met. Dep., Delhi*, **29**, Part 2, 1942.

33. Delhi, India Meteorological Department. Climatological charts of the India monsoon area. Poona, 1945.

34. KRISHNA RAO, P. R. and BHATIA, K. L.; Temperatures and humidities up to 3 kms. over Karachi. *Sci. Notes met. Dep. India, Delhi*, **7**, 1938, No. 78.

35. Poona, India Meteorological Department. Normal monthly percentage frequencies of upper winds at 4, 6, 8 and 10 km. above sea-level obtained from pilot balloon ascents. *Sci. Notes met. Dep. India, Delhi*, **6**, No. 66, 1933.

36. Poona, India Meteorological Department. Tables of monthly average frequencies of surface and upper winds up to 3 km. in India. *Sci. Notes met. Dep. India, Calcutta*, **2**, No. 17, A–D., 1930.

37. Poona, India, Meteorological Department. Normals of upper air data up to the end of 1935. *Upper Air Data, Delhi*, **12**, Part B, 1942, p. 206.

38. RAMANATHAN, K. R. and RAMAKRISHNAN, K. P.; Discussion of results of sounding balloon ascents at Poona and Hyderabad during the period October 1928 to December 1931. *Mem. India met. Dep., Delhi*, **26**, Part IV, 1934.

39. RAMANATHAN, K. R. and RAMAKRISHNAN, K. P.; The general circulation of the atmosphere over India and its neighbourhood. *Mem. India met. Dep., Delhi*, **26**, Part X, 1939.

Siam and East Indies

40. Bangkok, Hydrographic Service, Section of Meteorology. *Pilot balloon data*, 1936–39.

41. Batavia, Koninklijk Magnetisch en Meteorologisch Observatorium. Results of pilot balloon observations at and near Batavia in the years 1911–1918. *Verh. magn. met. Obs., Batavia*, No. 6, 1920.

42. BEMMELEN, W. VAN; The atmospheric circulation above Australasia according to the pilot balloon-observations made at Batavia. *Proc. Akad. Sci., Amsterdam*, **20**, 1918, p. 1313.

43. BEMMELEN, W. van; Die Wind-verhältnisse in den oberen Luftschichten nach Ballonvisierungen in Batavia. *Verh. magn. met. Obs., Batavia*, No. 1, 1911.

44. BRAAK, C.; Het Klimaat van Nederlandsch-Indië. Deel I. Algemeene Hoofdstukken. Deel II. Locale Klimatologie. *Verh. magn. met. Obs., Batavia*, No. 8 [1921] and 1929.

AFRICA

45. Cairo, Ministry of Public Works, Physical Department. *Met. Rep. 1932–37.* Cairo, 1935–44.

46. Cox, G. W. ; The circulation of the atmosphere over South Africa. *Mem. S. Afr. met. Off., Pretoria,* No. **1**, 1935.

47. Service Météorologique de l'Afrique Occidentale Française. Vent en altitude. *Mémento Serv. mét., Dakar,* No. 8, 1941.

48. HAMILTON, R. A. and ARCHBOLD, J. W. ; Meteorology of Nigeria and adjacent territory. *Quart. J.R. met. Soc., London,* **71**, 1945, p. 231.

49. London, Meteorological Office. A pilot's primer of west African weather. London, 1944.

50. London, Meteorological Office. Weather of the Sierra Leone peninsula. London, 1946.

51. PENNDORF, R. ; Die mittleren Temperaturverhältnisse über der Sahara. *Met. Z., Braunschweig,* **60**, 1943, p. 351.

52. Nairobi, British East African Meteorological Service. *Meteorological Reports for Northern Rhodesia.* Seasons 1933–1934 to 1936–1937.

53. Nairobi, British East African Meteorological Service. Upper wind frequencies. Tables of frequencies of the speed and direction of upper winds determined by pilot balloon observations at stations in British East Africa during the period 1927–43. Nairobi, 1946.

54. Pretoria, Meteorological Office. Upper winds of South Africa. *Rep. met. Off., Pretoria,* 1929, Appendix, p. 226, Pretoria, 1934.

55. Salisbury, Department of Agriculture. *Met. Rep. year ending 30th June, 1936.* Salisbury, 1937.

AUSTRALIA

56. Melbourne, R.A.A.F. Meteorological Service. Weather on the Australia Station, Vol. II. Local information.
    Part 1. Bismarck Archipelago. 1942.
    Part 2. Northern Australian Waters. 1942.
    Part 5. The Pacific Ocean between the Tropic of Capricorn and latitude 32° S., west of longitude 170° E., including the Australian coast from Rockhampton to Port Macquarie. 1943.
    Part 6. The south-west Tasman Sea (32°–46° S., 146°–160° E.) including the Australian coast from Port Macquarie to Wilson's Promontory and the eastern part of Tasmania. 1945.

NORTH AMERICA

57. GREGG, W. R. ; An aerological survey of the United States. Part II. Results of observations by means of pilot balloons. *Mon. Weath. Rev., Washington D.C.,* Supplement No. 26, 1926.

58. MALONE, T. F. ; A study of interdiurnal pressure and temperature variations in the free atmosphere over North America. *Pap. phys. Oceanogr. Met., Cambridge and Woods Hole, Mass.,* **9**, No. 4, 1946.

59. PENNDORF, R. and E. ; Die mittleren Verhältnisse der freien Atmosphäre über Pensacola (Golf von Mexico). *Met. Z., Braunschweig,* **61**, 1944, p. 62.

60. RATNER, B. ; Upper air average values of temperature, pressure and relative humidity over the United States and Alaska. *Weath. Bur. tech. Pap., Washington D.C.,* No. 6, 1945.

61. Royal Society, British National Committee for the Polar Year. British Polar Year expedition, Fort Rae, N.W. Canada, 1932–33. London, 1937.

62. STEVENS, L. A. ; Upper-air wind roses and resultant winds for the eastern section of the United States. *Mon. Weath. Rev., Washington D.C.,* Supplement No. 35, 1933.

SOUTH AMERICA

63. Buenos Aires, Dirección de Meteorología, Geofisca e Hidrología. *Carta del Tiempo.* 1941–44.

64. COYLE, J. R. ; A series of papers on the weather of South America. Rio de Janeiro. Part I 1942. Part II 1943.

65. Lima, Institut Nacional de Meteorología e Hidrología. Boletín anual meteorológico. Nos. 22–4, 1943–45.

66. Santiago, Oficina Meteorológica de Chile. Anuario meteorológico de Santiago, 1937 and 1939. Santiago, 1938 and 1940.

67. SERRA, A. ; Climatologia da troposfera. Rio de Janeiro, 1943.

68. SERRA, A. and RATISBONNA, L. ; As massas de ar da América do Sul. Rio de Janeiro, 1942.

OCEANIC ISLANDS

69. COULTER, J. W. ; Meteorological reports of the Mauna Kea expedition, 1935. *Bull. Amer. met. Soc., Milton Mass.*, **19**, 1938, p. 349.

70. DEPPERMAN, C. E. ; The upper air at Manila. *Publ. Manila Obs.*, **2**, 1934, No. 5.

71. DEPPERMAN, C. E. ; Upper air circulation (1–6 Km.) over the Philippines and adjacent regions. Manila, 1940.

72. London, Meteorological Office. Weather in the Indian Ocean. Vol. I. General Information. Vol. II. Local information. Part 6. A. East coast of India from Cape Comorin to the Ganges delta. B. Ceylon. London, 1940, reprinted 1944.

73. STONE, R. G. ; On the mean circulation of the atmosphere over the Caribbean. *Bull. Amer. met. Soc., Milton Mass.*, **23**, 1942, p. 4.

74. THOMSON, A. ; Scientific results of cruise VII of the *Carnegie* during 1928–1929 under the command of Captain J. P. Ault. Meteorology—II. Upper wind observations and results obtained on cruise VII of the *Carnegie*. Washington D.C., 1943.

APPENDIX I—COMPUTATION OF HEIGHT DIFFERENCES BETWEEN SUCCESSIVE STANDARD PRESSURE LEVELS FROM 500 MB. UPWARDS

In computing height differences above 500 mb. (§ 4), it was necessary to make some assumption as to the variation of temperature with height in the atmosphere as a whole. Between 500 and 130 mb. the variation of temperature is complicated by the existence of the tropopause and by the variation of its height; in this region of the atmosphere, therefore, a constant lapse rate cannot be assumed for the layer between any two standard pressure levels nor is an abrupt change to constant temperature feasible at the average height of the tropopause. A convenient approximation to actual conditions was obtained by inserting, between troposphere and stratosphere, a transition layer in which the lapse rate was half that in the troposphere. The boundaries of the transition layer were placed at 5,000 ft. above and below the average height of the tropopause, and the lapse rate taken for the troposphere was that used already between 700 and 500 mb. (about 1·8° C./1,000 ft.).

For convenience, let us take 1,000 ft. as unit of height and denote the average height of tropopause by Z_t. The lapse rates can then be tabulated as follows:

Layer	Range of height	Lapse rate
	1,000 ft.	°C./1,000 ft.
(i) Stratosphere	above $Z_t + 5$	0
(ii) Transition	between $Z_t + 5$ and $Z_t - 5$	0·9
(iii) Troposphere	below $Z_t - 5$	1·8

The temperature curve is given in Fig. 16.

All the computations described below are based upon the following formula in which height is expressed in 1,000 ft. units;

Height difference $= 0{\cdot}2211 \times$ (mean temperature of layer in °A.) $\times \log$ (ratio of pressures).

In the discussion which follows the symbols used are Z (in thousands of feet) the required height difference between two specified standard pressure levels, Z_c the height of the tropopause above the lower pressure level, and the symbols, given below, for the pressure and temperature at the critical levels:

Height 1,000 ft.		Pressure mb.	Temperature °A.
$Z + Z_t - Z_c$	upper pressure level (specified)	P'	..
$Z_t - Z_c$	lower pressure level (specified)	P	T
$Z_t + 5$	boundary between (i) and (ii)	P_1	..
$Z_t - 5$	boundary between (ii) and (iii)	P_2	..

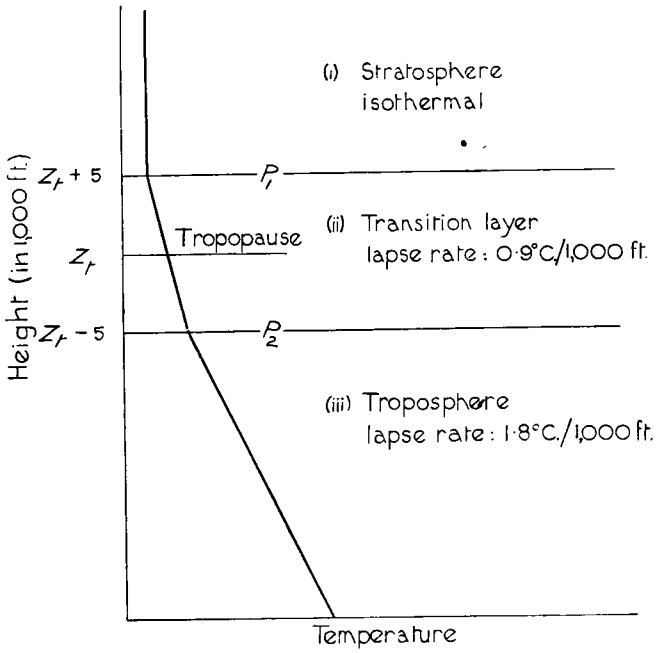

FIG. 16—VARIATION OF TEMPERATURE WITH HEIGHT—SCHEMATIC

Since the pressure levels P and P' may each be in any one of the layers, (i), (ii) or (iii) (see Fig. 16), six different orders of P', P, P_1 and P_2 appear to be possible (excluding cases in which P or P' equals P_1 or P_2). These will be classified according to the value of Z_c, the resulting classes being subdivided as necessary.

1. $Z_c \leqslant -5$. Both P and P' are in the stratosphere and the height difference is given by

$$Z = 0{\cdot}2211\ T \log (P/P'). \qquad .. \quad .. \quad (19)$$

2. $-5 < Z_c \leqslant +5$. Here, P is in the transition layer and P' is in the stratosphere or transition layer according as P_1 is greater or less than P'.

Now, the height difference $Z_c + 5$ between P and P_1 is given by

$$Z_c + 5 = 0{\cdot}2211\ [T - 0{\cdot}45\ (Z_c + 5)] \log (P/P_1).$$

Put $$\varkappa = \frac{Z_c + 5}{0{\cdot}2211\,[T - 0{\cdot}45\,(Z_c + 5)]}\,; \qquad \ldots\ \ldots (20)$$

then $\log (P/P_1) = \varkappa$ and P_1 is greater or less than P' according as $\varkappa$ is less or greater than $\log (P/P')$. This criterion gives the two sub-classes:—

2. (*a*) $\varkappa < \log (P/P')$. The pressure level P' is in the stratosphere; here, the temperature is constant and equal to $T - 0{\cdot}9\,(Z_c + 5)$, and so the height difference between P_1 and P' is given by

$$\begin{aligned} Z - (Z_c + 5) &= 0{\cdot}2211\,[T - 0{\cdot}9\,(Z_c + 5)] \log (P_1/P') \\ &= 0{\cdot}2211\,[T - 0{\cdot}9\,(Z_c + 5)].\,[\log (P/P') - \log (P/P_1)] \\ i.e.\ Z &= Z_c + 5 + 0{\cdot}2211\,[T - 0{\cdot}9\,(Z_c + 5)].\,[\log (P/P') - \varkappa] \qquad \ldots\ \ldots (21) \end{aligned}$$

2. (*b*) $\varkappa > \log (P/P')$. Both standard pressure levels are in the transition layer and so

$$Z = 0{\cdot}2211\,(T - 0{\cdot}45\,Z) \log (P/P'),$$

which gives $$Z = \frac{T}{0{\cdot}45 + 4{\cdot}523/\log (P/P')}\,. \qquad \ldots\ \ldots (22)$$

If $\varkappa = \log (P/P')$, $P' = P_1$ and $Z = Z_c + 5$.

3. $Z_c > +5$. Here P is in the troposphere. The case in which P' lies in the stratosphere does not occur; P' is in the troposphere or in the transition layer according as P_2 is less or greater than P'. The sub-classes are defined by a criterion λ such that

$$\lambda = \log (P/P_2) = \frac{Z_c - 5}{0{\cdot}2211\,[T - 0{\cdot}9\,(Z_c - 5)]}\,. \qquad \ldots\ \ldots (23)$$

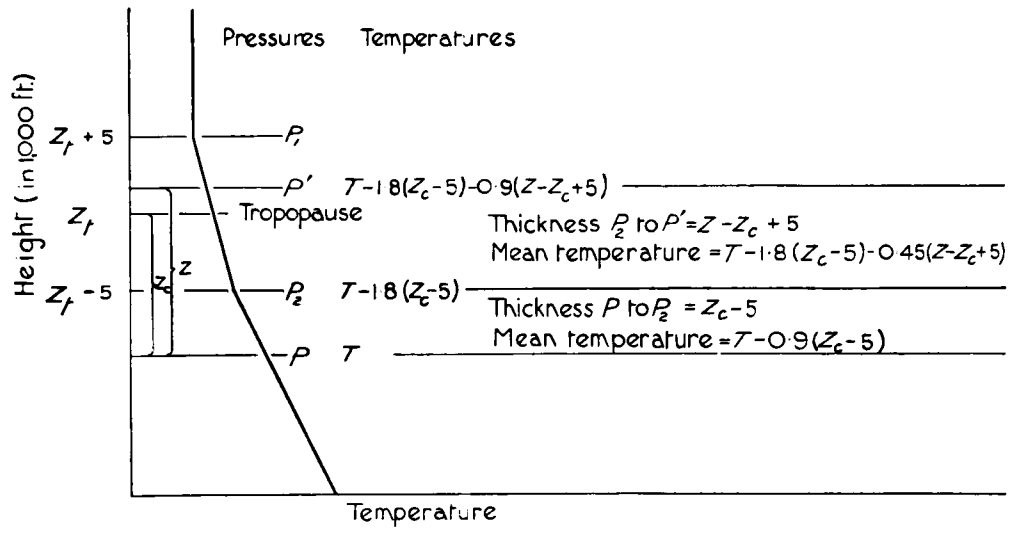

FIG. 17—POSITIONS OF PRESSURE LEVELS P AND P' FOR CASE 3(*a*) AND CORRESPONDING TEMPERATURES

3. (*a*) $\lambda < \log (P/P')$. The pressure level P' is in the transition layer (see Fig. 17) and the height difference between P_2 and P' is given by

$$Z - (Z_c - 5) = 0{\cdot}2211\,[T - 1{\cdot}8\,(Z_c - 5) - 0{\cdot}45\,(Z - Z_c + 5)] \log (P_2/P')$$

which gives $$Z = Z_c - 5 + \frac{T - 1{\cdot}8\,(Z_c - 5)}{0{\cdot}45 + 4{\cdot}523/[\log (P/P') - \lambda]} \qquad \ldots\ \ldots (24)$$

3. (*b*) $\lambda > \log (P/P')$. Both standard pressure levels are in the troposphere and we have, similar to 2 (*b*),

$$Z = \frac{T}{0{\cdot}9 + 4{\cdot}523/\log (P/P')} . \qquad .. \quad .. \quad (25)$$

Height difference between 500 and 300 mb.—For the parts of the world covered by the contour charts, the 500-mb. level was found to lie 12,000 ft. or more below the tropopause. The table of height differences used in the construction of the 300-mb. contours, therefore, entailed the use of formulæ (23), (24) and (25) only. These were evaluated for different temperatures, the appropriate values of P and P' having been inserted, *viz.* $P = 500$, $P' = 300$, giving $\log (P/P') = 0{\cdot}222$.

Height differences between 300 and 200 mb., 200 and 130 mb.—In the construction of the higher-level charts all five cases, 1, 2 (*a*), 2 (*b*), 3 (*a*), and 3 (*b*) occurred.

For the 200-mb. contours, $P = 300$, $P' = 200$, $\log (P/P') = 0{\cdot}176$ and the formulæ (19), (22) and (25) reduce to

$$(19)\ Z = 0{\cdot}0389\ T,$$
$$(22)\ Z = 0{\cdot}0383\ T,$$
$$(25)\ Z = 0{\cdot}0376\ T.$$

Formulæ (21) and (24) cannot be expressed in this simple form. For these substitute $0{\cdot}176$ for $\log (P/P')$, using $\varkappa$ or λ from (20) or (23).

For the 130-mb. contours, $P = 200$, $P' = 130$, $\log (P/P') = 0{\cdot}187$ and the formulæ are

$$(19)\ Z = 0{\cdot}0414\ T,$$
$$(22)\ Z = 0{\cdot}0406\ T,$$
$$(25)\ Z = 0{\cdot}0399\ T,$$

but again formulæ (21) and (24) cannot be expressed so simply. For these substitute $0{\cdot}187$ for $\log (P/P')$, $\varkappa$ or λ being given by (20) or (23).

Tables, giving Z for specified values of T and Z_c, were compiled from these formulæ.

APPENDIX II—USE OF PILOT-BALLOON OBSERVATIONS IN THE CONSTRUCTION OF WIND ROSES

In § 2 we showed how the frequency distribution of upper winds can be reconstructed, given the vector mean wind and a measure of the scatter such as the constancy q. In this part we set out a method by which these parameters may, in certain circumstances, be calculated approximately from the incomplete distribution given by a pilot-balloon summary, so that the true frequency distribution may be obtained.

At considerable heights many balloons are lost in the distance, and, as this generally happens with strong winds, an uncorrected summary is liable to lead to an underestimate of the frequency of strong winds, an error which may have disastrous results. The method described below is only applicable in regions or seasons of small cloud amount because clear days in cloudy regions may be associated with certain winds.

Summaries of pilot-balloon observations show a marked falling off in the number of observations at the higher levels. This is due to the following causes:—

(i) The bursting of the balloon at a lower level. This depends on the condition of the balloon, and may be supposed to affect all wind velocities in equal proportions.

(ii) The disappearance of the balloon in the distance. This affects only the higher wind velocities, and although the distance of the balloon at any instant depends, to a first approximation, on the resultant velocity of the whole layer of air which it has traversed, it is closely correlated with the velocity at the level under consideration.

(iii) The disappearance of the balloon in or behind cloud. It cannot be assumed that the distribution of the upper winds when much cloud is present resembles that on clear days; in fact there are probably marked differences in most cases.

(iv) Other causes, such as the abandonment of the ascent for various reasons, the drifting of the balloon " into the sun ", confusion with a star, etc. These may be regarded as " random " causes of loss. With them may be included cases in which the cause of loss is not stated.

No published tabulation of the frequency of the various causes of loss could be found, and the observations from six stations were accordingly analysed. These included :—

Iceland, Reykjavik (May 1942–June 1943), Kaldadarnes (May–June 1942), Akureyri (April 1942–January 1943);

Portugal, Lisbon (May 1942–June 1943);

Sudan, Khartoum (November 1935–October 1936);

Indian Ocean, Addu Atoll, 0° 41′ S., 73° 10′ E. (August 1942–February 1945).

In all there were 2,700 ascents. The causes of loss were: A (abandoned), 21 per cent.; B (balloon burst), 9 per cent.; C (lost in or behind cloud), 26 per cent.; D (lost in distance or haze), 14 per cent.; U (unknown or miscellaneous), 30 per cent. The percentage of ascents reaching different heights, and those lost below each height from different causes, are shown on the left-hand side of Table XV. Details for individual stations are shown in Table X, p. 15.

As the present investigation deals with wind roses in nearly cloudless regions or seasons, loss in cloud can be left out of account, and we are concerned only with the proportion lost by " random " causes (A, B, U) compared with those lost in the distance (D). At any given height we have actually n observations, and we require N, the total number which would have reached that height if none had been lost in the distance. This was calculated on the assumptions that, if the balloons lost in the distance could have been followed further, the losses by random causes would have been in the same proportion as those actually so lost, and that in any height interval the losses were uniformly distributed through the interval. The right-hand half of Table XV gives the calculated ratios $r = 100N/n$ for all six stations, and also for Addu Atoll (846 observations) to represent tropical oceanic conditions and Khartoum (568 observations) to represent a hazy region.

The method of calculation was briefly as follows: ignoring the ascents lost in cloud, the total number, n, reaching 1,000 ft. was computed. The number, b, lost from random causes (abandoned, burst, unknown and miscellaneous) in the layer 1,000–2,000 ft. was expressed as a fraction b/n. Let d be the number lost in the distance in the same layer. Consider a balloon lost in the distance at $2{,}000 - h$ ft. If it had not been so lost, the probability that it would have been lost by random causes in the layer of h ft. is assumed to be $(h/1{,}000) \times (b/n)$. Since losses in the distance are assumed to be uniformly distributed through the whole layer from 1,000 to 2,000 ft., h is to be assigned values at equal intervals from 0 to 1,000, so that the mean value of $h/1{,}000$ is $\frac{1}{2}$, and the number of balloons lost in the distance which would otherwise have

been lost by random causes is therefore $db/2n$. Hence the total number which would have been lost by random causes in the whole layer if none had been lost in the distance is not b but $b(1 + d/2n)$. In most cases the term $d/2n$ is small. This estimated loss, subtracted from the number known to have reached 1,000 ft., gives the number N which would have reached 2,000 ft. if none had been lost in the distance.

The same procedure is followed in the layer 2,000–3,000 ft., except that the number estimated to be lost by random causes must now be increased in the ratio N/n, where N denotes the number which would have been observed to reach 2,000 ft. if none had been lost in the distance, and n is the number actually observed. The loss suffered by N balloons in this layer by random causes is therefore $Nb(1 + d/2n)/n$ and this, subtracted from N, gives the new value of N at 3,000 ft. The same procedure is followed for all higher layers. The ratios $100N/n$ are then calculated and the values for successive heights are plotted against height and smoothed graphically.

TABLE XV—LOSSES OF PILOT BALLOONS, AND RATIOS $r = 100N/n$

A, abandoned; B, burst; C, cloud; D, distance or haze; U, unknown.

Height	Percentage reaching height	Percentage lost below height due to causes					Ratio $r = 100N/n$		
		A	B	C	D	U	6 Stations	Addu Atoll	Khartoum
ft.		*per cent.*					I	II	III
45,000	0·3	21·1	8·7	25·6	14·1	30·2	600	..	..
40,000	0·6	21·1	8·5	25·6	14·0	30·2	300	200	..
35,000	1·3	21·0	8·5	25·5	13·7	30·0	240	140	600
30,000	3	21·0	8·2	25·5	13·5	29·2	210	120	470
25,000	5	20·3	7·9	25·4	13·1	28·2	180	107	360
20,000	9	19·5	7·3	25·4	12·4	26·6	158	104	270
18,000	12	18·3	6·9	25·3	12·1	25·2	149	103	240
16,000	15	17·8	6·5	24·8	11·5	24·2	140	103	200
14,000	21	16·9	5·8	24·2	9·9	21·7	130	102	166
12,000	29	15·3	5·0	23·0	7·8	19·8	120	101	136
10,000	45	9·7	4·0	20·9	5·3	15·5	111	101	120
9,000	48	8·6	3·8	20·0	4·6	14·6	108	101	115
8,000	57	6·4	3·0	18·3	3·0	12·5	105	101	110
7,000	64	4·3	2·4	16·4	2·5	10·3	103	101	106
6,000	73	2·6	1·8	13·3	1·3	8·0	102	101	104
5,000	82	1·0	1·0	9·8	0·9	5·6	101	101	103
4,000	88	0·4	0·6	7·1	0·4	3·1	101	100	102
3,000	95	0·2	0·3	3·2	0·3	1·1	100	100	101
2,000	99	0·0	0·1	0·6	0·2	0·1	100	100	100
1,000	100	..	..	..	..	..	100	100	100

The figures in Tables X and XV show that the conditions vary greatly from one station to another. Either a hazy atmosphere or the prevalence of strong winds increases the percentage of balloons lost in the distance and so gives high values of r. The table can be used as a first approximation to estimate the proportion of balloons so lost, using columns I, II or III or interpolating between them, according to what is known of the local conditions.

The method of " completing " a pilot-balloon frequency summary, *i.e.* of making allowance for the missing observations, is one of trial and error. Various values of V_R and q are considered, and the calculated frequency distribution is compared with the observed frequency distribution for such of the lower speed ranges as can be assumed to be complete.

Table XVI gives a summary of 137 pilot-balloon observations (morning ascents only), June–September 1928–31, at 20,000 ft. over Bahrein (26° 0′ N. 50° 35′ E.). Frequencies are expressed as per mille of 137 to shorten subsequent calculations. The values Π are the sums of (central speed) × (per mille frequency) for each of the eight compass points, and the sum of all these gives $1{,}000V_S'$ where ′ indicates that the velocity is that given by the recorded observations. Similarly V_R' is given by

$$(1{,}000\ V_R')^2 = \{\Sigma(\Pi \cos \psi)\}^2 + \{\Sigma(\Pi \sin \psi)\}^2$$

where ψ is the angular departure of the mid direction of each group from north. Since V_R' is only a guide for determining V_R, it is not necessary to correct for the grouping of the directions. The constancy q' is given by $100V_R'/V_S'$. Since the majority of the missing winds can safely be assumed to have blown from near the prevailing direction, q' gives the lower limit in estimating q.

TABLE XVI—UPPER WINDS AT 20,000 FT. OVER BAHREIN, JUNE–SEPTEMBER

137 observations. Mean cloud amount 0·4 tenths.

Speed	N.	NE.	E.	SE.	S.	SW.	W.	NW.	All directions
kt.				*per mille*					
0–10	..	..	..	..	..	..	..	..	328 } 854
10–20	73	139	80	73	15	37	29	80	526 }
20–30	22	15	44	14	..	7	8	15	125
30–50	7	..	7	..	..	..	..	7	21
All speeds	102	154	131	87	15	44	37	102	1000
Π	1925	2460	2580	1445	225	730	635	1855	$13495 = 1000\ V_S'$
$\Pi \cos \psi$	+1925	+1732	0	−1019	−225	−515	0	+1308	$+3206 = \Sigma(\Pi \cos \psi)$
$\Pi \sin \psi$	0	+1732	+2580	+1019	0	−515	−635	−1308	$+2873 = \Sigma(\Pi \sin \psi)$

$V_S' = 13{\cdot}5 \quad V_R' = 4{\cdot}3 \quad q' = 32$

The next step is to determine the limiting speed, if any, above which the observations are incomplete owing to losses in the distance. The simplest method is to compare the total frequencies for " All directions " with those derived from the appropriate theoretical summary (Appendix IV) taking $V_R = V_R'$ and $q = q'$. At Bahrein $q' = 32$ and $V_R' = 4{\cdot}3$ kt. The comparison gives us the following table.

TABLE XVII—FREQUENCIES OF WIND STRENGTH AT 20,000 FT. OVER BAHREIN, JUNE–SEPTEMBER

Speed	V/V_R	Theoretical $q = 32$, $V_R = 4{\cdot}3$	Observed $q' = 32$, $V_R' = 4{\cdot}3$
kt.		*per mille*	
0–10	0 – 2·32	348	328
10–20	2·33– 4·65	459	526
20–30	4·66– 6·95	165	125
30–50	6·96–11·64	29	21

The method of determining the total frequencies was described in § 2.

The observed frequencies are too high for the range 10–20 kt. and too low for ranges above 20 kt. Hence we assume that the observations are " complete " up to 20 kt. The observed values are too low in the range 0–10 kt.; this is to be expected, since a higher value of V_R would decrease the theoretical frequency in the lowest speed range. This is another indication that the value of 4·3 for V_R is too low.

In some cases the comparison does not at first sight give a clear answer to the question whether the series is " complete ". Thus at 10,000 ft. over Helwan, March–May (671 observations), the frequencies are as follows :—

Speed	$q' = 65$, $V_R' = 12{\cdot}3$ kt. Theoretical	Observed
kt.	*per mille*	
0– 2	17 (11)	9 (6)
3–13	296 (197)	329 (220)
14–27	483 (324)	458 (307)
28–40	177 (119)	177 (119)
Over 40	27 (18)	27 (18)

The figures in brackets show the actual numbers of observations and the theoretical frequencies reduced to a total of 671 for comparison. The agreement is very good for the higher speeds; for the lower speeds the differences, though appreciable, are irregular. Application of the chi-square test to the figures in brackets shows that if the observations are " complete " and the distribution normal, differences of this magnitude would arise by chance 5 times in 100. It is doubtful whether the series is " complete " or not, but in any case the number of missing observations due to selective causes such as loss in the distance cannot be very great, and it seems to be safe to accept the distribution without " completion ", *i.e.* to assume that the irregularities in the observed distribution are due to random causes and not to a bias in favour of [illegible] er speeds. Note that if the same value of chi-square had been found with the frequencies of the higher speeds systematically smaller than those given by theory, we should have regarded the series as " incomplete ".

Another example is at 10,000 ft. over Insalah, September–November. The observed distribution of 99 observations, well spaced in time, and the theoretical distribution ($q = 20$) are :

$q' = 18$, $V_R' = 3{\cdot}03$ kt.

Speed	Theoretical	Observed
kt.		
0– 2	2·4	0
3–13	43·4	43
14–27	45·4	45
28–40	7·4	9
Over 40	0·4	2

With these groupings of frequencies the chi-square test is not possible, but the fit obviously is very good. We therefore accept the series as " complete ".

The method of determining the total frequencies was described in § 2.

The observed frequencies are too high for the range 10–20 kt. and too low for ranges above 20 kt. Hence we assume that the observations are " complete " up to 20 kt. The observed values are too low in the range 0–10 kt.; this is to be expected, since a higher value of V_R would decrease the theoretical frequency in the lowest speed range. This is another indication that the value of 4·3 for V_R is too low.

In some cases the comparison does not at first sight give a clear answer to the question whether the series is " complete ". Thus at 10,000 ft. over Helwan, March–May (671 observations), the frequencies are as follows :—

Speed	$q' = 65$, $V_R' = 12{\cdot}3$ kt. Theoretical	Observed
kt.	*per mille*	
0– 2	17 (11)	9 (6)
3–13	296 (197)	329 (220)
14–27	483 (324)	458 (307)
28–40	177 (119)	177 (119)
Over 40	27 (18)	27 (18)

The figures in brackets show the actual numbers of observations and the theoretical frequencies reduced to a total of 671 for comparison. The agreement is very good for the higher speeds; for the lower speeds the differences, though appreciable, are irregular. Application of the chi-square test to the figures in brackets shows that if the observations are " complete " and the distribution normal, differences of this magnitude would arise by chance 5 times in 100. It is doubtful whether the series is " complete " or not, but in any case the number of missing observations due to selective causes such as loss in the distance cannot be very great, and it seems to be safe to accept the distribution without " completion ", *i.e.* to assume that the irregularities in the observed distribution are due to random causes and not to a bias in favour of the lower speeds. Note that if the same value of chi-square had been found with the observed frequencies of the higher speeds systematically smaller than those given by theory, we should have regarded the series as " incomplete ".

Another example is at 10,000 ft. over Insalah, September–November. The observed distribution of 99 observations, well spaced in time, and the theoretical distribution ($q = 20$) are :

$q' = 18$, $V_R' = 3{\cdot}03$ kt.

Speed	Theoretical	Observed
kt.		
0– 2	2·4	0
3–13	43·4	43
14–27	45·4	45
28–40	7·4	9
Over 40	0·4	2

With these groupings of frequencies the chi-square test is not possible, but the fit obviously is very good. We therefore accept the series as " complete ".

In practice it is found that, save in exceptionally hazy regions, pilot-balloon summaries are generally sufficiently "complete" up to 10,000 ft., but at 20,000 ft. and above many of the higher speeds are missing.

Returning to the table for Bahrein, we have found that it is "complete", *i.e.* unbiassed in respect of wind speeds, up to a speed of 20 kt. The next stage is to compute from this part of the distribution values of q and V_R and also the resultant direction α, given by

$$\tan \alpha = \Sigma(\Pi \sin \psi)/\Sigma(\Pi \cos \psi) \ .$$

In computing these, corrections should be applied for grouping of the observations.*

In § 2 it was shown that a "long-period" wind distribution is symmetrical about the resultant direction, so that the latter can be found from the lower speed groups only. In an incomplete summary the omissions in the higher speeds are not necessarily symmetrical about the vector mean wind, owing to differences in visibility or in the wind structure of the lower layers for different wind directions at 20,000 ft. The resultant direction is therefore calculated only from the speed ranges which are accepted as unbiassed. Other parameters computed from this part of the frequency summary are distinguished by a double dash; for Bahrein,

$$V_R'' = 3{\cdot}3 \text{ kt.}, \ q'' = 25, \ \alpha = 40°.$$

From Table XV we find that the percentage ratio r of the probable total number of ascents reaching 20,000 ft., including those lost in the distance, to those followed to that height lies between 104 (Addu Atoll) and 270 (Khartoum). Since the region is neither exceptionally clear or calm nor exceptionally hazy or windy, the value of r is probably near the average figure of 158. Since we are working with only part of the observed summary however, we have to multiply these limits by $1{,}000/F''$, where F'' is the frequency per mille in the unbiassed part of the table. For Bahrein we find from Table XVI that F'' is 854, whence the percentage ratio r'' of the total number of observations to those in the range 0–20 kt. lies between 122 and 316, and probably near 185.

For any given value of q, we can calculate from Tables XXI–XXXIII the value of q'' for that part of the frequency summary for which the values of V/V_R are less than any given value. The ratio between the total (all directions) for all speeds and that for all speeds less than V/V_R gives us the value of r''. In the same way we can calculate the vector mean velocity of this limited part of the distribution in the terms of V_R, and so obtain the ratio V_R/V_R''. For example, with $q = 80$, we have the values of q'', V_R/V_R'' and r'', shown in Table XVIII.

TABLE XVIII—VALUES OF q'', V_R/V_R'' AND r''

Upper limit of V/V_R	q''	V_R/V_R''	r''
0·8	55	3·48	426
1·0	62	2·46	279
1·2	68	1·90	203
1·4	72	1·57	160
1·6	75	1·36	135
1·8	77	1·22	120
2·0	78	1·13	111

Thus for every pair of values of q and q'' there are corresponding values of V_R/V_R'' and r''. Isopleths of these values are shown in Fig. 18.

* Briefly, the rule is: for any direction, subtract the frequency of the direction preceding it (clockwise) from that of the direction following it, divide by the frequency of the direction itself and multiply by 15/8. This gives the positive or negative correction in degrees.

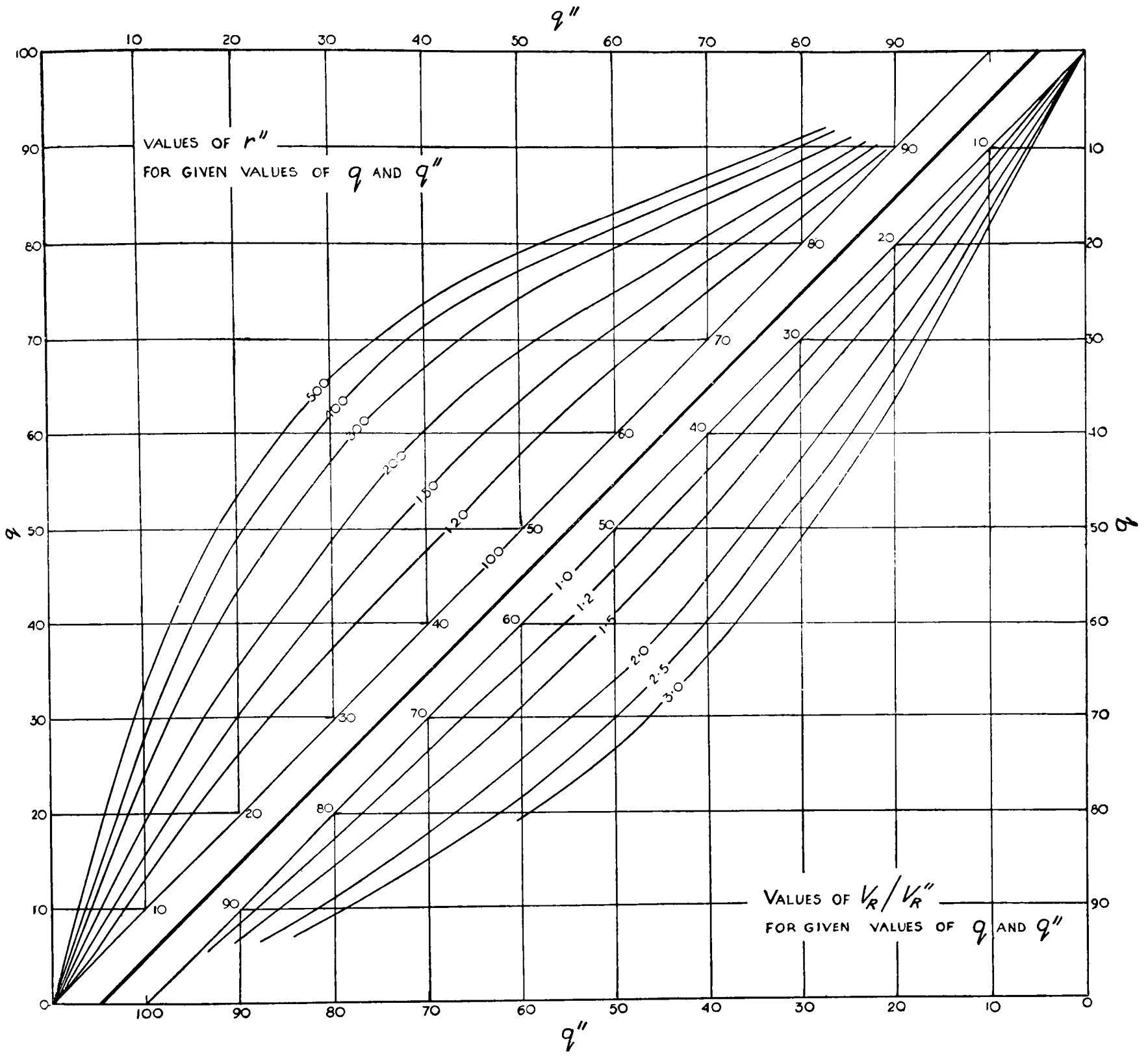

FIG. 18—VALUES OF r'' AND V_R/V_R'' FOR GIVEN VALUES OF q AND q''

From Fig. 18 we find that with $q'' = 25$ and r'' between 122 and 316 with a most probable value of about 185, q must lie between 32 and 52 with a most probable value of about 41. Since $q' = 32$ and q cannot be less than q', this also fixes the lower limit at 32.

We will choose three values of q for testing purposes. The three most convenient in the neighbourhood of $q = 41$ are 35, 40 and 45; the corresponding values of V_R/V_R'' are read from Fig. 18; V_R is obtained by multiplying these values by $V_R'' = 3{\cdot}3$ kt.

q	35	40	45
V_R/V_R''	1·79	2·34	2·95
V_R	5·9	7·7	9·7

Theoretical frequencies for the ranges 0–10, 10–20 and over 20 kt. are worked for each pair of values of q and V_R by the method of § 2. The total of these will be 1,000, but this refers to the total of a " complete " distribution, which is $r/100$ times the total of the observed summary. Before comparing with the observed per mille frequencies therefore, the theoretical frequencies need to be multiplied by $r/100$, *i.e.* by

$$\frac{r''}{100} \cdot \frac{F''}{1{,}000}$$

where r'' is the value in Fig. 9 corresponding with $q'' = 25$ and the value of q selected for testing. The comparison of the observed with the three theoretical distributions selected for testing is shown in the following table :

TABLE XIX—OBSERVED AND THEORETICAL WIND FREQUENCIES AT 20,000 FT. OVER BAHREIN

	Theoretical frequency			Observed frequency
kt.		*per mille*		
0–10	285 } 770	287 } 846	309 } 939	328 } 854
10–20	485 }	559 }	630 }	526 }
Over 20	421	641	998	(146)
Total	1,191	1,487	1,937	(1,000)
Assumed values				
q	35	40	45	32–52
V_R	5·9	7·7	9·7	⩾5·1
r	119	149	194	104–158–270

Agreement between observed and theoretical frequency for the whole of the range 0–20 kt. is very close when q is taken as 40 and is not improved when q is 41. We therefore adopt for Bahrein at 20,000 ft. the values $q = 40$, $V_R = 7{\cdot}7$ kt.

The numbers in brackets (" observed ") denote that here some observations are missing. The total of each of the theoretical distributions is approximately $10r$. It will be noted that as q and V_R increase, r increases, for a greater number of missing observations of high speeds will have to be added to the observed (" incomplete ") summary to give the greater values of q and V_R. Also, the more q is increased the greater tendency there is for observations to cluster about the vector mean. In the example taken here, V_R falls in the range 0–20 kt. and so the frequency for this part of the distribution increases as q increases, and only for the true value of q will it agree with the observed frequency for this range.

One might expect a possible check to be given by the ratio between the frequencies in the ranges 0–10 and 10–20 kt. This is 0·62 in the observed values, while with $q = 40$ it is only 0·51 and with $q = 35$, 0·59. To obtain a ratio of 0·62 we should have to reduce q to 32, the extreme limit of the possible range. In practice however we often find a tendency for too many observations to be placed in the lowest speed range, so that all that this ratio tells us is that q is not less than 32, which we know already.

A more reliable check is obtained by comparing the theoretical and observed frequencies of different directions in the unbiassed part of the distribution for which directions are given, in this case 10–20 kt. The result is shown in Fig. 19. The broken line representing the theoretical

frequencies is a reasonably good smoothing of the full line representing the observed frequencies, and suggests that the parameters used ($q = 40$, $V_R = 7{\cdot}7$ kt.) are sufficiently accurate. The theoretical " completed " summary is shown in Table XX with the actual numbers of observations in brackets for comparison. The total theoretical frequency is $r \times$ (number observed) = 204.

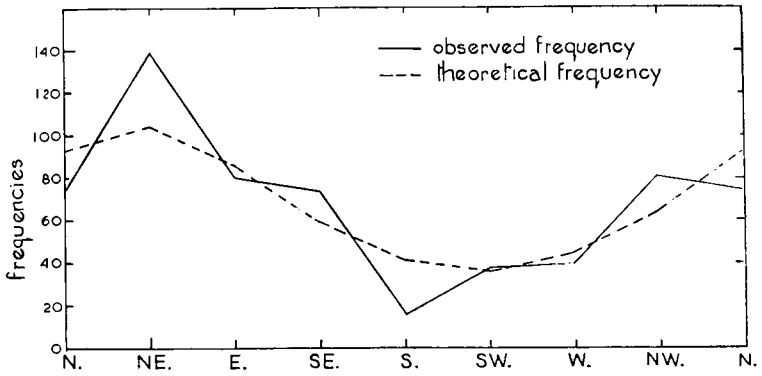

FIG. 19—FREQUENCIES IN RANGE 10–20 kt. AT 20,000 FT. OVER BAHREIN
expressed as per mille of actual observations
June–September

TABLE XX—THEORETICAL WIND FREQUENCIES AT 20,000 FT. OVER BAHREIN

$q = 40$, $V_R = 7{\cdot}7$ kt.

Speed	N.	NE.	E.	SE.	S.	SW.	W.	NW.	Total
kt.									
0–10	..	..	..	..	..	..	..	..	39·4 (45)
10–20	13·5 (10)	15·2 (19)	12·6 (11)	8·6 (10)	5·9 (2)	5·2 (5)	6·3 (4)	9·3 (11)	76·6 (72)
	1·6 (3)	14·1 (2)	10·4 (6)	5·6 (2)	3·1 (—)	2·5 (1)	3·4 (1)	6·4 (2)	57·1 (17)
Over 30	7·1 (1)	9·4 (—)	6·1 (1)	2·4 (—)	1·0 (—)	0·7 (—)	1·2 (—)	3·0 (1)	30·9 (3)
Total	32·2 (14)	38·7 (21)	29·1 (18)	16·6 (12)	10·0 (2)	8·4 (6)	10·9 (5)	18·7 (14)	204·0 (137)

APPENDIX III—LIST OF SYMBOLS

b = number of losses of pilot-balloon observations in a specified layer due to random causes

d = number of losses of pilot-balloon observations in a specified layer due to distance or haze

F = approximate theoretical frequency

F'' = frequency per mille in the unbiassed part of a wind summary

g = acceleration due to gravity

m = ratio, v/V_R or V_R/v, less than unity

N = number of winds which would have been recorded had no balloons been lost in distance or haze

n = actual number of winds recorded

P = standard pressure level; in Appendix I the lower of two levels

P' = the upper of two standard pressure levels

P_1 = pressure level 5,000 ft. above the tropopause

P_2 = pressure level 5,000 ft. below the tropopause

P_m = pressure level of σ_m

p = pressure

p_0 = surface pressure

Q = a parameter in the relation between q and σ

q = constancy of winds = $100V_R/V_S$

q' = constancy computed from an " incomplete " wind summary

q'' = value of q computed from the unbiassed part of a wind summary

R = gas constant

r = ratio, $100N/n$

r'' = ratio of N to the number of winds in the unbiassed part of a wind summary

T = temperature

T_0 = surface temperature

T_m = temperature at the level of σ_m

V = wind speed

V_a = average speed in a specified direction

$\mathbf{V_R}$ = vector mean wind

V_R = magnitude of $\mathbf{V_R}$, sometimes referred to as vector mean speed

V_S = scalar mean wind, *i.e.* average (or mean) speed

V_R' = values of V_R computed from an " incomplete " wind summary

V_S' = value of V_S computed from an " incomplete " wind summary

V_R'' = value of V_R given by the unbiassed part of a wind summary

$\mathbf{v}$ = vector deviation of a wind from the vector mean wind summary

v = magnitude of $\mathbf{v}$

x = ratio, v/V_R

$\bar{x}$ = parameter, $V_R \cos \phi$

Z = height of P' above P

Z_c = height of the tropopause above the pressure level, P

Z_t = height of the tropopause above M.S.L.

Z_{700} = height of 700-mb. level above the surface

Z_{500} = height of 500-mb. level above the surface

z = transformed variable, $(V - \bar{x})/\sigma$

α = resultant wind direction, *i.e.* direction of $\mathbf{V_R}$

β = lapse rate of temperature with height

γ = proportion

θ = angle which $\mathbf{v}$ makes with $\mathbf{V_R}$

$\varkappa$ = criterion, log (P/P_1)

λ = criterion, log (P/P_2)

Π = sum of (central speed) × (per mille frequency) in each speed range for a specified direction

ρ = air density

σ = standard vector deviation, root mean square of v

σ_{700}, σ_{500}, ⋮, σ_{130} = standard vector deviation of winds at 700 mb., 500 mb.,.....130 mb.

σ_m = maximum value of σ in the variation of σ with height

σ_0 = standard vector deviation of surface winds

ϕ = angle which a wind makes with $\mathbf{V_R}$ (except in the footnote to Table IX)

ψ = angular departure from north, through east

APPENDIX IV—TABLES FOR THE CONSTRUCTION OF WIND ROSES; FREQUENCY DISTRIBUTION

TABLE XXI

$q = 98$ $\sigma/V_R = 0{\cdot}28$

V/V_R \ ϕ	0–20	20–40	40–60	All directions
	per mille			
0·0–0·1	—	—	—	—
0·1–0·2	—	—	—	—
0·2–0·3	—	—	—	—
0·3–0·4	0·2	0·1	—	0·6
0·4–0·5	1·1	0·3	—	2·8
0·5–0·6	4·8	0·9	—	11·4
0·6–0·7	15·1	2·1	0·1	34·6
0·7–0·8	36·0	3·7	0·1	79·6
0·8–0·9	65·5	5·0	—	141·0
0·9–1·0	90·9	5·1	—	192·0
1·0–1·1	96·6	4·0	—	201·2
1·1–1·2	78·8	2·4	—	162·4
1·2–1·3	49·5	1·1	—	101·2
1·3–1·4	23·9	0·4	—	48·6
1·4–1·5	8·9	0·1	—	18·0
1·5–1·6	2·6	—	—	5·2
1·6–1·7	0·6	—	—	1·2
1·7–1·8	0·1	—	—	0·2
All speeds	474·6	25·2	0·2	1000·0

TABLE XXII

$q = 97$ $\sigma/V_R = 0{\cdot}37$

V/V_R \ ϕ	0–20	20–40	40–60	60–80	All directions
			per mille		
0·0–0·1	—	—	—	—	—
0·1–0·2	0·1	—	—	—	0·2
0·2–0·3	0·3	0·2	0·1	—	1·2
0·3–0·4	1·2	0·7	0·2	—	4·2
0·4–0·5	3·6	1·7	0·4	0·1	11·6
0·5–0·6	9·0	3·5	0·6	0·1	26·4
0·6–0·7	18·7	6·1	0·7	—	51·0
0·7–0·8	32·7	8·9	0·8	—	84·8
0·8–0·9	48·5	11·1	0·7	—	120·6
0·9–1·0	61·3	11·8	0·5	—	147·2
1·0–1·1	66·3	10·7	0·4	—	154·8
1·1–1·2	61·4	8·3	0·2	—	139·8
1·2–1·3	48·7	5·6	0·1	—	108·8
1·3–1·4	33·2	3·2	—	—	72·8
1·4–1·5	19·5	1·6	—	—	42·2
1·5–1·6	9·8	0·7	—	—	21·0
1·6–1·7	4·2	0·2	—	—	8·8
1·7–1·8	1·6	0·1	—	—	3·4
1·8–1·9	0·5	—	—	—	1·0
1·9–2·0	0·1	—	—	—	0·2
2·0–2·1	—	—	—	—	—
All speeds	420·7	74·4	4·7	0·2	1000·0

TABLE XXIII

$q = 95$ $\sigma/V_R = 0{\cdot}47$

V/V_R \ ϕ	0–20	20–40	40–60	60–80	80–100	100–120	120–140	140–160	160–180	All directions
					per mille					
0·0–0·2	0·2	0·2	0·2	0·1	0·1	0·1	0·1	0·1	—	2·2
0·2–0·4	3·1	2·3	1·2	0·5	0·2	0·1	—	—	—	14·8
0·4–0·6	15·1	8·8	3·2	0·8	0·2	—	—	—	—	56·2
0·6–0·8	42·9	20·0	4·8	0·7	0·1	—	—	—	—	137·0
0·8–1·0	77·4	28·9	4·6	0·4	—	—	—	—	—	222·6
1·0–1·2	91·8	27·6	3·0	0·1	—	—	—	—	—	245·0
1·2–1·4	73·1	17·7	1·3	—	—	—	—	—	—	184·2
1·4–1·6	39·3	7·7	0·3	—	—	—	—	—	—	94·6
1·6–1·8	14·4	2·3	0·1	—	—	—	—	—	—	33·6
1·8–2·0	3·6	0·5	—	—	—	—	—	—	—	8·2
2·0–2·2	0·6	0·1	—	—	—	—	—	—	—	1·4
2·2–2·4	0·1	—	—	—	—	—	—	—	—	0·2
All speeds	361·6	116·1	18·7	2·6	0·6	0·2	0·1	0·1	—	1000·0

TABLE XXIV

$q = 90$ $\sigma/V_R = 0{\cdot}64$

V/V_R \ ϕ	0–20	20–40	40–60	60–80	80–100	100–120	120–140	140–160	160–180	All directions
					per mille					
0·0–0·2	0·7	0·7	0·6	0·5	0·4	0·4	0·3	0·3	0·3	8·4
0·2–0·4	4·8	4·0	2·9	1·9	1·1	0·7	0·4	0·3	0·3	32·8
0·4–0·6	14·2	10·6	6·1	2·9	1·3	0·6	0·3	0·2	0·1	72·6
0·6–0·8	29·2	19·3	8·9	3·2	1·0	0·3	0·1	0·1	0·1	124·4
0·8–1·0	45·0	26·5	9·9	2·6	0·5	0·1	0·1	—	—	169·4
1·0–1·2	54·2	28·4	8·4	1·6	0·3	0·1	—	—	—	186·0
1·2–1·4	51·8	24·1	5·8	0·8	0·1	—	—	—	—	165·2
1·4–1·6	39·6	16·5	3·1	0·3	0·1	—	—	—	—	119·2
1·6–1·8	24·4	9·1	1·4	0·1	—	—	—	—	—	70·0
1·8–2·0	12·2	4·0	0·5	0·1	—	—	—	—	—	33·6
2·0–2·2	4·9	1·4	0·2	—	—	—	—	—	—	13·0
2·2–2·4	1·6	0·4	0·1	—	—	—	—	—	—	4·2
2·4–2·6	0·4	0·1	—	—	—	—	—	—	—	1·0
2·6–2·8	0·1	—	—	—	—	—	—	—	—	0·2
All speeds	283·1	145·1	47·9	14·0	4·8	2·2	1·2	0·9	0·8	1000·0

TABLE XXV

$q = 80$ $\sigma/V_R = 0{\cdot}93$

V/V_R \ ϕ	0–20	20–40	40–60	60–80	80–100	100–120	120–140	140–160	160–180	All directions
					per mille					
0·0–0·2	1·0	1·0	0·9	0·9	0·8	0·7	0·7	0·7	0·6	14·6
0·2–0·4	4·3	4·0	3·4	2·8	2·2	1·7	1·4	1·2	1·1	44·2
0·4–0·6	9·4	8·2	6·4	4·5	3·0	2·0	1·5	1·1	1·0	74·2
0·6–0·8	15·7	13·0	9·0	5·6	3·2	1·9	1·1	0·8	0·7	102·0
0·8–1·0	21·9	17·2	10·8	5·8	2·9	1·4	0·8	0·5	0·4	123·4
1·0–1·2	26·7	19·8	11·2	5·3	2·2	0·9	0·4	0·2	0·2	133·8
1·2–1·4	28·6	20·0	10·3	4·2	1·5	0·5	0·2	0·1	0·1	131·0
1·4–1·6	27·2	18·1	8·4	3·0	0·9	0·3	0·1	—	—	116·0
1·6–1·8	23·3	14·6	6·1	1·9	0·5	0·1	0·1	—	—	93·2
1·8–2·0	17·9	10·7	4·0	1·1	0·2	0·1	—	—	—	68·0
2·0–2·2	12·4	7·0	2·4	0·5	0·1	—	—	—	—	44·8
2·2–2·4	7·8	4·2	1·3	0·3	—	—	—	—	—	27·2
2·4–2·6	4·4	2·2	0·6	0·1	—	—	—	—	—	14·6
2·6–2·8	2·3	1·1	0·3	—	—	—	—	—	—	7·4
2·8–3·0	1·1	0·5	0·1	—	—	—	—	—	—	3·4
3·0–3·2	0·5	0·2	—	—	—	—	—	—	—	1·4
3·2–3·4	0·2	0·1	—	—	—	—	—	—	—	0·6
3·4–3·6	0·1	—	—	—	—	—	—	—	—	0·2
All speeds	204·8	141·9	75·2	36·0	17·5	9·6	6·3	4·6	4·1	1000·0

TABLE XXVI

$q = 70$ $\sigma/V_R = 1{\cdot}24$

V/V_R \ ϕ	0–20	20–40	40–60	60–80	80–100	100–120	120–140	140–160	160–180	All directions
						per mille				
0·0–0·2	0·8	0·8	0·8	0·8	0·7	0·7	0·7	0·7	0·6	13·2
0·2–0·4	3·1	3·0	2·8	2·4	2·1	1·9	1·7	1·5	1·4	39·8
0·4–0·6	6·0	5·6	4·8	4·0	3·2	2·6	2·1	1·8	1·7	63·6
0·6–0·8	9·3	8·5	6·9	5·2	3·8	2·8	2·1	1·8	1·6	84·0
0·8–1·0	12·5	11·0	8·5	6·0	4·0	2·7	1·9	1·5	1·3	98·8
1·0–1·2	15·4	12·9	9·4	6·1	3·8	2·3	1·5	1·1	0·9	106·8
1·2–1·4	17·1	14·1	9·6	5·8	3·3	1·8	1·1	0·8	0·6	108·4
1·4–1·6	17·8	14·1	9·2	5·1	2·6	1·3	0·7	0·5	0·4	103·4
1·6–1·8	17·2	13·3	8·2	4·2	2·0	0·9	0·5	0·3	0·2	93·6
1·8–2·0	15·6	11·6	6·7	3·2	1·4	0·6	0·3	0·2	0·1	79·4
2·0–2·2	13·5	9·6	5·2	2·3	0·9	0·3	0·1	0·1	—	64·0
2·2–2·4	10·6	7·4	3·8	1·6	0·6	0·2	0·1	—	—	48·6
2·4–2·6	8·0	5·5	2·7	1·0	0·3	0·1	—	—	—	35·2
2·6–2·8	5·7	3·7	1·7	0·6	0·2	0·1	—	—	—	24·0
2·8–3·0	3·8	2·5	1·1	0·3	0·1	—	—	—	—	15·6
3·0–3·2	2·5	1·5	0·6	0·2	—	—	—	—	—	9·6
3·2–3·4	1·5	0·9	0·5	0·1	—	—	—	—	—	6·0
3·4–3·6	0·8	0·5	0·2	—	—	—	—	—	—	3·0
3·6–3·8	0·4	0·3	0·1	—	—	—	—	—	—	1·6
3·8–4·0	0·3	0·1	—	—	—	—	—	—	—	0·8
4·0–4·2	0·1	0·1	—	—	—	—	—	—	—	0·4
Over 4·2	0·1	—	—	—	—	—	—	—	—	0·2
All speeds	162·1	127·0	82·8	48·9	29·0	18·3	12·8	10·3	8·8	1000·0

TABLE XXVII

$q = 60$ $\sigma/V_R = 1{\cdot}60$

V/V_R \ ϕ	0–20	20–40	40–60	60–80	80–100	100–120	120–140	140–160	160–180	All directions
						per mille				
0·0–0·4	2·7	2·6	2·6	2·4	2·3	2·2	2·1	2·0	2·0	41·8
0·4–0·8	9·7	9·2	8·3	7·2	6·1	5·2	4·5	4·0	3·9	116·2
0·8–1·2	17·2	15·6	13·1	10·4	7·9	6·0	4·8	4·0	3·6	165·2
1·2–1·6	22·4	19·6	15·4	11·1	7·6	5·2	3·8	3·0	2·6	181·4
1·6–2·0	23·8	20·1	14·7	9·6	5·9	3·7	2·4	1·7	1·5	166·8
2·0–2·4	21·1	17·3	11·7	7·0	3·9	2·1	1·3	0·9	0·7	132·0
2·4–2·8	16·1	12·6	8·0	4·3	2·2	1·1	0·6	0·4	0·2	91·0
2·8–3·2	10·5	8·0	4·7	2·3	1·0	0·5	0·2	0·1	0·1	54·8
3·2–3·6	5·9	4·3	2·4	1·1	0·4	0·2	0·1	0·1	—	29·0
3·6–4·0	2·9	2·0	1·1	0·4	0·2	0·1	—	—	—	13·4
4·0–4·4	1·3	0·8	0·4	0·2	0·1	—	—	—	—	5·6
4·4–4·8	0·5	0·3	0·1	0·1	—	—	—	—	—	2·0
4·8–5·2	0·2	0·1	—	—	—	—	—	—	—	0·6
5·2–5·6	0·1	—	—	—	—	—	—	—	—	0·2
All speeds	134·4	112·5	82·5	56·1	37·6	26·3	19·8	16·2	14·6	1000·0

TABLE XXVIII

$q = 50$ $\sigma/V_R = 2{\cdot}04$

V/V_R \ ϕ	0–20	20–40	40–60	60–80	80–100	100–120	120–140	140–160	160–180	All directions
						per mille				
0·0–0·4	1·8	1·8	1·8	1·7	1·7	1·6	1·6	1·5	1·5	30·0
0·4–0·8	6·2	5·9	5·6	5·1	4·6	4·2	3·8	3·6	3·5	85·0
0·8–1·2	10·6	10·0	9·0	7·8	6·6	5·6	4·8	4·4	4·1	125·8
1·2–1·6	14·3	13·2	11·3	9·2	7·4	5·8	4·7	4·1	3·8	147·6
1·6–2·0	16·3	14·7	12·1	9·3	6·9	5·1	4·0	3·3	2·9	149·2
2·0–2·4	16·3	14·4	11·4	8·3	5·8	4·0	2·9	2·3	2·0	134·8
2·4–2·8	14·7	12·7	9·6	6·6	4·3	2·8	1·9	1·4	1·2	110·4
2·8–3·2	12·0	10·1	7·3	4·7	2·9	1·8	1·1	0·8	0·7	82·8
3·2–3·6	8·8	7·3	5·0	3·1	1·8	1·0	0·6	0·4	0·4	56·8
3·6–4·0	6·0	4·8	3·2	1·8	1·0	0·5	0·3	0·2	0·2	36·0
4·0–4·4	3·7	2·9	1·8	1·0	0·5	0·2	0·1	0·1	0·1	20·8
4·4–4·8	2·1	1·6	1·0	0·5	0·2	0·1	0·1	—	—	11·2
4·8–5·2	1·1	0·8	0·5	0·2	0·1	0·1	—	—	—	5·6
5·2–5·6	0·5	0·4	0·2	0·1	0·1	—	—	—	—	2·6
5·6–6·0	0·2	0·2	0·1	—	—	—	—	—	—	1·0
6·0–6·4	0·1	0·1	—	—	—	—	—	—	—	0·4
All speeds	114·7	100·9	79·9	59·4	43·9	32·8	25·9	22·1	20·4	1000·0

TABLE XXIX

$q = 40$ $\sigma/V_R = 2{\cdot}64$

V/V_R \ ϕ	0–20	20–40	40–60	60–80	80–100	100–120	120–140	140–160	160–180	All directions
						per mille				
0·0–0·6	2·7	2·6	2·6	2·5	2·4	2·4	2·3	2·3	2·2	44·0
0·6–1·2	8·5	8·4	7·8	7·2	6·6	6·0	5·6	5·3	5·1	121·0
1·2–1·8	13·6	13·0	11·8	10·4	8·9	7·7	6·8	6·2	5·9	168·6
1·8–2·4	16·6	15·5	13·5	11·3	9·2	7·5	6·3	5·5	5·1	181·0
2·4–3·0	16·8	15·3	12·9	10·2	7·8	6·0	4·8	4·0	3·7	163·0
3·0–3·6	14·5	13·0	10·5	7·9	5·7	4·1	3·1	2·5	2·3	127·2
3·6–4·2	10·9	9·6	7·5	5·4	3·6	2·5	1·8	1·4	1·2	87·8
4·2–4·8	7·3	6·2	4·7	3·2	2·0	1·3	0·9	0·7	0·6	53·8
4·8–5·4	4·3	3·6	2·6	1·7	1·0	0·6	0·4	0·3	0·2	29·4
5·4–6·0	2·2	1·9	1·3	0·8	0·4	0·2	0·2	0·1	0·1	14·4
6·0–6·6	1·1	0·8	0·6	0·3	0·2	0·1	0·1	—	—	6·4
6·6–7·2	0·4	0·4	0·2	0·1	0·1	—	—	—	—	2·4
7·2–7·8	0·2	0·1	0·1	—	—	—	—	—	—	0·8
7·8–8·4	0·1	—	—	—	—	—	—	—	—	0·2
All speeds	99·2	90·4	76·1	61·0	47·9	38·4	32·3	28·3	26·4	1000·0

TABLE XXX

$q = 30$ $\sigma/V_R = 3{\cdot}68$

V/V_R \ ϕ	0–20	20–40	40–60	60–80	80–100	100–120	120–140	140–160	160–180	All directions
						per mille				
0·0– 0·6	1·5	1·4	1·4	1·4	1·4	1·3	1·3	1·3	1·3	24·6
0·6– 1·2	4·4	4·3	4·2	4·1	3·9	3·7	3·6	3·4	3·4	70·0
1·2– 1·8	7·2	7·1	6·7	6·3	5·8	5·4	5·0	4·8	4·7	106·0
1·8– 2·4	9·4	9·1	8·5	7·7	6·9	6·2	5·7	5·3	5·1	127·8
2·4– 3·0	10·6	10·2	9·3	8·3	7·2	6·3	5·6	5·1	4·9	135·0
3·0– 3·6	10·9	10·3	9·2	8·0	6·7	5·7	4·9	4·4	4·2	128·6
3·6– 4·2	10·2	9·5	8·4	7·1	5·8	4·7	4·0	3·5	3·3	113·0
4·2– 4·8	8·9	8·2	7·0	5·8	4·6	3·6	3·0	2·5	2·4	92·0
4·8– 5·4	7·2	6·6	5·5	4·4	3·4	2·6	2·1	1·8	1·6	70·4
5·4– 6·0	5·4	4·9	4·1	3·1	2·4	1·8	1·4	1·1	1·0	50·4
6·0– 6·6	3·8	3·4	2·8	2·1	1·5	1·1	0·9	0·7	0·6	33·8
6·6– 7·2	2·5	2·3	1·8	1·3	0·9	0·7	0·5	0·4	0·3	21·4
7·2– 7·8	1·6	1·4	1·1	0·8	0·5	0·4	0·2	0·2	0·2	12·8
7·8– 8·4	1·0	0·8	0·6	0·4	0·3	0·2	0·1	0·1	0·1	7·2
8·4– 9·0	0·5	0·5	0·3	0·2	0·2	0·1	0·1	—	—	3·8
9·0– 9·6	0·3	0·2	0·2	0·1	0·1	—	—	—	—	1·8
9·6–10·2	0·1	0·1	0·1	0·1	—	—	—	—	—	0·8
10·2–10·8	0·1	0·1	—	—	—	—	—	—	—	0·4
Over 10·8	0·1	—	—	—	—	—	—	—	—	0·2
All speeds	85·7	80·4	71·2	61·2	51·6	43·8	38·4	34·6	33·1	1000·0

TABLE XXXI

$q = 20$ $\sigma/V_R = 5{\cdot}62$

V/V_R \ ϕ	0–20	20–40	40–60	60–80	80–100	100–120	120–140	140–160	160–180	All directions
						per mille				
0– 1	1·7	1·7	1·7	1·7	1·7	1·7	1·6	1·6	1·6	30·0
1– 2	5·2	5·1	5·0	4·9	4·7	4·6	4·4	4·4	4·3	85·2
2– 3	8·1	8·0	7·7	7·3	6·9	6·6	6·3	6·0	6·0	125·8
3– 4	10·0	9·8	9·3	8·7	8·1	7·5	7·0	6·7	6·5	147·2
4– 5	10·7	10·3	9·7	8·8	8·0	7·3	6·7	6·3	6·1	147·8
5– 6	10·1	9·7	9·0	8·1	7·1	6·4	5·7	5·3	5·1	133·0
6– 7	8·7	8·3	7·6	6·7	5·8	5·0	4·5	4·1	3·9	109·2
7– 8	6·9	6·5	5·8	5·1	4·3	3·6	3·2	2·9	2·7	82·0
8– 9	5·0	4·7	4·2	3·5	2·9	2·4	2·1	1·9	1·7	56·8
9–10	3·4	3·1	2·8	2·3	1·9	1·5	1·3	1·1	1·0	36·8
10–11	2·2	1·9	1·7	1·4	1·1	0·9	0·7	0·6	0·6	22·2
11–12	1·2	1·1	0·9	0·8	0·6	0·5	0·4	0·3	0·3	12·2
12–13	0·7	0·6	0·5	0·4	0·3	0·2	0·2	0·2	0·2	6·6
13–14	0·3	0·3	0·3	0·2	0·1	0·1	0·1	0·1	0·1	3·2
14–15	0·2	0·1	0·1	0·1	0·1	0·1	—	—	—	1·4
15–16	0·1	0·1	0·1	—	—	—	—	—	—	0·6
All speeds	74·5	71·3	66·4	60·0	53·6	48·4	44·2	41·5	40·1	1000·0

TABLE XXXII

$q = 10$ $\sigma/V_R = 11{\cdot}3$

V/V_R \ ϕ	0–20	20–40	40–60	60–80	80–100	100–120	120–140	140–160	160–180	All directions
	per mille									
0– 2	1·7	1·7	1·7	1·7	1·7	1·7	1·7	1·7	1·7	30·6
2– 4	5·0	5·0	4·9	4·9	4·8	4·7	4·7	4·6	4·6	86·4
4– 6	7·6	7·6	7·4	7·2	7·1	6·9	6·7	6·6	6·6	127·4
6– 8	9·2	9·0	8·8	8·5	8·2	7·9	7·6	7·5	7·4	148·2
8–10	9·4	9·3	9·0	8·6	8·2	7·8	7·5	7·3	7·2	148·6
10–12	8·7	8·5	8·2	7·8	7·4	6·9	6·6	6·3	6·2	133·2
12–14	7·3	7·1	6·8	6·4	5·9	5·5	5·3	5·0	4·9	108·4
14–16	5·6	5·5	5·2	4·8	4·4	4·1	3·8	3·6	3·5	81·0
16–18	4·0	3·8	3·6	3·4	3·1	2·8	2·6	2·4	2·3	56·0
18–20	2·6	2·5	2·3	2·2	1·9	1·8	1·6	1·5	1·5	35·8
20–22	1·6	1·5	1·4	1·3	1·2	1·0	0·9	0·9	0·8	21·2
22–24	0·9	0·9	0·8	0·7	0·6	0·5	0·5	0·5	0·5	11·8
24–26	0·5	0·5	0·4	0·4	0·3	0·3	0·3	0·2	0·2	6·2
26–28	0·3	0·2	0·2	0·2	0·2	0·2	0·1	0·1	0·1	3·2
28–30	0·1	0·1	0·1	0·1	0·1	0·1	0·1	—	—	1·4
Over 30	0·1	0·1	0·1	—	—	—	—	—	—	0·6
All speeds	64·6	63·3	60·9	58·2	55·1	52·2	50·0	48·2	47·5	1000·0

TABLE XXXIII

$q = 0$

V/σ	Frequency for 20° range	All directions	V/σ	Frequency for 20° range	All directions
	per mille			*per mille*	
0·0–0·2	2·2	39	1·6–1·8	2·1	38
0·2–0·4	6·1	109	1·8–2·0	1·1	20
0·4–0·6	8·6	155	2·0–2·2	0·6	10
0·6–0·8	9·5	171	2·2–2·4	0·3	5
			2·4–2·6	0·1	1·8
0·8–1·0	8·9	160	2·6–2·8	—	0·7
1·0–1·2	7·2	131	2·8–3·0	—	0·2
1·2–1·4	5·3	96			
1·4–1·6	3·5	63	All speeds	55·5	1000·0

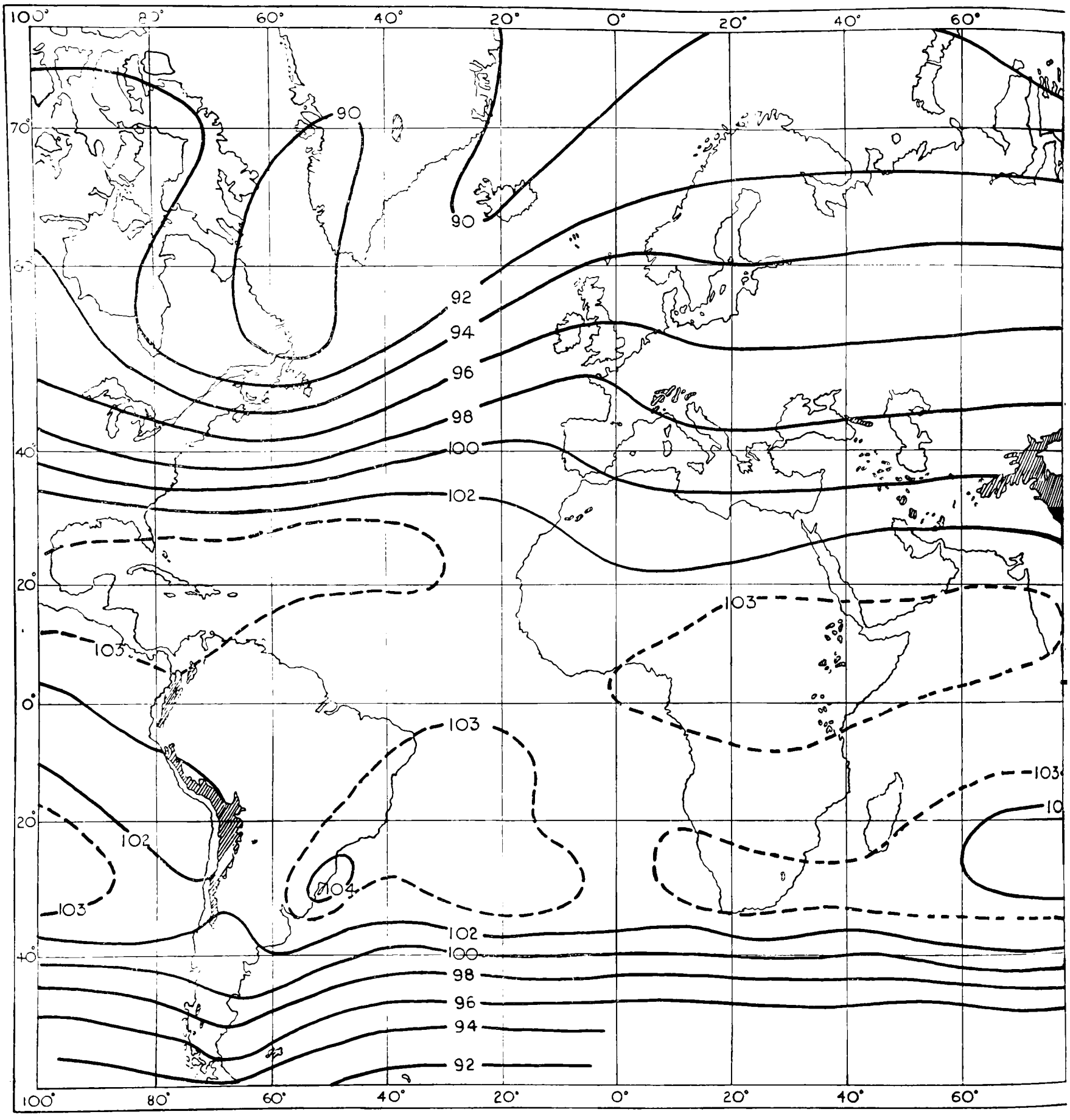

CONTOURS

Height of isobaric surface is given in hundreds of feet

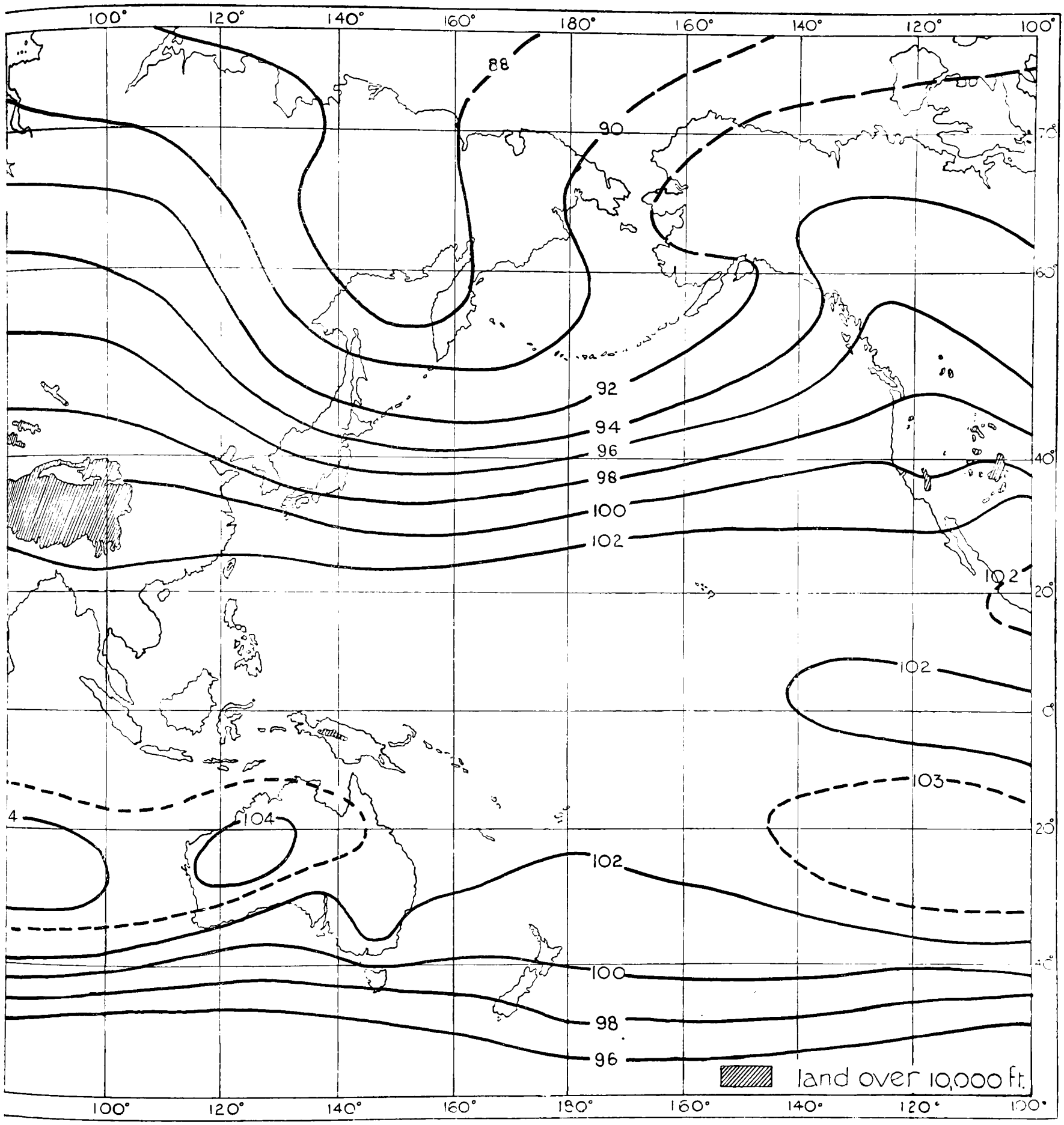

CONTOURS

Height of isobaric surface is given in hundreds of feet

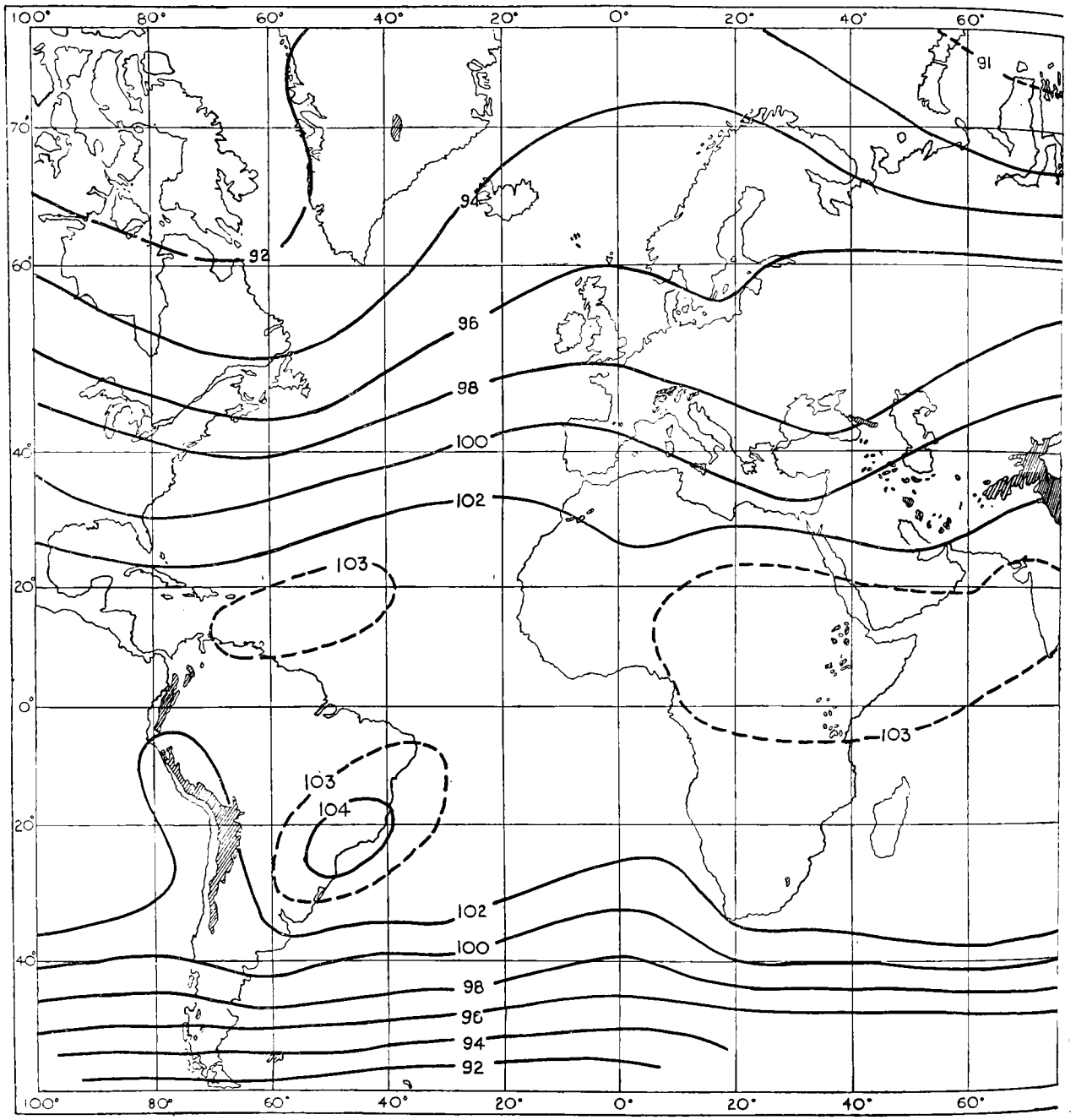

CONTOURS

Height of isobaric surface is given in hundreds of feet

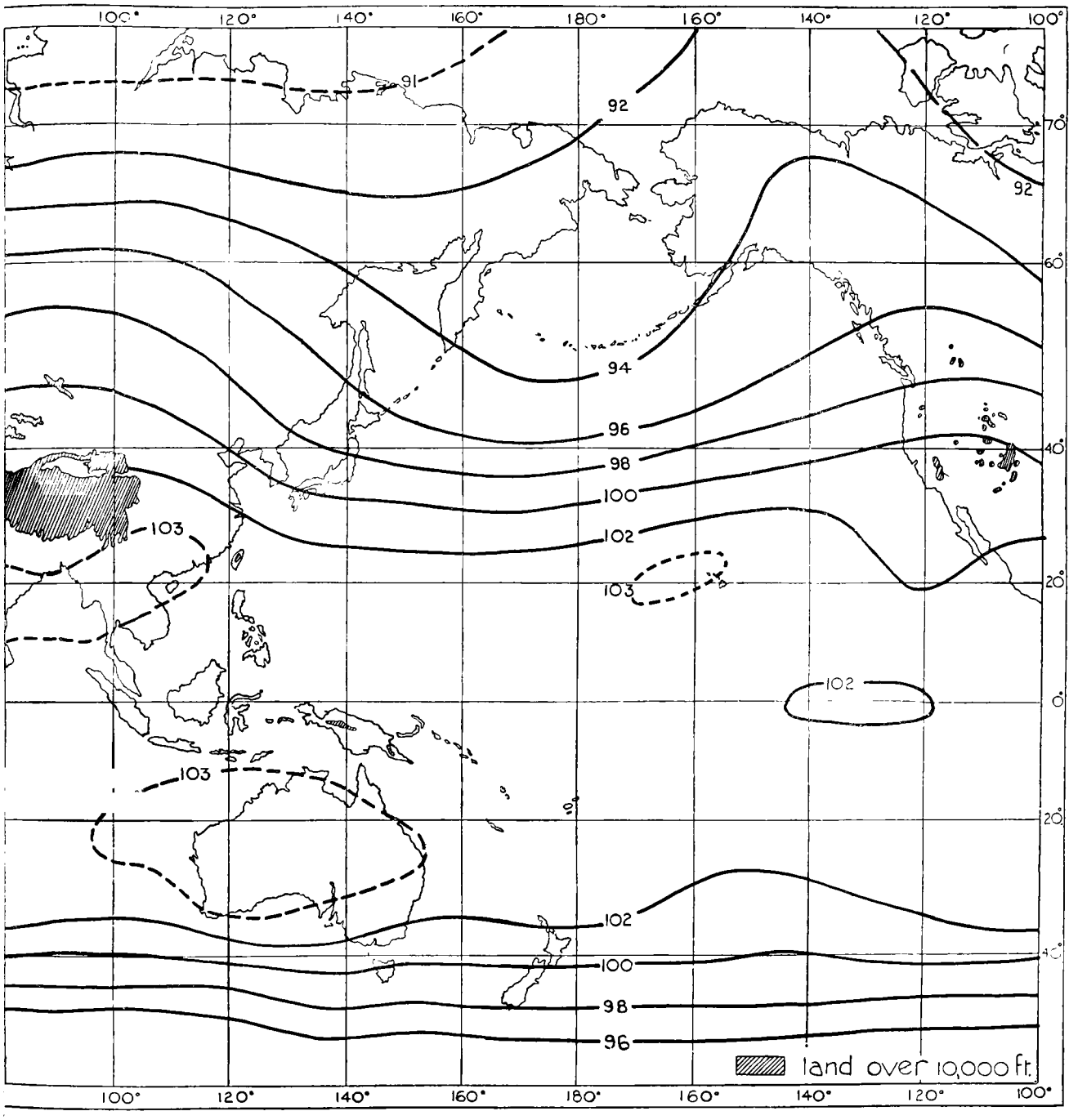

CONTOURS

Height of isobaric surface is given in hundreds of feet

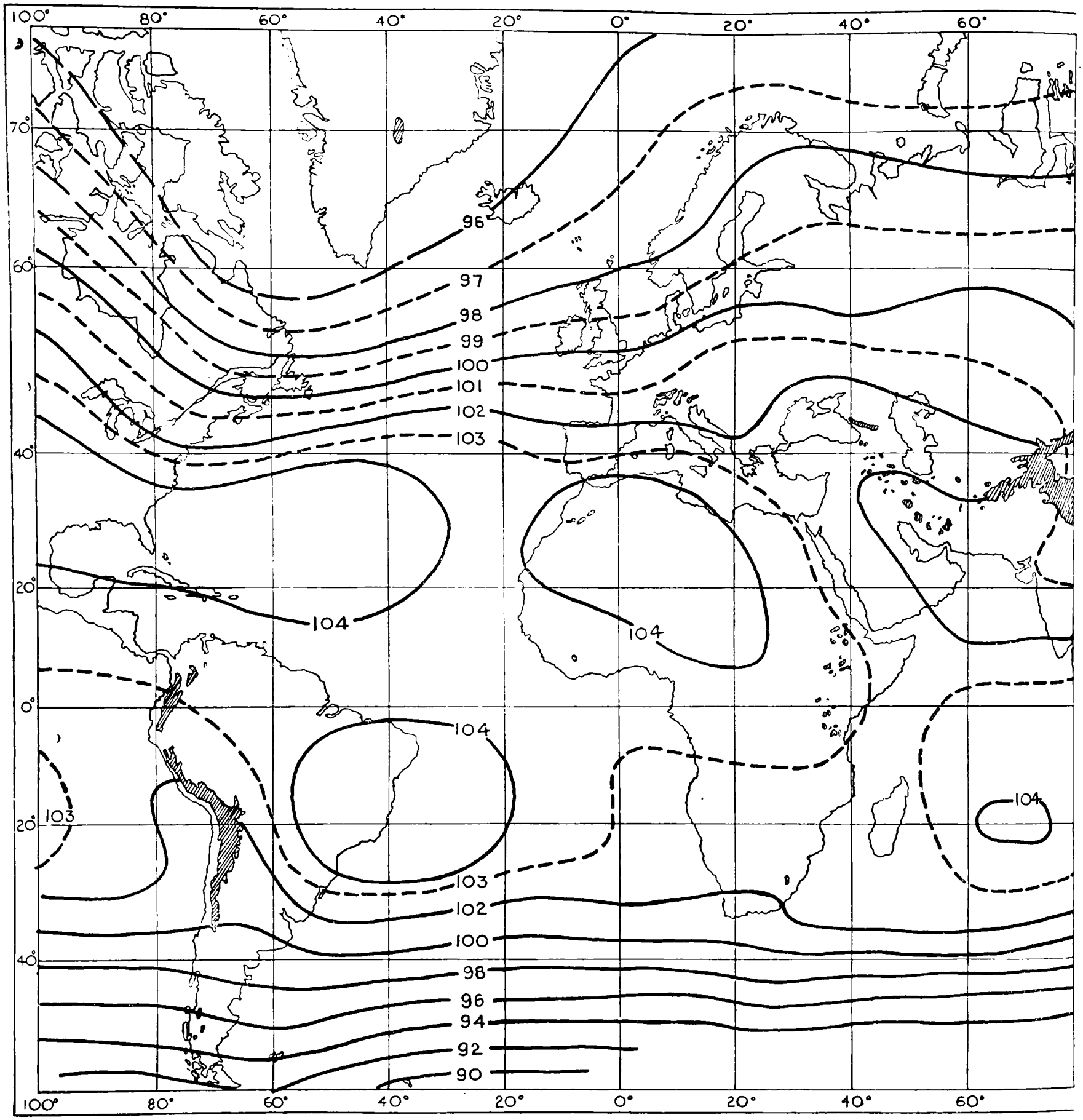

CONTOURS

Height of isobaric surface is given in hundreds of feet

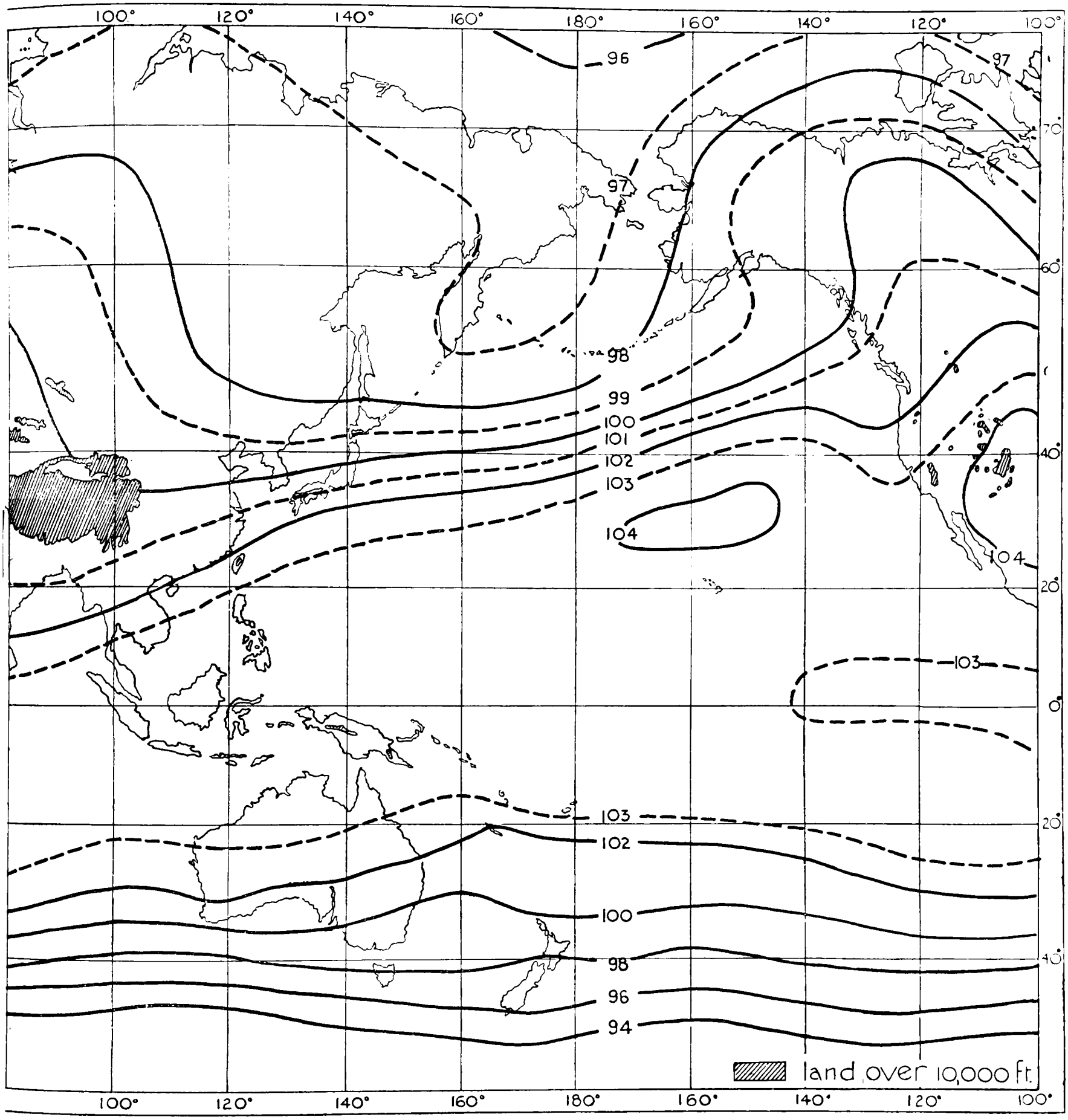

CONTOURS

Height of isobaric surface is given in hundreds of feet

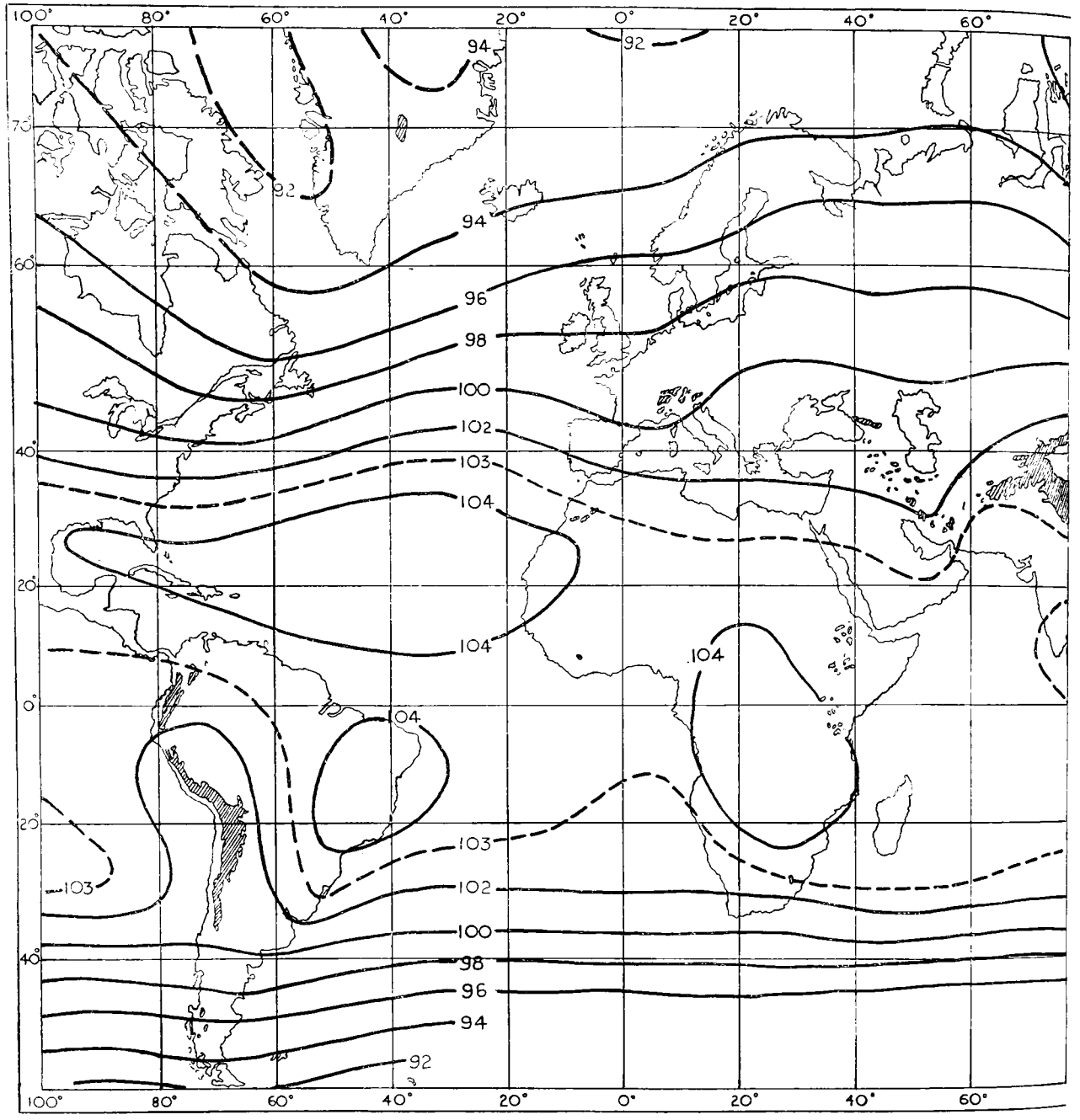

CONTOURS

Height of isobaric surface is given in hundreds of feet

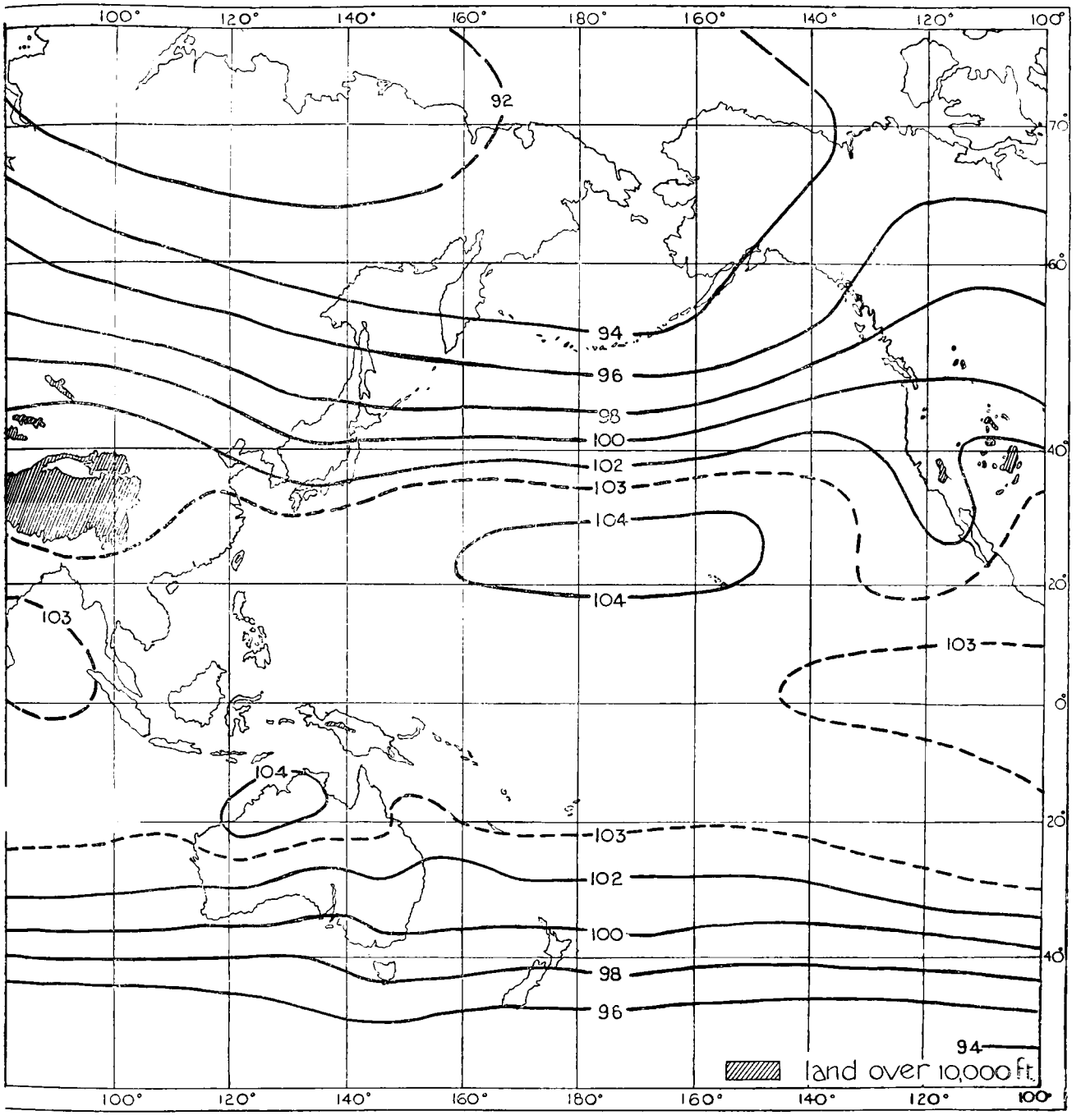

CONTOURS

Height of isobaric surface is given in hundreds of feet

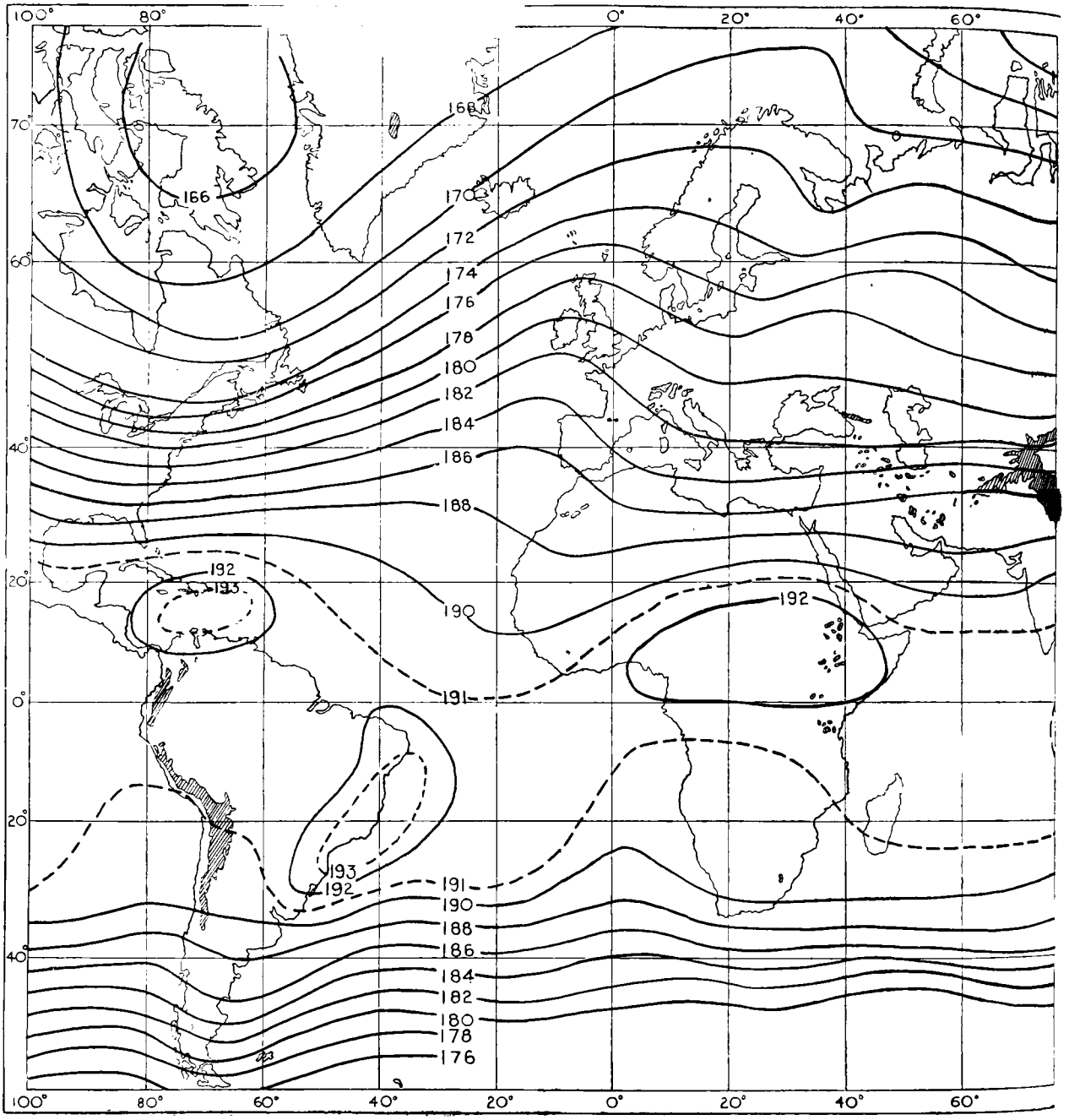

CONTOURS

Height of isobaric surface is given in hundreds of feet

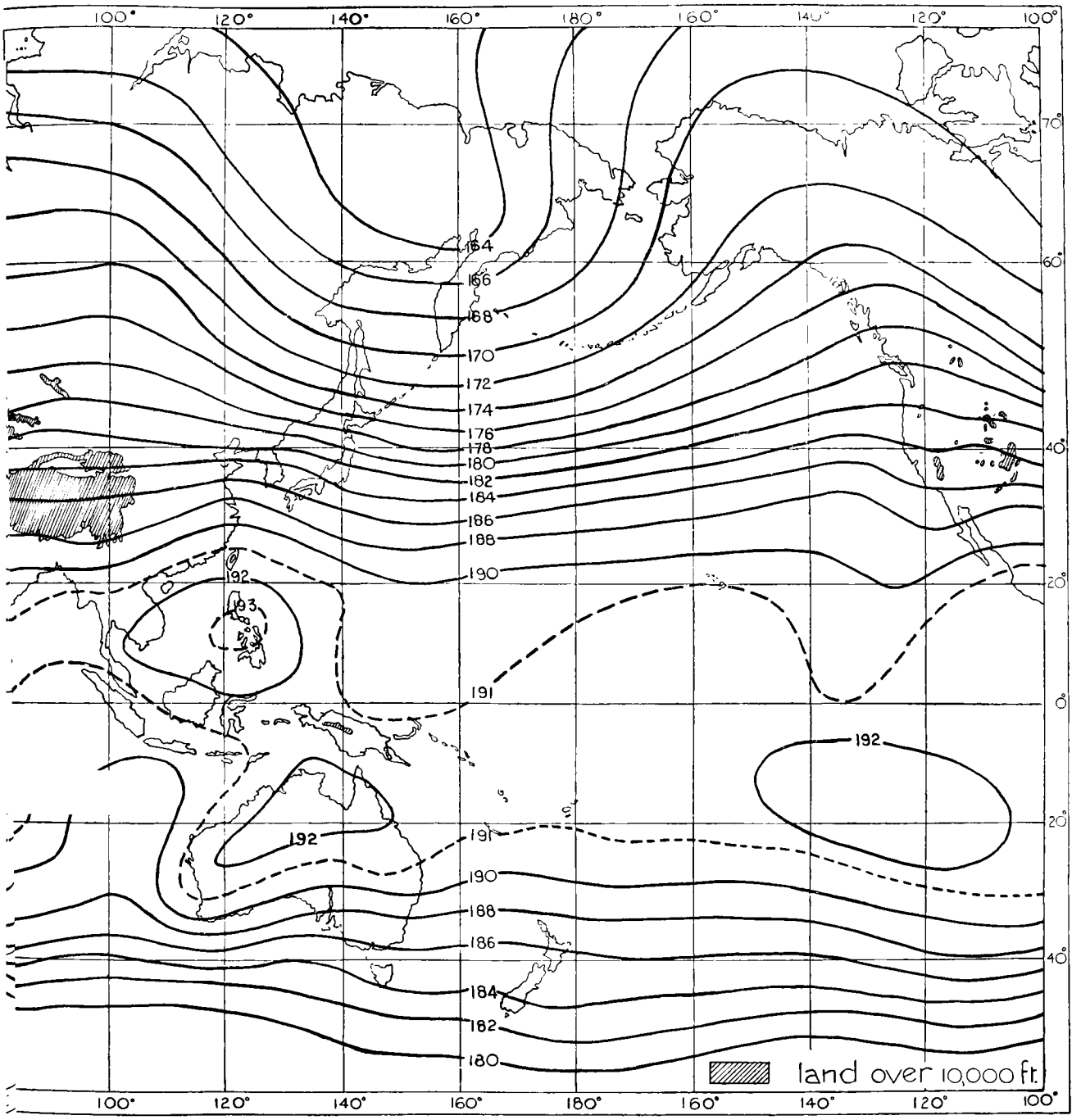

CONTOURS

Height of isobaric surface is given in hundreds of feet

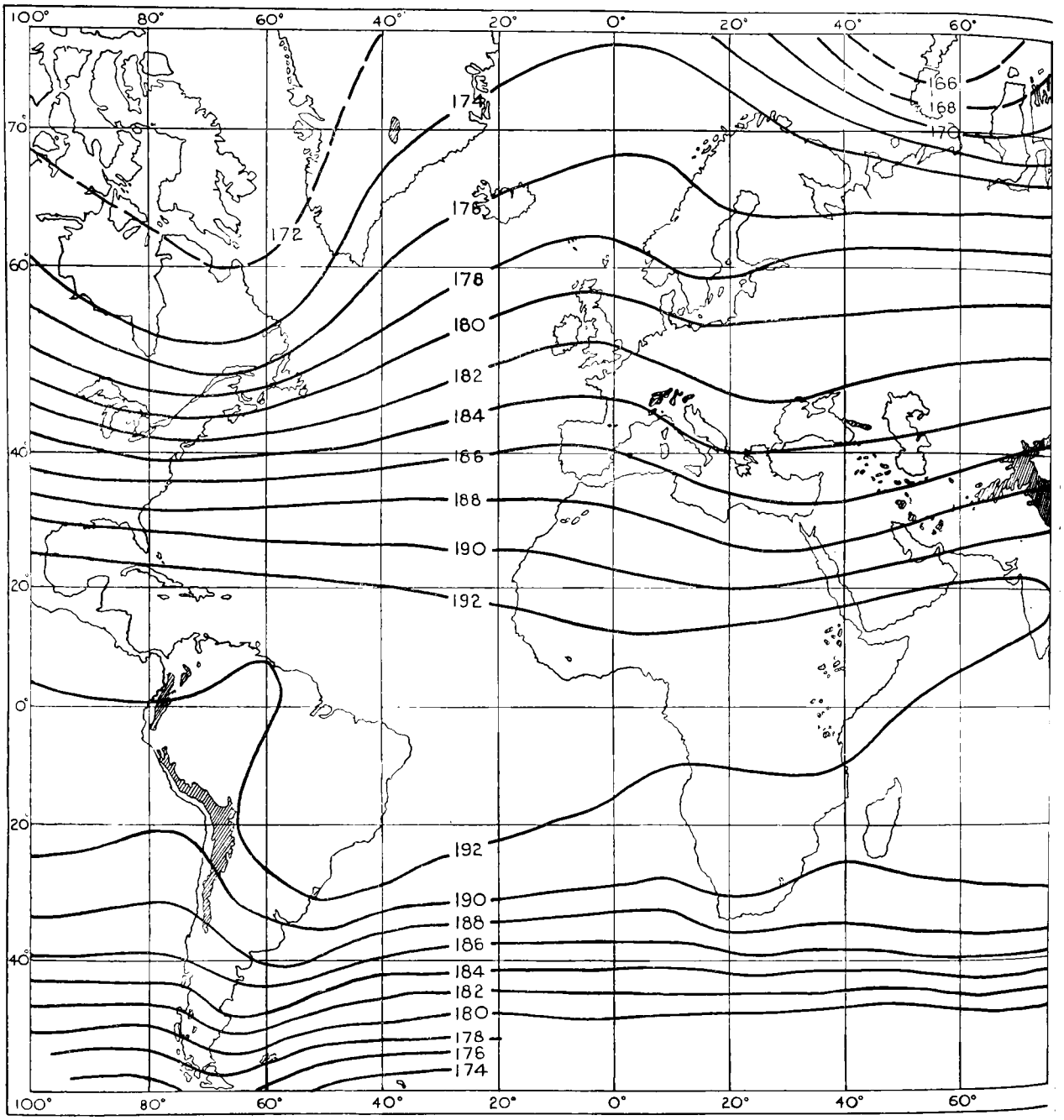

CONTOURS

Height of isobaric surface is given in hundreds of feet

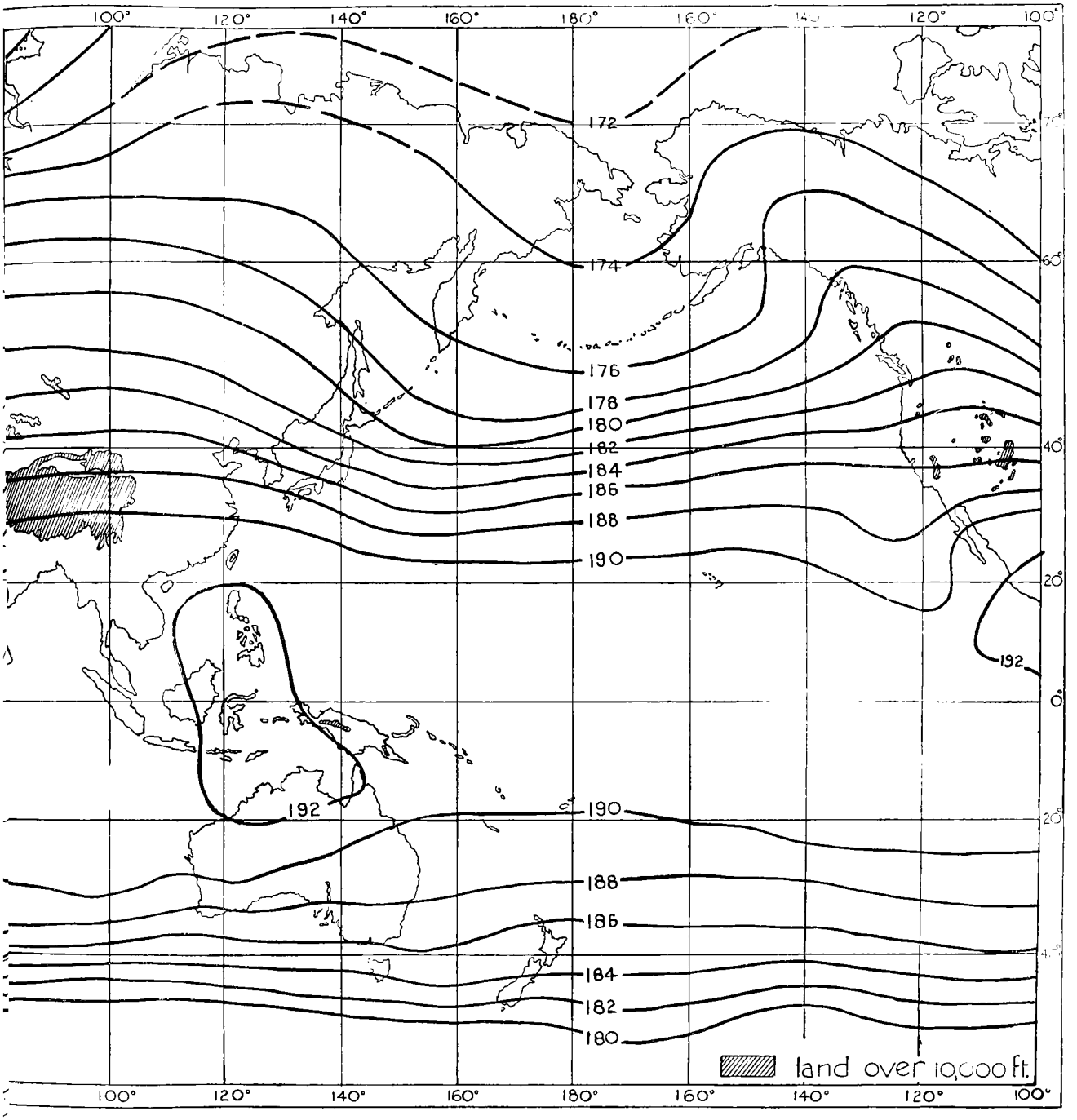

CONTOURS

Height of isobaric surface is given in hundreds of feet

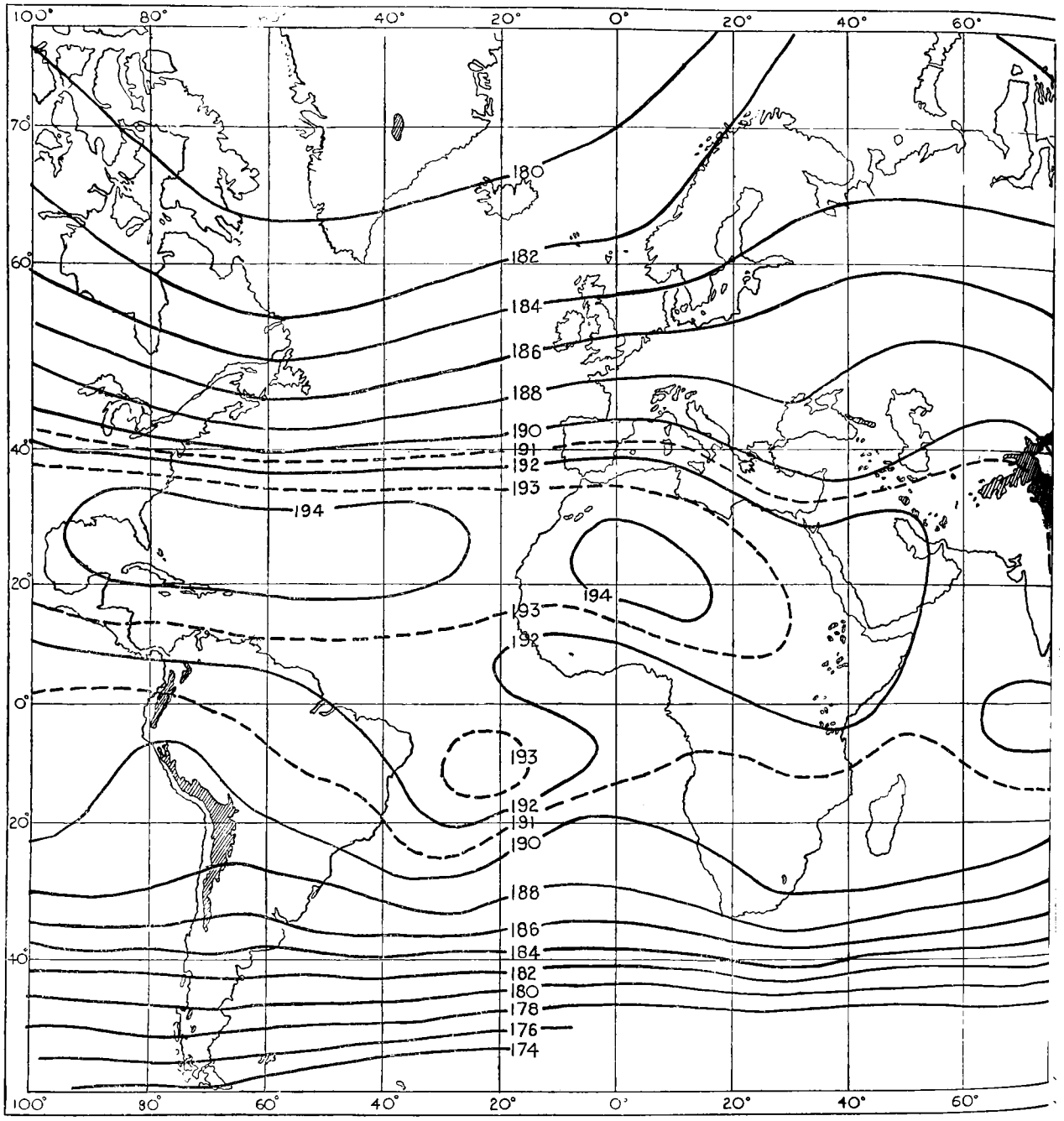

CONTOURS

Height of isobaric surface is given in hundreds of feet

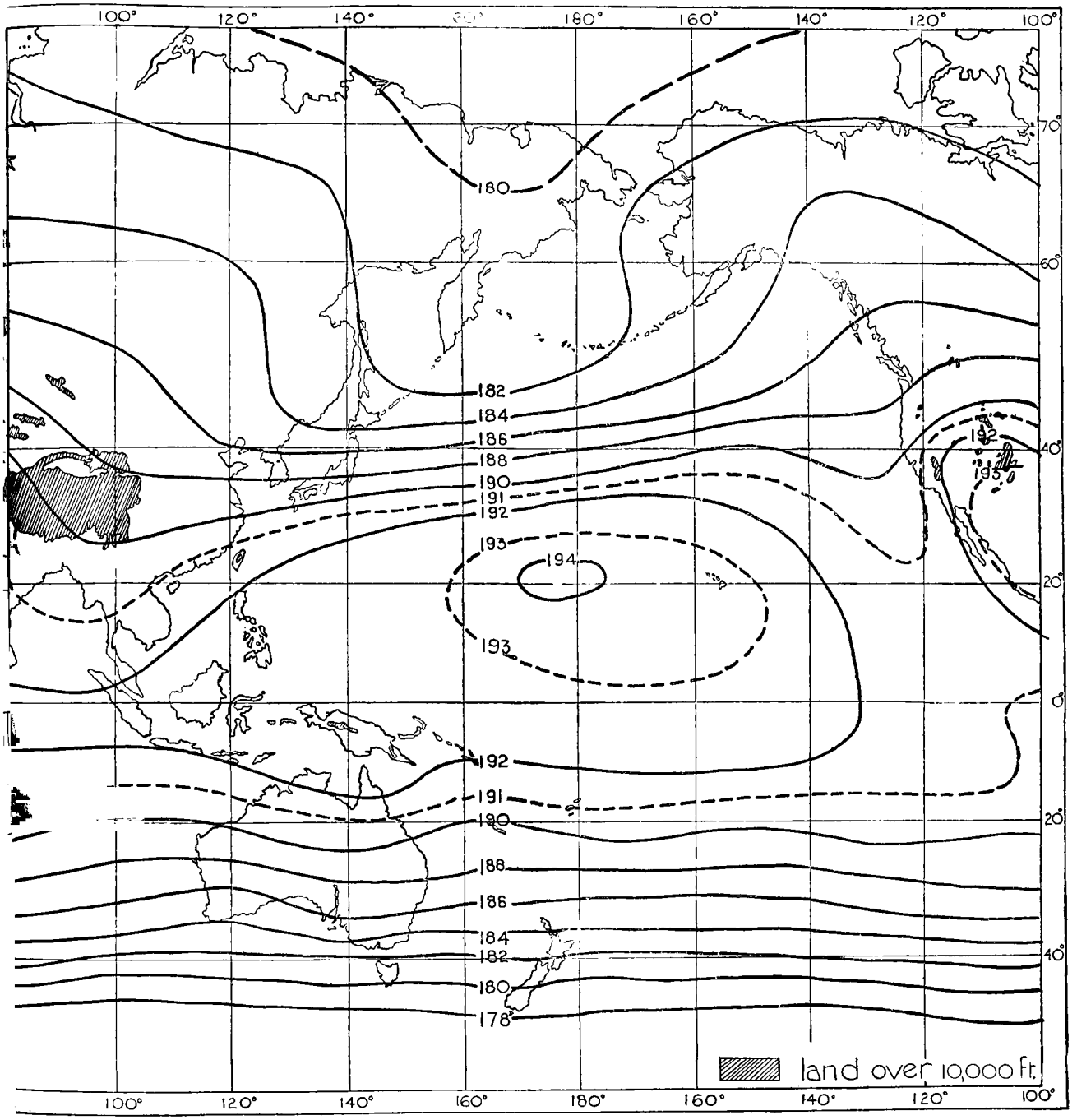

CONTOURS

Height of isobaric surface is given in hundreds of feet

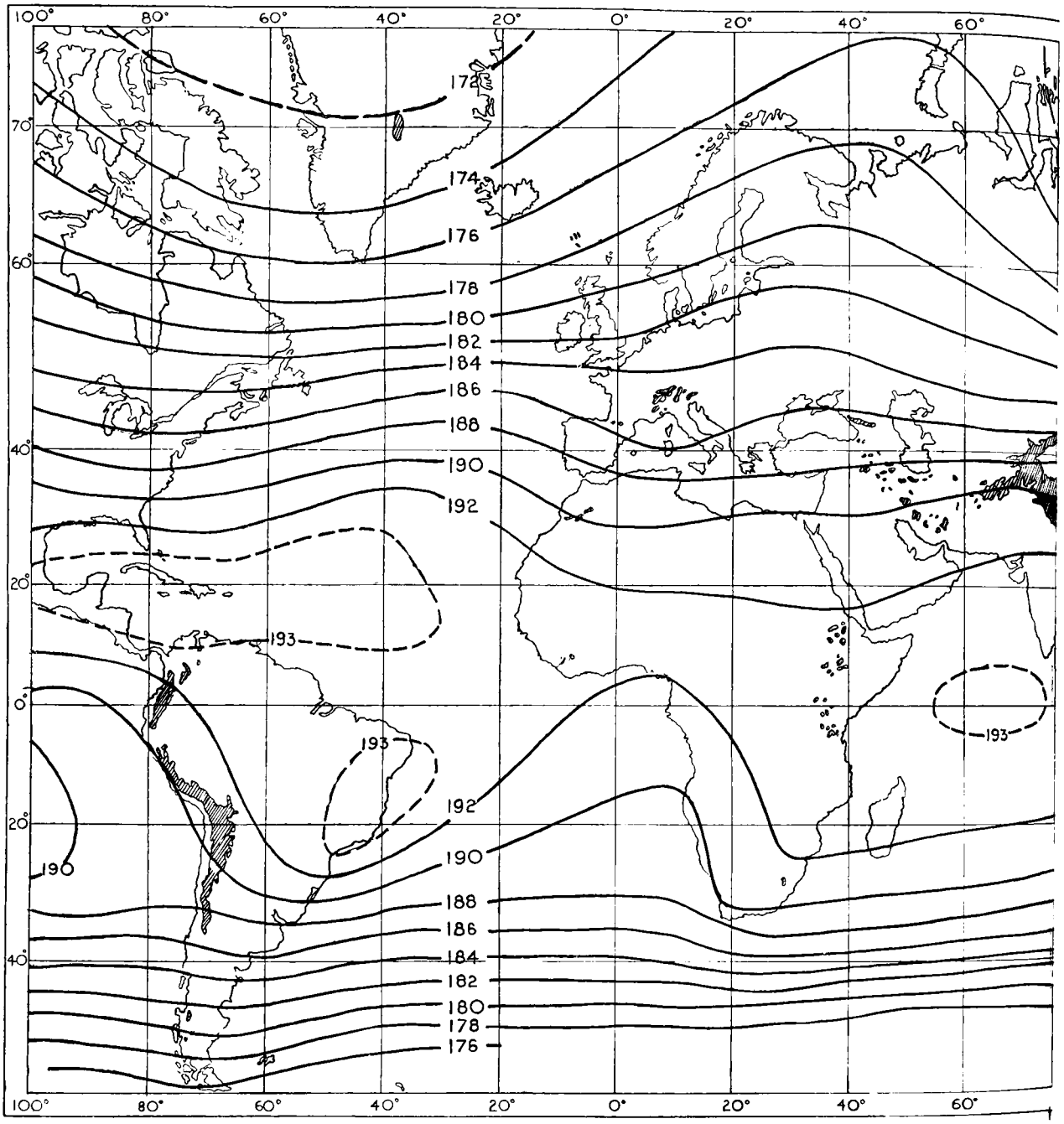

CONTOURS

Height of isobaric surface is given in hundreds of feet

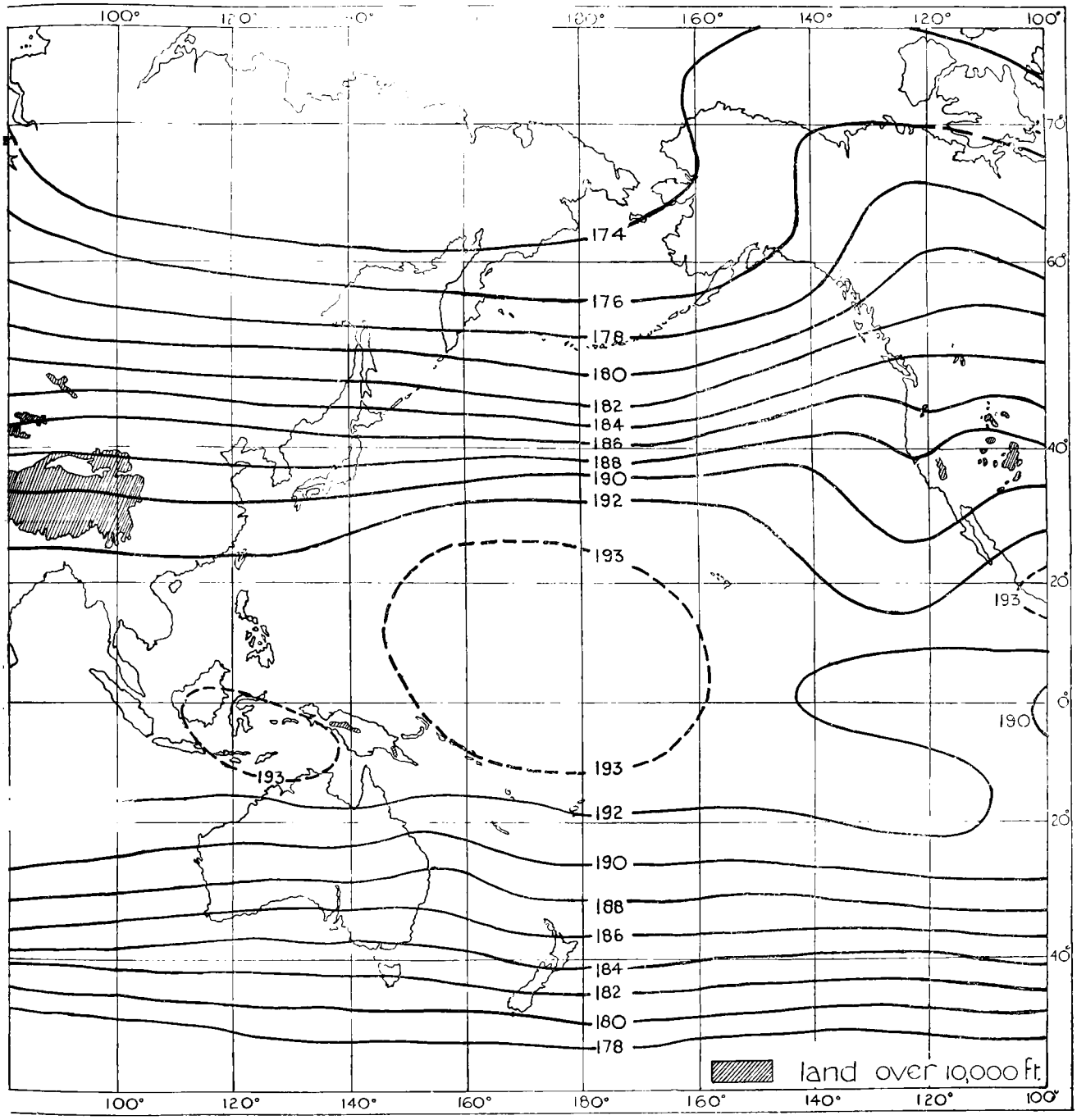

CONTOURS

Height of isobaric surface is given in hundreds of feet

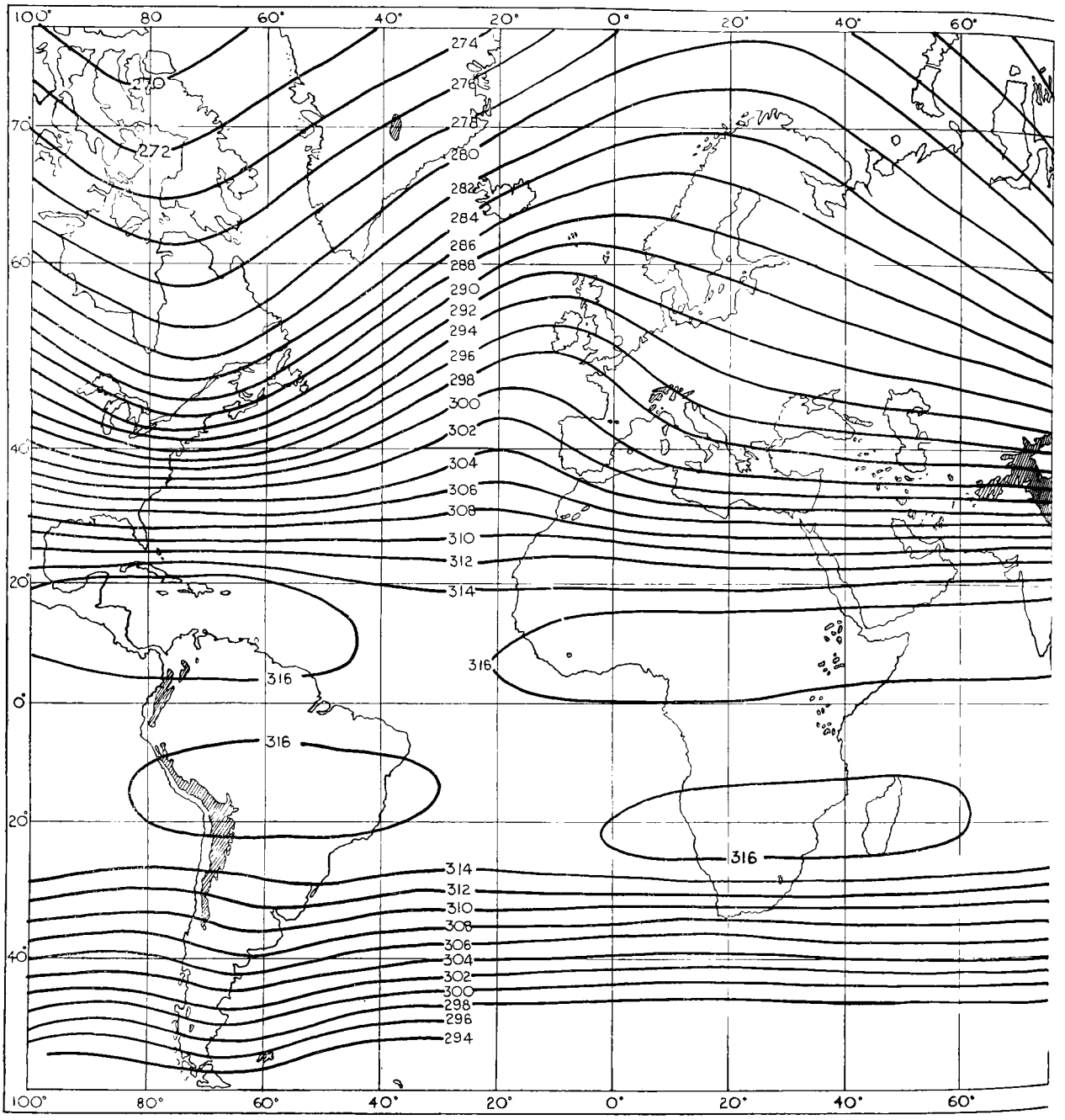

CONTOURS

Height of isobaric surface is given in hundreds of feet

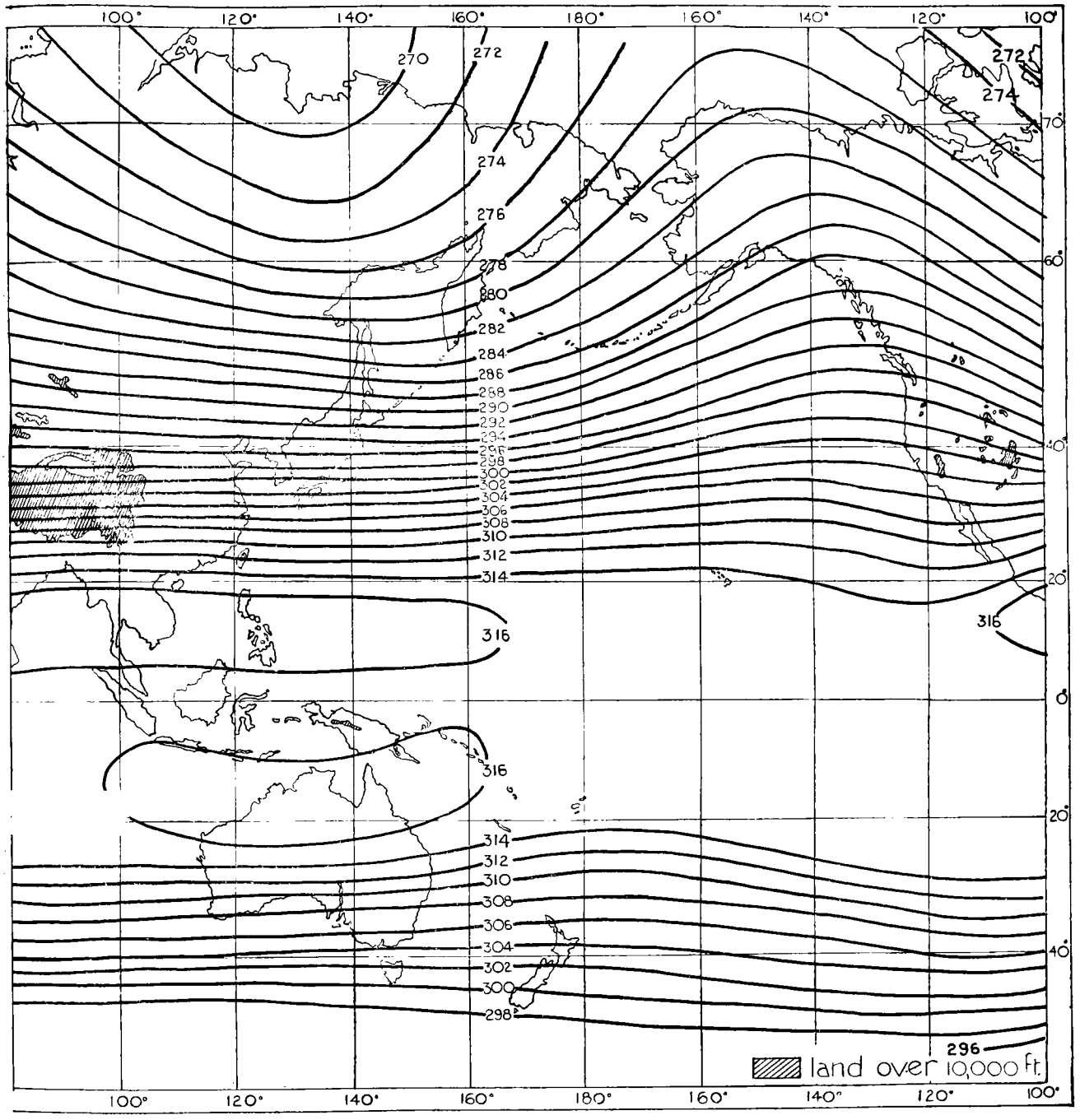

CONTOURS

Height of isobaric surface is given in hundreds of feet

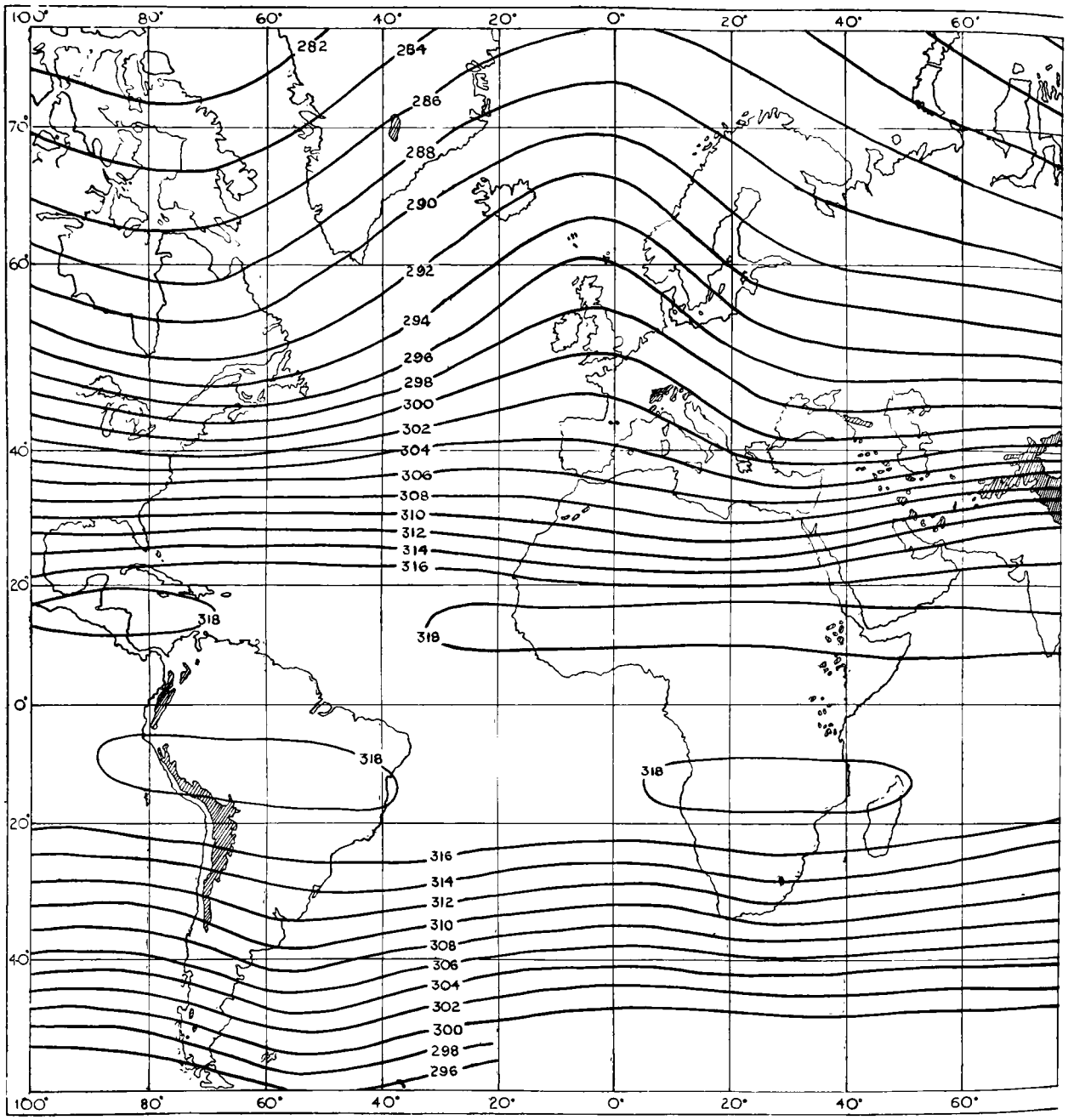

CONTOURS

Height of isobaric surface is given in hundreds of feet

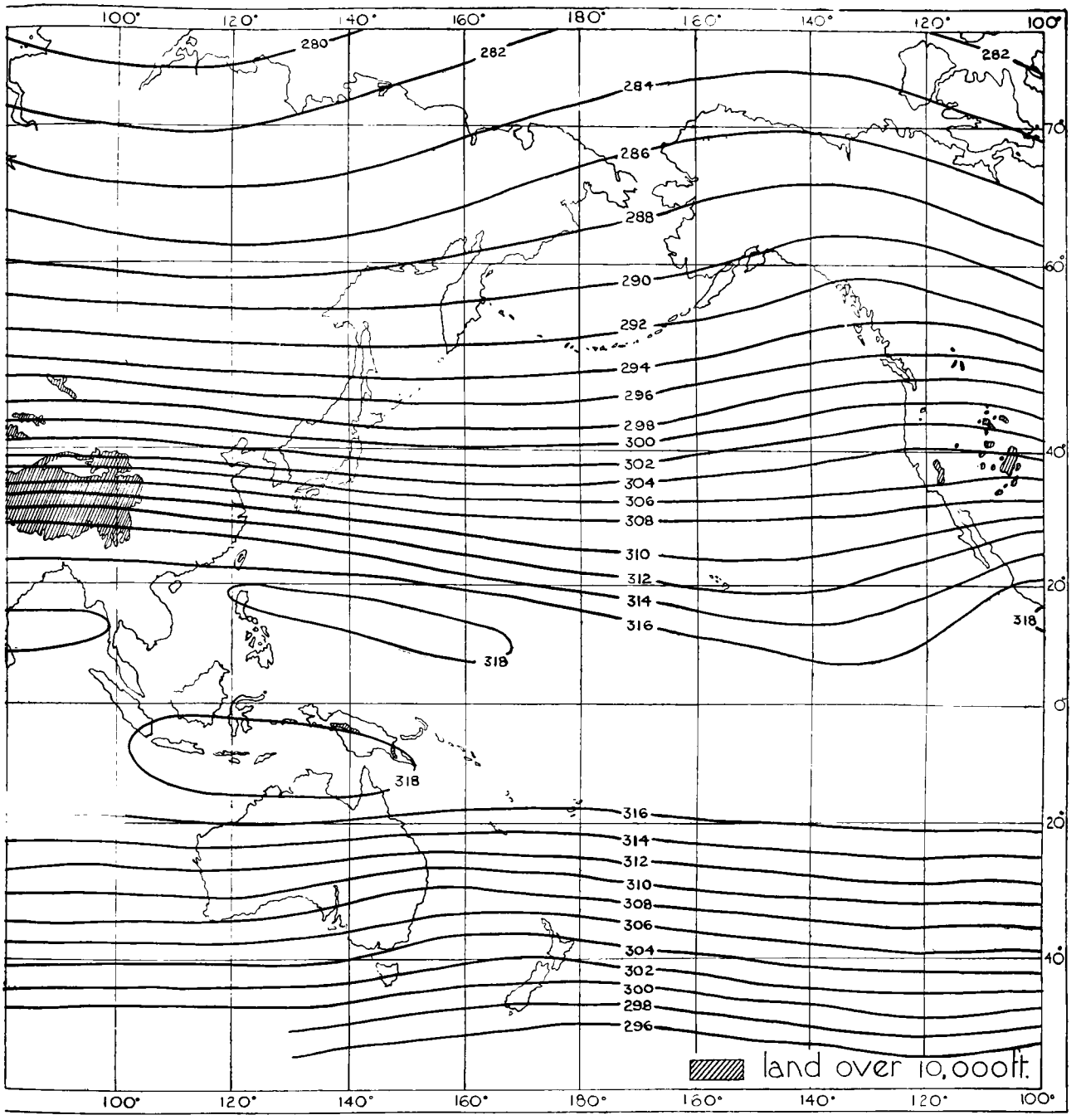

CONTOURS

Height of isobaric surface is given in hundreds of feet

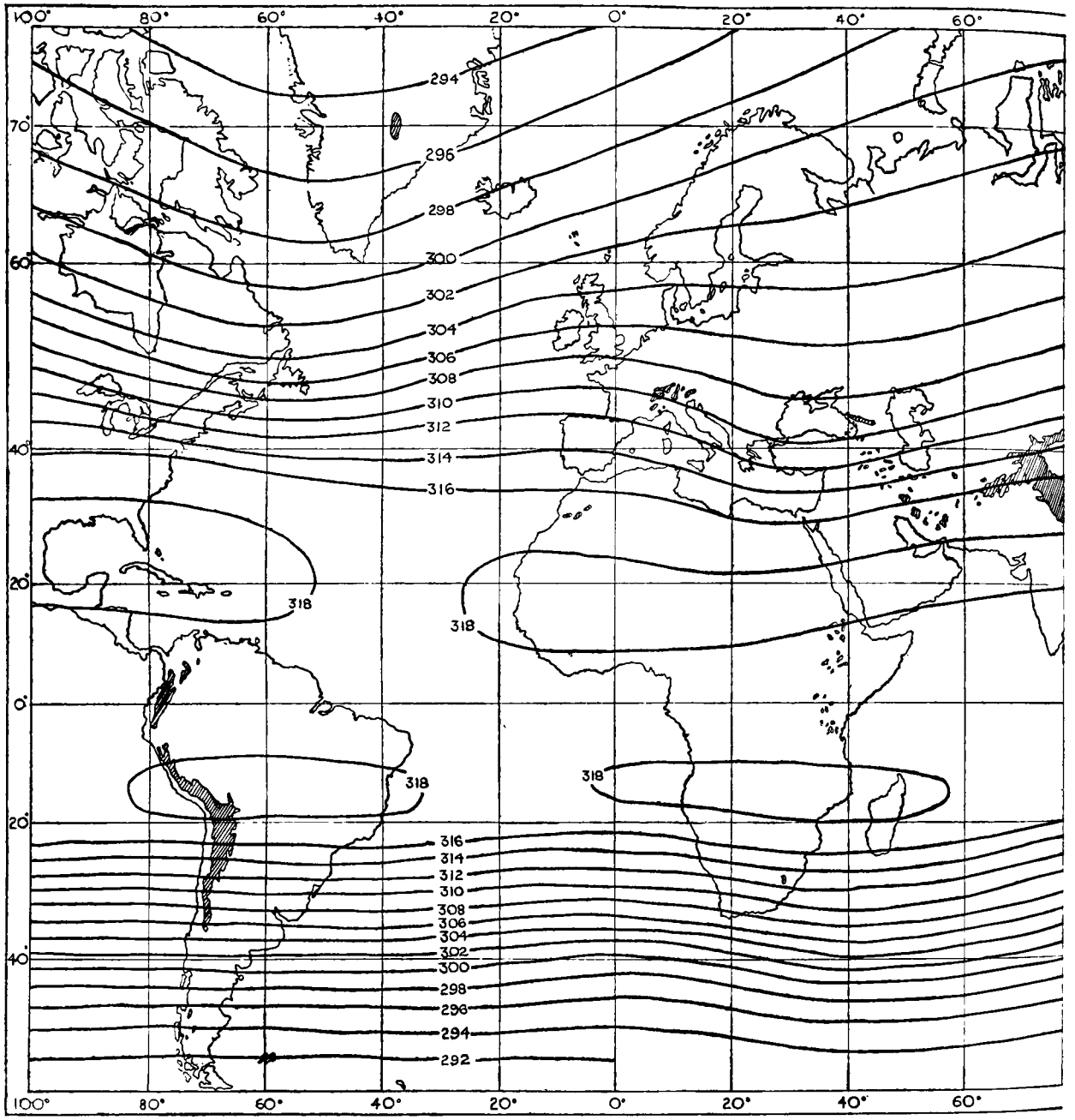

CONTOURS

Height of isobaric surface is given in hundreds of feet

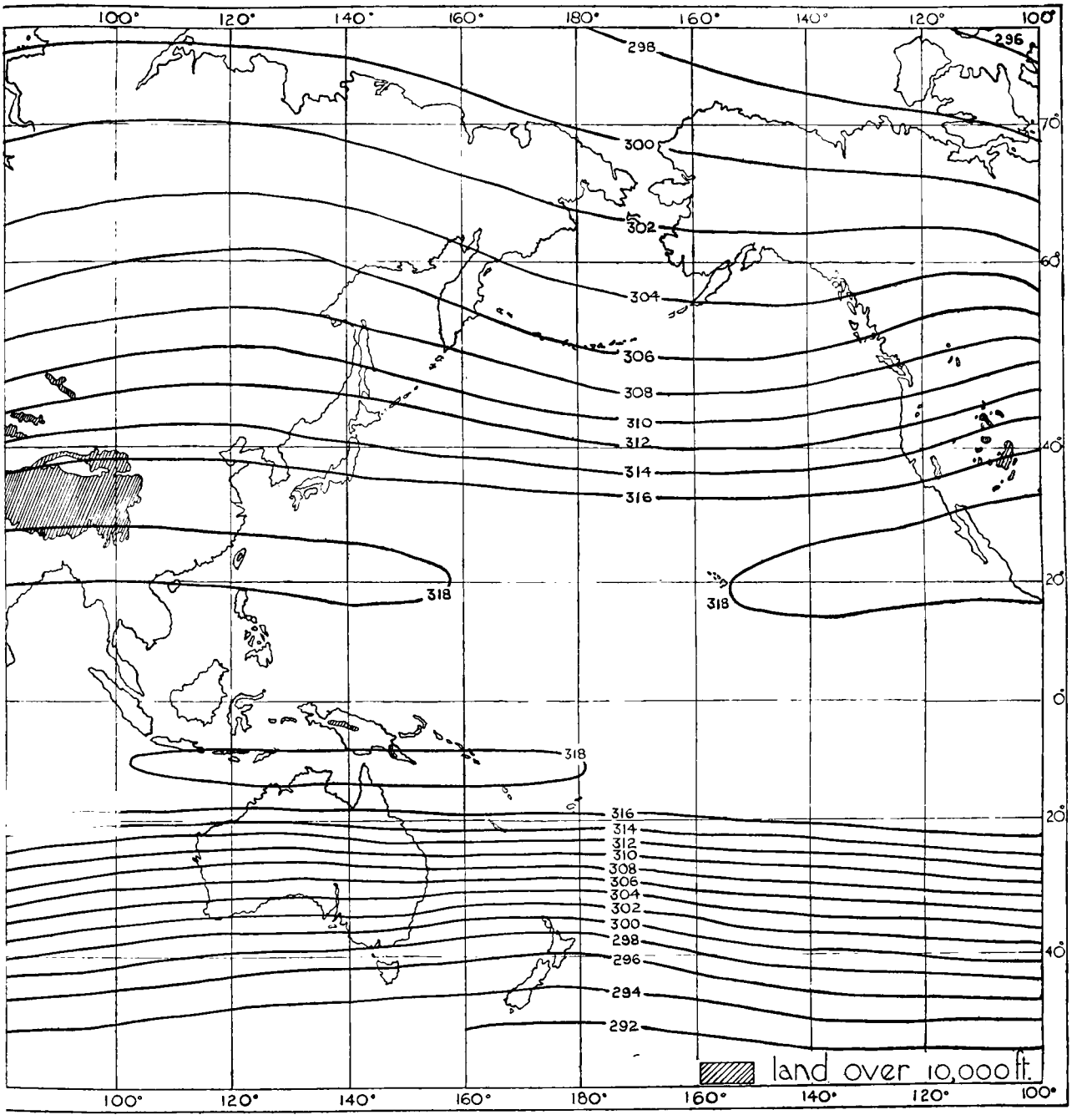

CONTOURS

Height of isobaric surface is given in hundreds of feet

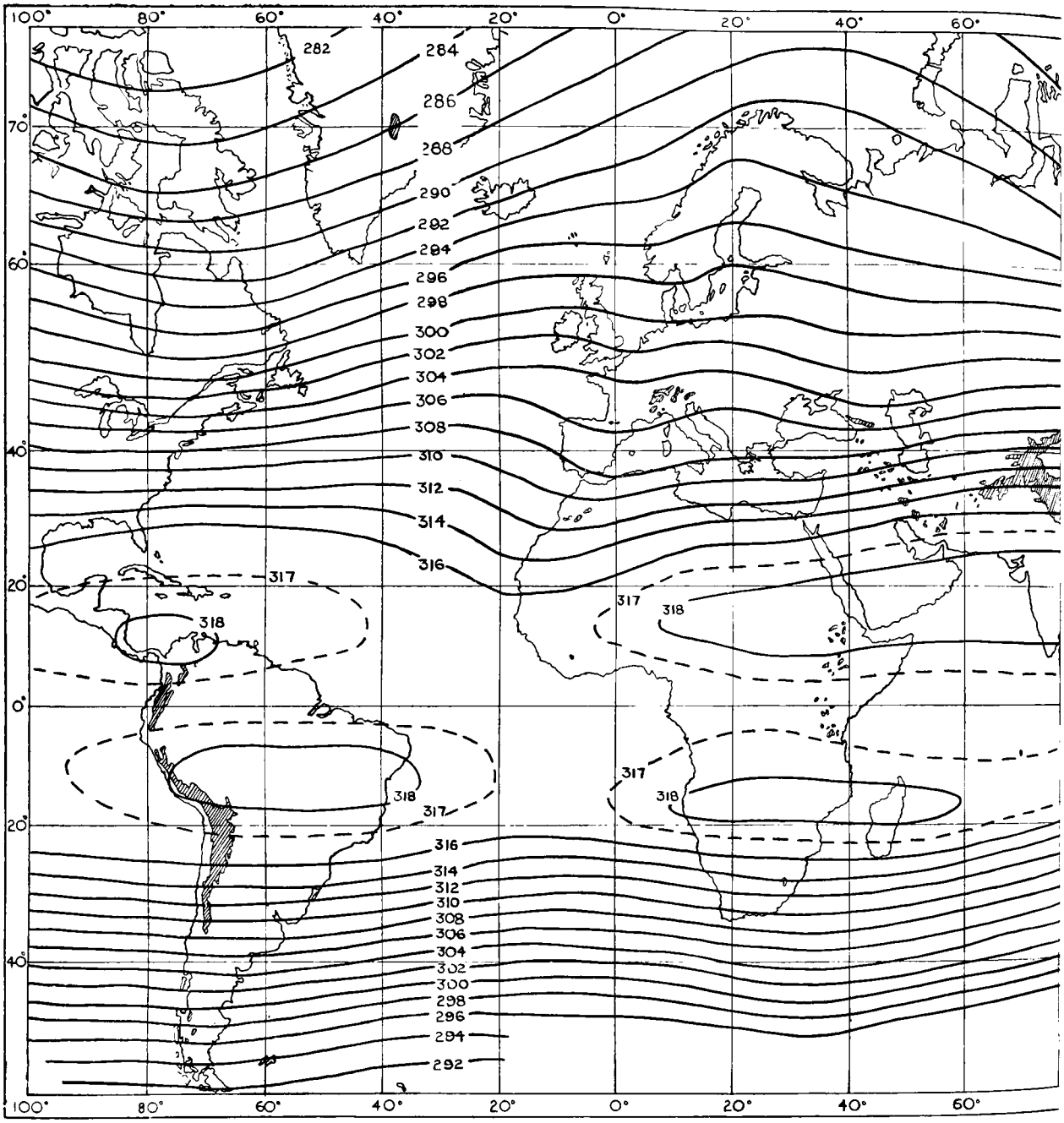

CONTOURS

Height of isobaric surface is given in hundreds of feet

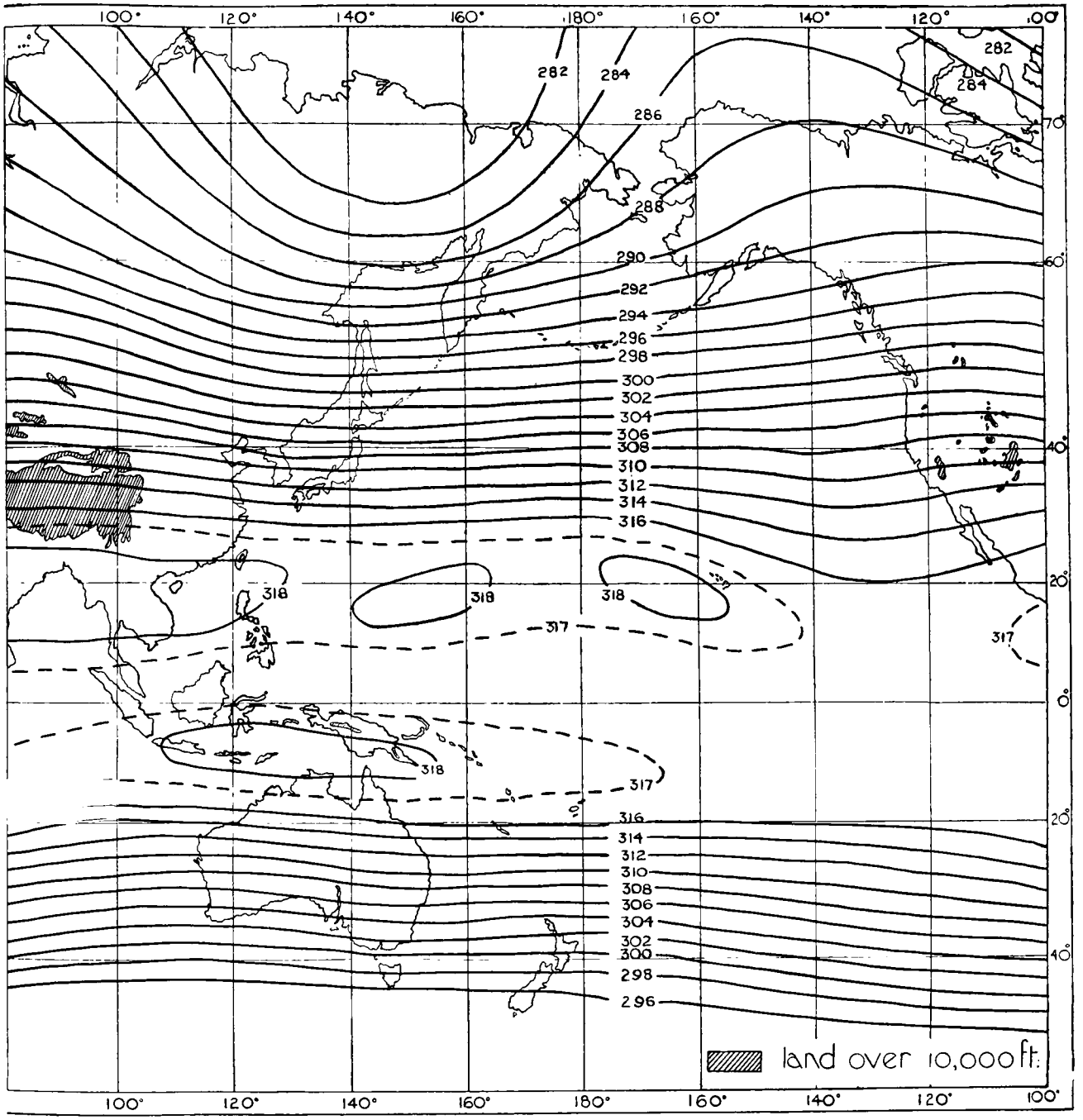

CONTOURS

Height of isobaric surface is given in hundreds of feet

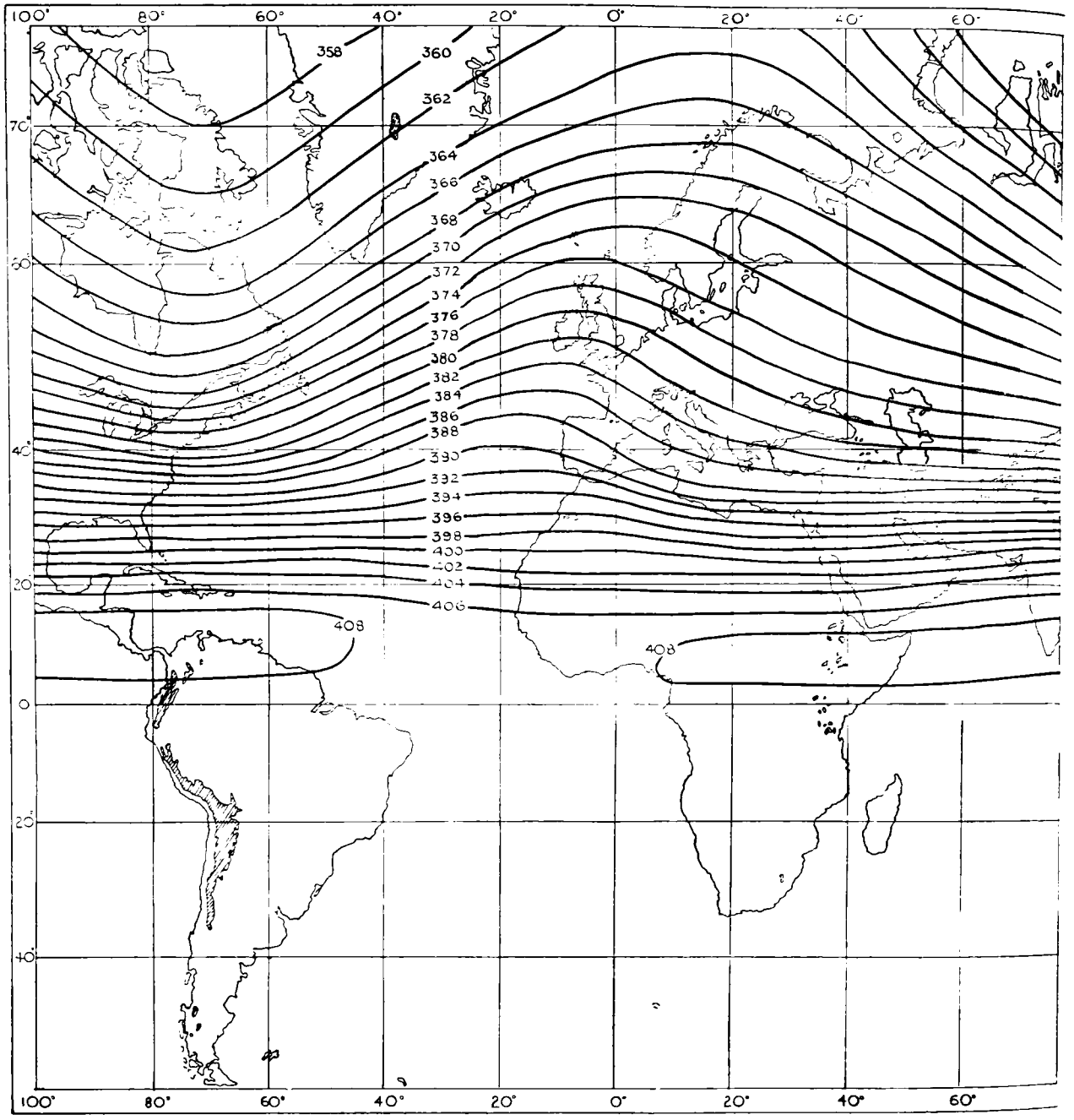

CONTOURS

Height of isobaric surface is given in hundreds of feet

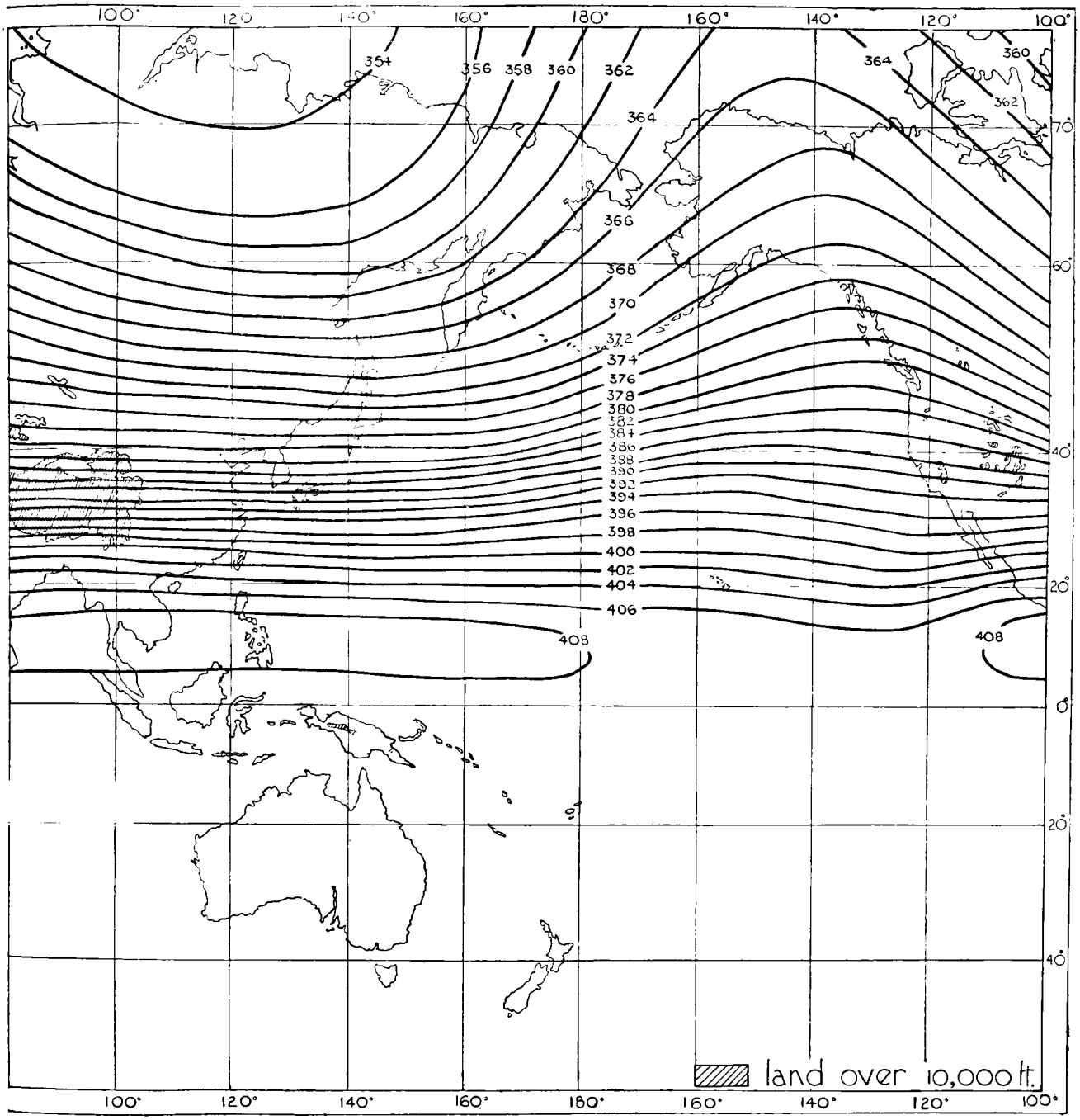

CONTOURS

Height of isobaric surface is given in hundreds of feet

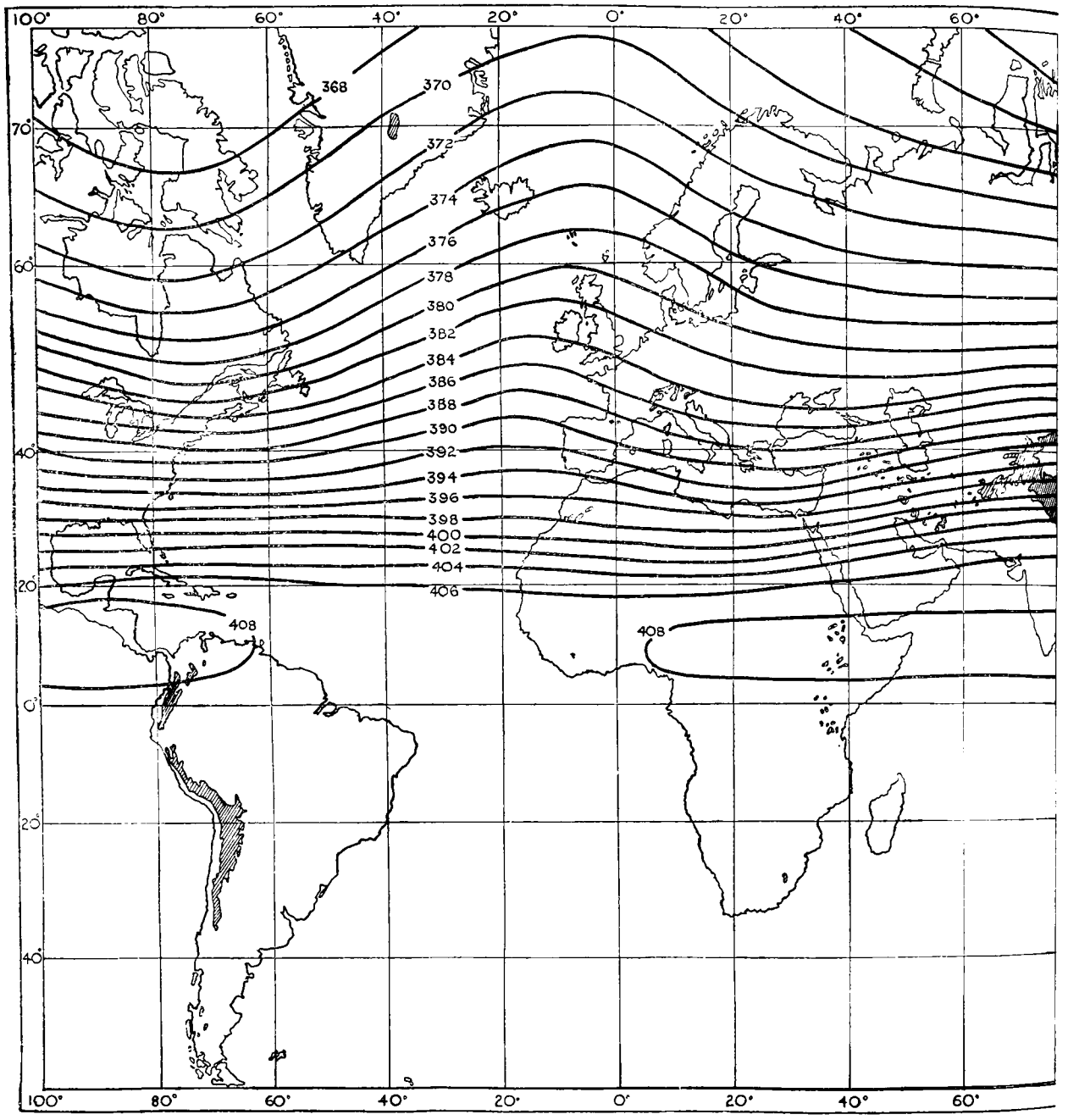

CONTOURS

Height of isobaric surface is given in hundreds of feet

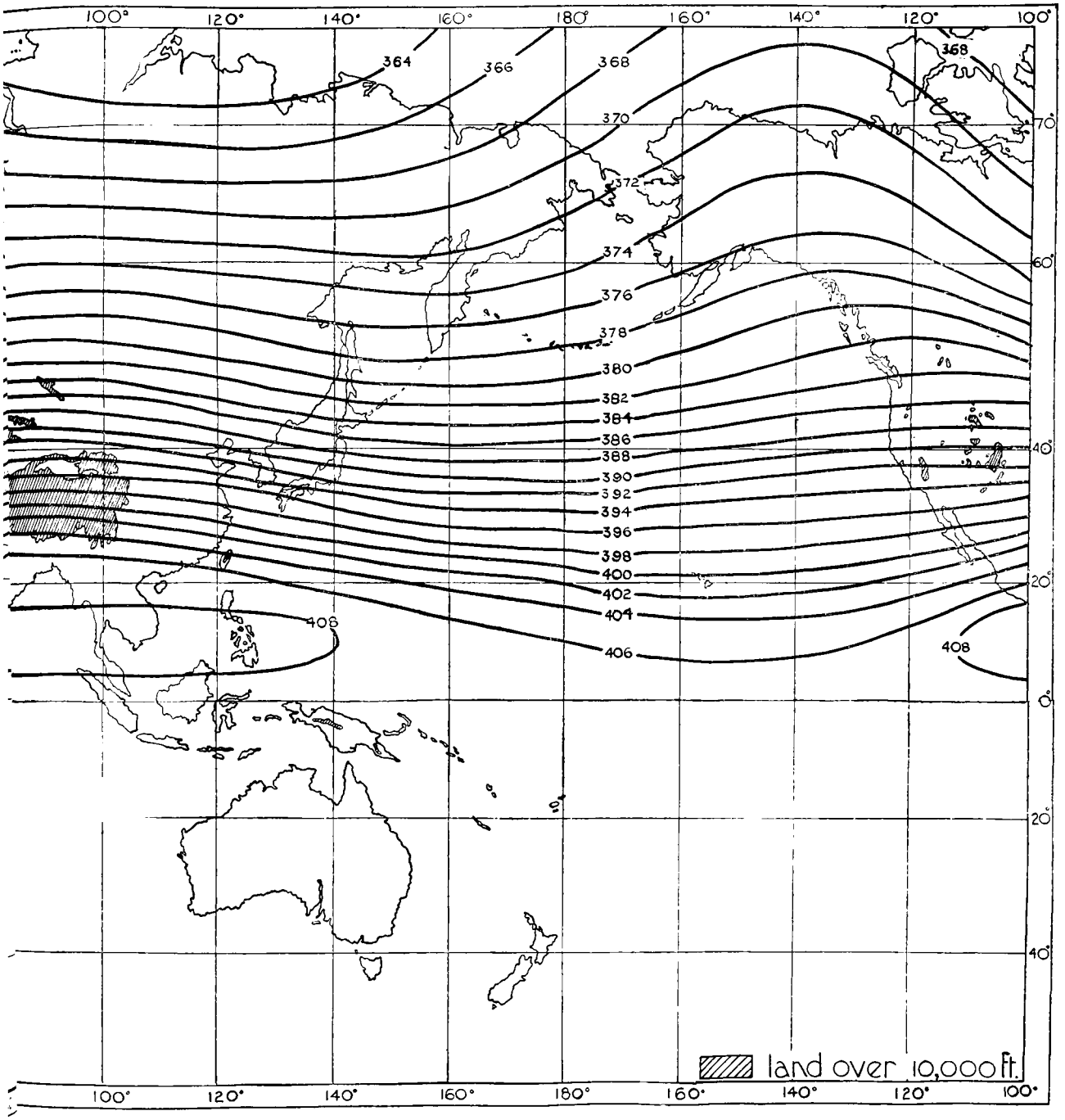

CONTOURS

Height of isobaric surface is given in hundreds of feet

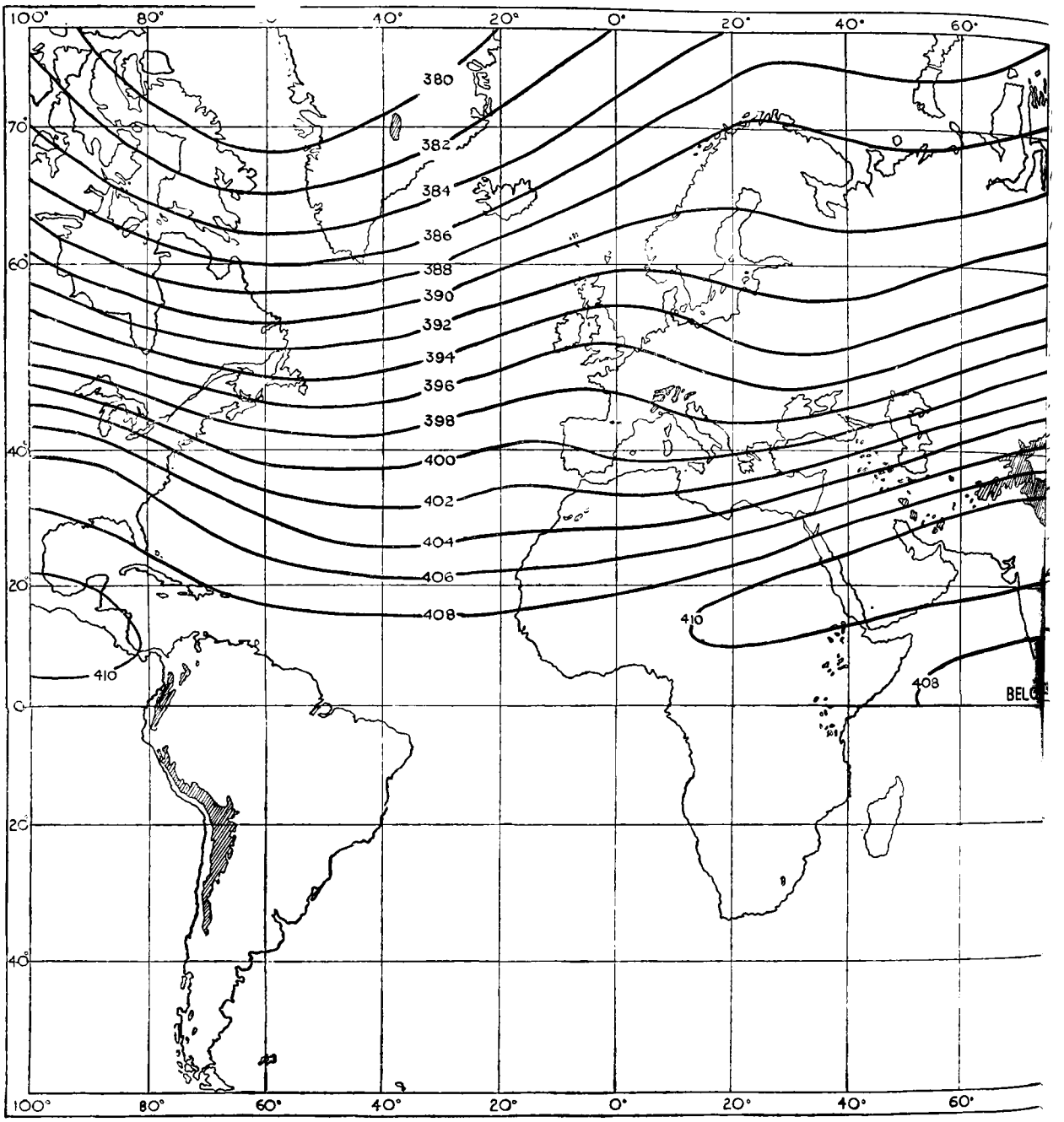

CONTOURS

Height of isobaric surface is given in hundreds of feet

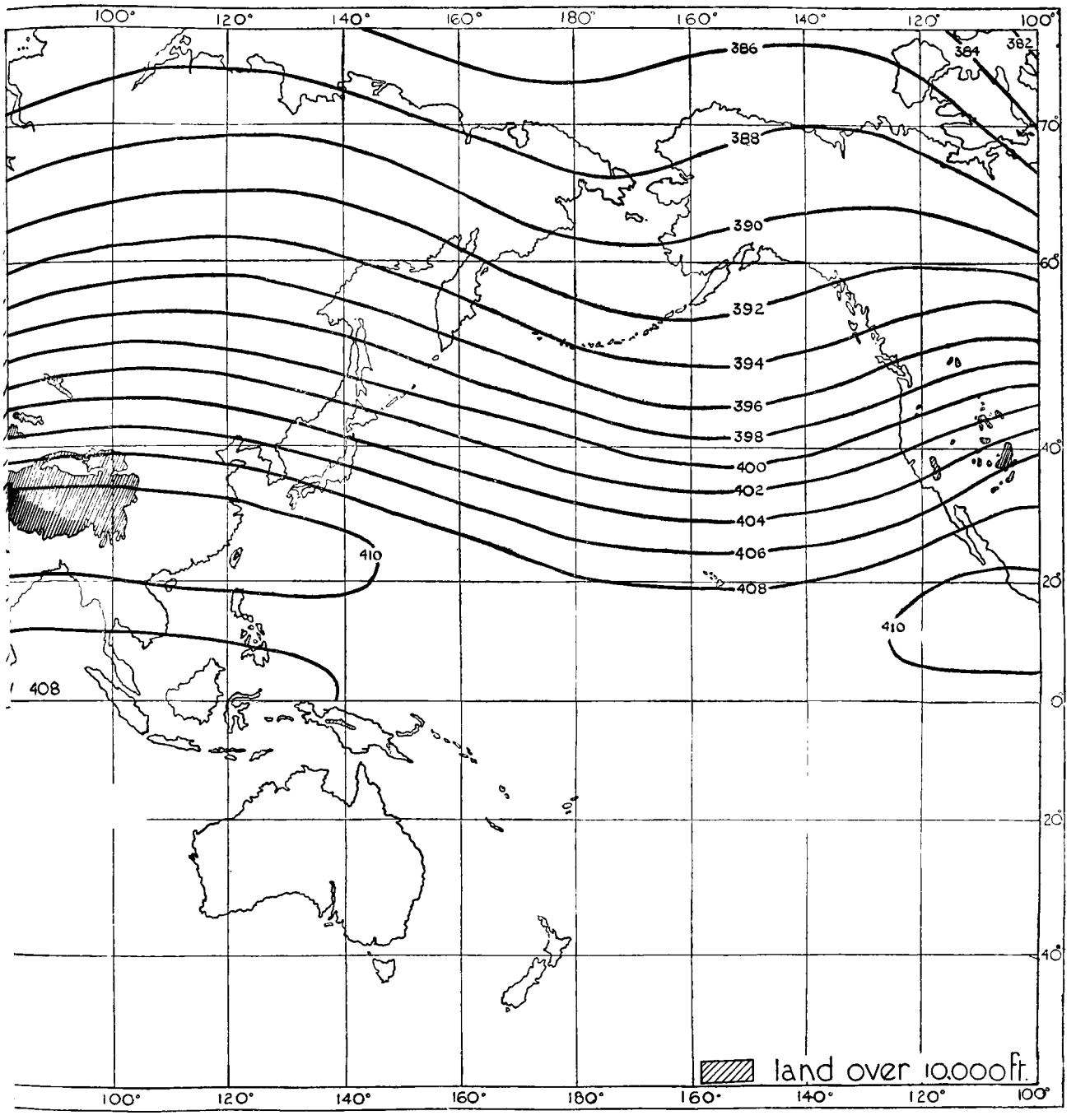

CONTOURS

Height of isobaric surface is given in hundreds of feet

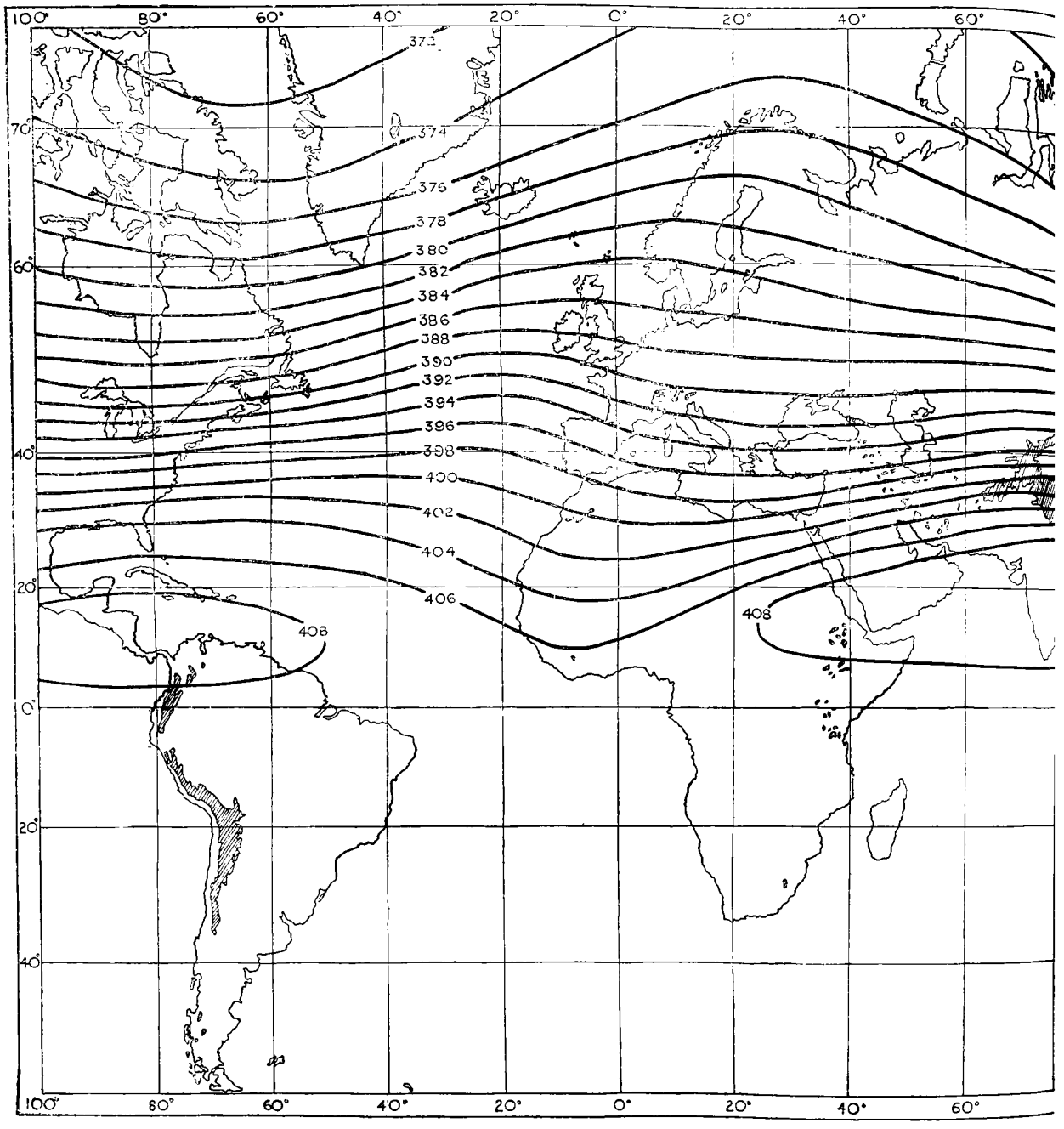

CONTOURS

Height of isobaric surface is given in hundreds of feet

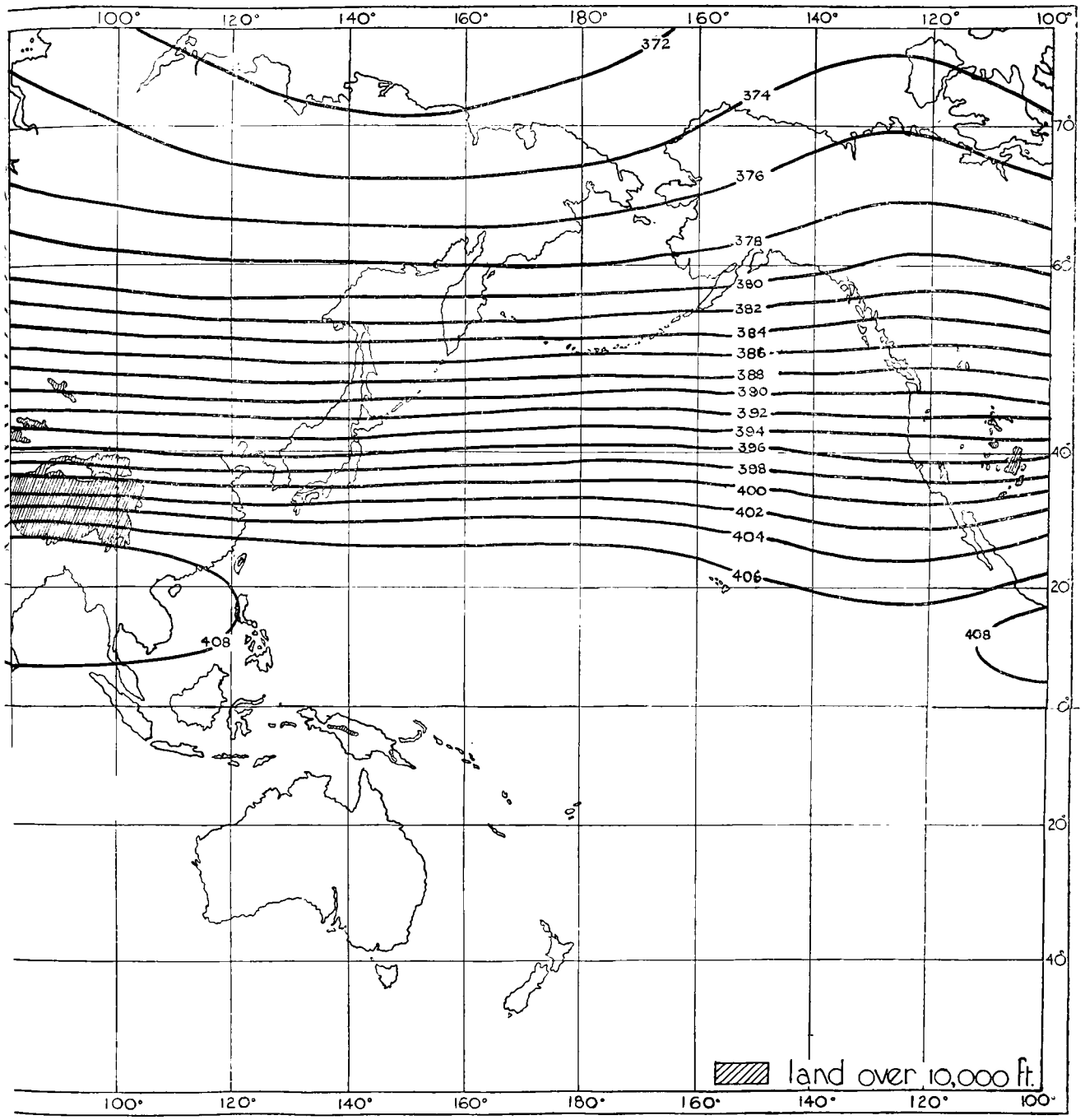

CONTOURS

Height of isobaric surface is given in hundreds of feet

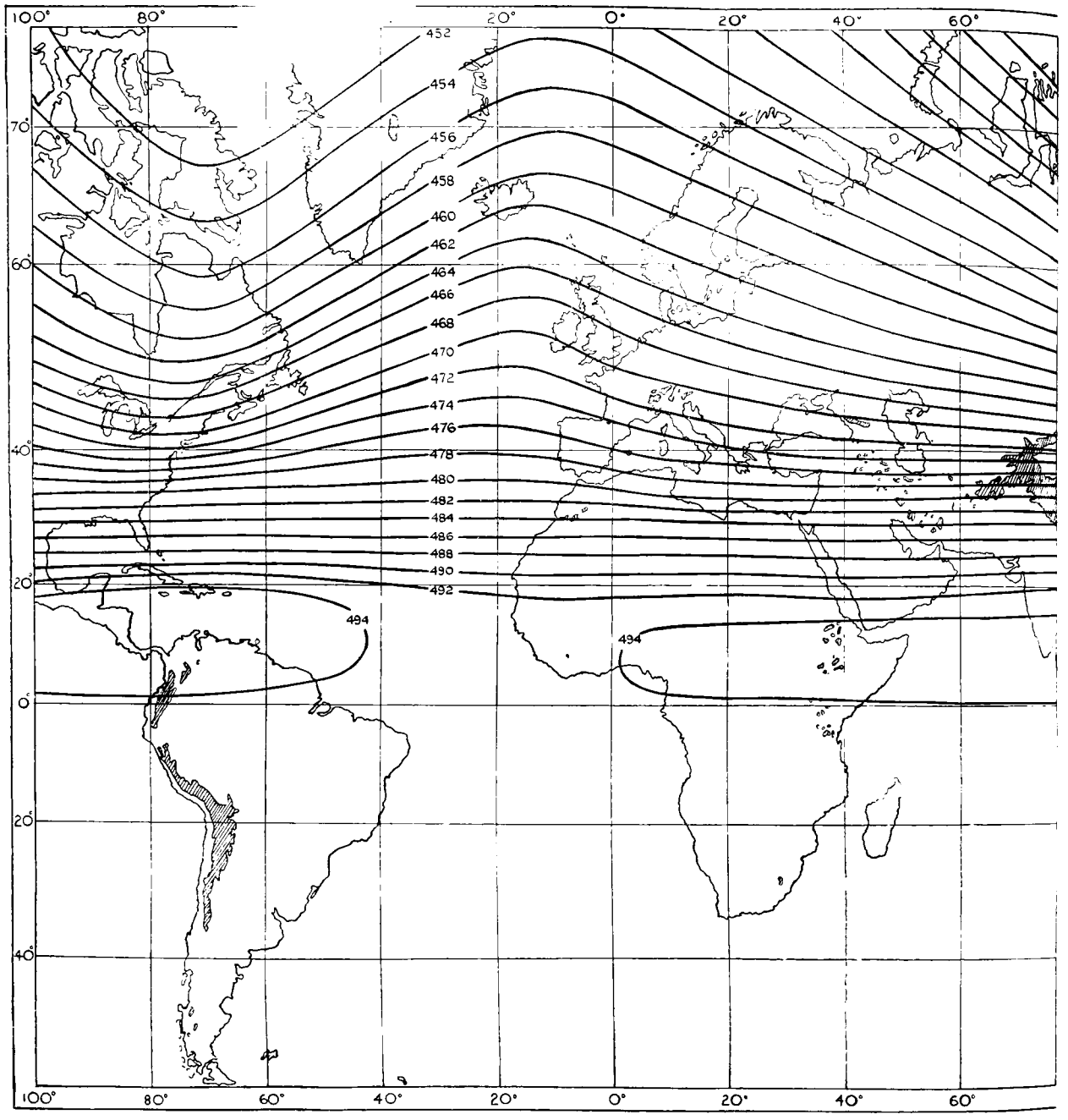

CONTOURS

Height of isobaric surface is given in hundreds of feet

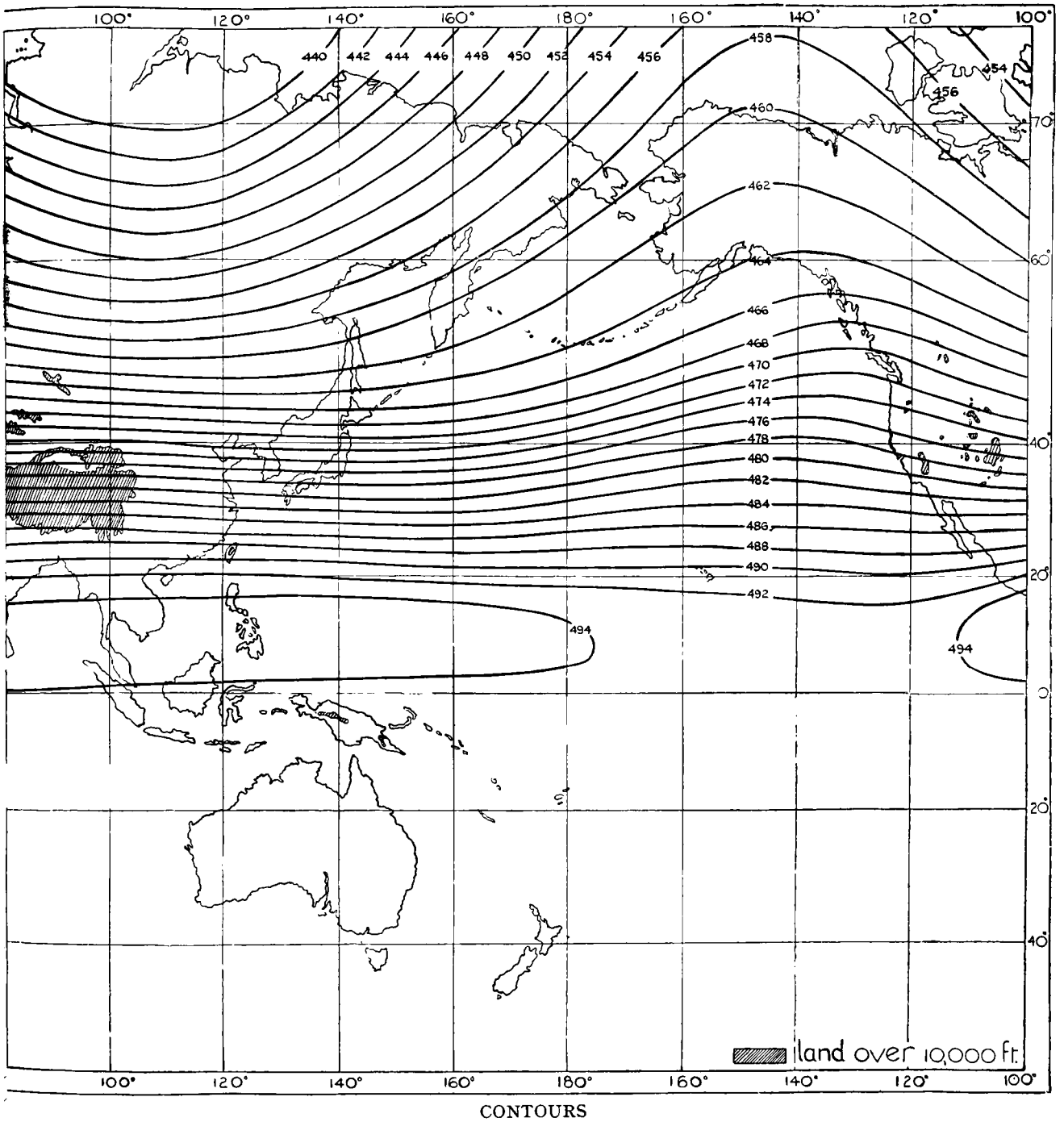

CONTOURS

Height of isobaric surface is given in hundreds of feet

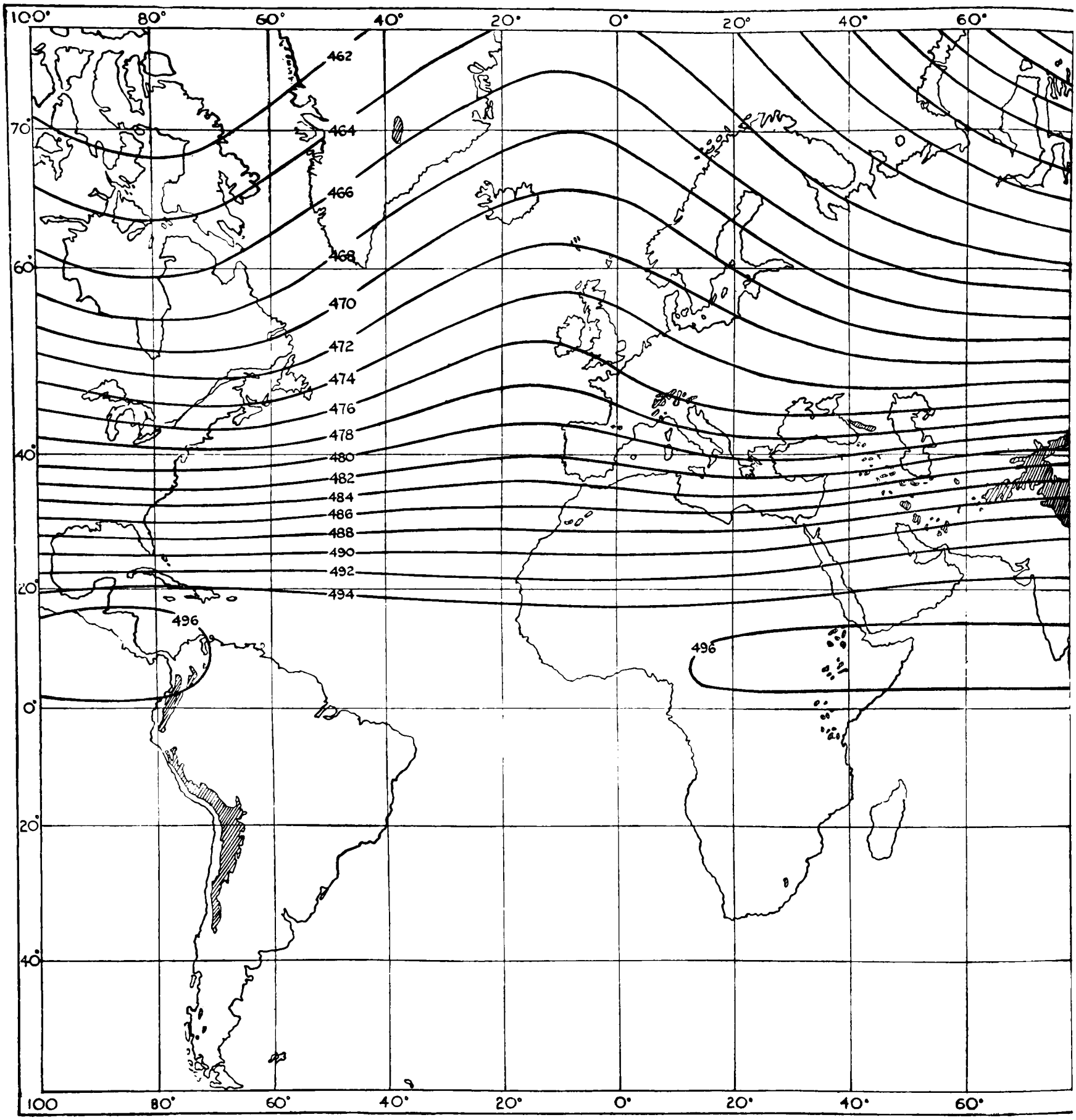

CONTOURS

Height of isobaric surface is given in hundreds of feet

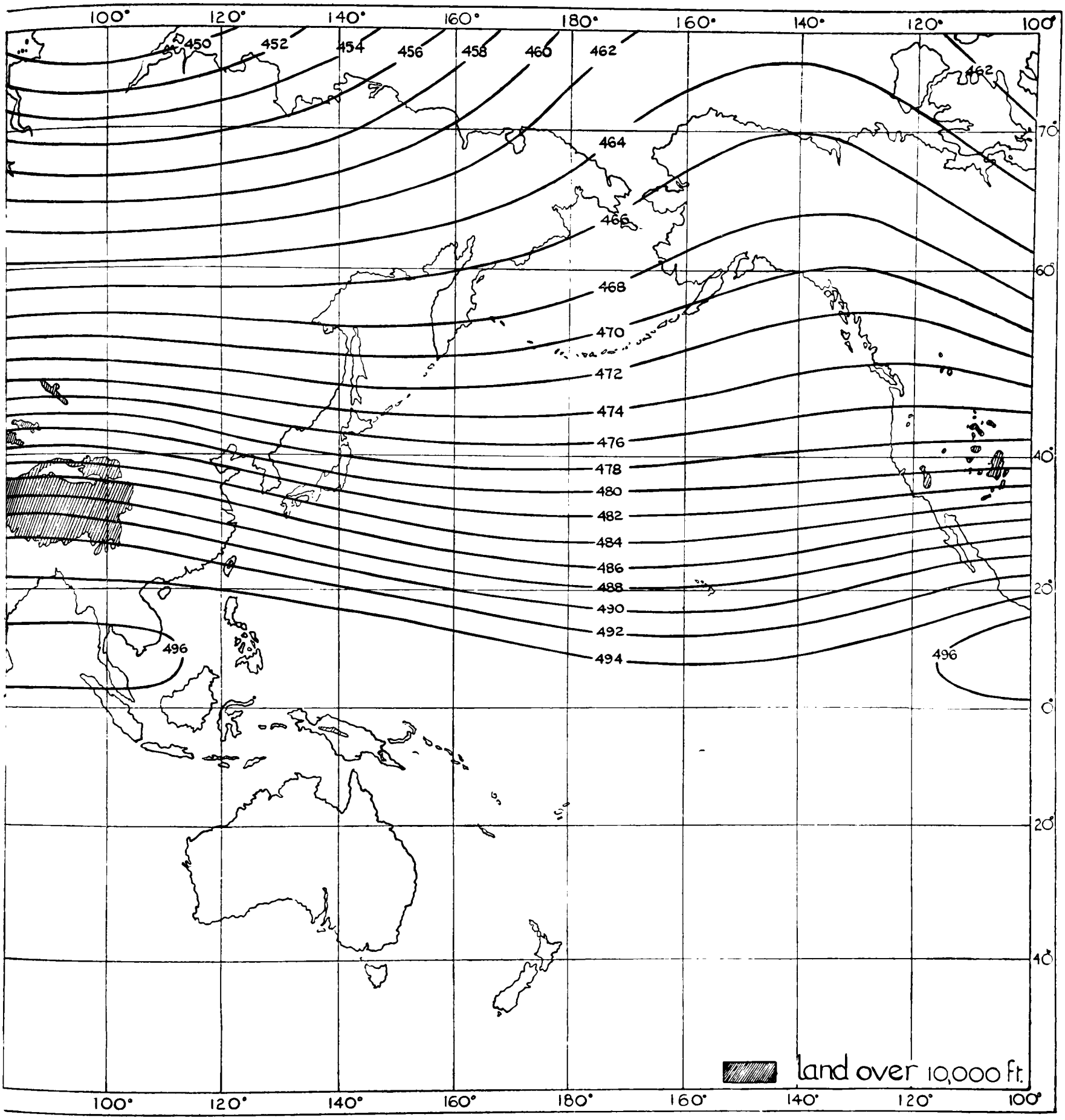

CONTOURS

Height of isobaric surface is given in hundreds of feet

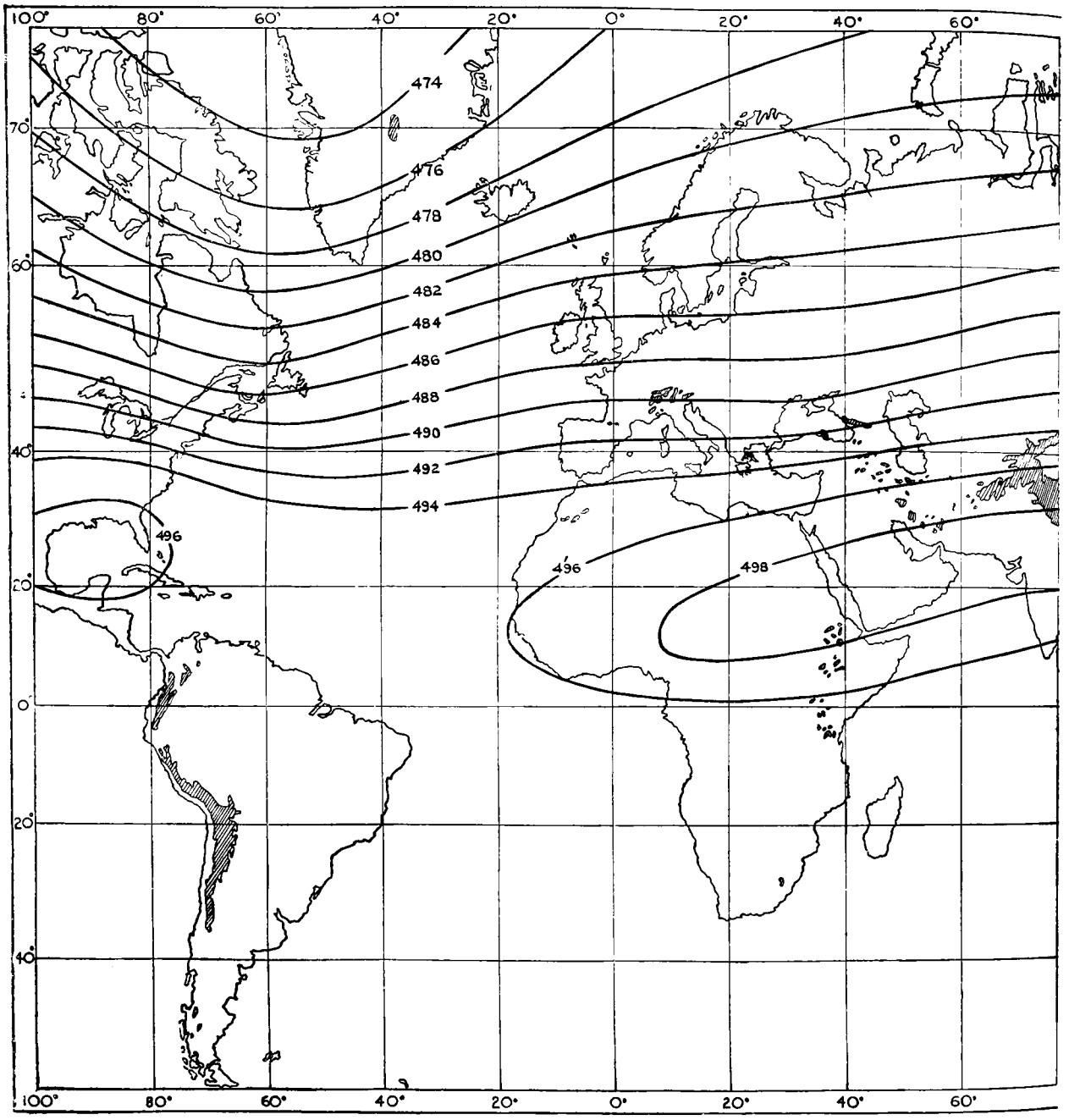

CONTOURS

Height of isobaric surface is given in hundreds of feet

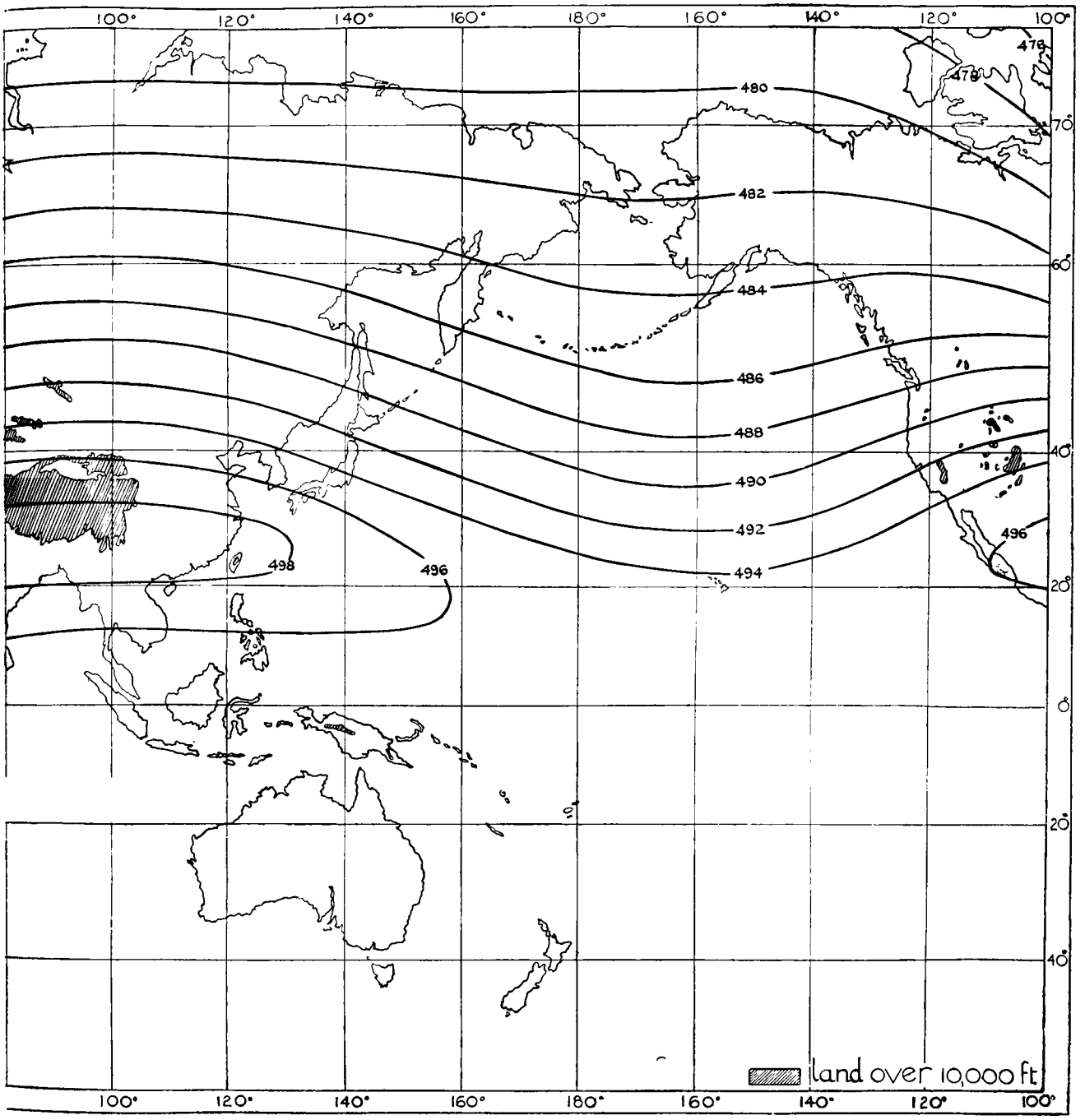

CONTOURS

Height of isobaric surface is given in hundreds of feet

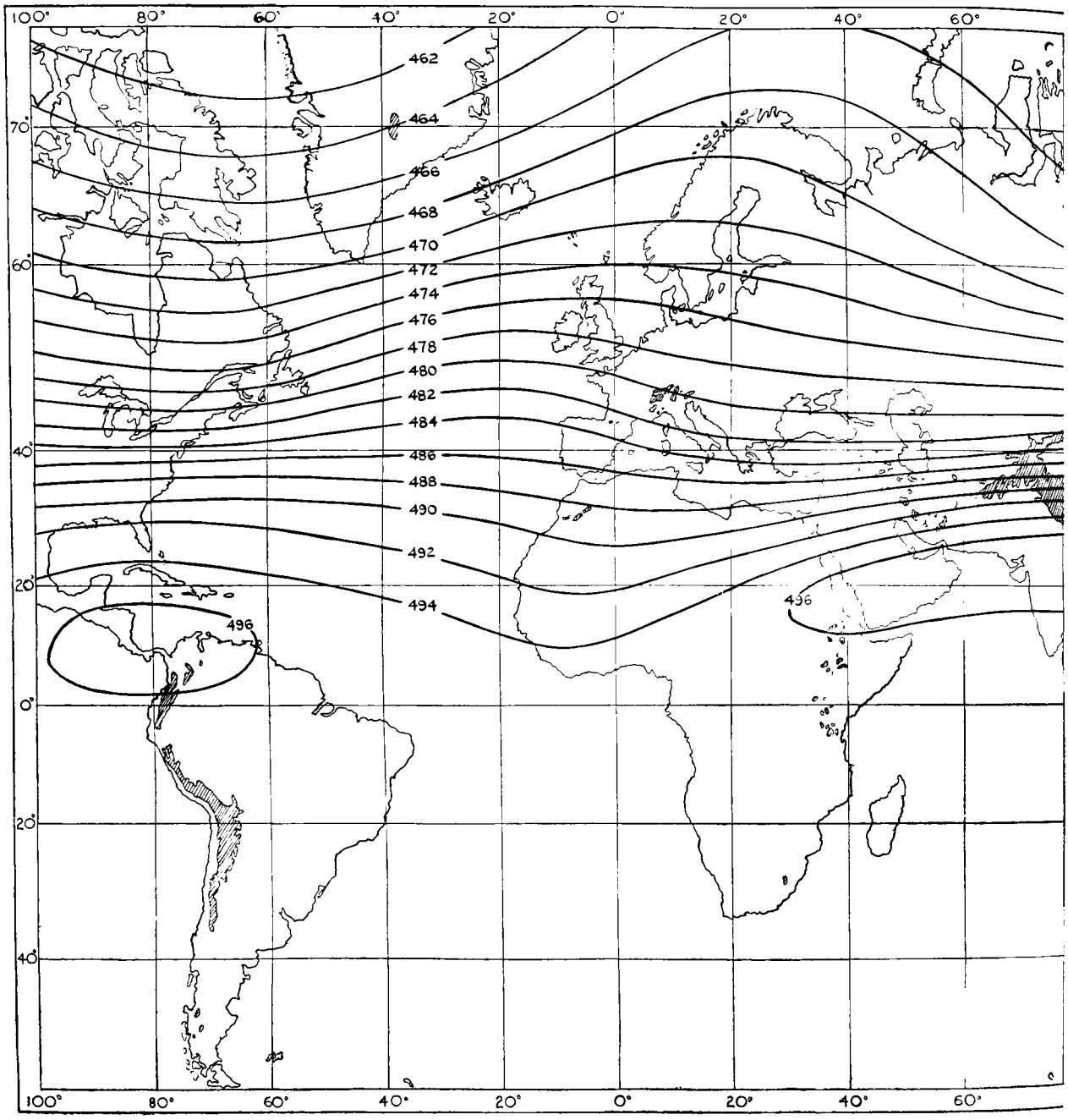

CONTOURS

Height of isobaric surface is given in hundreds of feet

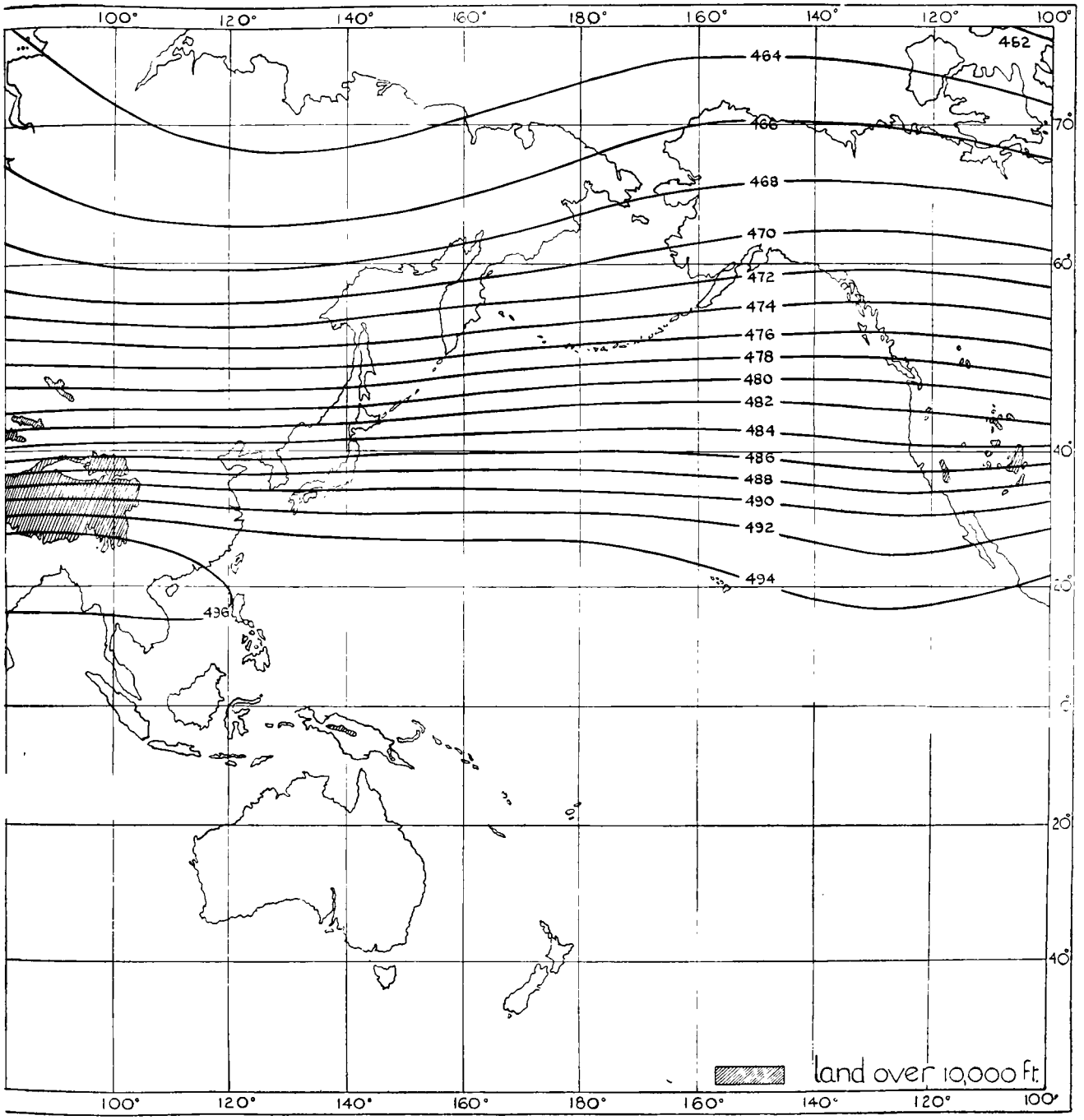

CONTOURS

Height of isobaric surface is given in hundreds of feet

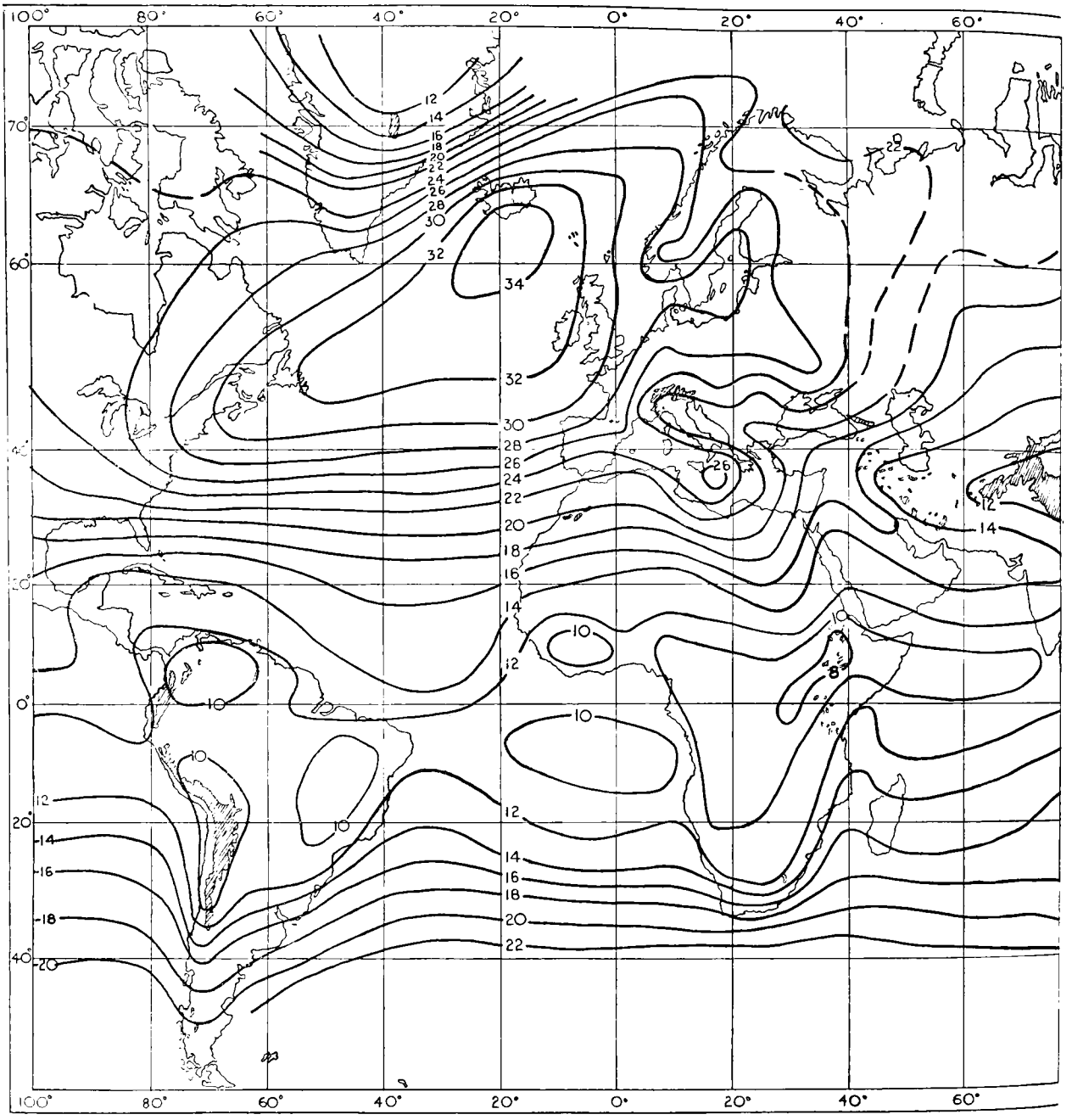

STANDARD VECTOR DEVIATION (knots)

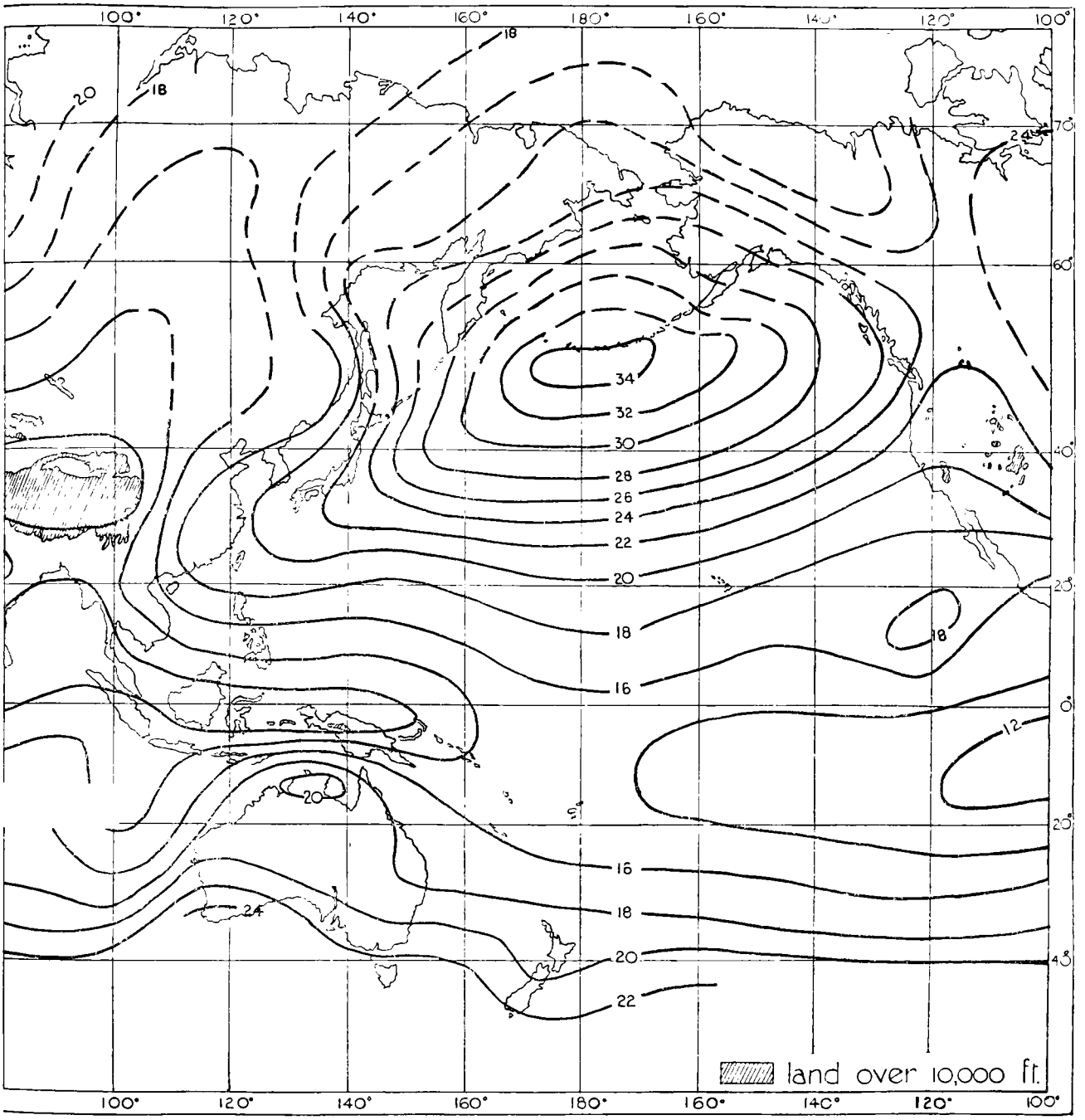

STANDARD VECTOR DEVIATION (knots)

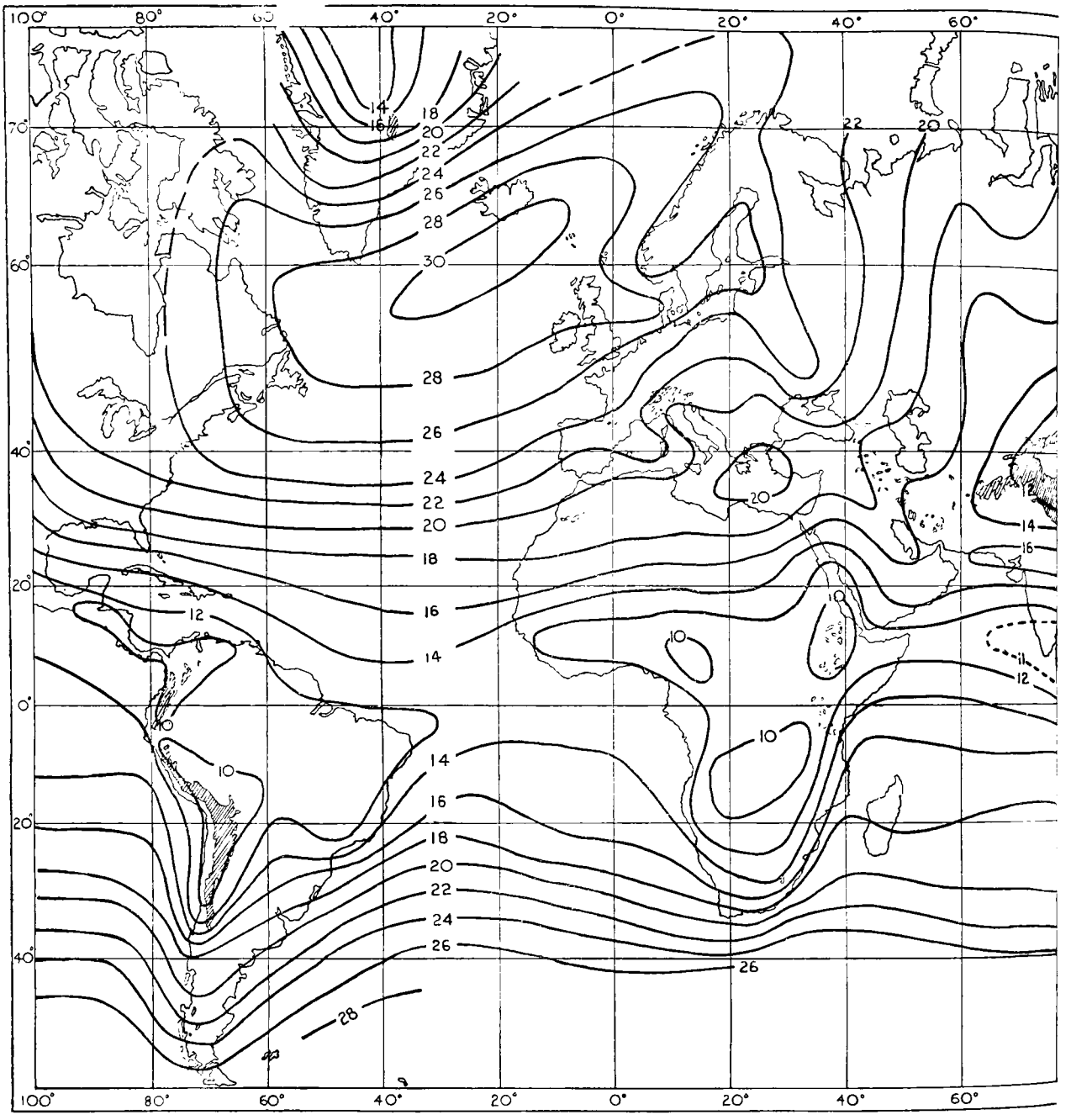

STANDARD VECTOR DEVIATION (knots)

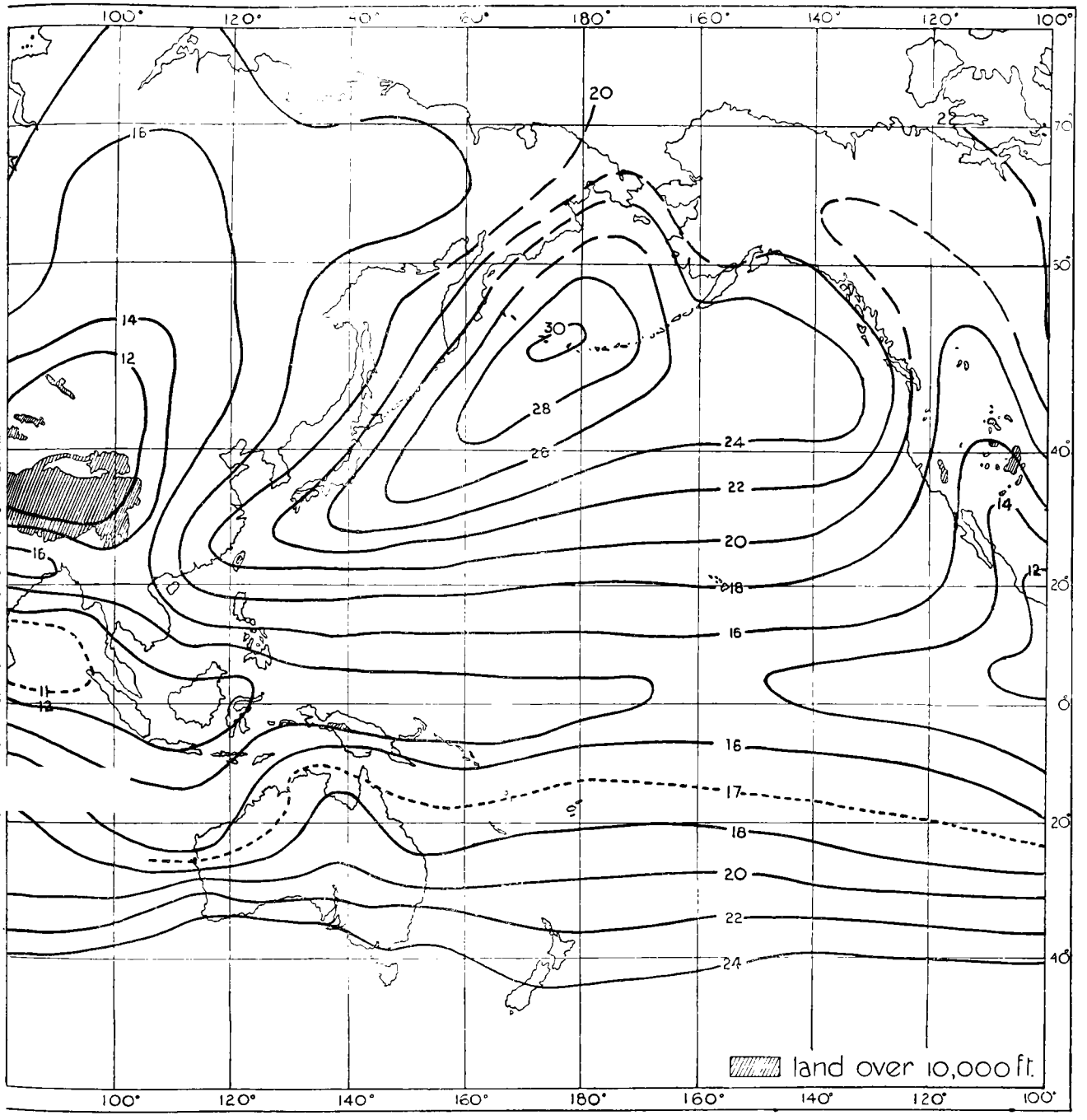

STANDARD VECTOR DEVIATION (knots)

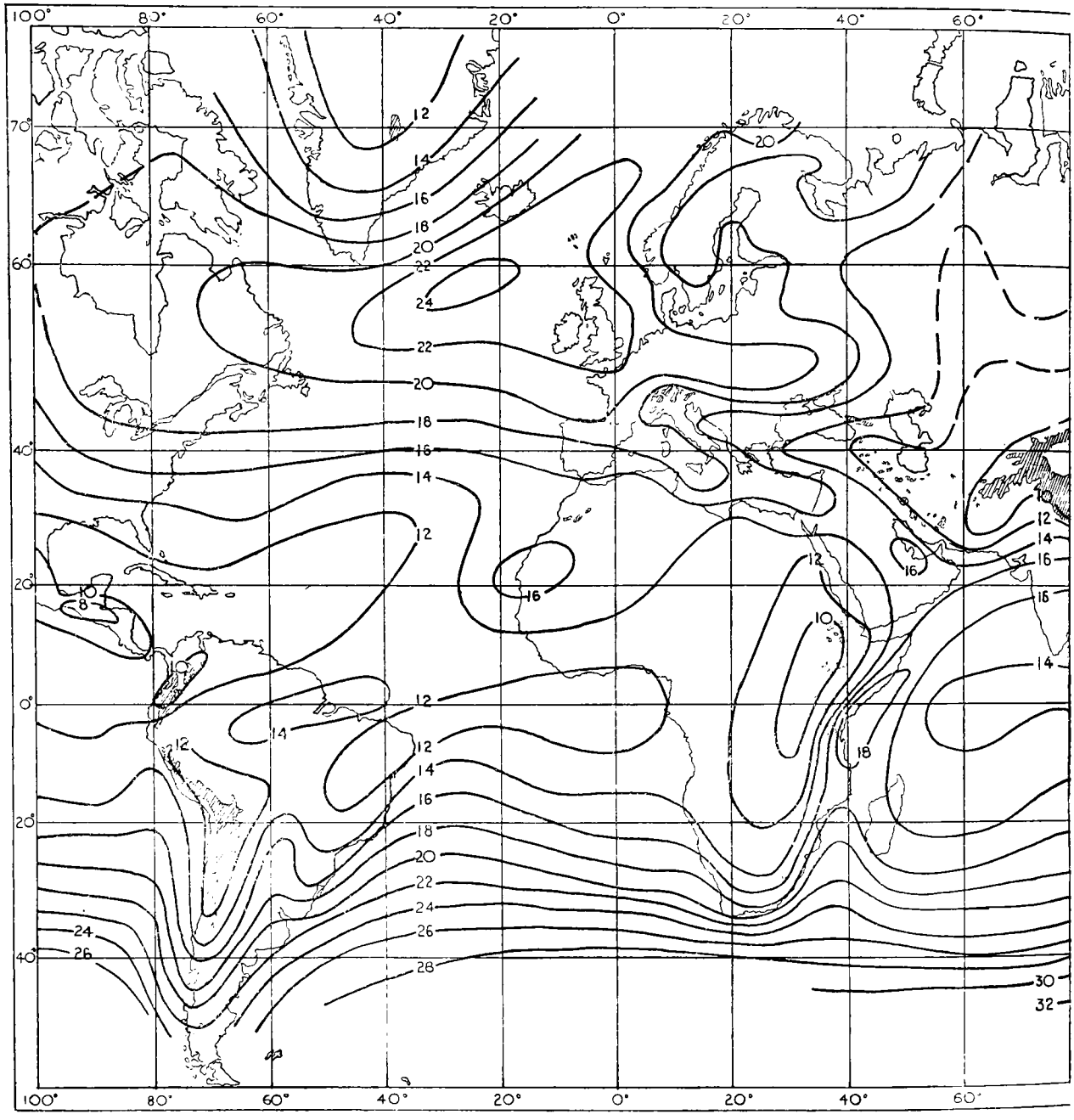

STANDARD VECTOR DEVIATION (knots)

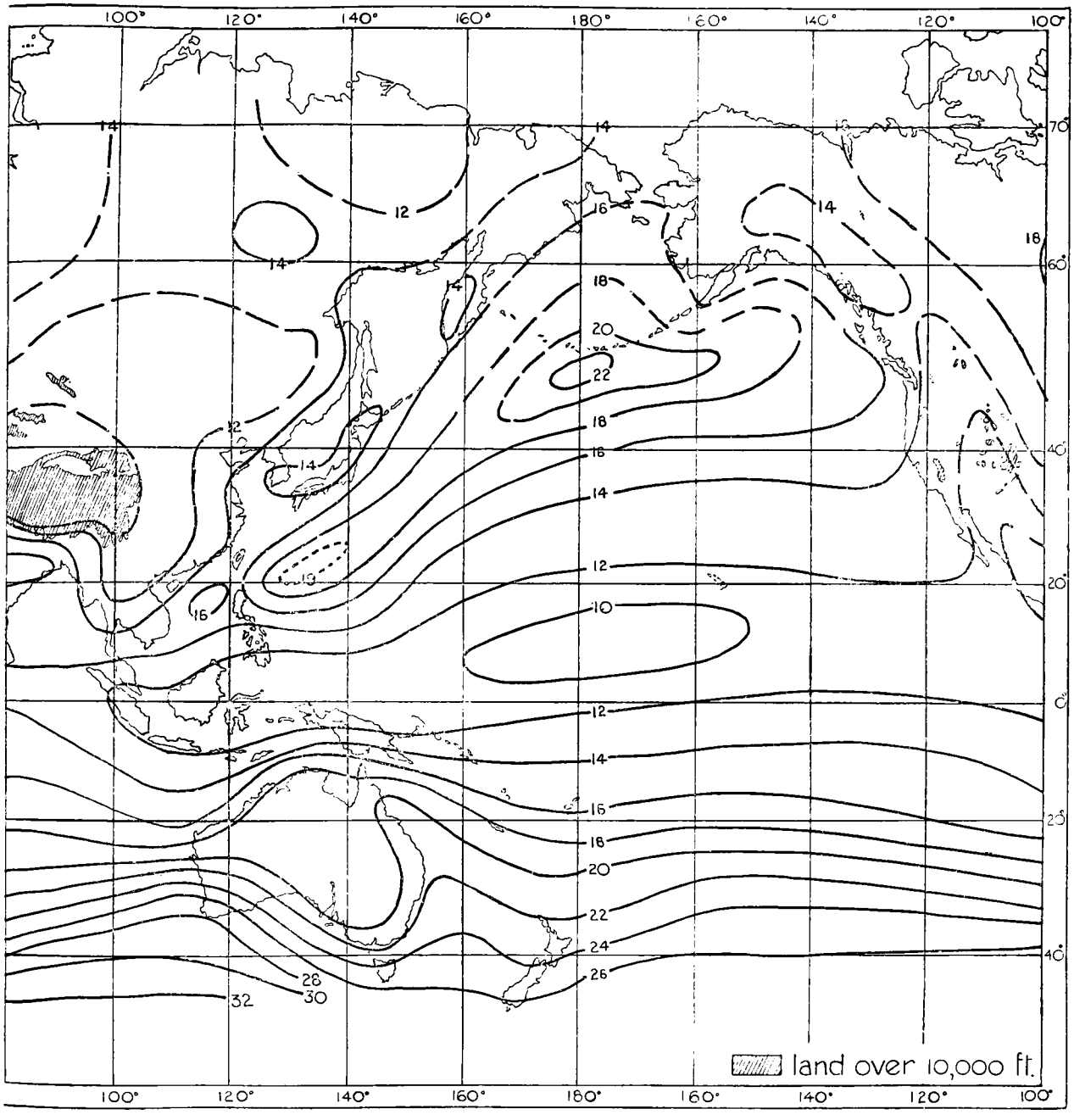

STANDARD VECTOR DEVIATION (knots)

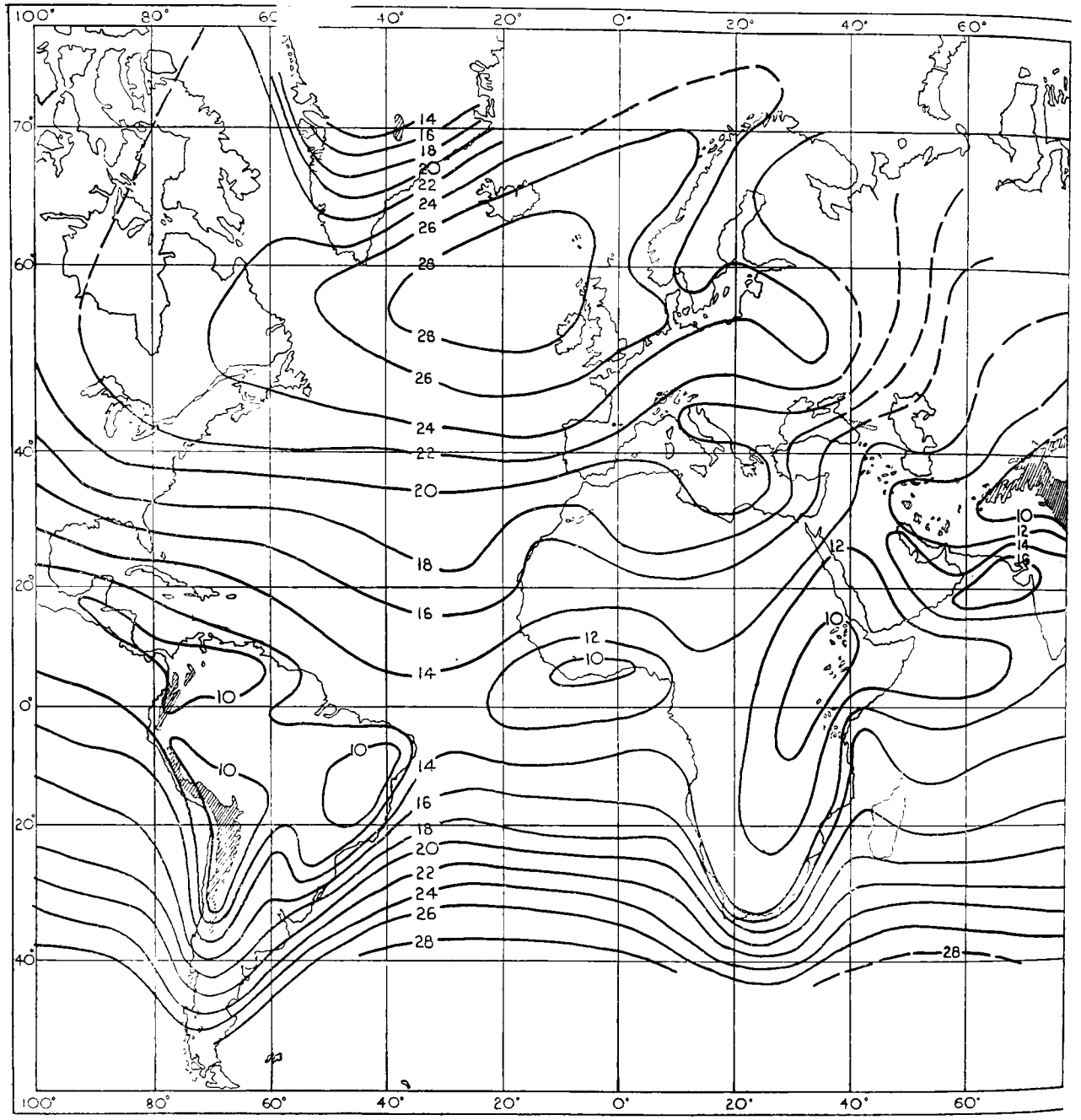

STANDARD VECTOR DEVIATION (knots)

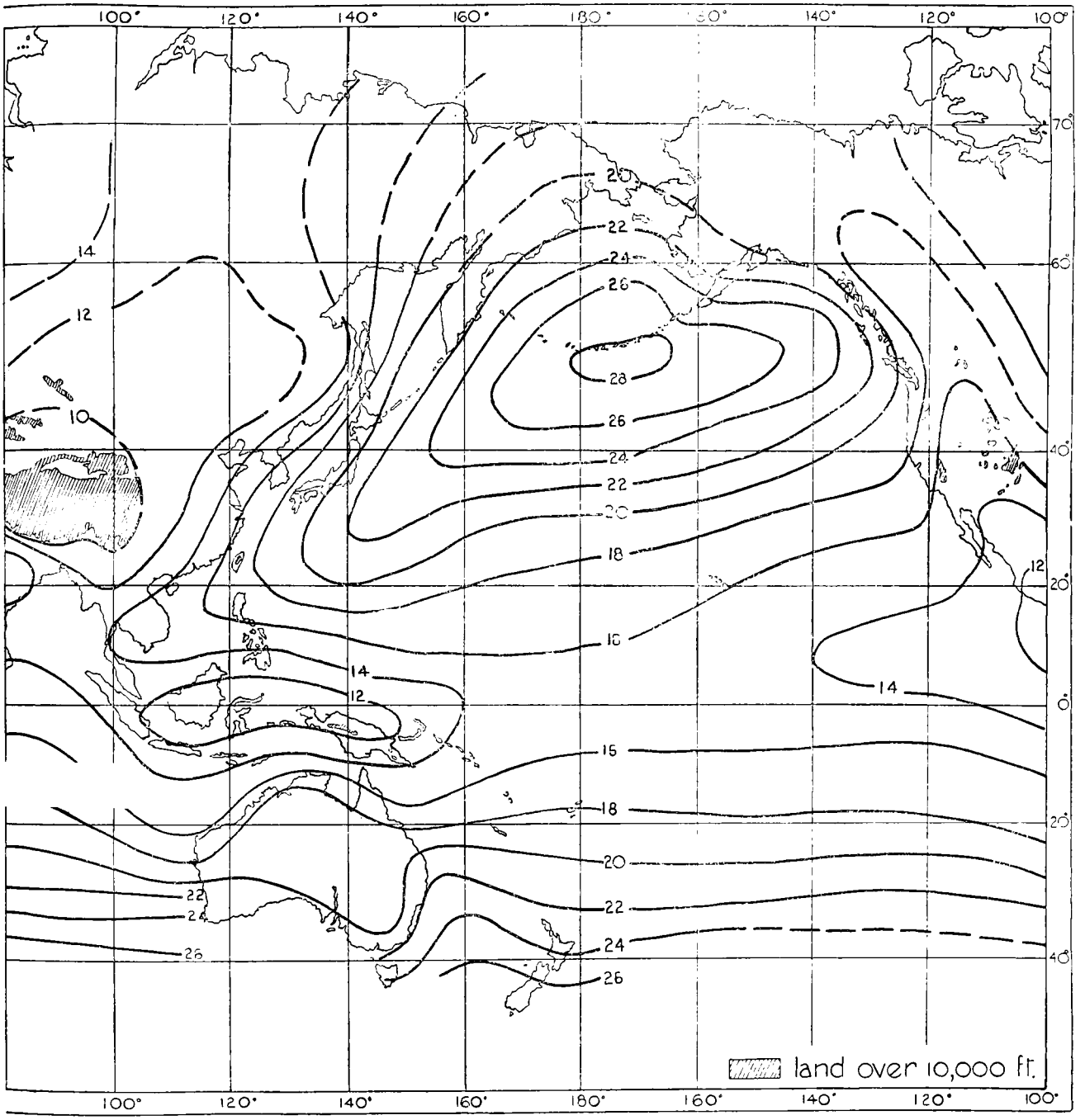

STANDARD VECTOR DEVIATION (knots)

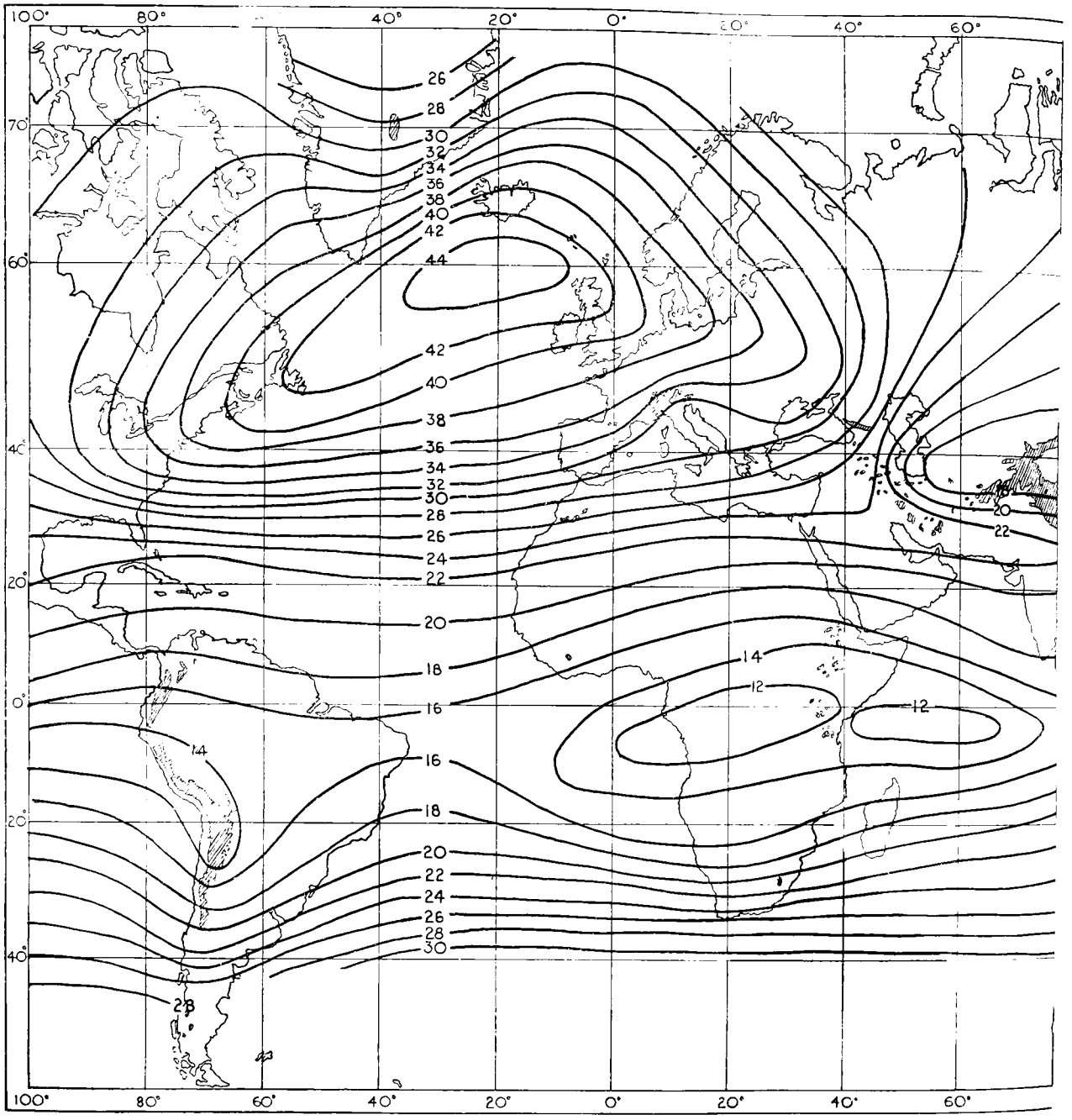

STANDARD VECTOR DEVIATION (knots)

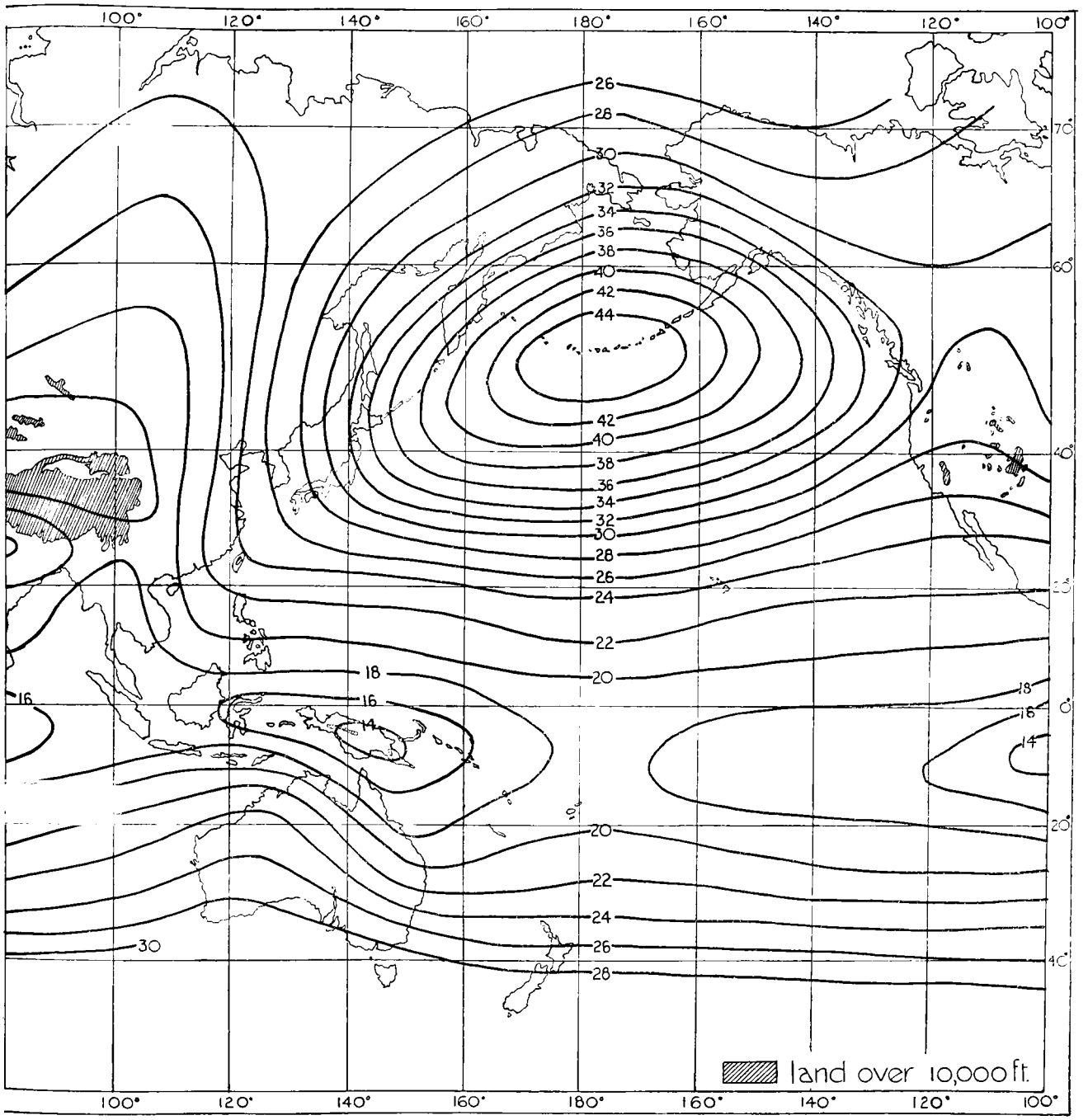

STANDARD VECTOR DEVIATION (knots)

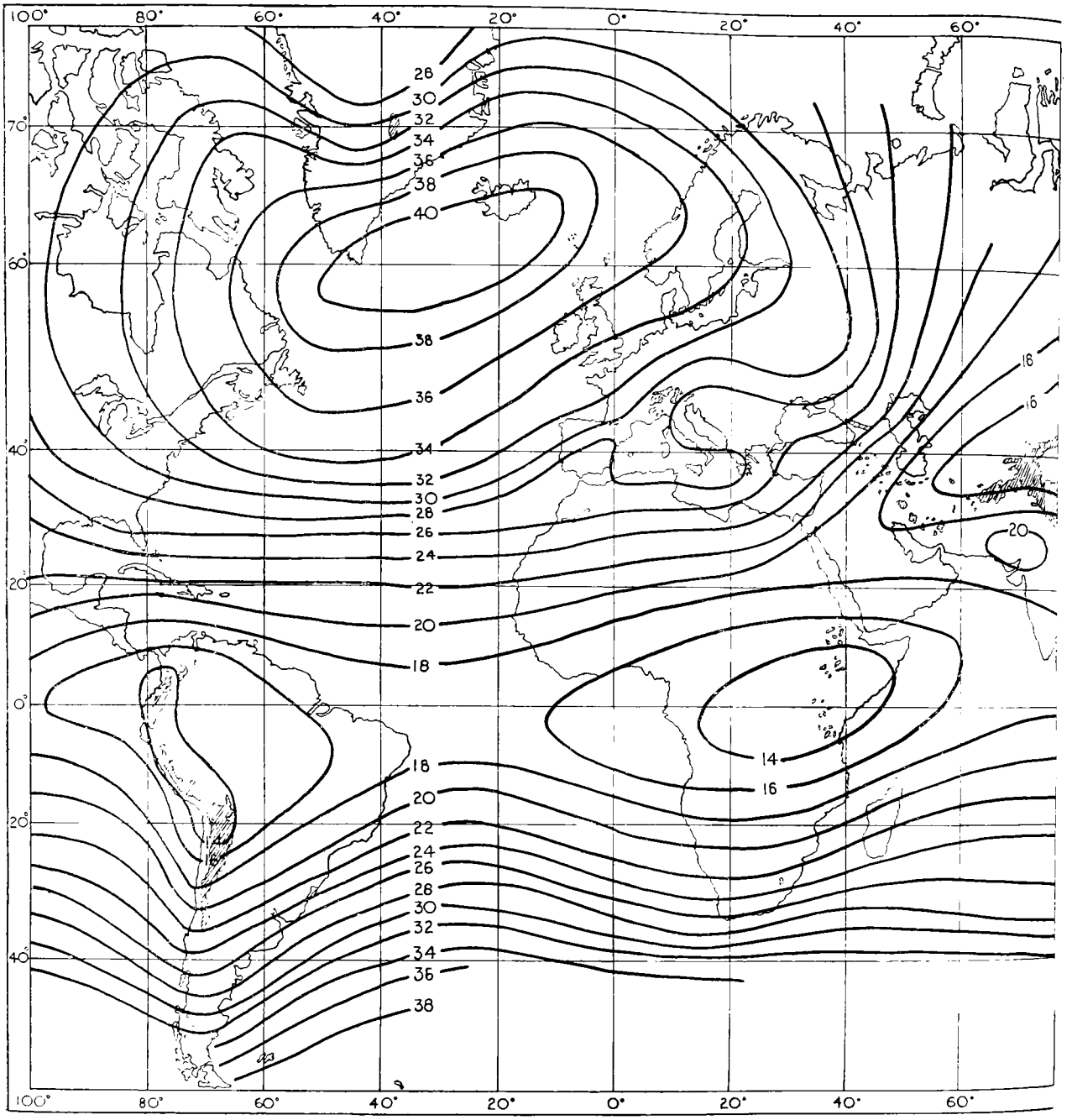

STANDARD VECTOR DEVIATION (knots)

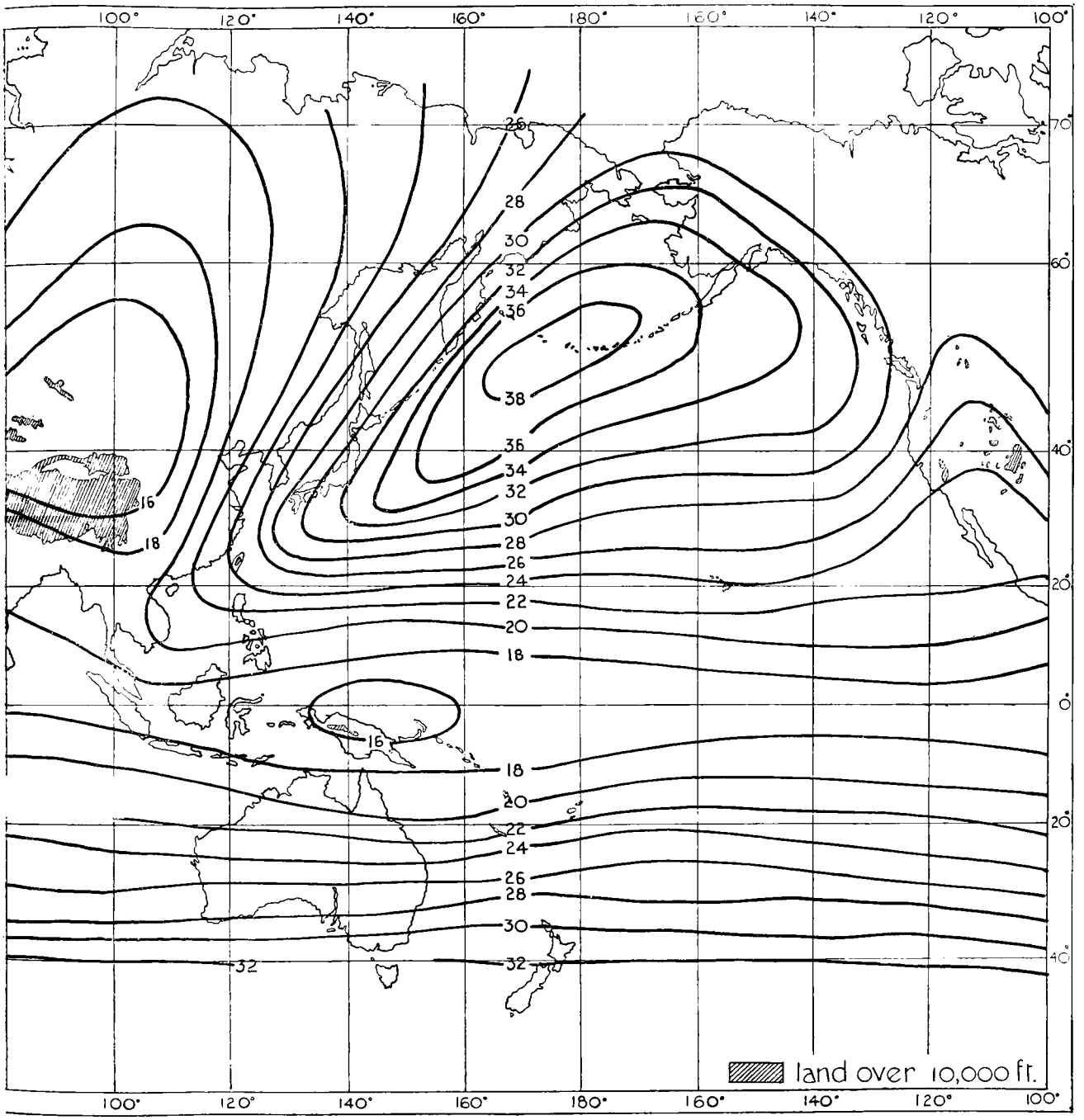

STANDARD VECTOR DEVIATION (knots)

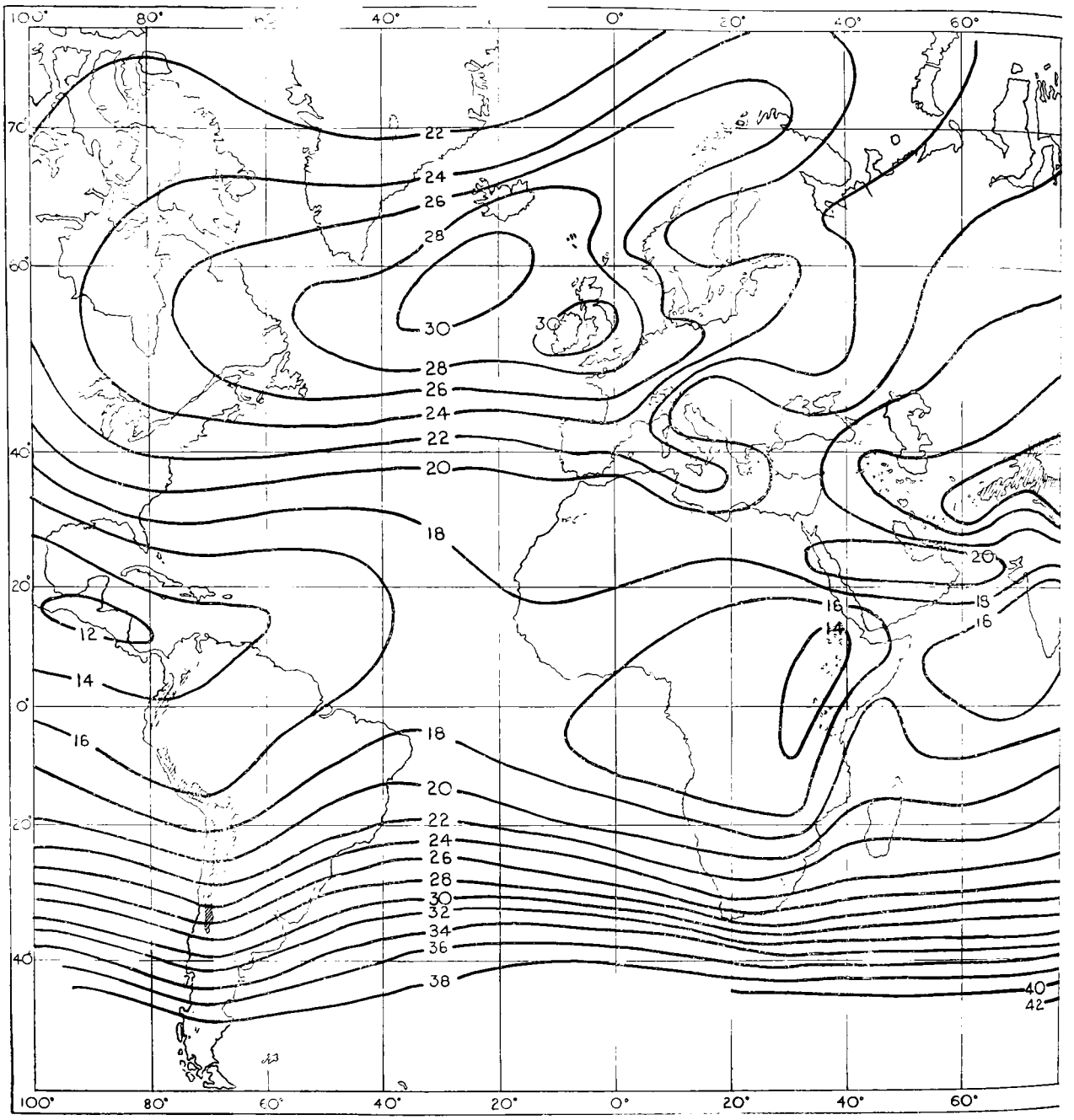

STANDARD VECTOR DEVIATION (knots)

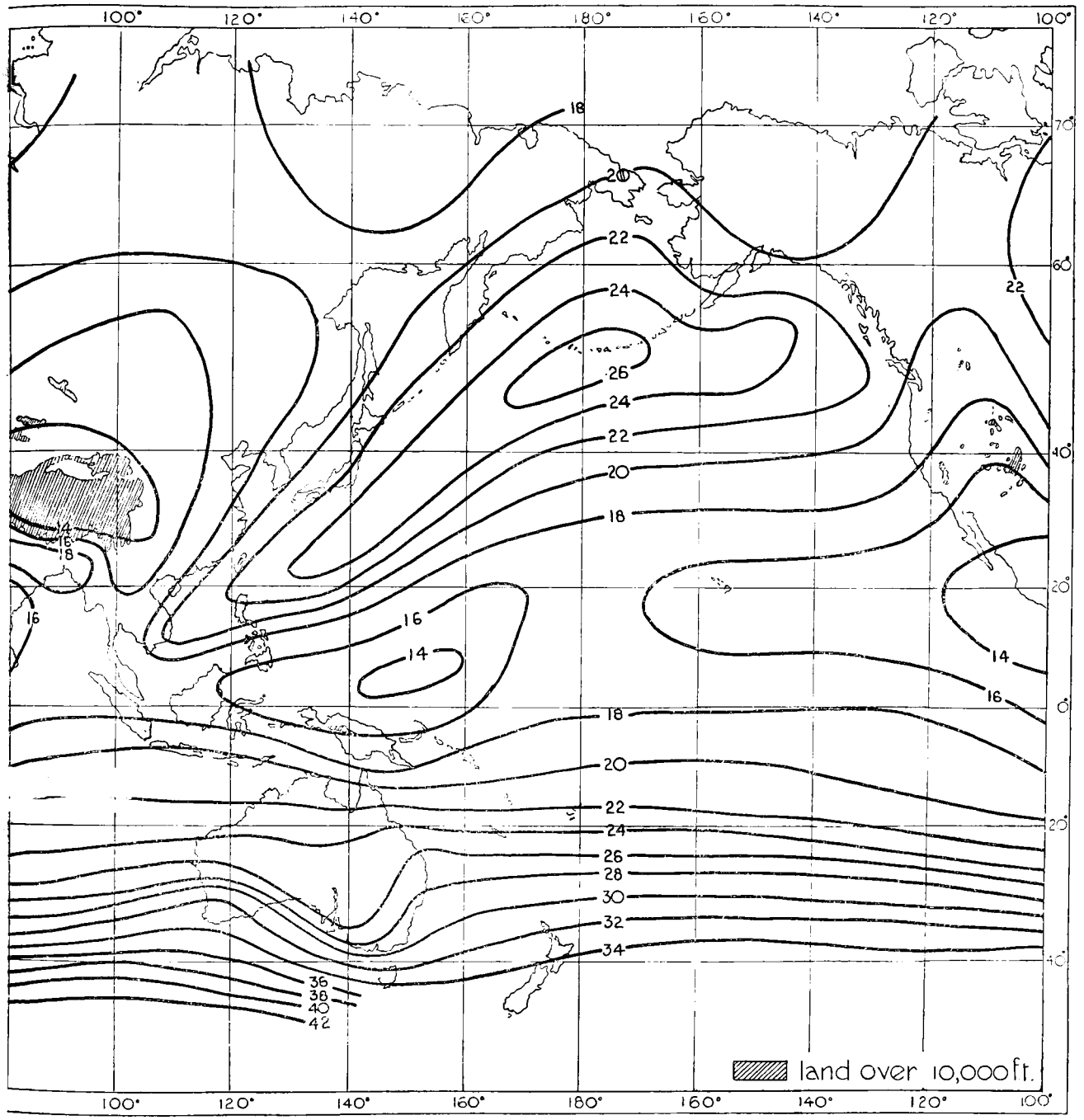

STANDARD VECTOR DEVIATION (knots)

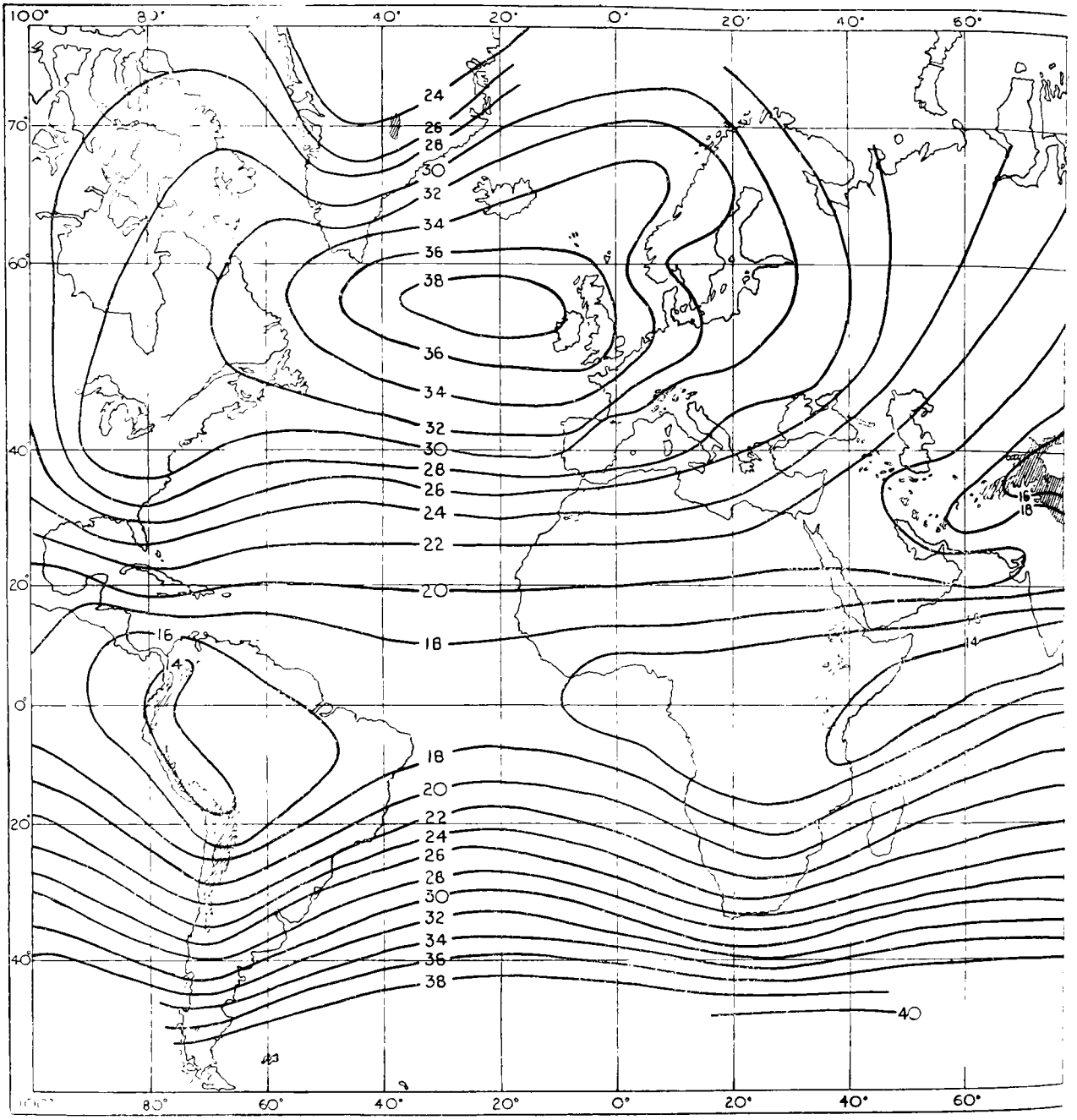

STANDARD VECTOR DEVIATION (knots)

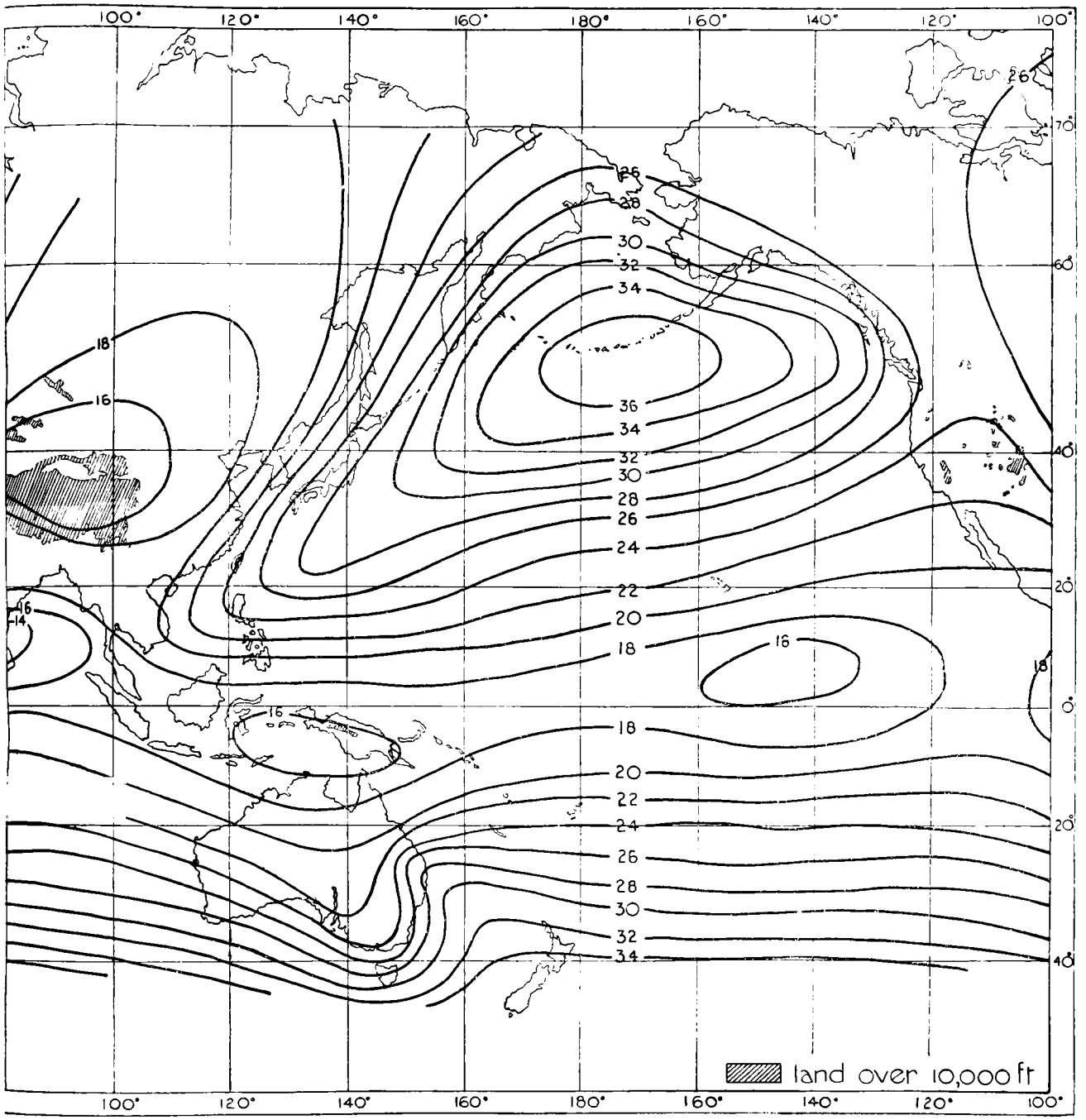

STANDARD VECTOR DEVIATION (knots)

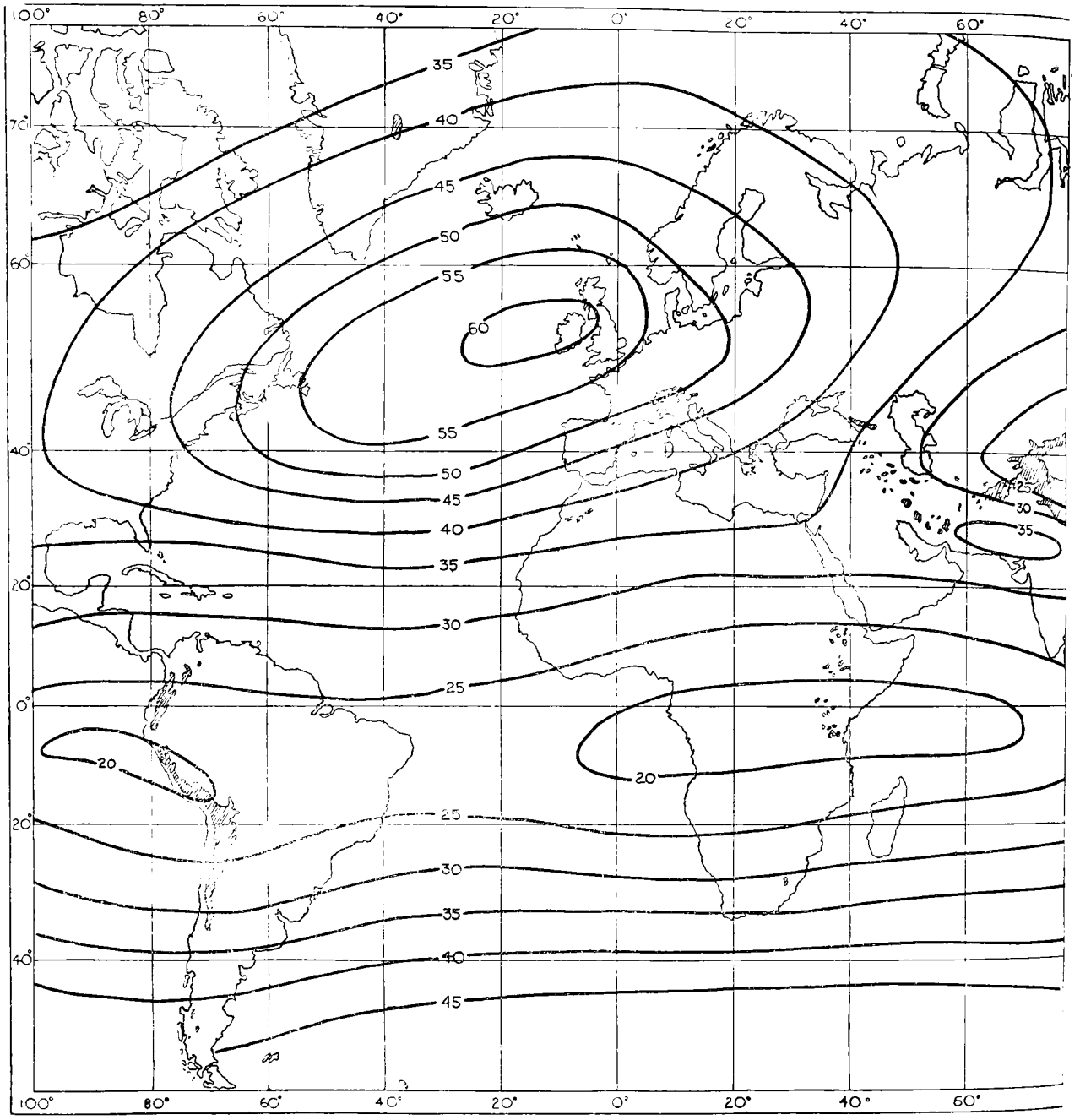

STANDARD VECTOR DEVIATION (knots)

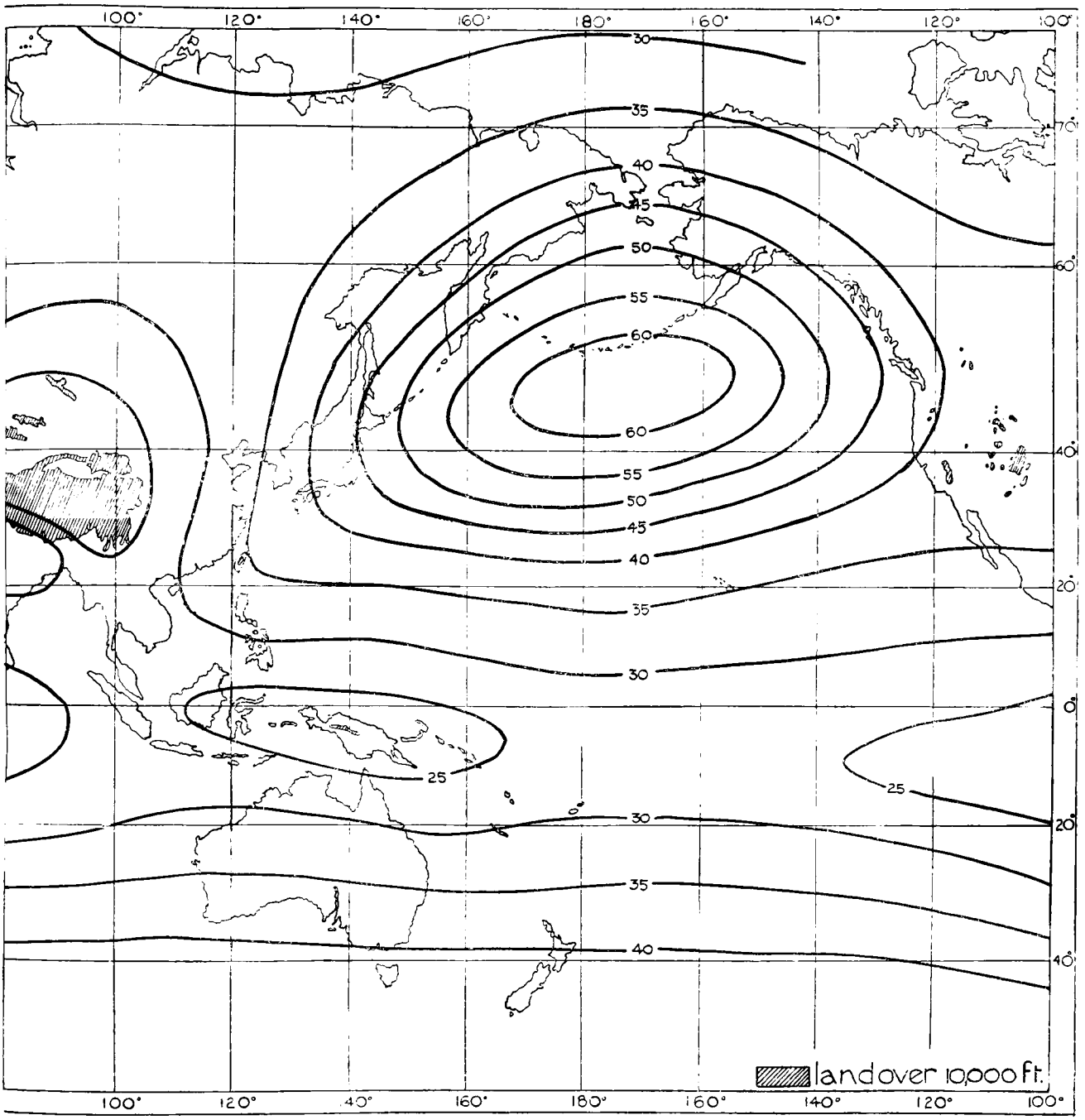

STANDARD VECTOR DEVIATION (knots)

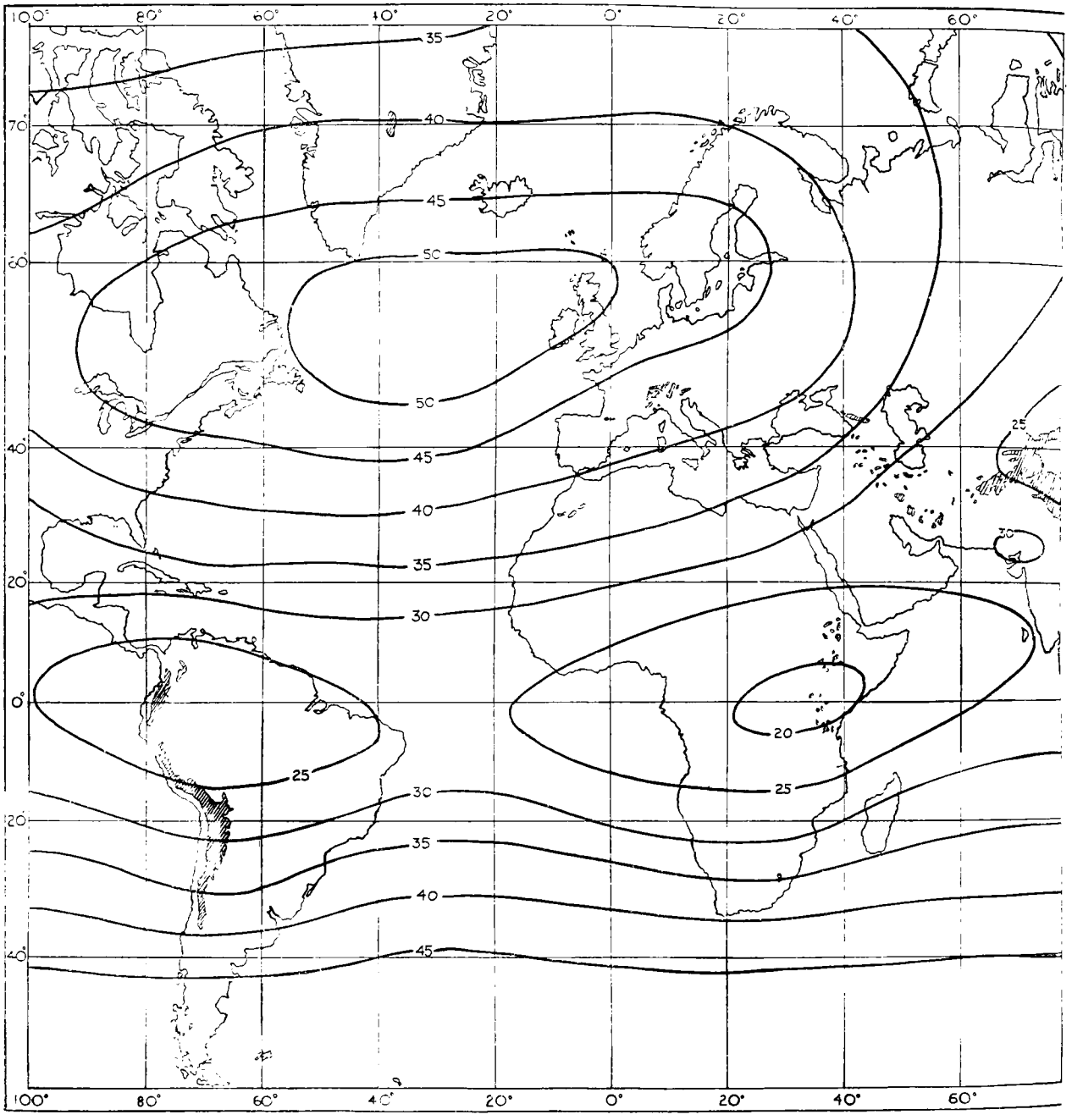

STANDARD VECTOR DEVIATION (knots)

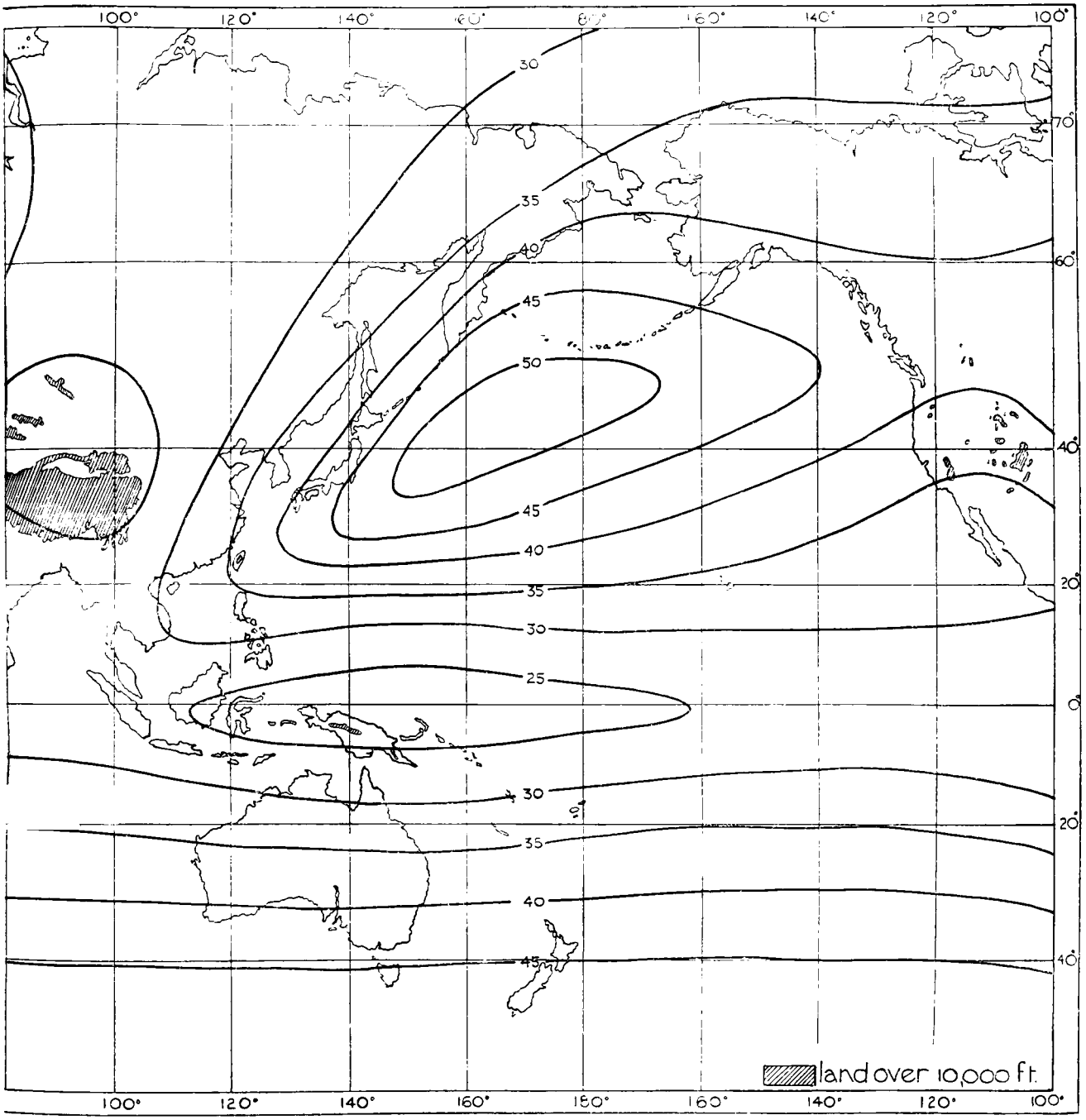

STANDARD VECTOR DEVIATION (knots)

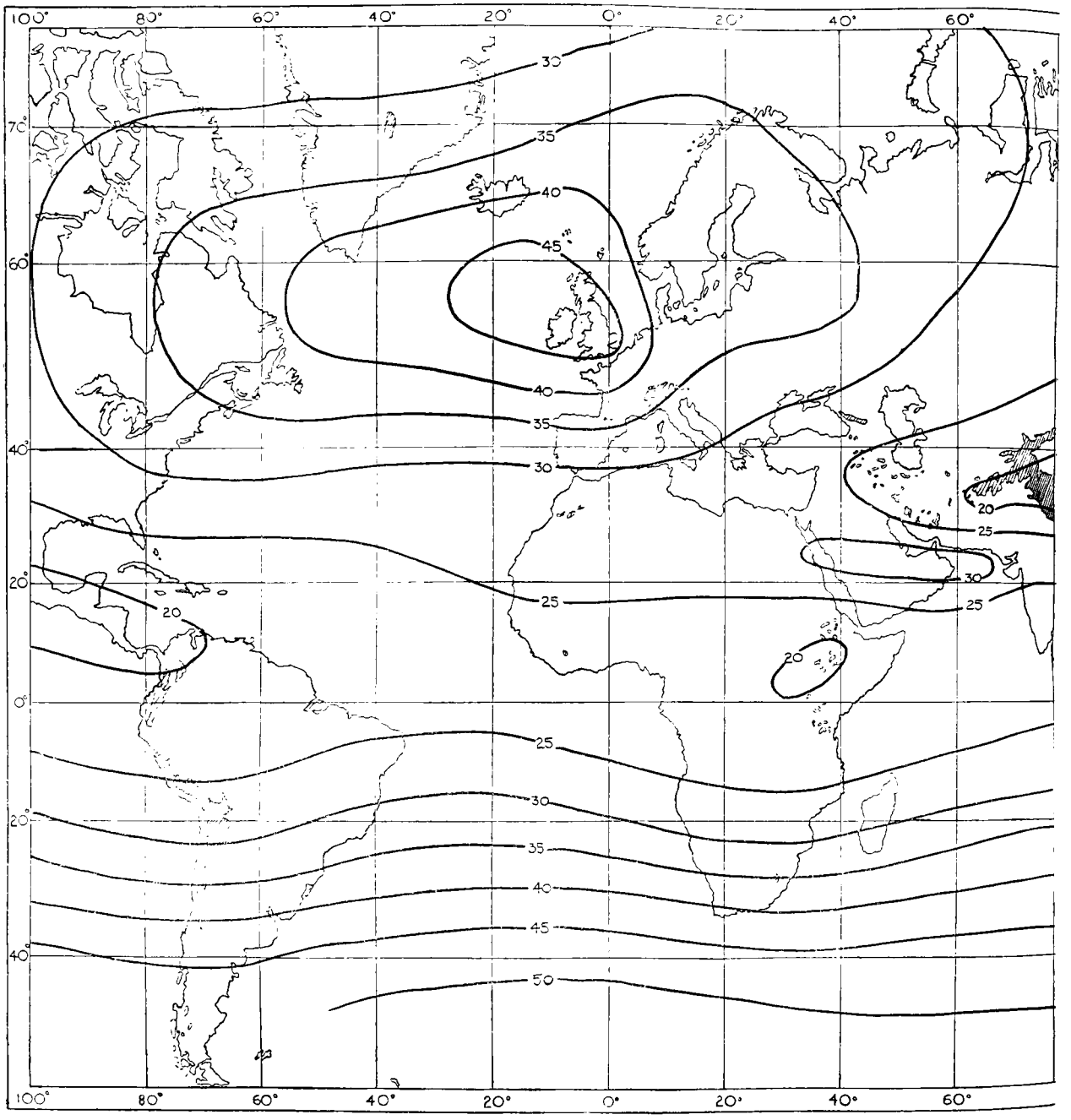

STANDARD VECTOR DEVIATION (knots)

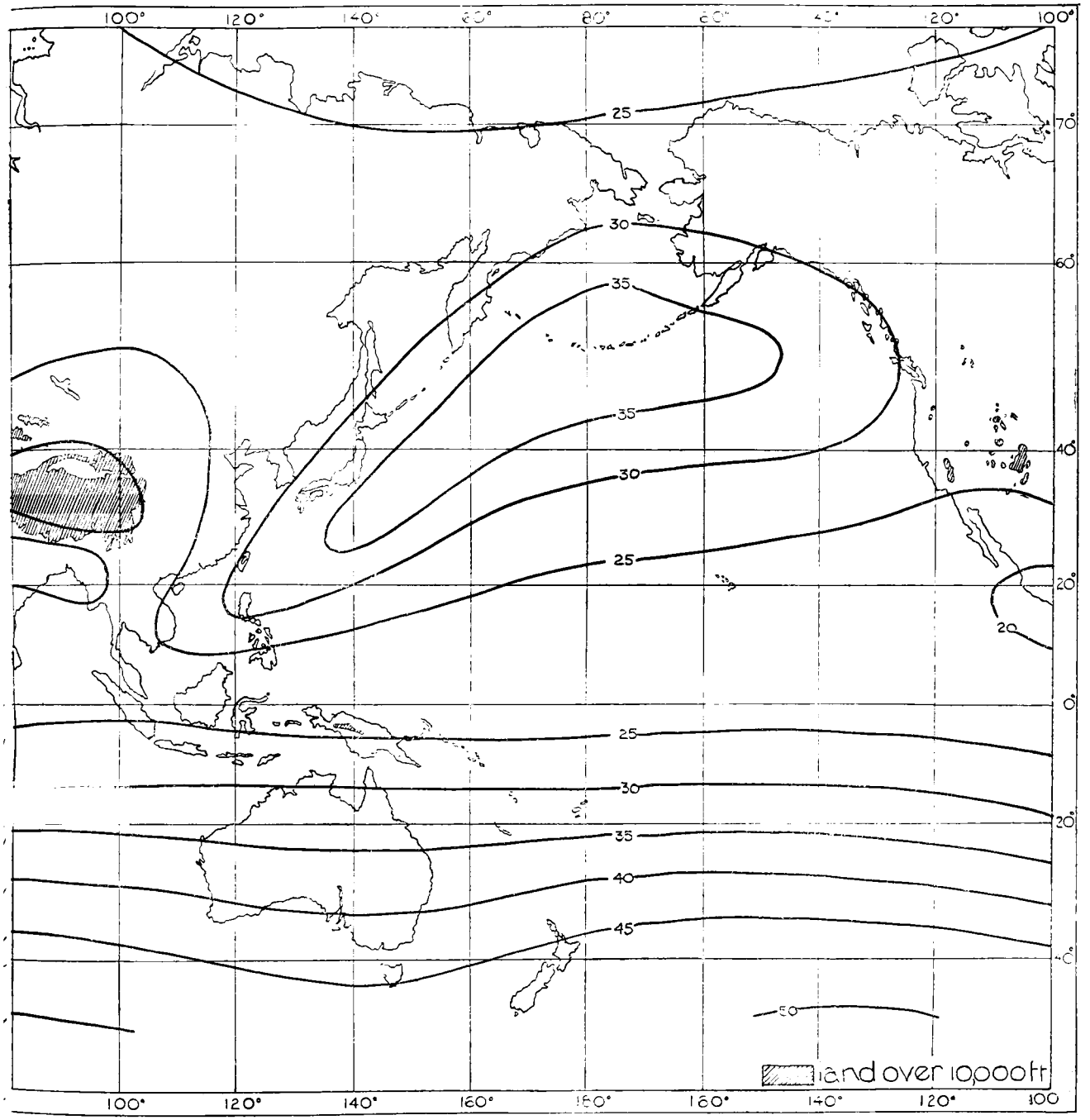

STANDARD VECTOR DEVIATION (knots)

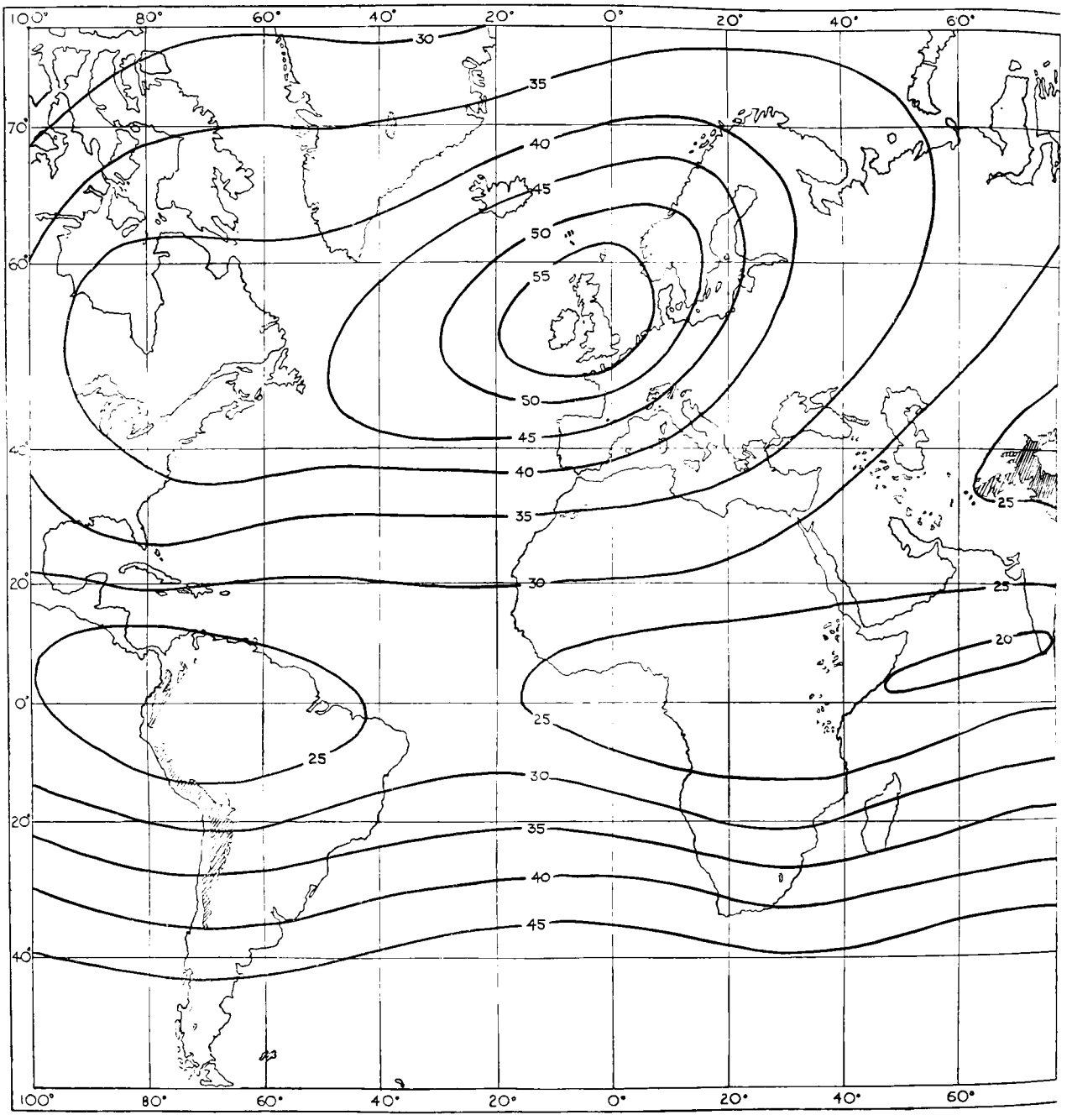

STANDARD VECTOR DEVIATION (knots)

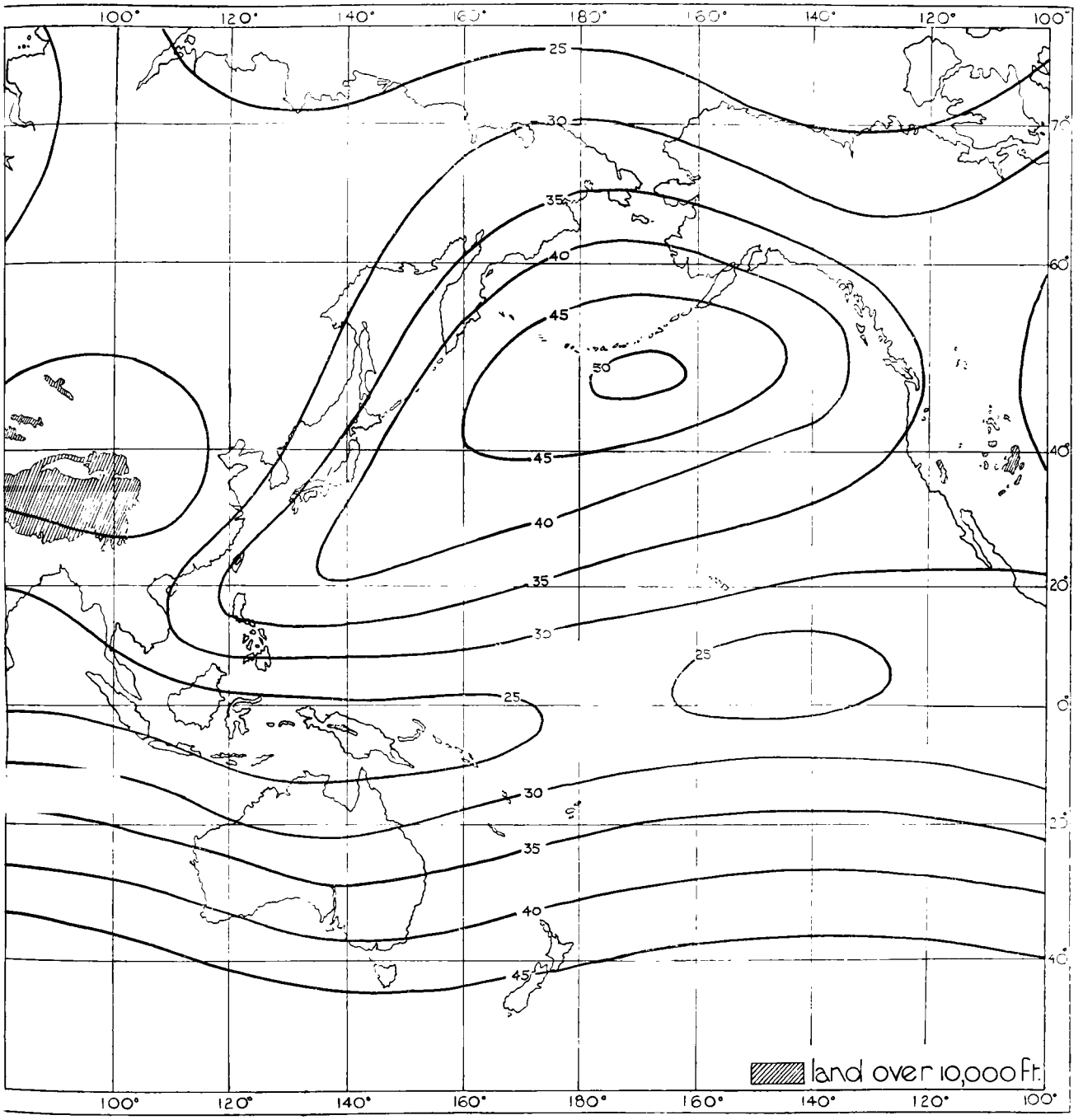

STANDARD VECTOR DEVIATION (knots)

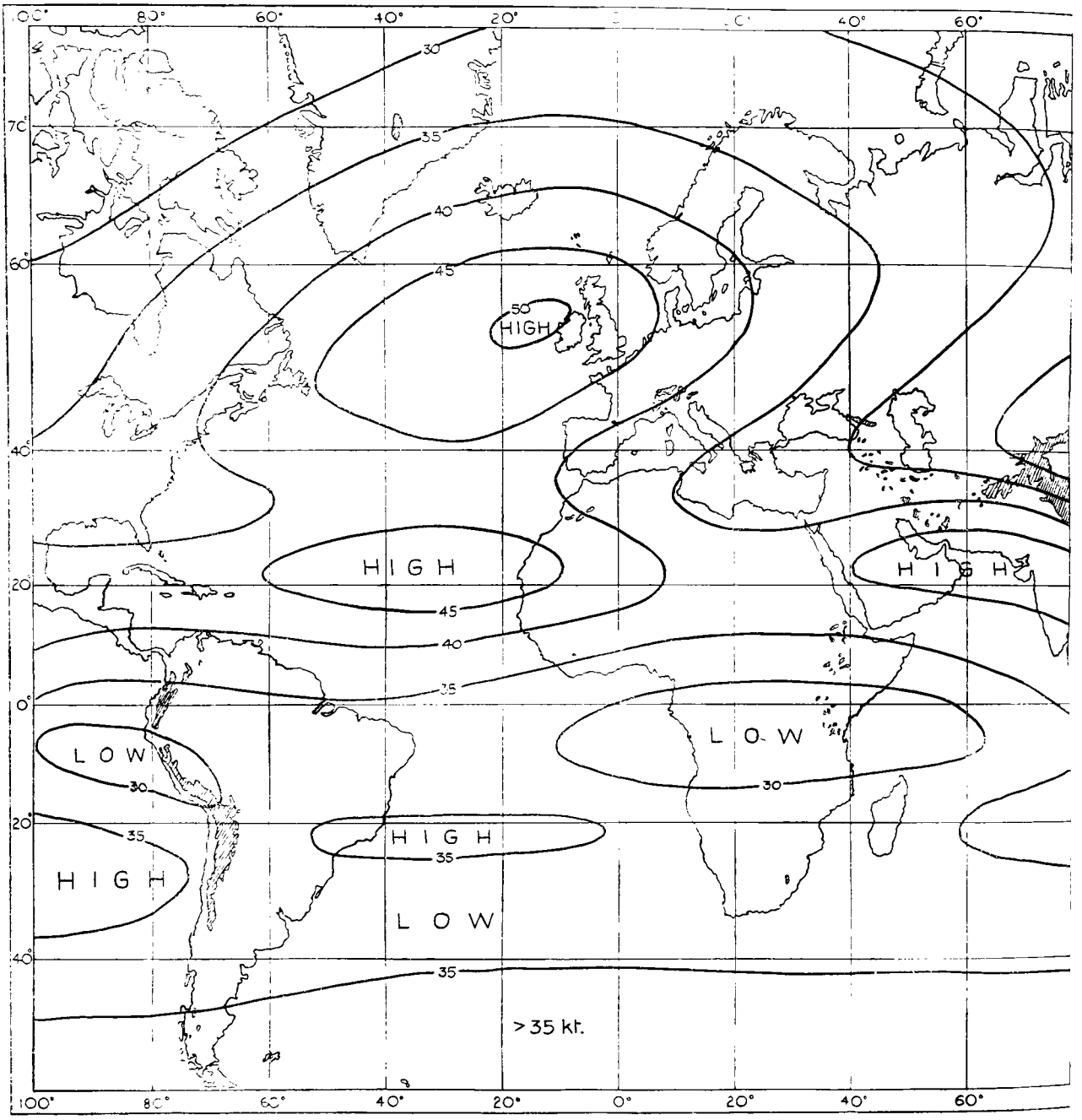

STANDARD VECTOR DEVIATION (knots)

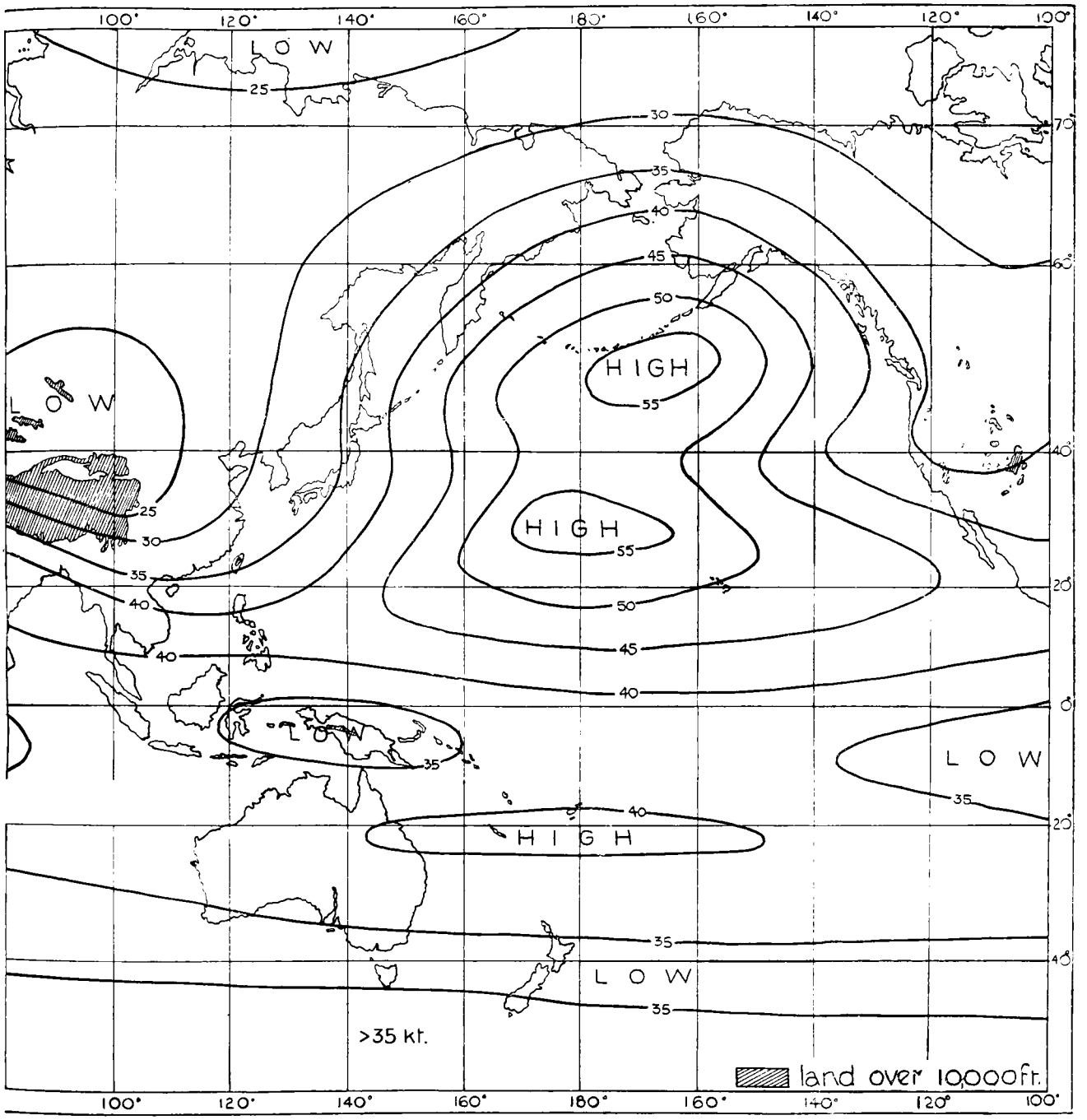

STANDARD VECTOR DEVIATION (knots)

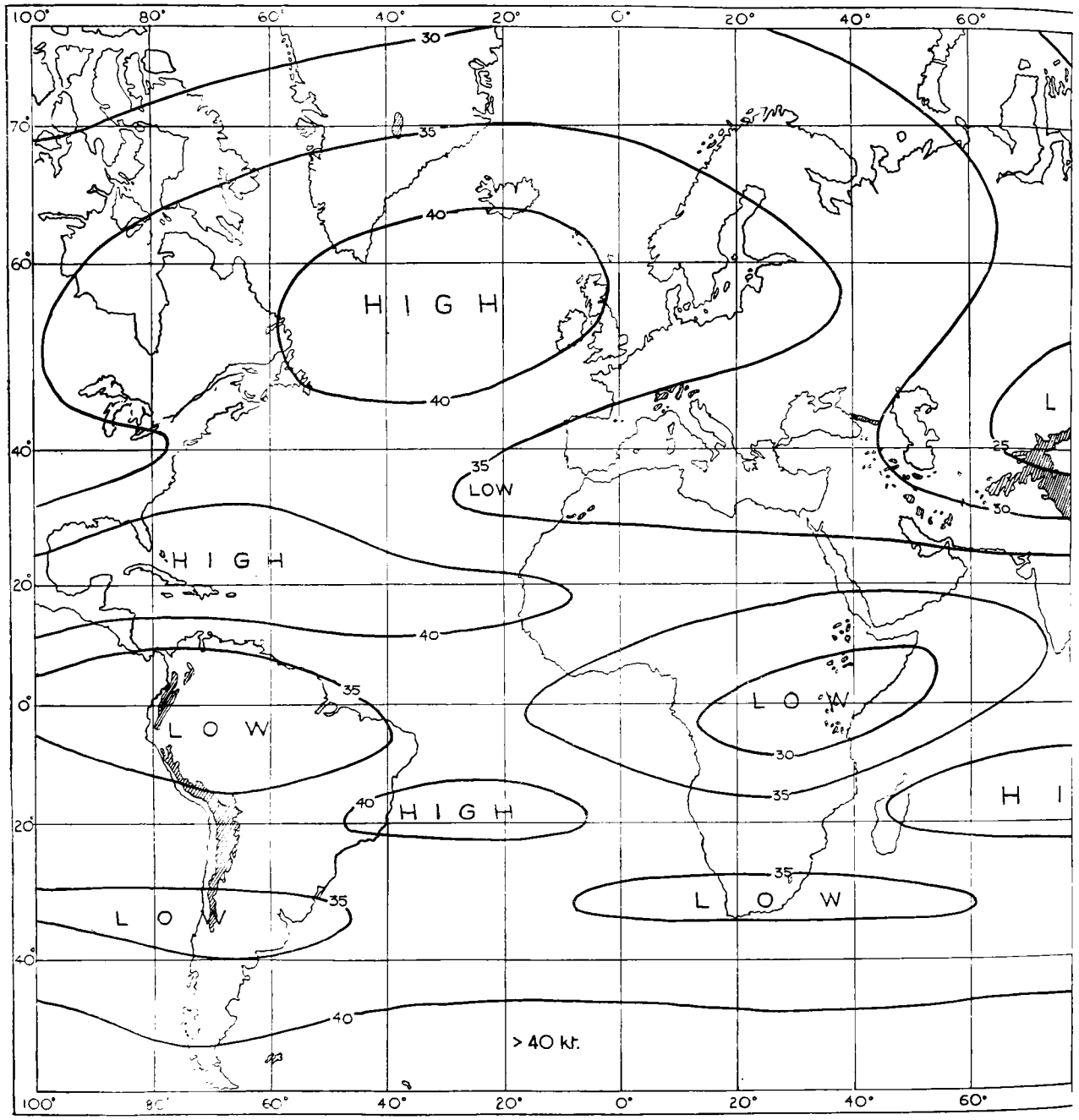

STANDARD VECTOR DEVIATION (knots)

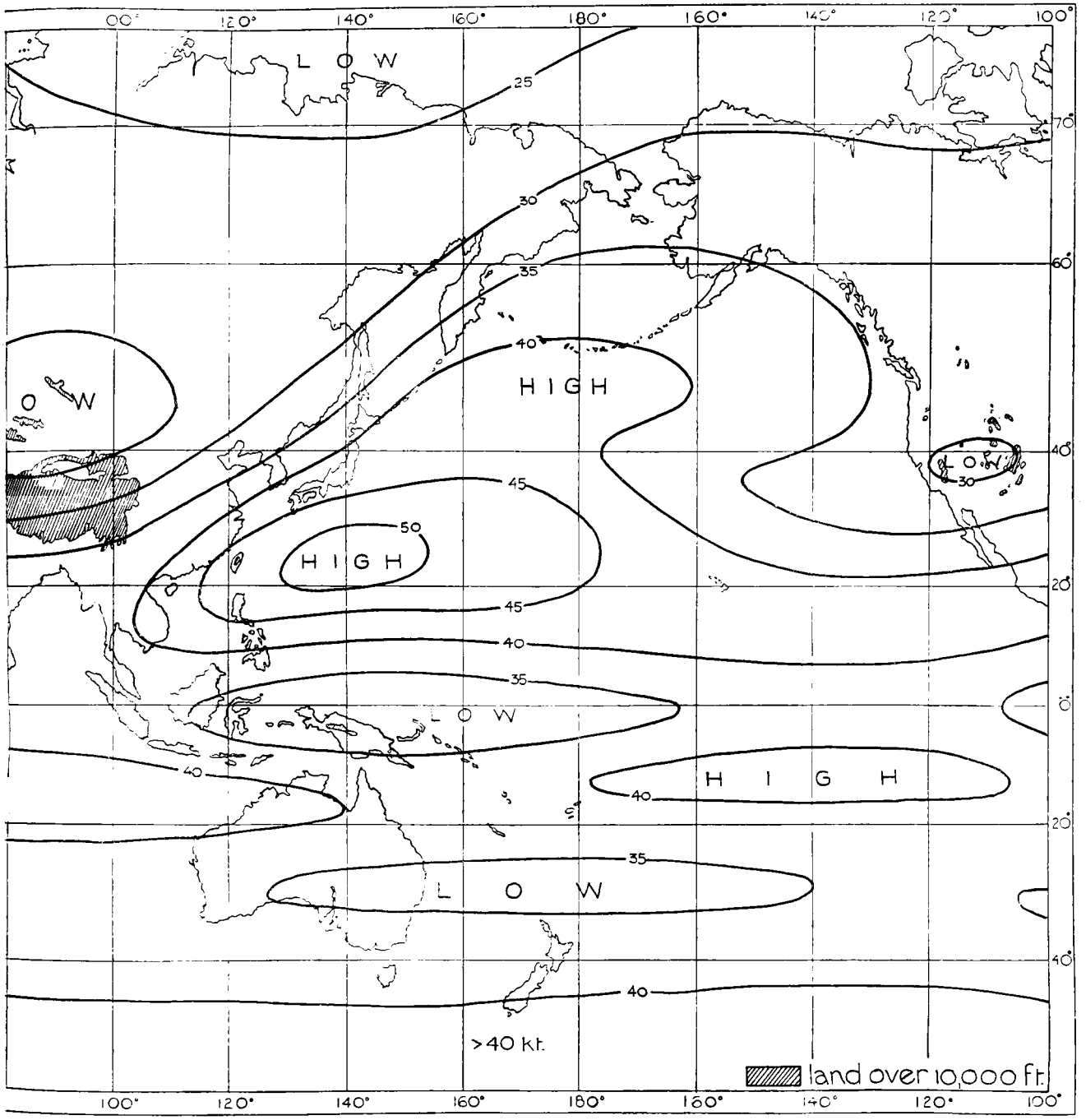

STANDARD VECTOR DEVIATION (knots)

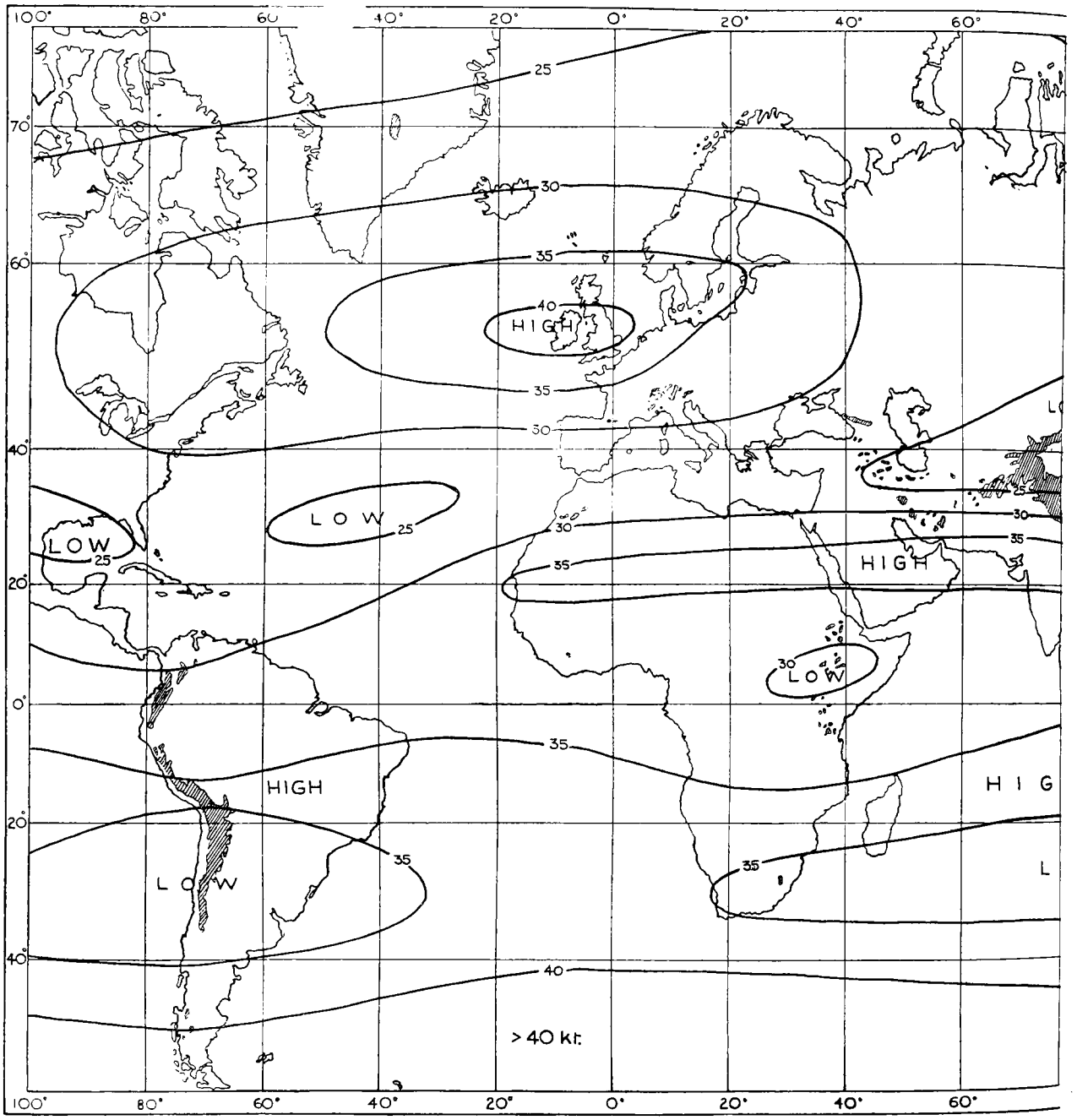

STANDARD VECTOR DEVIATION (knots)

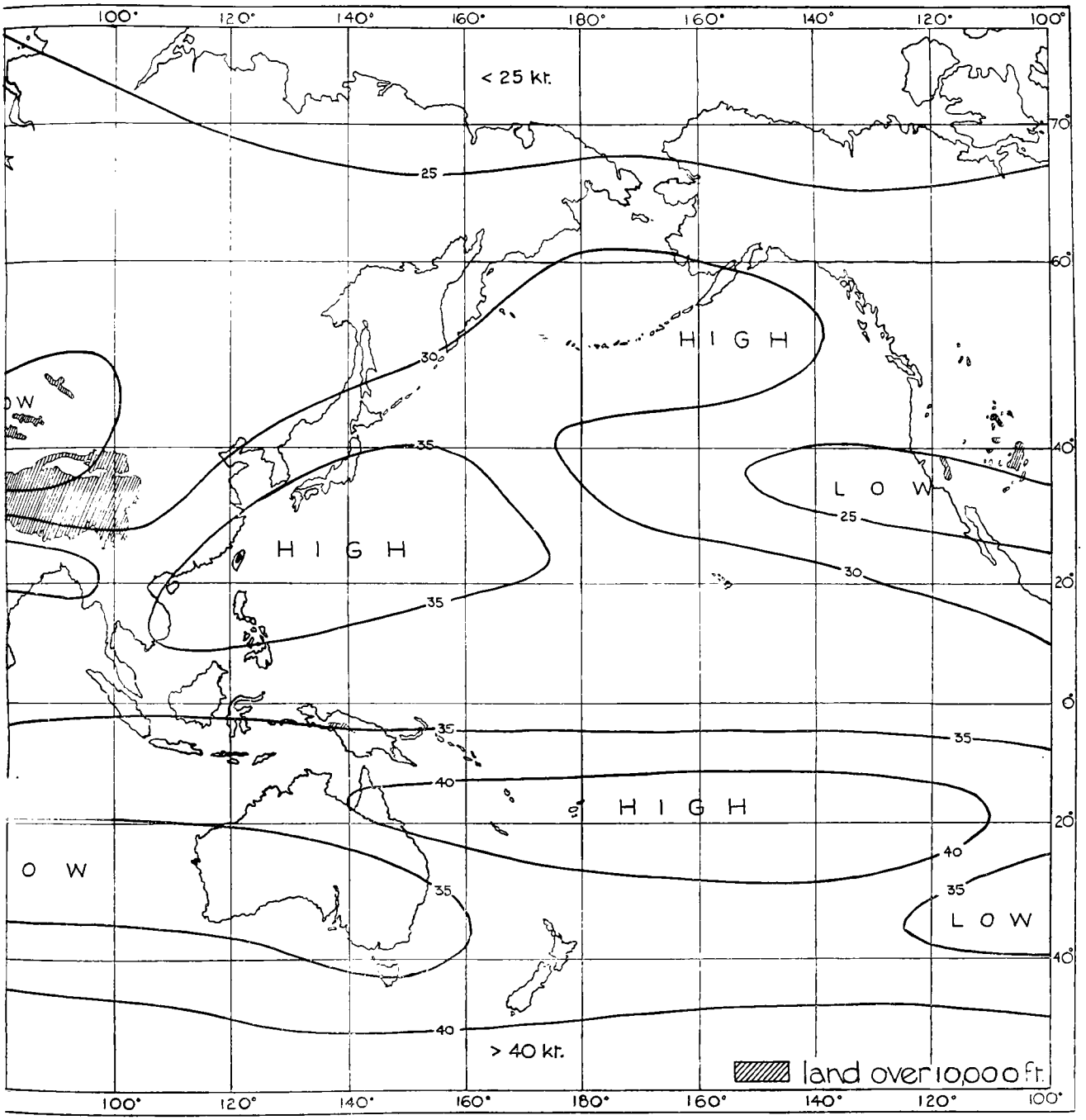

STANDARD VECTOR DEVIATION (knots)

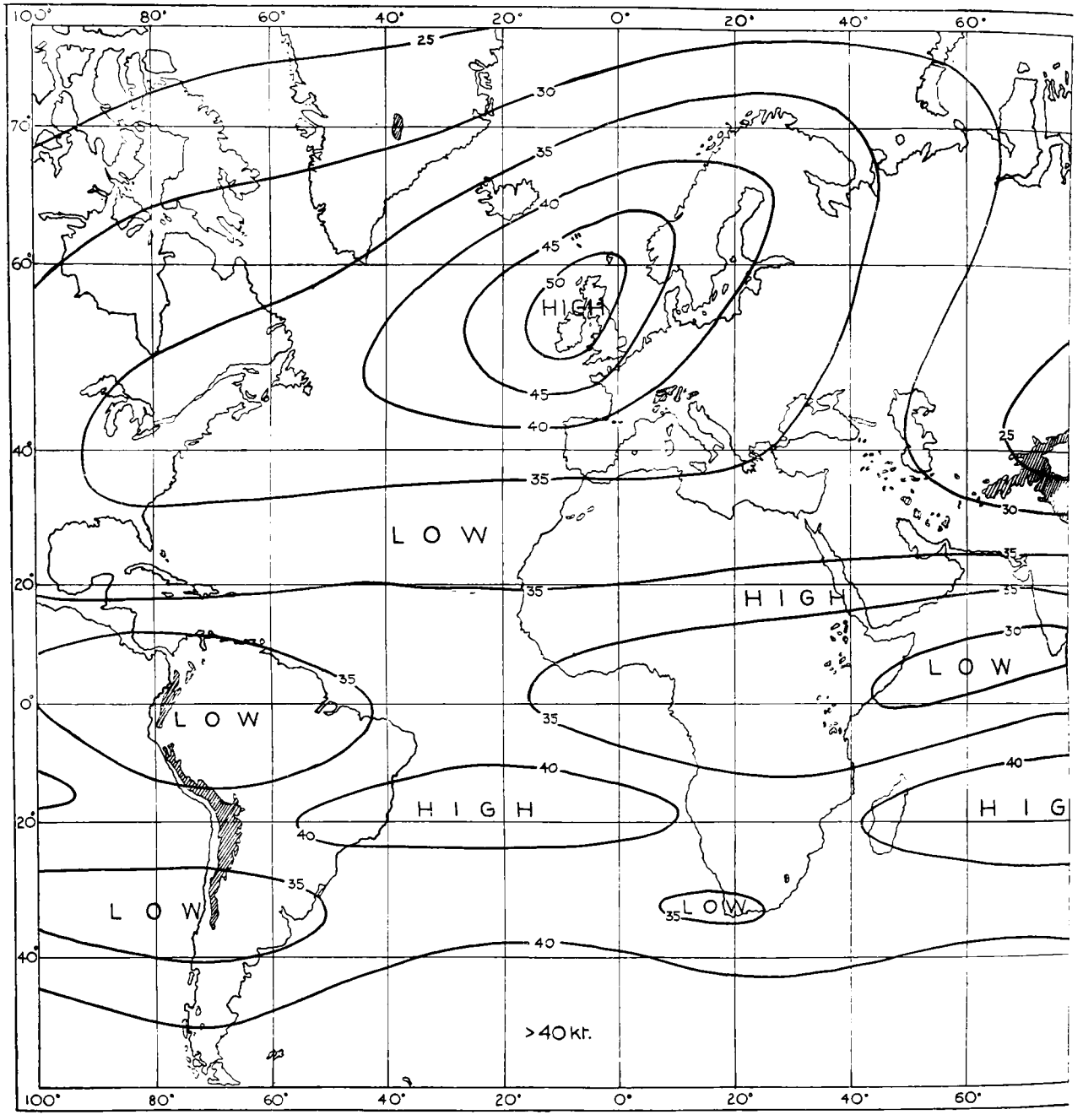

STANDARD VECTOR DEVIATION (knots)

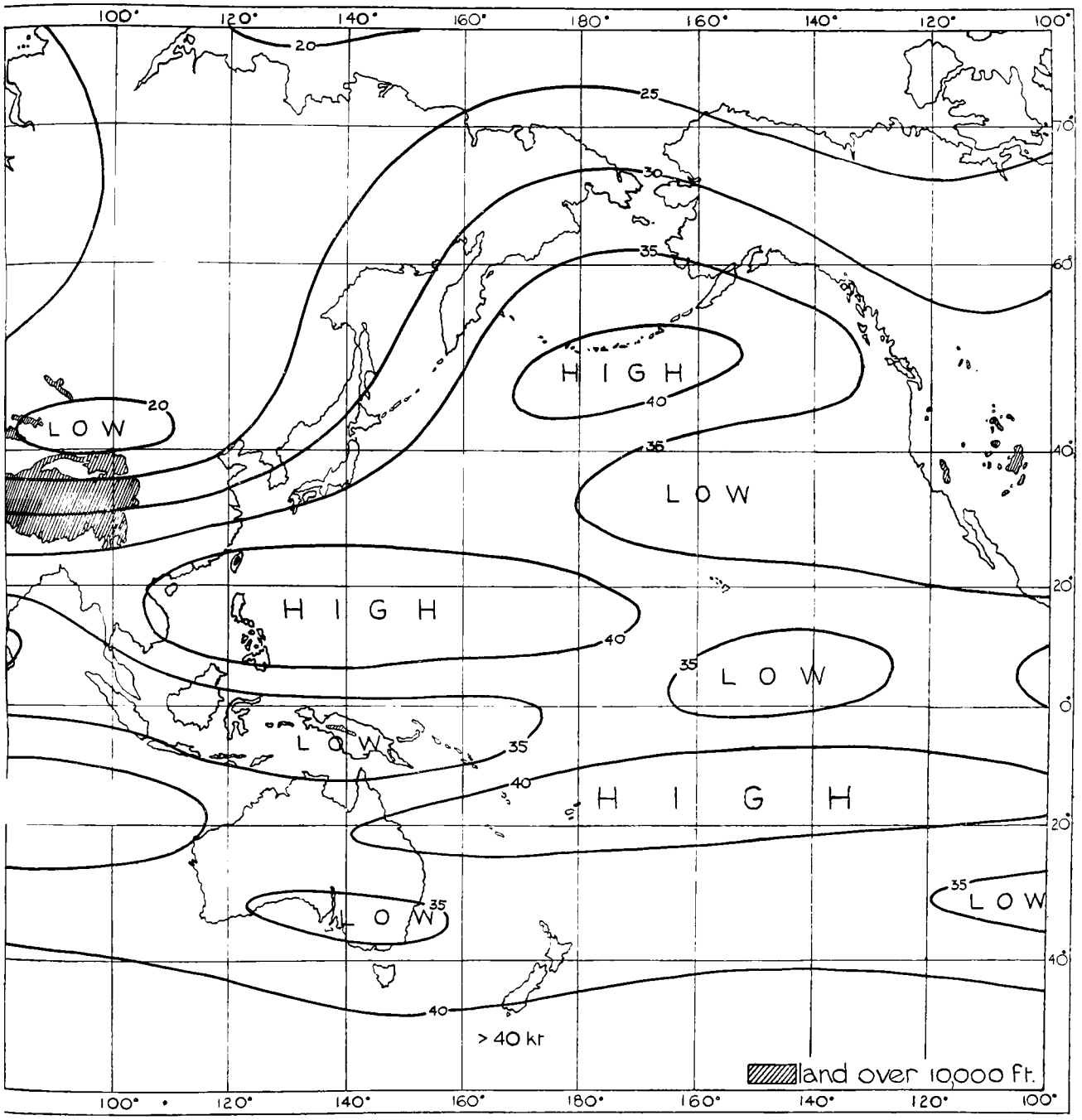

STANDARD VECTOR DEVIATION (knots)

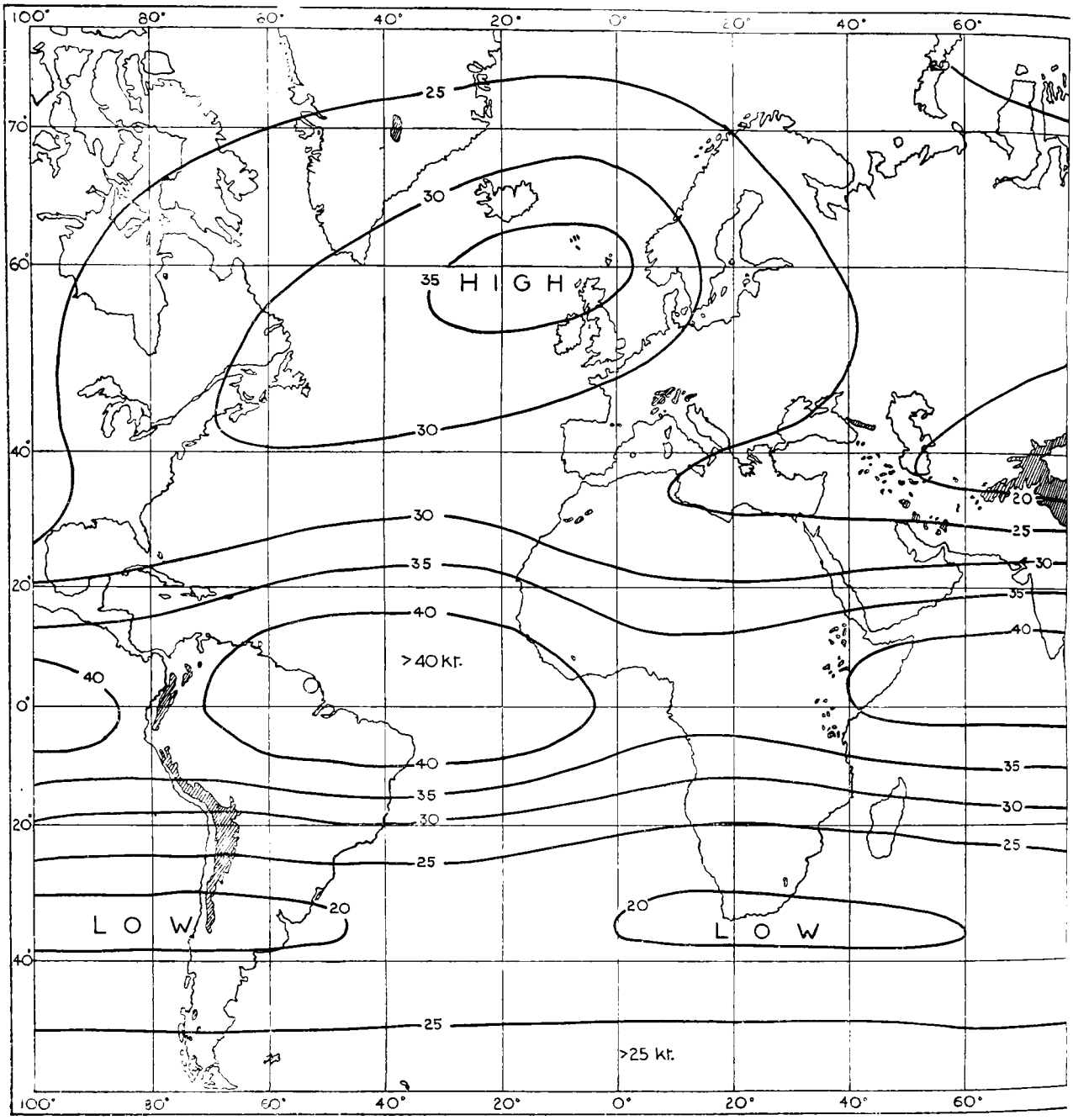

STANDARD VECTOR DEVIATION (knots)

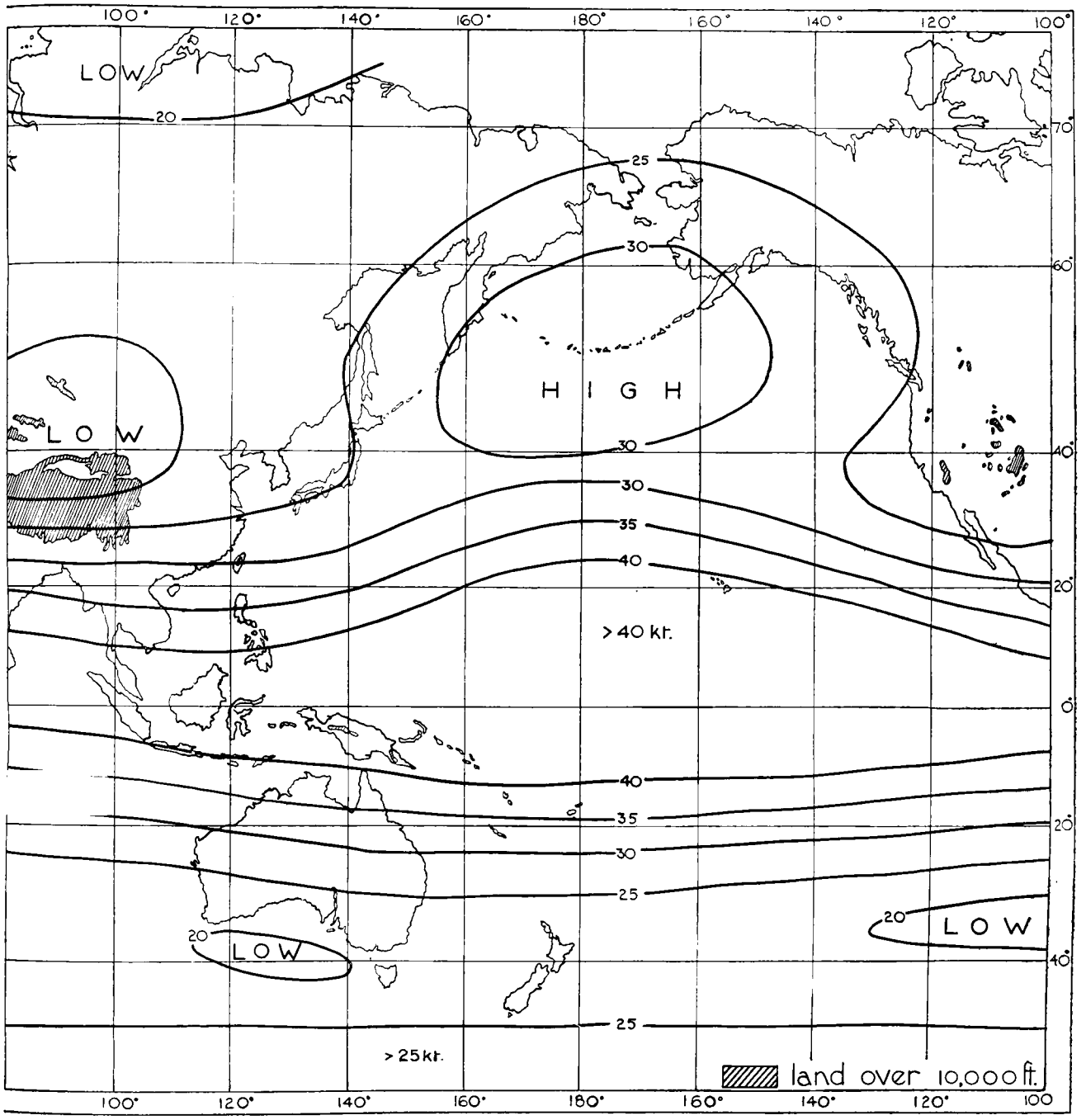

STANDARD VECTOR DEVIATION (knots)

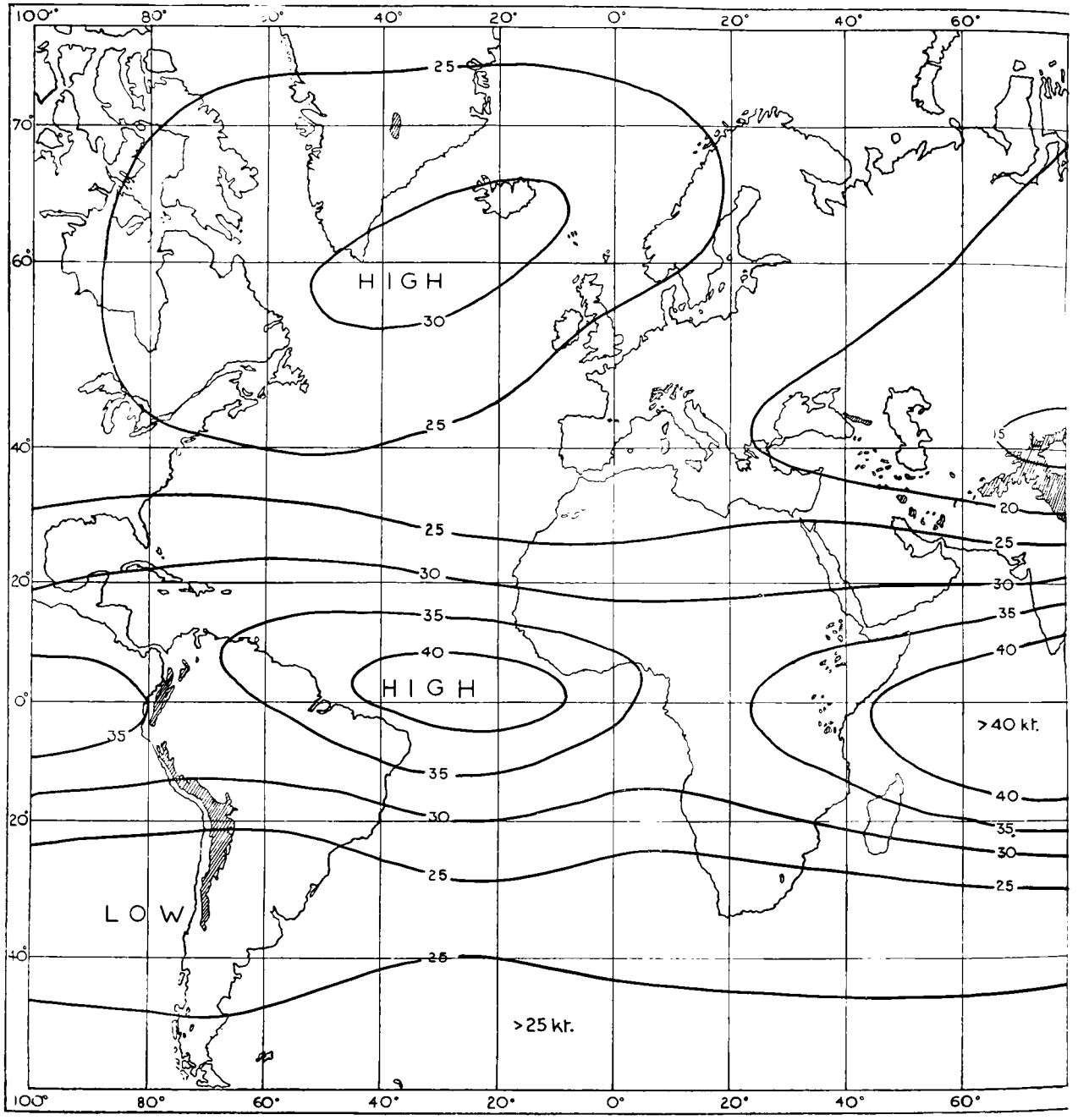

STANDARD VECTOR DEVIATION (knots)

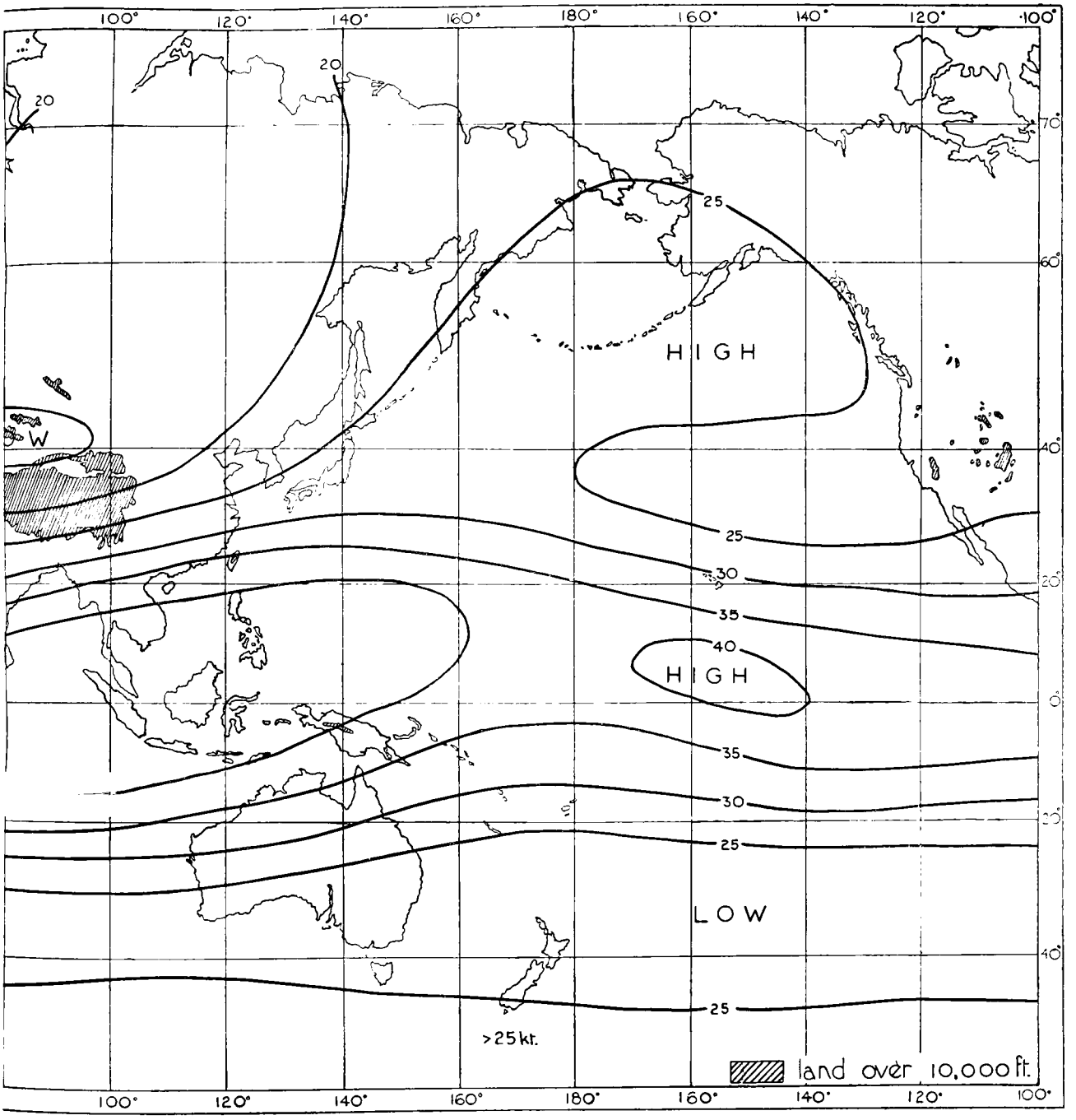

STANDARD VECTOR DEVIATION (knots)

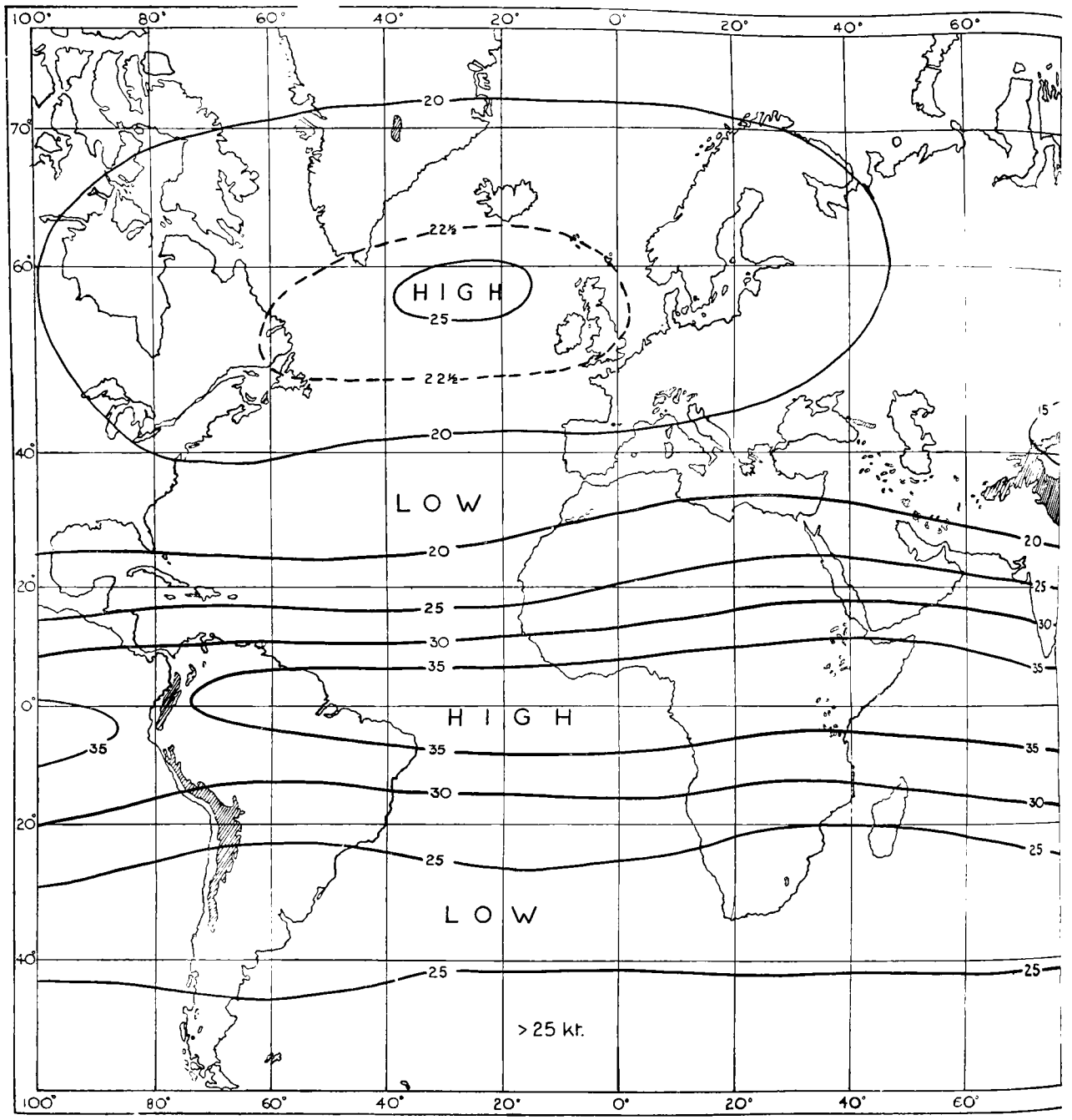

STANDARD VECTOR DEVIATION (knots)

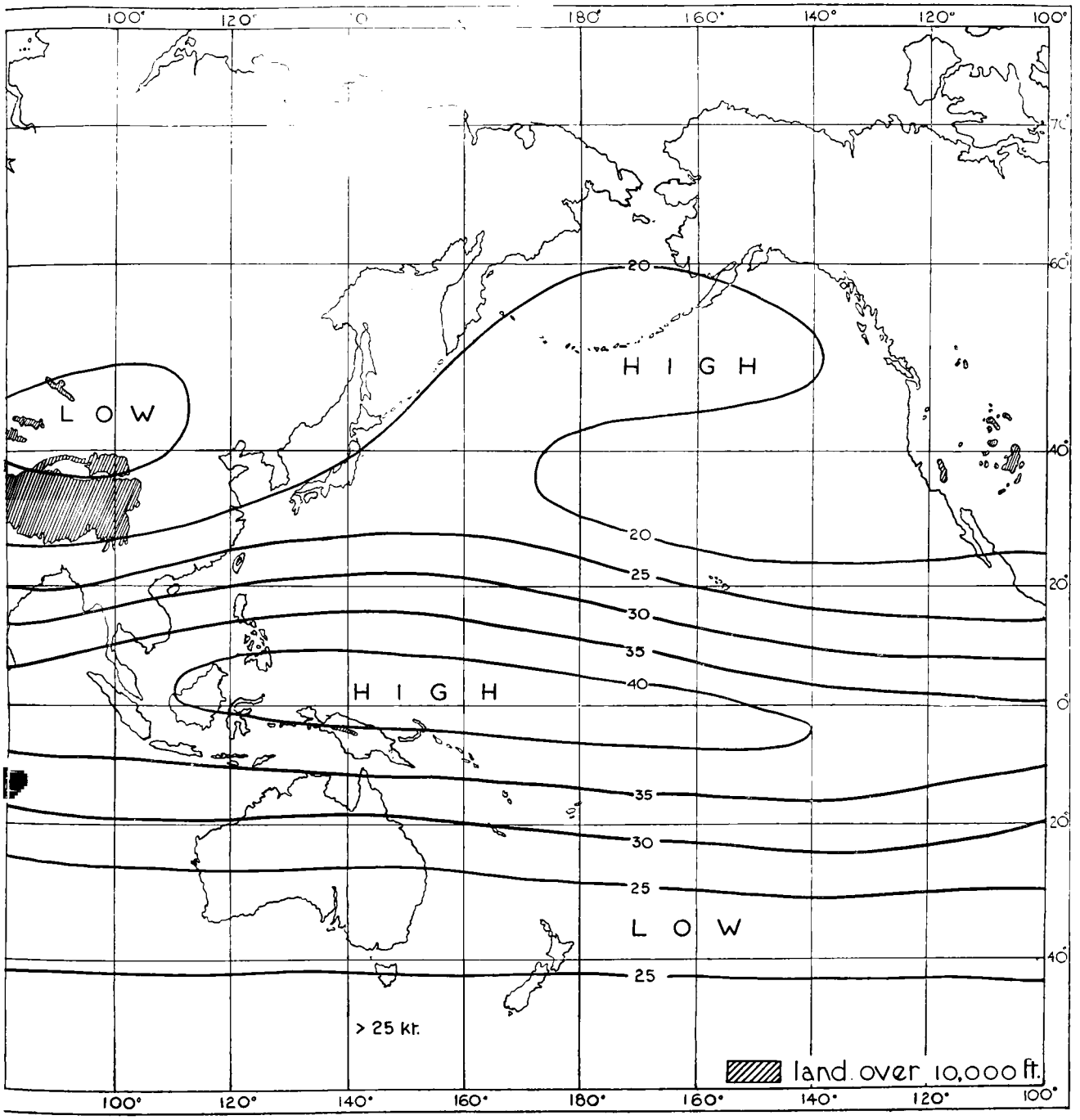

STANDARD VECTOR DEVIATION (knots)

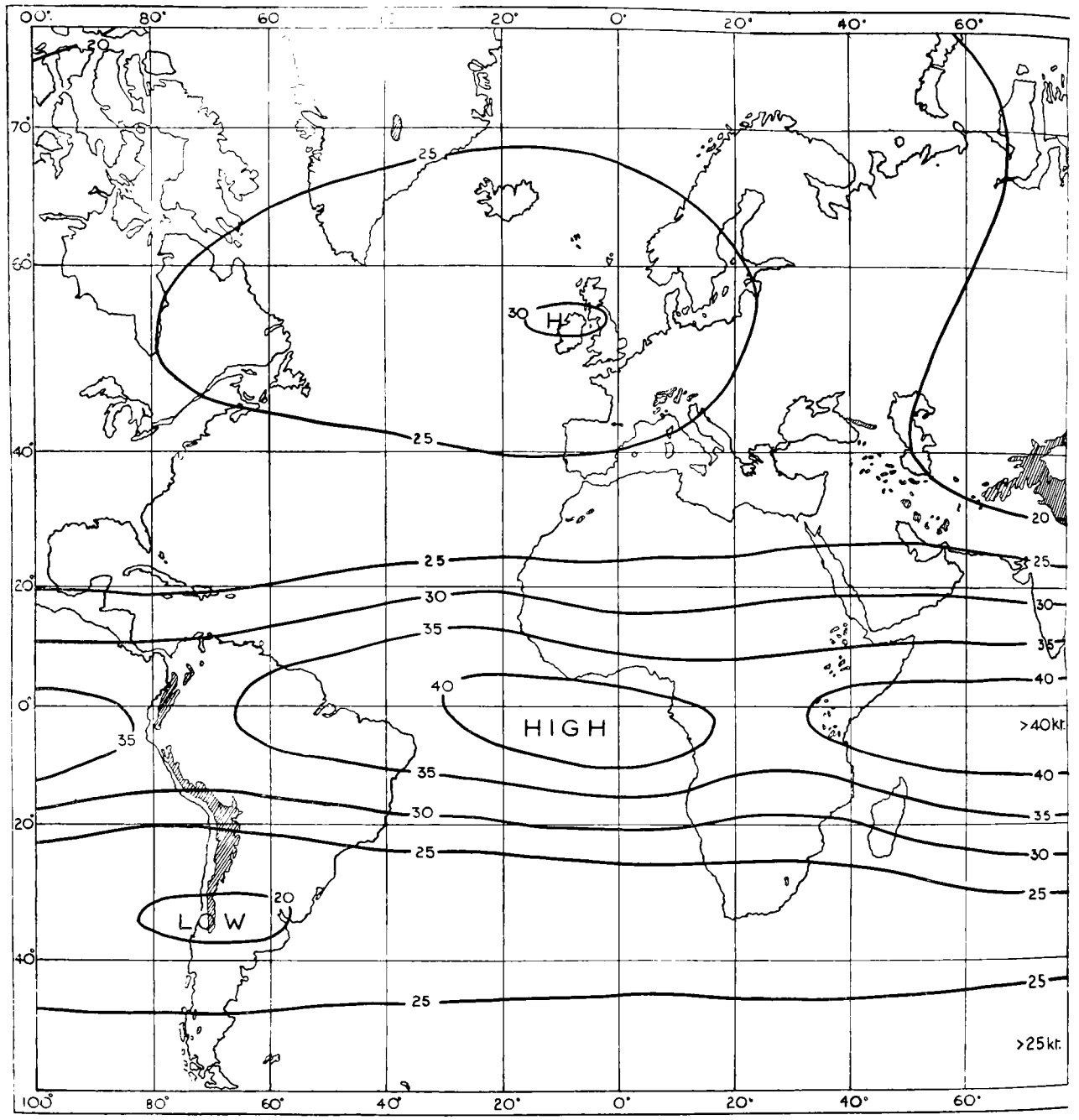

STANDARD VECTOR DEVIATION (knots)

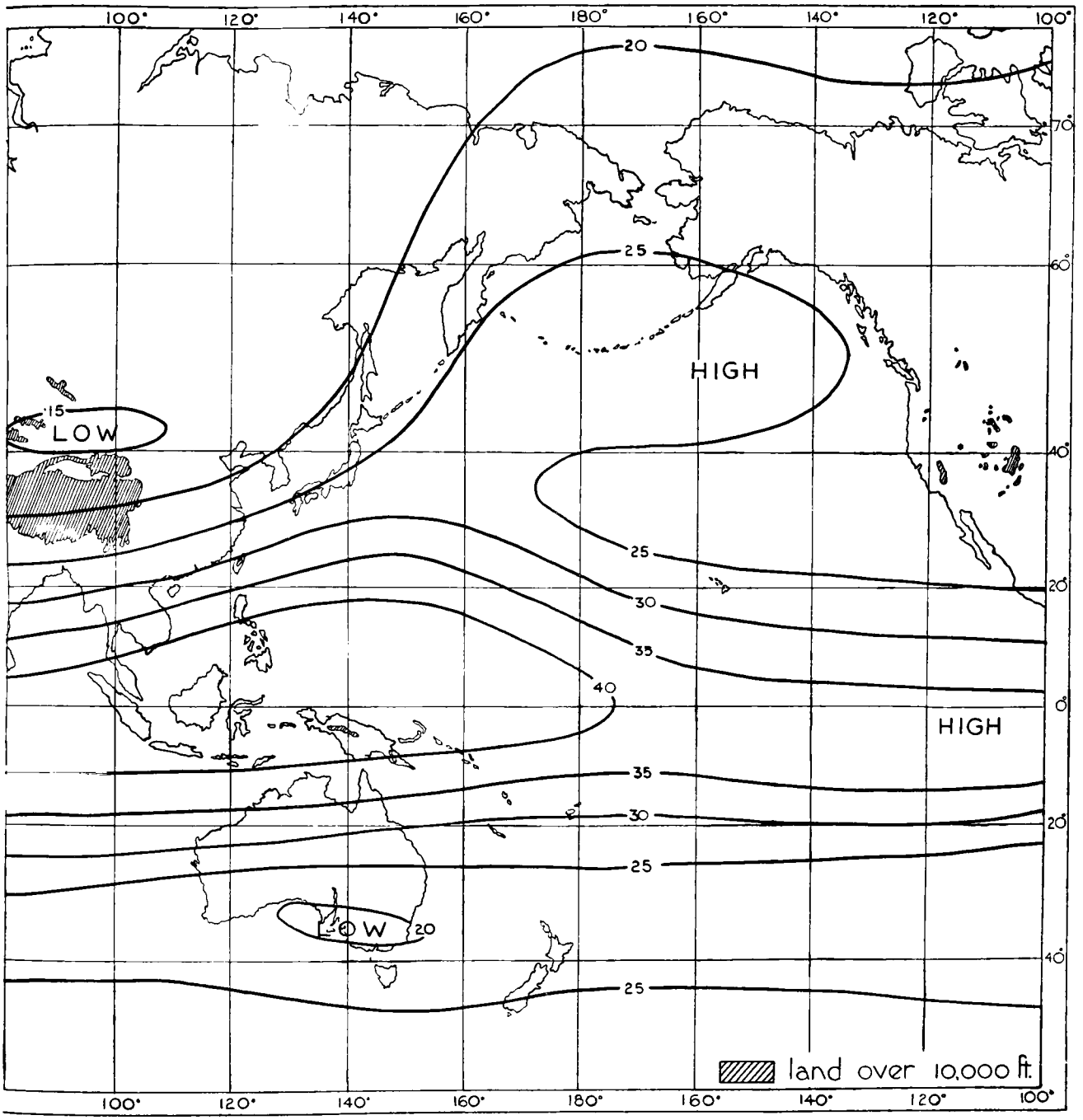

STANDARD VECTOR DEVIATION (knots)

700 mb. DEC.-FEB.

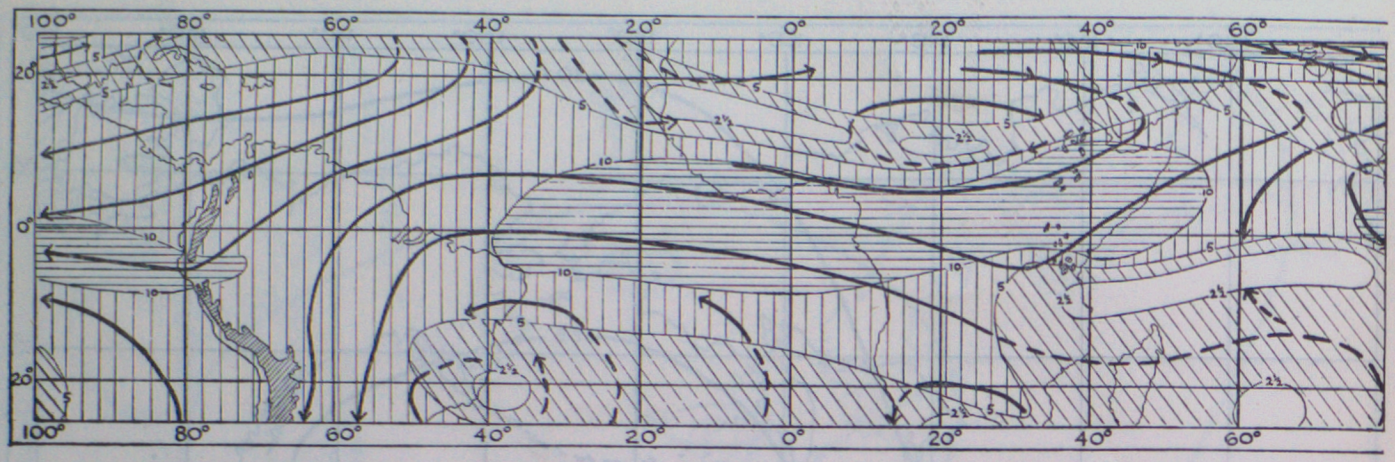

700 mb. MAR.-MAY

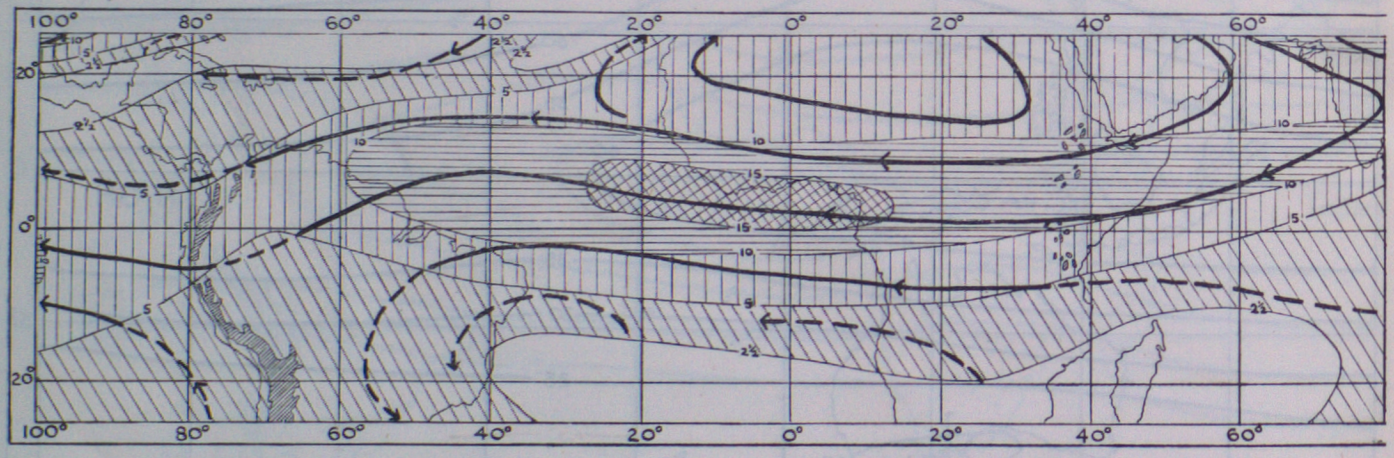

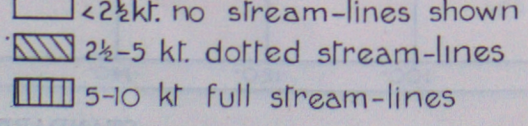

STREAM-LINES IN THE INTERTROPICAL BELT

DEC.-FEB. 700 mb.

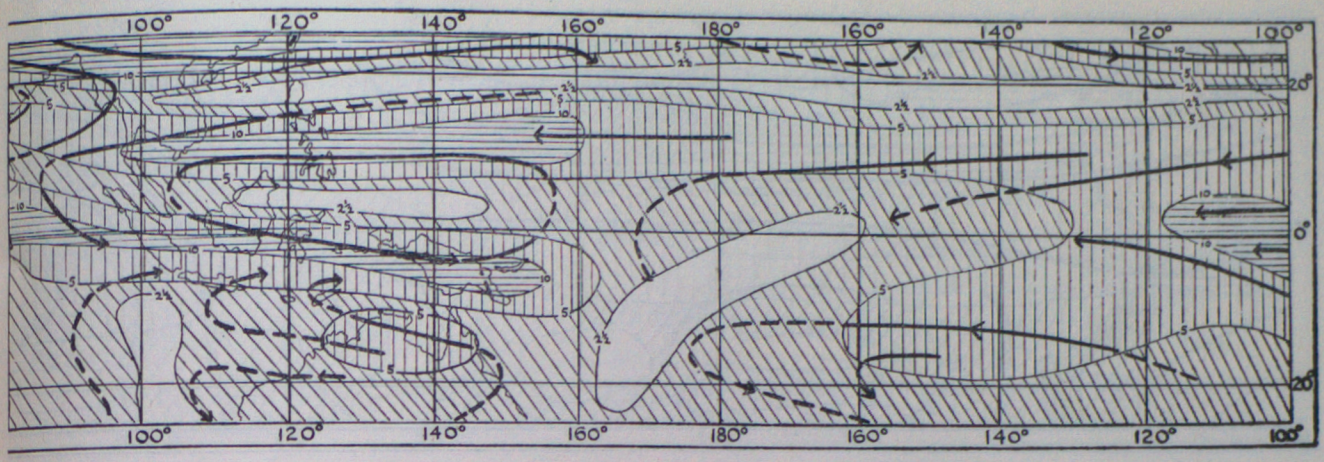

MAR.-MAY 700 mb.

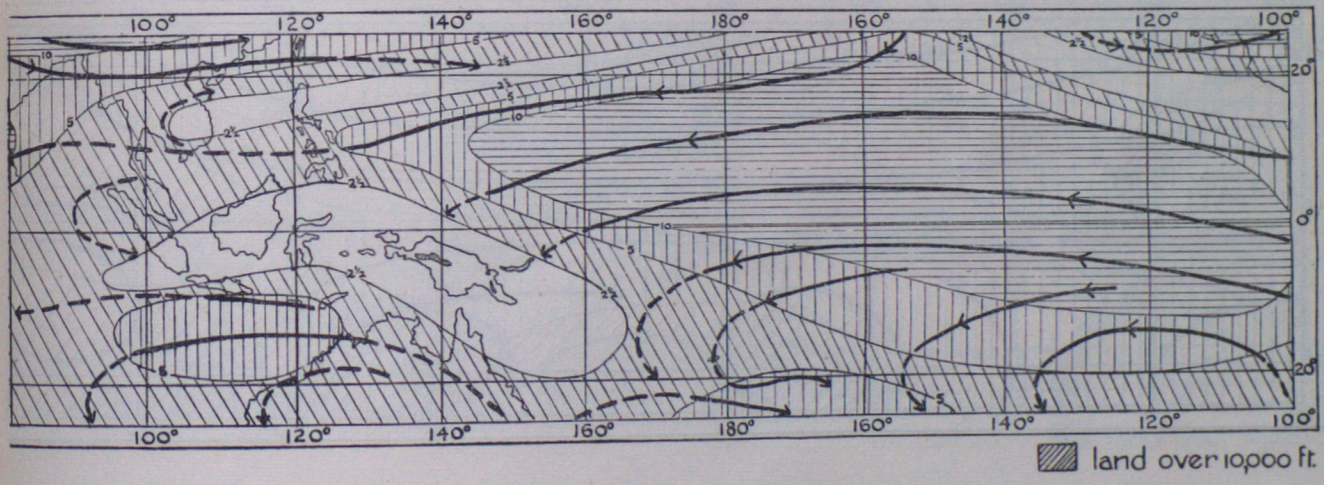

10-15 kt. Full stream-lines
15-20 kt. Full stream-lines
> 20 kt Full stream-lines

STREAM-LINES IN THE INTERTROPICAL BELT

700 mb. JUNE-AUG.

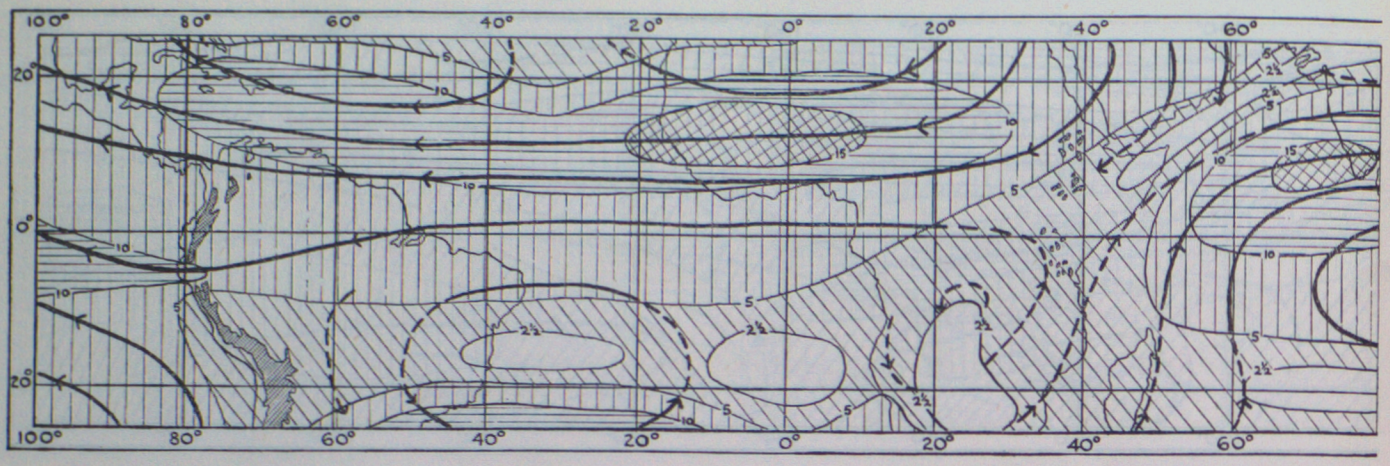

700 mb. SEPT.-NOV.

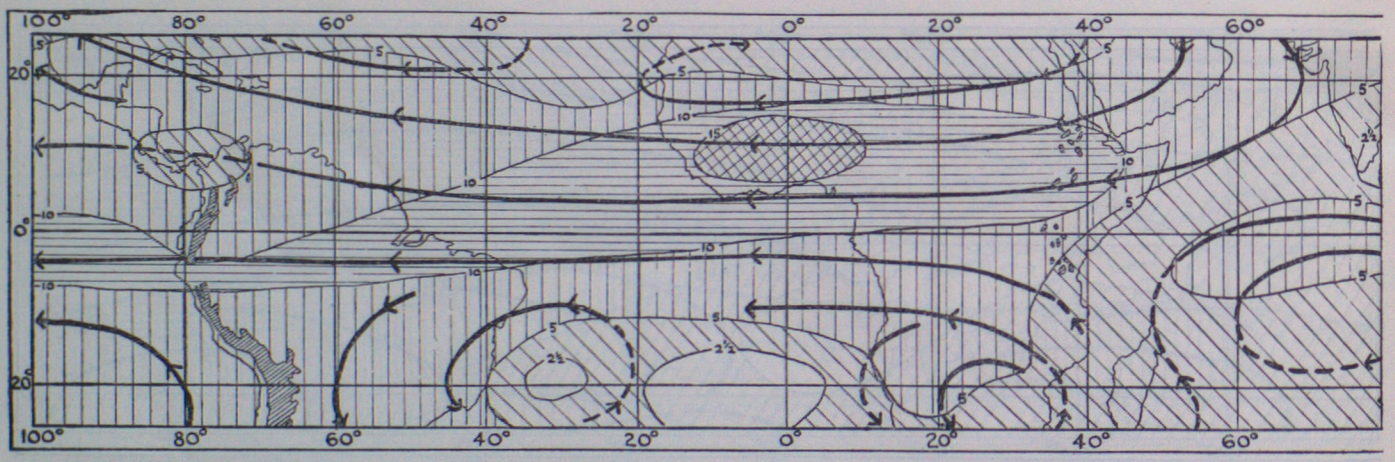

< 2½ kt. no stream-lines shown
2½-5 kt. dotted stream-lines
5-10 kt. full stream-lines

STREAM-LINES IN THE INTERTROPICAL BELT

JUNE-AUG. 700 mb.

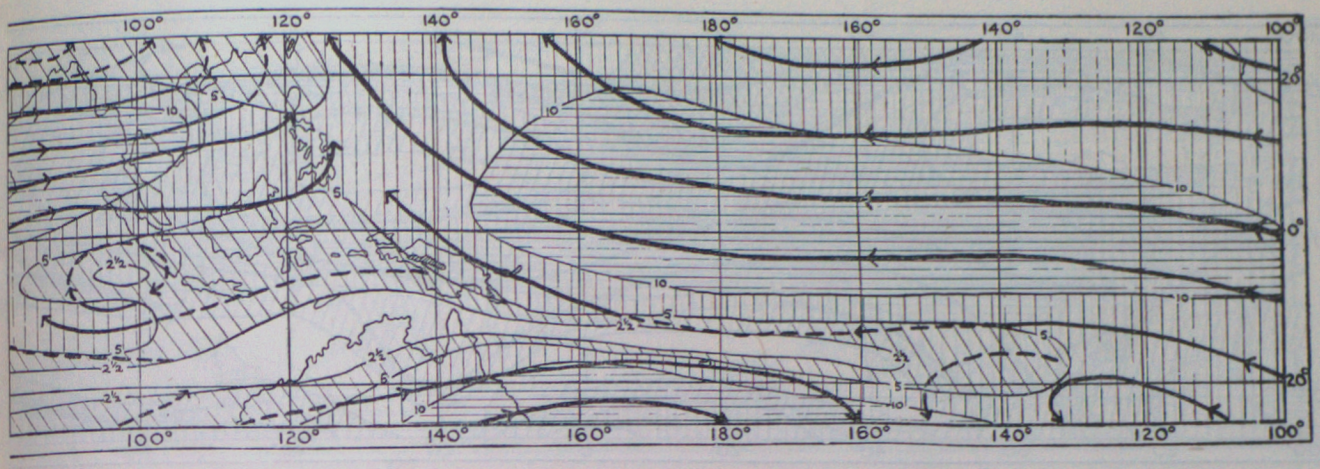

SEPT.-NOV. 700 mb.

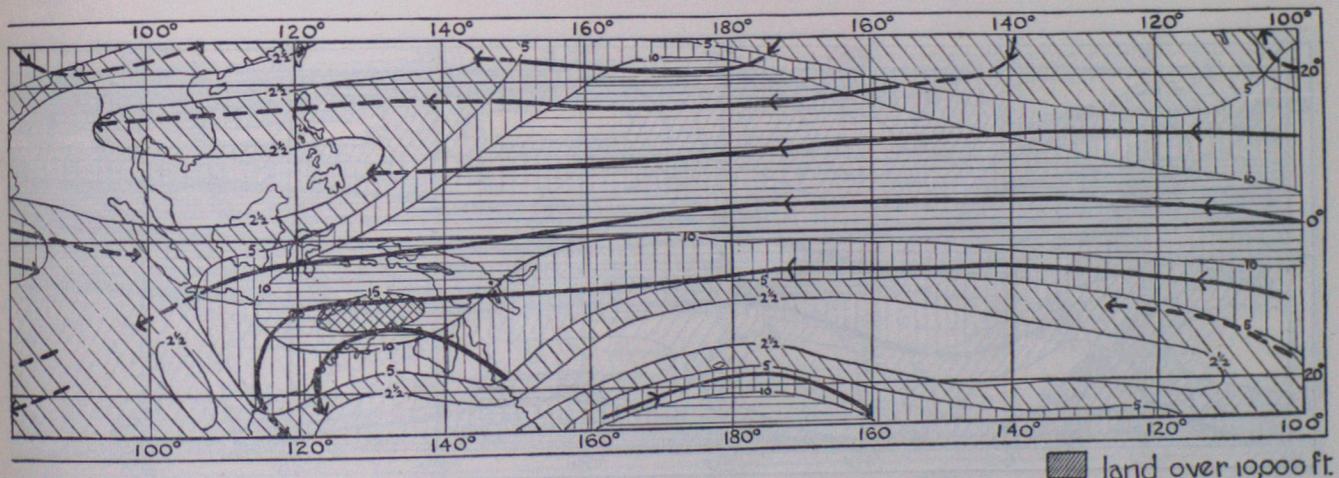

10–15 kt. full stream-lines
15–20 kt. full stream-lines
> 20 kt. full stream-lines

STREAM-LINES IN THE INTERTROPICAL BELT

500 mb. DEC.-FEB.

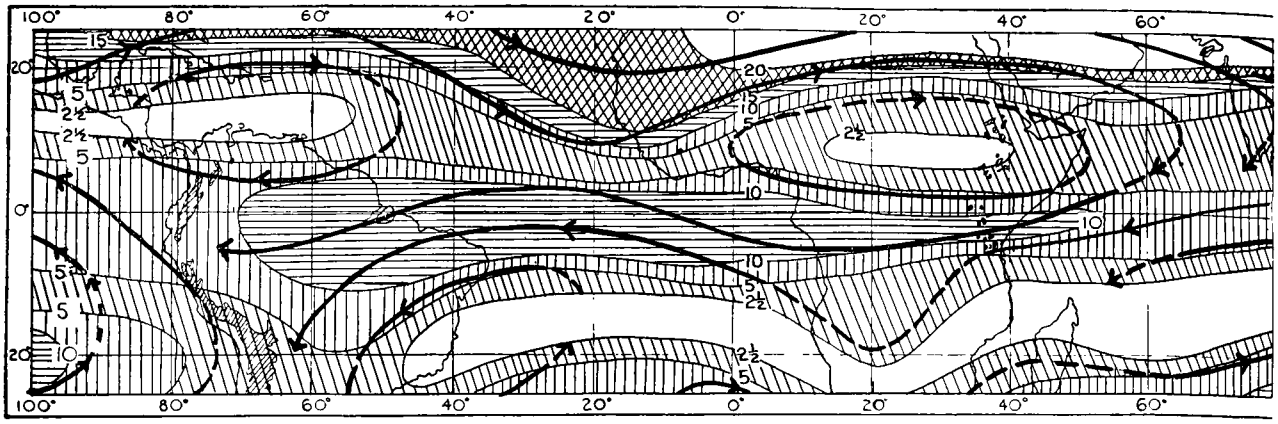

500 mb. MAR.-MAY

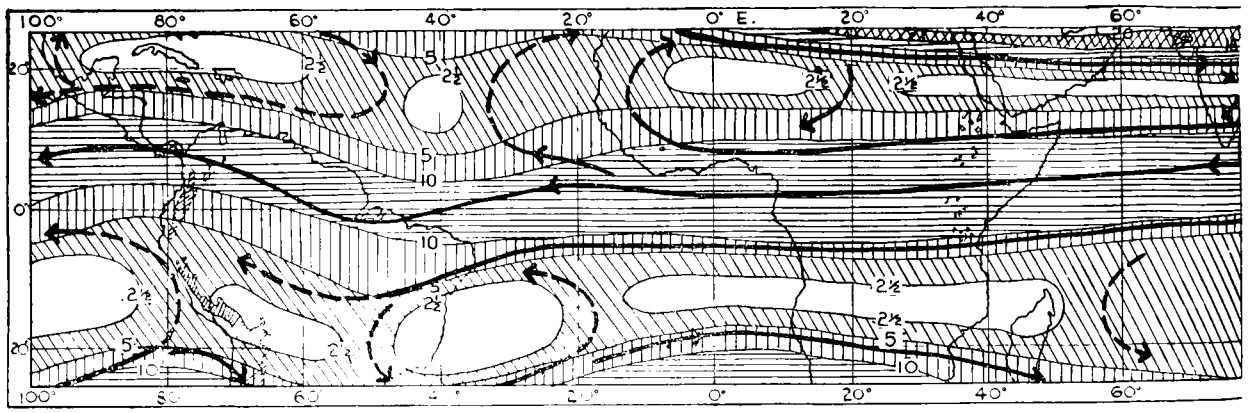

<2½kt. no stream-lines shown
2½-5 kt. dotted stream-lines
5-10 kt. full stream-lines

STREAM-LINES IN THE INTERTROPICAL BELT

DEC.-FEB. 500 mb.

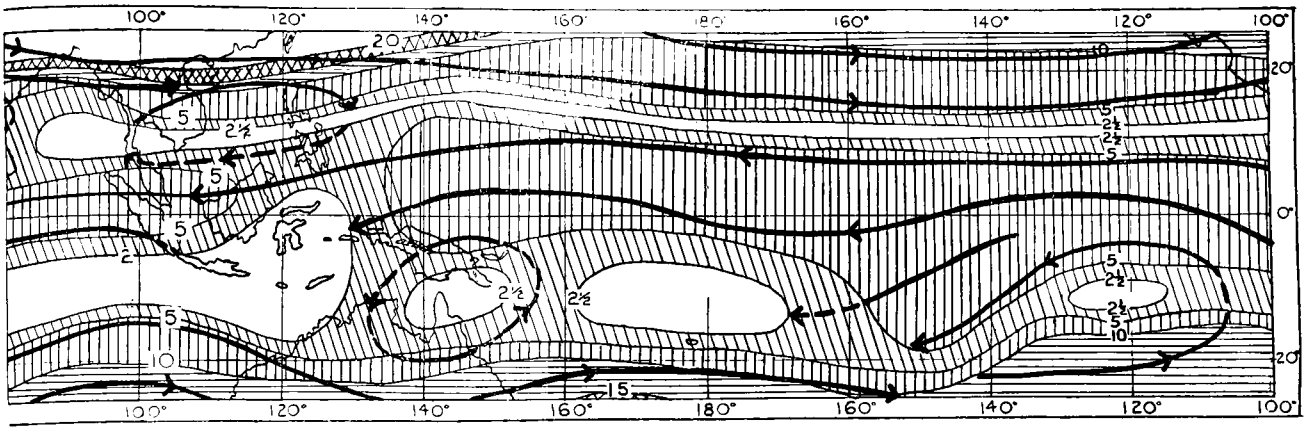

MAR.-MAY 500 mb.

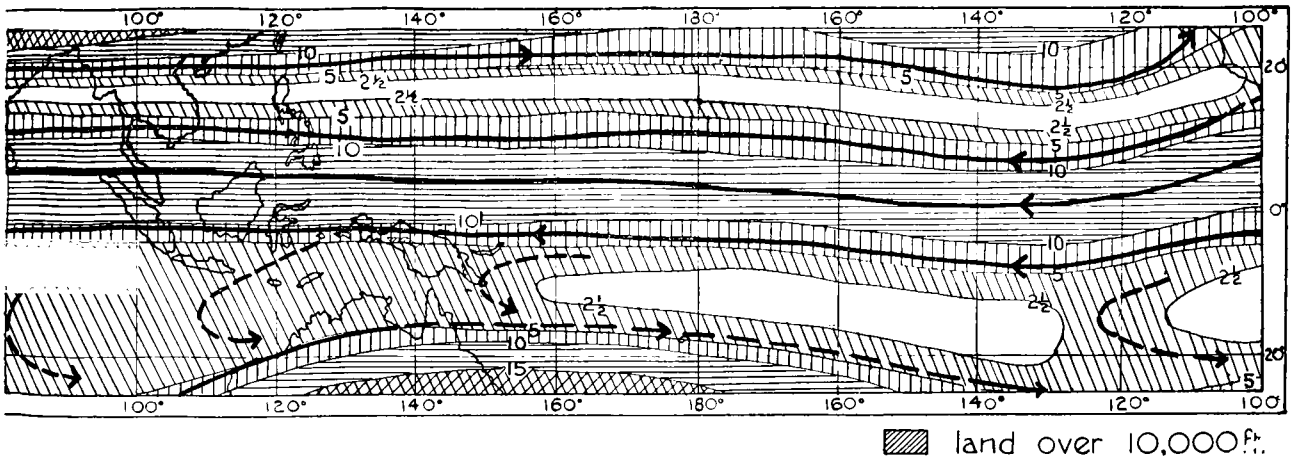

10-15 kt. full stream-lines
15-20 kt. full stream-lines
>20 kt. full stream-lines

STREAM-LINES IN THE INTERTROPICAL BELT

500 mb. JUNE-AUG.

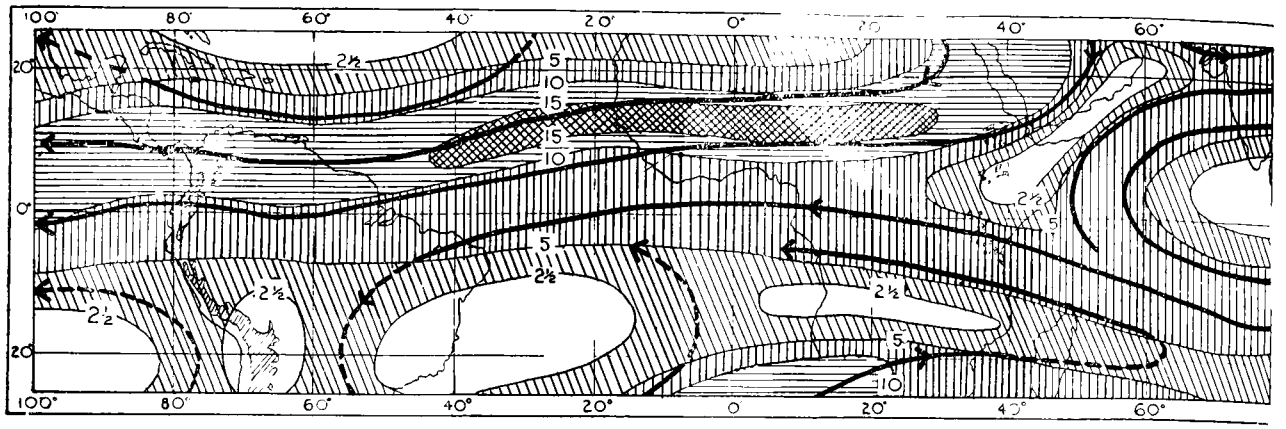

500 mb. SEPT.-NOV.

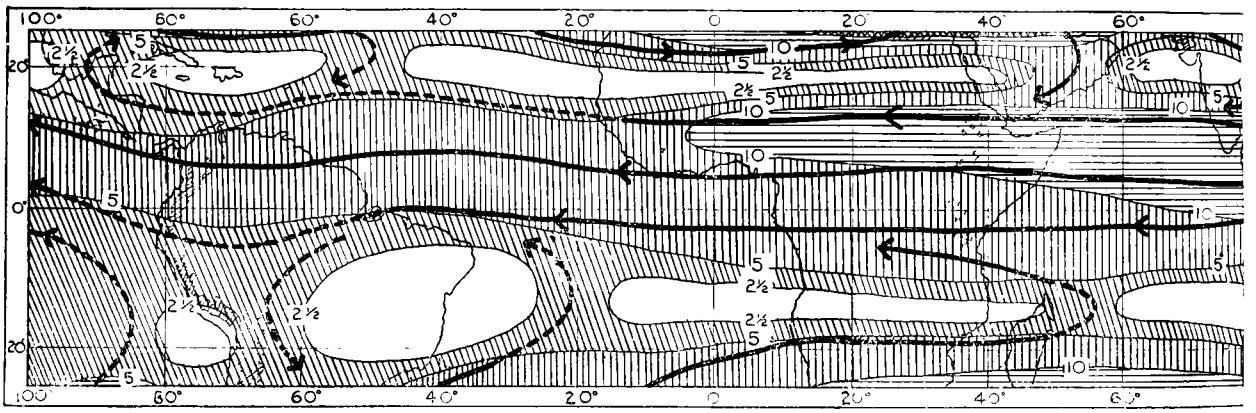

<2½kt. no stream-lines shown
2½-5 kt. dotted stream-lines
5-10 kt. full stream-lines

STREAM-LINES IN THE INTERTROPICAL BELT

JUNE-AUG. 500 mb.

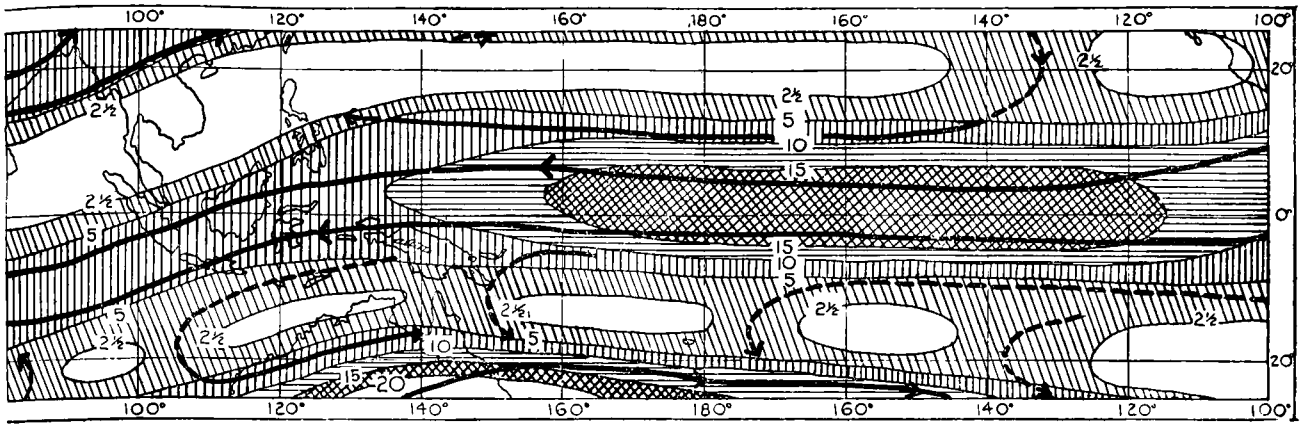

SEPT.-NOV. 500 mb.

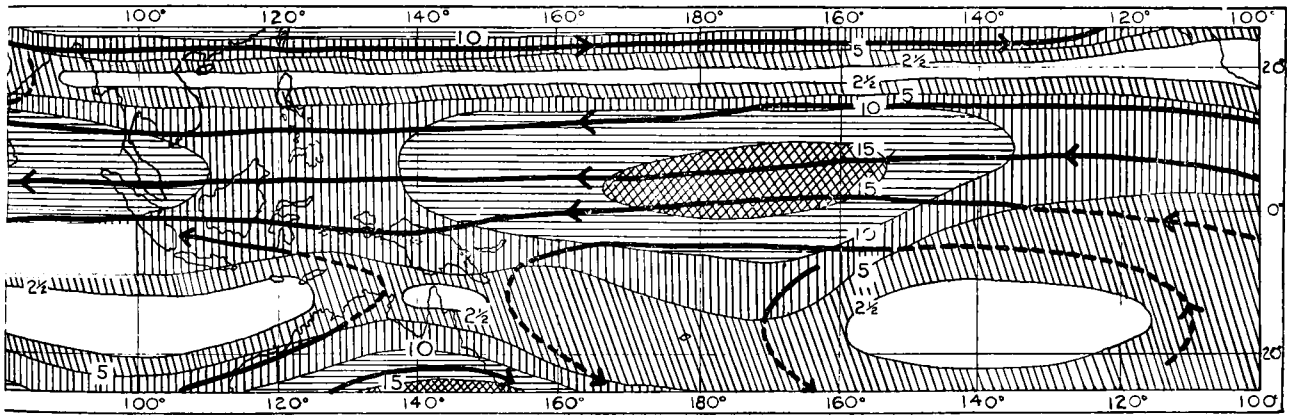

land over 10,000 ft.

10-15 kt. full stream-lines
15-20 kt. full stream-lines
> 20 kt. full stream-lines

STREAM-LINES IN THE INTERTROPICAL BELT

300 mb. DEC.-FEB.

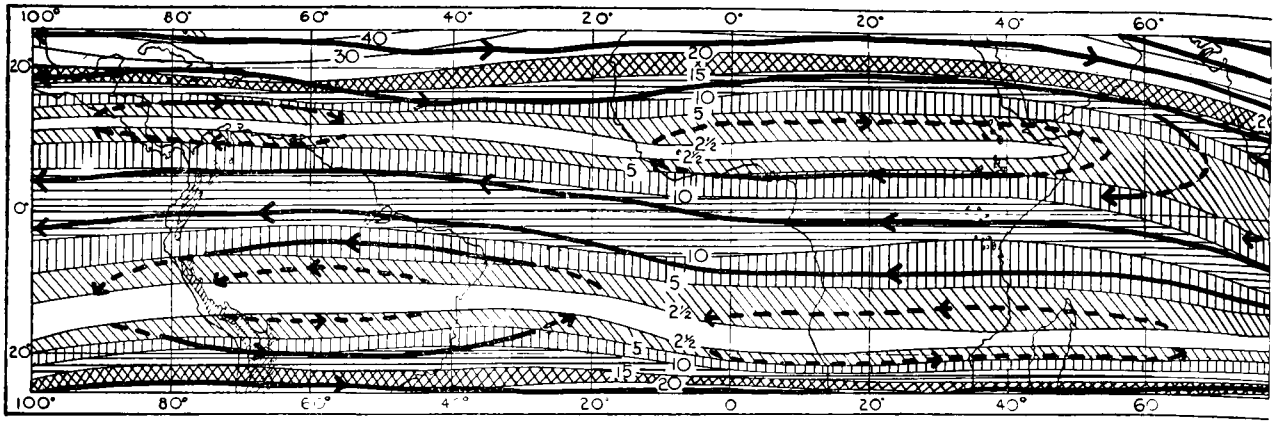

300 mb. MAR.-MAY

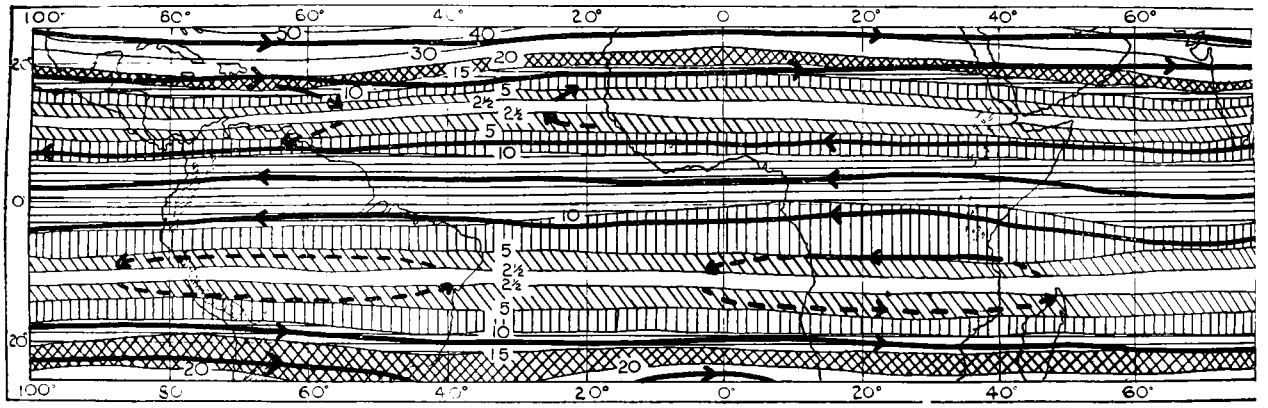

<2½kt. no stream lines shown
2½–5 kt. dotted stream-lines
5–10 kt. full stream-lines

STREAM-LINES IN THE INTERTROPICAL BELT

DEC.-FEB. 300 mb.

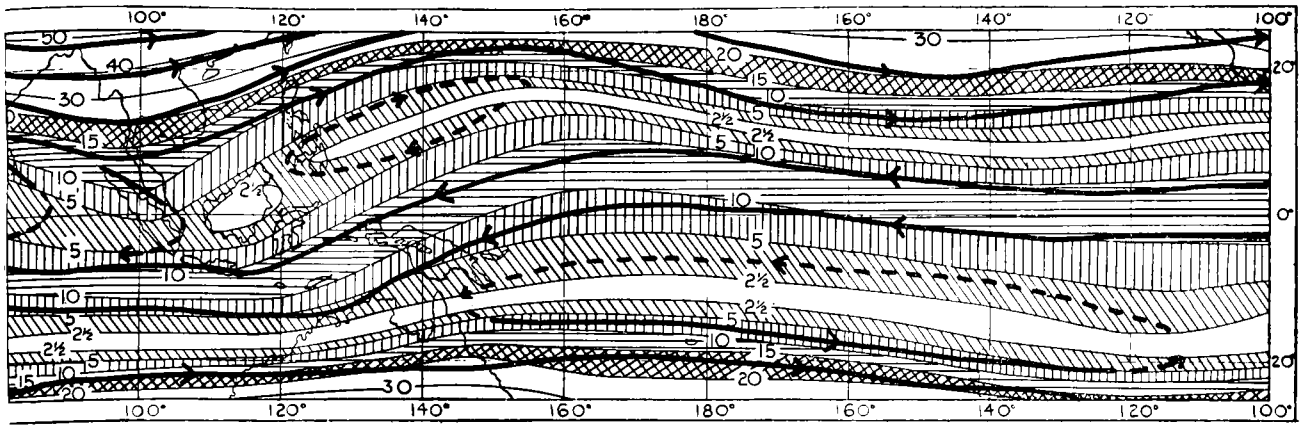

MAR.-MAY 300 mb.

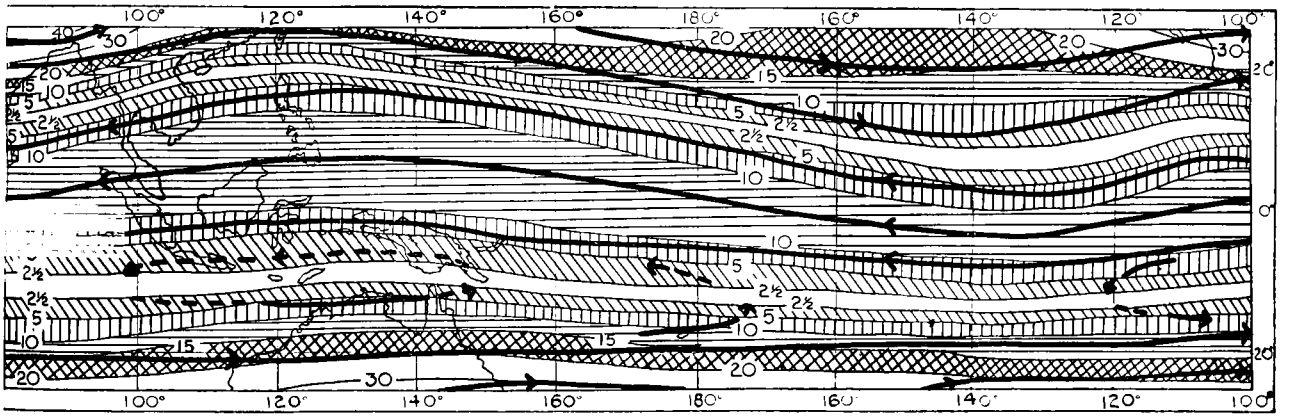

land over 10,000 ft

10-15 kt. full stream-lines
15-20 kt. full stream-lines
> 20 kt. full stream-lines

STREAM-LINES IN THE INTERTROPICAL BELT

300 mb. JUNE-AUG.

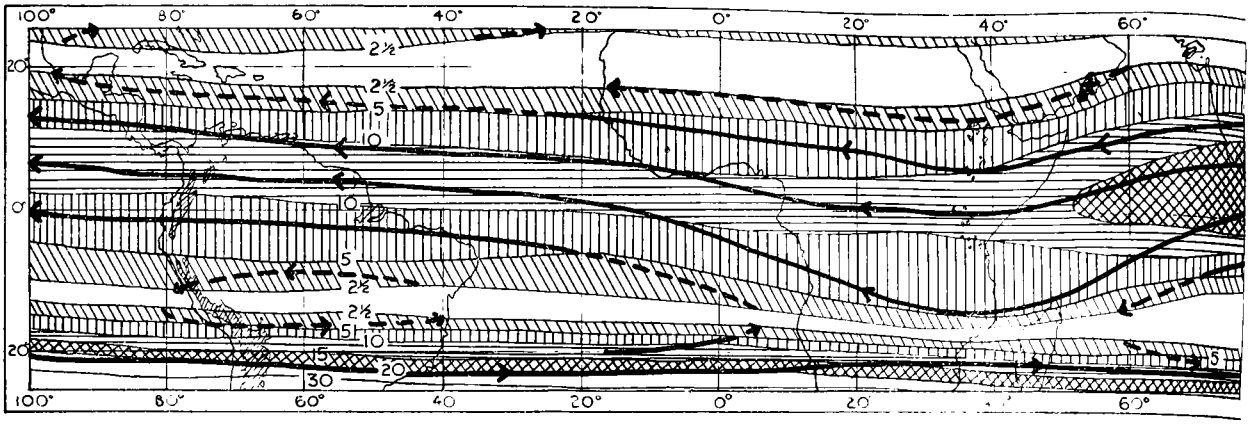

300 mb. SEPT.-NOV.

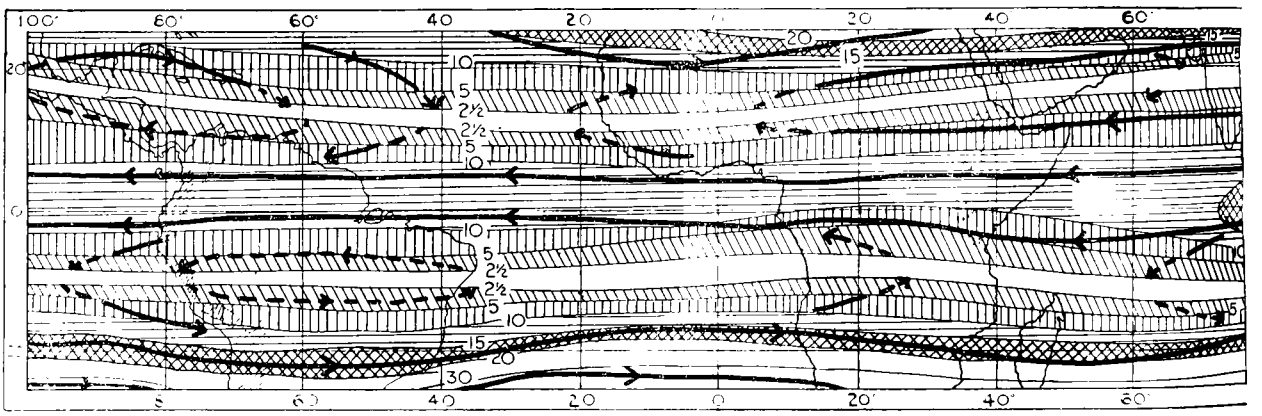

<2½ kt. no stream-lines shown
2½-5 kt. dotted stream-lines
5-10 kt. full stream-lines

STREAM-LINES IN THE INTERTROPICAL BELT

JUNE-AUG. 300 mb.

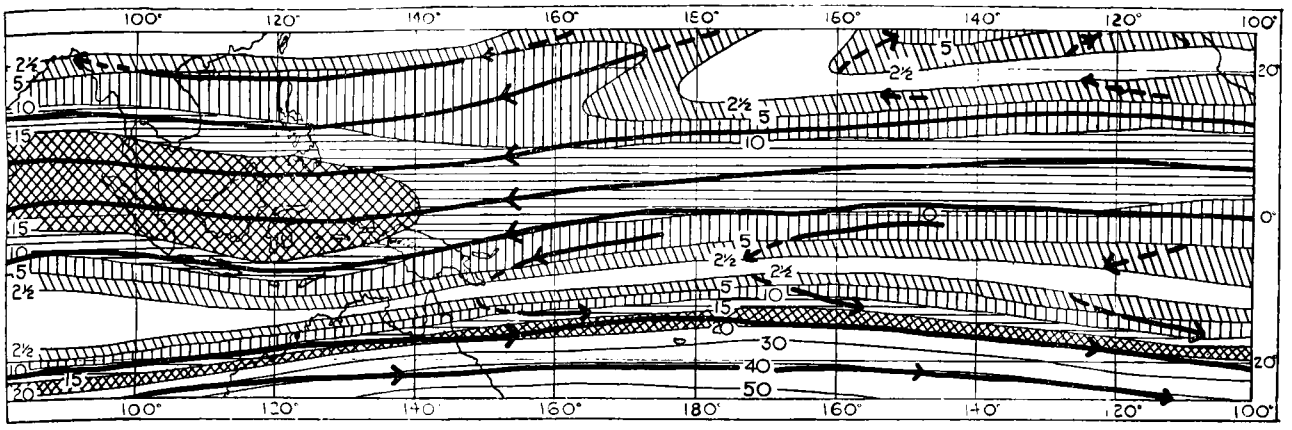

SEPT.-NOV. 300 mb.

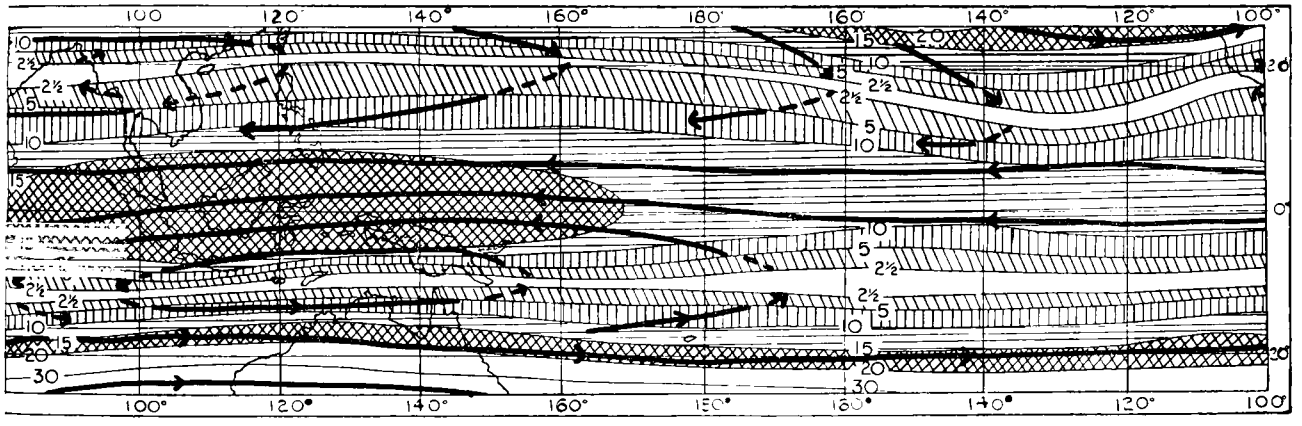

land over 10,000 ft.

10-15 kt. full stream-lines
15-20 kt. full stream-lines
> 20 kt. full stream-lines

STREAM-LINES IN THE INTERTROPICAL BELT

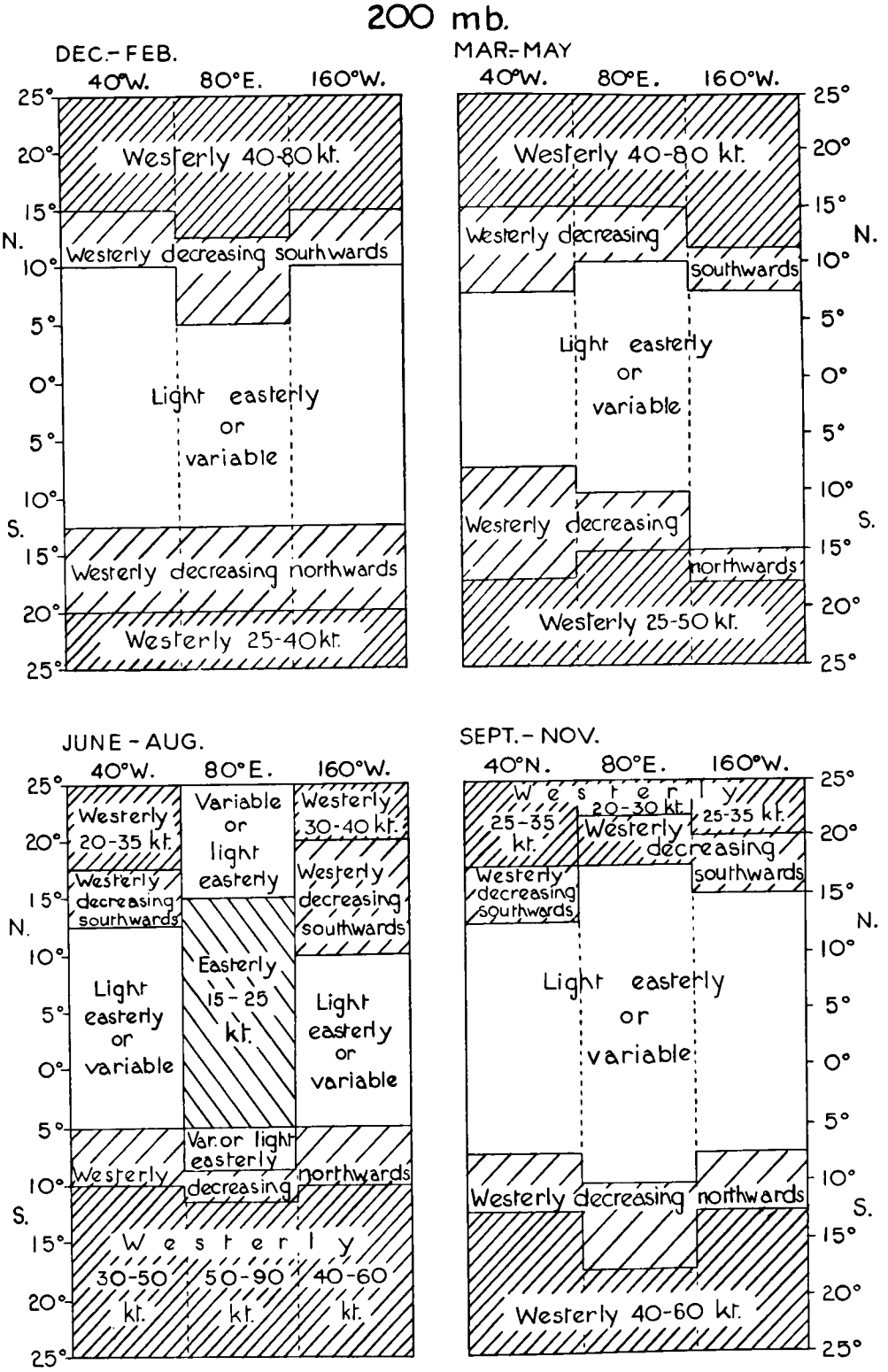

WIND SPEED AND DIRECTION IN THE INTERTROPICAL BELT

(89462) Wt 2409/M. 238 K6 8/50 Hw.